Investigating the role of chitin deacetylation in *Magnaporthe oryzae*

Ivey Geoghegan

Linacre College

University of Oxford

A thesis submitted for the degree of
Doctor of Philosophy
October 2015

Abstract

The fungal cell wall is a highly complex and dynamic structure. It plays a critical role in maintaining cellular integrity, as well as forming the interfacial barrier with the environment. It comprises a matrix of interconnected polysaccharides and proteins, which can change in response to altered environmental conditions, during interactions with other organisms, or during cellular growth and morphogenesis. One such observed change is the deacetylation of chitin to chitosan, a reaction catalysed by a family of carbohydrate esterase enzymes known as chitin deacetylases (CDAs). In phytopathogenic species, such as the rice blast fungus *Magnaporthe oryzae*, chitosan has been shown to be a component of the cell wall during pathogenic interactions. Here, it was hypothesized that the deacetylation of chitin acts as a 'stealth mechanism', by both protecting the fungal cell wall from plant chitinase activity, and by preventing the activation of plant defence responses. In addition, differences in the physical and chemical properties of chitin and chitosan are such that chitin deacetylation may also be required for cell wall modification during cellular morphogenesis. In order to test these hypotheses, the role of chitin deacetylation in appressorium development and vegetative growth were investigated.

During germling morphogenesis, chitosan staining revealed that chitin deacetylation occurs both prior to, and during, appressorium development. Through the creation of single, double and triple deletion strains of three CDAs (*CBP1*, *CDA2* and *CDA3*), chitosan was shown to be necessary for appressorium development on artificial surfaces. However, chitin deacetylation is not required for appressorium development on plant surfaces, arguing against its role in morphogenesis. Exogenous application of chitosan and chemical inducers of appressorium development revealed that chitosan is instead required for germling adhesion and surface sensing. Fluorescent tagging of these CDAs and colocalization with chitin synthase VII suggests that the deacetylation of chitin may involve close association/collaboration between these two families of enzymes.

Chitin deacetylation also occurs in the septa and lateral walls of vegetative hyphae. Two further CDAs (*CDA1* and *CDA4*) were characterized by gene deletion and fluorescent protein tagging, and were found to be required for chitin deacetylation in these locations. Although chitin deacetylation was dramatically reduced in the deletion strains,

no defects in growth or morphology were observed. This again argues against a role for chitin deacetylation in morphogenesis, and also suggests that chitosan is not a crucial structural component of the cell wall. However, mCherry fusions of Cda4 provided further evidence of possible collaboration between CDAs and chitin synthases.

Lastly, the role of chitosan hydrolysis was investigated. Cell wall hydrolases have long been hypothesized to have roles in cell wall modification during morphogenesis. To test this hypothesis, strains were created in which the gene encoding the sole chitosanase (*CSN*) in *M.oryzae* was either deleted or overexpressed. However, these strains proved to be identical to the WT strain under all conditions tested. In addition, a promoter fusion revealed only weak expression of *CSN* in vegetative hyphae. Chitosanase therefore appears not to have a role in cell wall modification during morphogenesis, but its true purpose remains unclear.

In summary, the data in this thesis do not support the original hypotheses regarding the roles of chitin deacetylation or chitosan hydrolysis. Instead, novel roles for chitosan were unmasked, which demonstrate the complex and multifaceted nature of the cell wall. Novel mechanistic insights into chitin deacetylation were also revealed, which suggest that our current knowledge of chitin synthesis and deacetylation is far from complete.

Acknowledgements

First and foremost, I must thank Professor Sarah Gurr for her supervision and support over the past 4 years. Dr Mark Fricker has also been a source of much valuable insight over the course of this DPhil. Additional thanks go to Dr Ian Moore, for being my stand-in supervisor. I must also acknowledge all other members of the Gurr lab: Marketa Samalova, Sarena Che Omar, Elizabeth Birch and Molly Dewey for all their help, advice, cake and coffee-time chat. Valuable technical assistance was provided by Sarah Rodgers and Caroline O'Brian. Many other members of the Department of Plant Sciences have also made valuable contributions over the course of my DPhil, but are too numerous to list here. Lastly, I must thank my family for their support.

This DPhil was funded by a BBSRC CASE studentship in collaboration with Puricore.

Contents

List of Figures

Acronyms

AFM Atomic Force Microscopy.

BSA Bovine Serum Albumin.

cAMP cyclic-adenosine monophosphate.

CDA Chitin Deacetylase.

cDNA Complementary DNA.

CFW Calcofluor White.

CHS Chitin Synthase.

CM Complete Medium.

COS488 Alexa Fluor 488 tagged chitosan oligomer.

CR Congo Red.

DAG 1,2 Dioctanol-*sn*-glycerol.

DEPC Diethylpyrocarbonate.

ELISA Enzyme-Linked Immunosorbant Assay.

FITC Fluorescein isothiocyanate.

FPKM Fragments Per Kilobase of exon per Million fragments mapped.

gDNA Genomic DNA.

GlcNAc *N*-Acetylglucosamine.

GPCR G-Protein Coupled Receptor.

GPI Glycosylphosphatidyl Inositol.

HDD 1,16 hexadecanediol.

hr Hours.

IBMX 3-isobutyl-1-methylxanthine.

min Minutes.

OGA488 Alexa Fluor 488 tagged Oligo Galacturonic Acid.

PAMP Pathogen Associated Molecular Pattern.

PBS Phosphate Buffered Saline.

PBS/T Phosphate Buffered Saline + 0.05% (v/v) Tween 20.

PCR Polymerase Chain Reaction.

PEC Polyelectrolyte Complex.

PGA Poly-galacturonic Acid.

PRR Pattern Recognition Receptor.

PTI PAMP Triggered Immunity.

ROS Reactive Oxygen Species.

RT-PCR Reverse Transcription-Polymerase Chain Reaction.

sec Seconds.

TEM Transmission Electron Microscopy.

TGN Trans-Golgi Network.

WGA Wheat Germ Agglutinin.

Chapter 1

General introduction

1.1 *Magnaporthe oryzae*: Pathogen and model organism

1.1.1 Overview

The rice blast fungus *Magnaporthe oryzae* is a filamentous ascomycete and a hemibiotrophic pathogen of rice. *M.oryzae* is a member of the *Magnaporthe grisea* species complex, and can cause disease in over 50 different grass species, including barley and wheat, making it a potential threat to a number of major food crops (Ou, 1985). Although precise figures for crop losses resulting from *M.oryzae* infection are few, and confounded by additional factors such as insect pests and abiotic factors, there is no doubt that this pathogen causes significant crop losses, even with the use of various control strategies. Epidemics of *M.oryzae* infection can cause devastating yield losses of over 90% (Thinlay et al., 2000), although even in non-epidemic years, losses are in the region of 10% - 30% (Skamnioti and Gurr, 2009). In many Asian countries, rice constitutes a significant proportion of the daily calories consumed, and so such crop losses can be a major cause of under-nourishment in these populations. Compounding these problems, global population is projected to increase to over 9 billion by 2050, with much of this increase occurring in developing countries with a high dependency on rice production (Lee, 2011). Therefore, more food will have to be produced from a cultivatable land area that is the same, if not smaller than that currently used. Increases in crop production must also occur in the face of adverse abiotic factors such as drought or flooding, which may well become more prevalent and severe as a result of climate change (Wheeler and von Braun, 2013). Thus, the study of *Magnaporthe oryzae* is essential if we are to successfully combat rice blast disease and safeguard future rice production. In addition, this fungus is not only important as a pathogen in its own right, but can also be used as a model organism for the study of hemibiotrophy and appressorium-driven infection in other phytopathogenic fungi. *M.oryzae* has a fully sequenced genome, can be grown *in vitro* and is genetically tractable - it is possible to investigate gene function by making targeted gene deletions, or to investigate protein localization by expression of fluorescent protein fusions. The use of these tools and resources has generated a wealth of information regarding the life-cycle of this fungus and the mechanisms by which it is able to successfully infect rice plants.

1.1.2 Life-cycle of *Magnaporthe oryzae*

Primary infection of rice plants by *M.oryzae* generally occurs as a result of conidial dispersal from the conidiophores of vegetatively growing fungus, or the sporulating lesions of an infected plant. Vegetative growth of *M.oryzae* can include growth on dead residue from a previous crop, infected seed, or growth on other grass species. Dispersal of these three-celled pyriform structures, by wind or dew-drop splash (Ou, 1985), leads to contact between the conidia and the aerial surface of a rice plant. Following this initial contact, the conidium immediately adheres to the plant surface due to the presence of spore tip mucilage which is a glycoprotein-rich secretion from the apex of the conidium (Hamer et al., 1988). Subsequent germination of conidia requires the presence of free water, and results in the growth of a polarized germ tube, usually from the apical cell of the conidium. At this stage, sensing of various physical and chemical stimuli by the germling occurs, which is crucial for inducing the formation of a dome-shaped structure known as the appressorium. Surface hydrophobicity is one of the most important stimuli; even in the absence of a leaf surface, appressorium development can be induced by an artificial hydrophobic surface, such as Teflon. The precise mechanism by which hydrophobicity is sensed by germlings remains mysterious, but is known to be dependant upon the G-protein coupled receptor (GPCR) Pth11 (DeZwaan et al., 1999), and the hydrophobin Mpg1 (Talbot et al., 1993, 1996), a protein which self-assembles into amphipathic monolayers at hydrophilic-hydrophobic interfaces (Sunde et al., 2008). Chemical stimuli are of equal importance to physical stimuli; in the absence of hydrophobicity, appressorium formation can be induced by cutin monomers (e.g. 1,16-hexadecanediol), the perception of which also appears to be dependant upon Pth11 (DeZwaan et al., 1999). Plant waxes also induce appressorium development, although via a separate signalling pathway. The integral membrane protein Sho1 and the signalling mucin Msb2 are reported to have overlapping functions in the sensing of waxes in *M.oryzae* (Liu et al., 2011). These proteins (particularly Msb2) also appear to be involved in the sensing of physical surface cues, a function that is conserved amongst a number of species of phytopathogenic fungi (Lanver et al., 2010; Leroch et al., 2015; Pérez-Nadales and Di Pietro, 2011). Downstream of these aforementioned receptors, lie two main signalling cascades: Activation of Pth11 by surface hydrophobicity and cutin monomers leads to an increase in intracellular levels

of the second messenger cAMP, which in turn activates the cAMP dependant protein kinase, CpkA (Choi and Dean, 1997; Mitchell and Dean, 1995). Msb2 and Sho1 both act upstream of a kinase cascade, the activation of which results in the phosphorylation and activation of the MAP kinase Pmk1 (Liu et al., 2011). However, it is also likely that cross-talk also exists between these two pathways (Li et al., 2012). Following activation of CpkA and Pmk1, various transcription factors (e.g. Mstu1 (Nishimura et al., 2009)) are in turn activated, leading to the upregulation of genes necessary to bring about appressorium development.

The appressorium is a melanized, dome-shaped cell that is necessary for the penetration of plant cells by the fungus. Once formed, the appressorium accumulates high concentrations of glycerol (de Jong et al., 1997), due to the break-down of intracellular stores of other molecules, such as lipids or trehalose (Thines et al., 2000). The accumulation of this glycerol results in the build up of extraordinary turgor pressure (up to 8 Mpa) in the appressorium (Howard et al., 1991). This is dependant upon the presence of melanin in the cell wall of the appressorium. Here, melanin acts both as a barrier to prevent diffusion of glycerol out of the appressorium, and contributes to the physical strength of the wall (Chumley et al., 1990; Howard et al., 1991). The turgor pressure is necessary for the penetration of the plant cells by a thin hypha called the penetration peg.

Once the plant cell has been successfully penetrated, the initial growth phase of *M.oryzae* is biotrophic and therefore symptomless. Invasion hyphae, surrounded by the plant-derived Extra Invasive-Hyphal membrane (EIHM), spread between adjacent cells via plasmodesmata (Kankanala et al., 2007). Successful colonisation of the plant depends upon the production and secretion of effector proteins, which subvert host cellular processes in order to create conditions conducive to the biotrophic growth of the fungus. Effectors can be divided into two types, depending upon their method of secretion - Those that are delivered into the cytoplasm of the plant cell in a golgi-independant manner via the Biotrophic Interfacial Complex (BIC) (a plant membrane-derived structure), and those that are delivered into the apoplast in a golgi-dependant manner (Khang et al., 2010; Giraldo et al., 2013). Following $\sim$72 hr of biotrophic growth, the fungus switches to a necrotrophic growth phase. At this stage, the fungal hyphae spread rapidly through

the plant, causing death of the plant cells, and resulting in the appearance of the disease lesions that are characteristic of rice blast disease. Under conditions of high humidity, conidiation occurs and thus the cycle begins again (Wilson and Talbot, 2009).

The entire infection cycle of *M.oryzae* takes just 5-7 days, meaning that many cycles of infection can occur within a single growing season (i.e. it is polycyclic). As well as being able to infect all aerial parts of the plant (including leaves, stems and panicles), *M.oryzae* has also been found to infect the roots of rice plants. In this case, the fungus follows a different developmental programme that is more typical of root-specific pathogens, such as *Gaeumannomyces graminis* (Sesma and Osbourn, 2004).

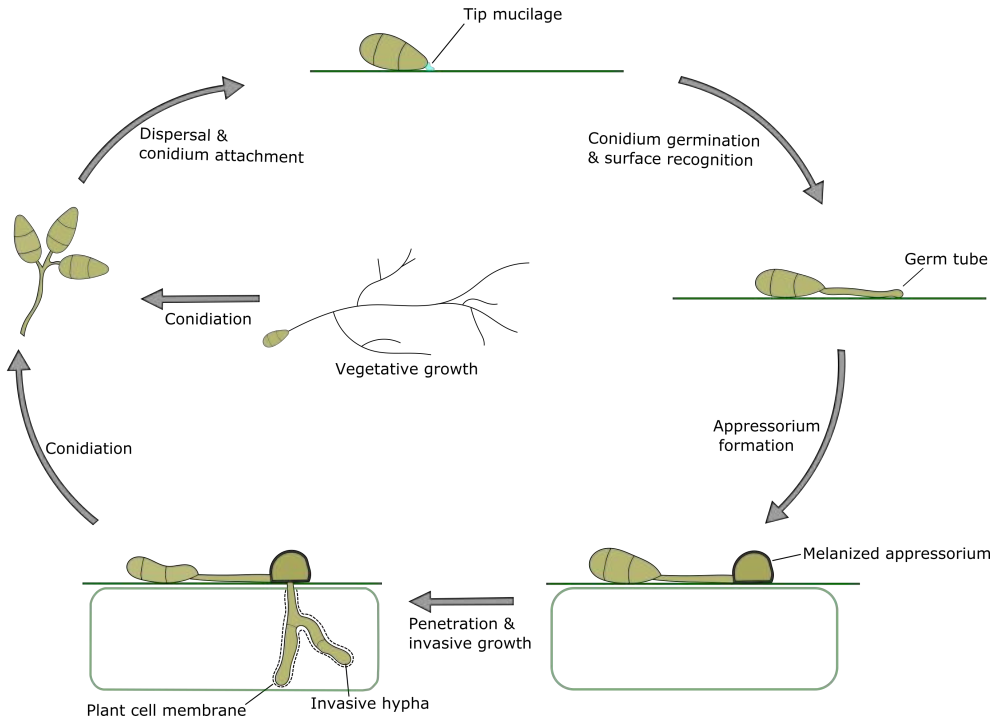

Figure 1.1: The life-cycle of the rice blast fungus, *Magnaporthe oryzae*. Infection begins with the dispersal of conidia, by wind or dew-drop splash. Conidia which land on the aerial part of a plant adhere, and germinate in the presence of free water. Appressorium development is induced by perception of various physical and chemical factors present on the plant surface. Generation of high turgor pressures within the appressorium results in penetration of the leaf. The invasive hyphae ramify throughout the plant, spreading from cell to cell. After ∼5 days conidiation occurs, and the cycle begins again. Adapted from Wilson and Talbot (2009).

1.1.3 Current control strategies

Given the extremely destructive nature of this pathogen, the control of *M.oryzae* is clearly of great importance. Current strategies can be broadly divided into those based on plant disease resistance through breeding, and those afforded by chemical control strategies.

In most of the rice cultivars grown, resistance to *M.oryzae* is imparted by a single dominant *Resistance* (*R*) gene. Currently, over 100 *R* genes have been discovered in rice, although of these, only 20 have been cloned and characterized (Wu et al., 2015). An *R* gene encodes a protein that recognizes an *M.oryzae* protein, termed an Avirulence (Avr) protein. Currently, over 40 *AVR* genes have been identified (Zhang and Xu, 2014). *AVR* genes generally encode effectors expressed in the invasive hyphae of *M.oryzae*. Delivery of these effectors into plant cells (as discussed in Section 1.1.2) leads to interaction (either direct or indirect) between the Avr protein and the R protein. This triggers the hypersensitive response, and therefore death of the invading fungus. Unfortunately, *R* genes may only recognize certain strains of *M.oryzae*, limiting their efficacy in the field. In addition, the resistance imparted by such *R* genes can be short-lived, particularly when deployed in the large monocultures typical of modern farming methods. Strong selection pressure leads to mutation or deletion of the cognate *AVR* genes in *M.oryzae*, allowing it to overcome the plant resistance (Skamnioti and Gurr, 2009). However, these problems can be somewhat alleviated by the presence of multiple *R* genes in a single cultivar, the use of broad-spectrum *R* genes, and/or the use of cultivar mixtures.

Chemical control strategies can complement the use of resistant cultivars, providing an additional layer of control against strains not recognized by resistance genes, or against other species of fungal pathogen. Fungicides represent the main chemical control strategy, particularly in the more resource-rich farming economies such as Japan, which represents 46% of the global rice-blast fungicide market, despite growing only 2% of the world's rice (Skamnioti and Gurr, 2009). Most fungicides directly disrupt a key cellular process in order to attenuate fungal growth and development. Melanin biosynthesis inhibitors (MBIs), are one of the most widely-used fungicides of this type (Skamnioti and Gurr, 2009). This class of fungicide can be further subdivided depending on which step is inhibited: MBI-Ds, such as carpromatid, which inhibits the scytalone dehydratase enzyme (Kurahashi et al., 1997), and MBI-Rs, such as tricyclazole, a systemic fungicide

which inhibits polyhydroxyl-napthalene reductase (Froyd et al., 1976; Tokousbalides and Sisler, 1978). In either case, application of these fungicides results in the loss of melanin, which is a key component of the cell wall in the appressorium, as discussed previously (Section 1.1.2). However, the inhibition of melanin biosynthesis is only effective at preventing plant infection when implemented prior to appressorium development and plant penetration by the fungus. Other fungicides, such as isoprothiolane are effective in disrupting fungal growth at any stage in development. Isoprothiolane is an inhibitor of the Kennedy pathway for phosphatidylcholine biosynthesis, and therefore causes disruption of fungal membranes (Kodama et al., 1979; Yoshida et al., 1984). It is systemic, being absorbed by the plant following application, meaning that direct application onto the fungus is not required (Uesugi, 2001). The fungal plasma membrane is also the target of another group of fungicides, the sterol biosynthesis inhibitors. This group can be subdivided into four classes, depending on which particular enzyme is inhibited. Of these, propiconazole, an inhibitor of a cytochrome P-450 monooxygenase, is one of the most widely-used against *M.oryzae* (Leroux, 2003). Finally, the strobilurins (e.g. azoxystrobin), which are derivatives of naturally occurring secondary metabolites produced by lignocellulytic fungi, inhibit mitochondrial respiration by preventing electron transfer between cytochrome b and cytochrome c_1 (Godwin et al., 1992) (Becker et al., 1981). Apart from application of fungicides, pathogenic fungi can also be controlled indirectly, through activation of plant defence responses. Probenazole triggers the accumulation of salicylic acid in treated plants (Yoshioka et al., 2001), thereby causing the upregulation of a host of genes involved in plant systemic acquired resistance (SAR) (Iwai et al., 2007). This potentially increases plant resistance to not only *M.oryzae*, but also to a broad-spectrum of fungi, bacteria and viruses.

As with plant resistance genes however, the emergence of fungal resistance to these chemical treatments is problematic. Although some fungicides, such as MBI-Rs, have remained effective after decades of use, others, such as carpromatid have only been able to be used for a few years before resistant *M.oryzae* strains emerged (Yamaguchi et al., 2002). In addition, whilst some fungi evolve fungicide resistance, others exhibit inherent insensitivity to certain types of fungicide, for example *Cryptococcus* species to the echinocandins and *Aspergillus terreus* to amphotericin B to name but a few (Denning

and Bromley, 2015). The cost of such fungicides must also be taken into consideration. In some cases, the cost of fungicides (e.g. echinocandins) is such that their use in agriculture is simply not economically viable. Taken together, it is clear that the search for novel fungicides is a necessary and continuous process. The targets of fungicides need to be both essential to the normal development and integrity of the fungal cell, and specific to fungi, in order to avoid deleterious effects in the host. The fungal cell wall fulfils these requirements: it is essential for cellular integrity, as well as structurally and compositionally unique to fungi. Additionally, as many enzymes involved in cell wall synthesis and remodelling are extracellular, the cell permeability of the fungicides need not be of primary concern. Although some fungicides targeting cell wall related processes have been developed (discussed later), our limited understanding of the processes underpinning cell wall synthesis and remodelling is preventing full exploitation of this target. Thus, investigating mechanisms of cell wall synthesis and remodelling could be extremely valuable in tackling pathogenic fungi.

1.2 The fungal cell wall

1.2.1 Overview

The fungal cell wall is a complex structure comprising a matrix of interconnected polysaccharides and proteins. Traditionally, the cell wall was considered as nothing more than the inert extracellular 'armour' of the fungal cell, maintaining cellular integrity in the face of the challenging environmental conditions faced by fungi during the course of their life-cycle. In more recent years however, the cell wall has been found to be a highly dynamic structure, with roles that extend far beyond being a simple protective shell. Cellular morphogenesis, for example, is heavily influenced by the composition of the cell wall, and *vice versa*. The cell wall acts as a physical constraint to any changes in cell size or shape, and so any alteration to these parameters requires both the cell and the cell wall to change in a harmonious and regulated manner. In this way, cellular integrity is maintained whilst allowing the underlying cell to undergo morphogenesis. Consequently, cell wall structure and composition is observed to change considerably during cellular development, as well as differing according to cell type. The importance of this process

has been demonstrated countless times by chemical or genetic perturbation of the cell wall, which often results in catastrophic morphogenic defects.

As the outermost part of the fungus, the cell wall also forms the interface between the fungal cell and its environment. This is particularly significant during pathogenic interactions between a fungus and its host, and there are numerous examples of how fungi significantly alter the composition of their cell wall during pathogenic interactions (detailed in the following subsections). Rather than simply being a reaction to a change in environment, it could instead be argued that these compositional changes allow a fungus to specifically tailor the outcome of a pathogenic interaction to its favour.

M.oryzae represents an ideal system in which to study the cell wall of a filamentous plant pathogen, where the inter-relationships between the different roles of the wall considered above can be investigated. The genetically tractable nature of this organism means that functional analysis and localization of any protein with a putative role in cell wall synthesis or remodelling is possible. As a phytopathogenic fungus that produces infection-specific structures (e.g. appressoria, penetration hyphae), *M.oryzae* also provides an opportunity to explore how the structure, composition and synthesis of the cell wall changes both during plant infection and during the development of these specialized cell-types. Of particular interest are the trade-offs which likely exist between the roles of the cell wall in cellular integrity, cellular morphogenesis and pathogen-host interactions. In the following sections, our current knowledge of cell wall composition, synthesis and remodelling is reviewed, with a particular emphasis on pathogenic fungi.

1.2.2 Structure and Synthesis

The structure and composition of the cell wall is known to vary considerably between different fungal species, and over the course of the fungal life-cycle. Presenting an accurate model for the structure of the cell wall that is applicable to all cell-types in all species of fungi is therefore impossible. This difficulty is compounded by the fact that the majority of research into the fungal cell wall has been conducted in just a few species, including *Saccharomyces cerevisiae* (Lesage and Bussey, 2006), *Candida albicans* (Klis et al., 2001) and *Aspergillus fumigatus* (Bernard and Latgé, 2001). Despite this, there is evidence that the structure and synthesis of the main cell wall components (chitin

and glucans) are widely conserved in fungi. A generalised model of the fungal cell wall, broadly applicable to most species of fungi and cell-types is presented in Figure 1.2. Much of the evidence for overall wall structure has resulted from ultrastructural imaging of *S.cerevisiae* and *C.albicans* cells by transmission electron microscopy (TEM). These studies have revealed that the cell wall in these species has a laminar structure, comprising an electron-transparent inner layer and an electron-dense outer layer (Cappellaro et al., 1994; Lesage and Bussey, 2006; Tokunaga et al., 1986). The inner layer is composed of an interconnected matrix of chitin and glucans, whereas the outer layer is composed of mannoproteins which are also cross-linked to the underlying polysaccharides. However, this laminar structure is not necessarily applicable to all fungi, and the manner in which different cell wall components are interlinked also differs widely between species. In the following sections, the synthesis and remodelling of the major components of the fungal cell wall are reviewed.

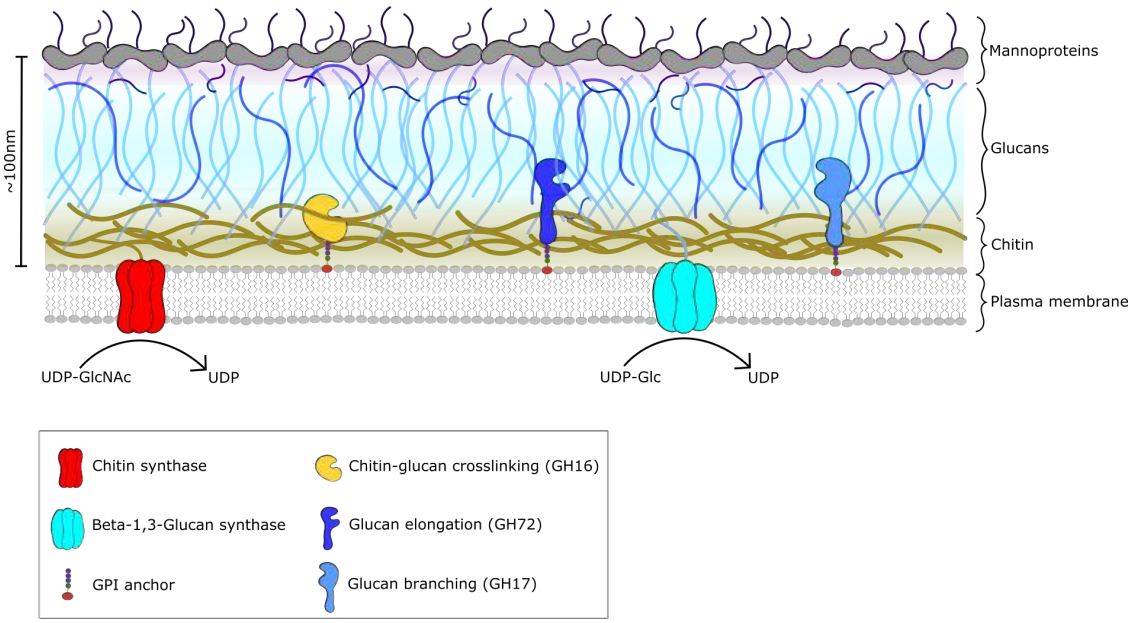

Figure 1.2: Cartoon of the fungal cell wall, showing the major components and enzymes involved in biosynthesis and remodelling. The wall is observed to have a layered structure, in which crystalline chitin forms the innermost layer. α1,3- β1,3- and β1,6- glucans constitute the majority of the cell wall by mass, and form the middle/outer layer. In some species, the outermost layer of the wall is dominated by highly glycosylated proteins (mannoproteins), although in others these are more likely interspersed throughout the wall. The major synthase enzymes are chitin and β1,3-glucan synthase; these are integral membrane proteins that extrude chains of chitin and β1,3-glucan respectively, into the cell wall. Remodelling of these components is performed by a series of GPI-anchored enzymes, which elongate, branch and cross-link polysaccharides.

Glucan synthesis

Glucans are usually the most abundant polysaccharides in the cell wall, the major species of which are β1,3-glucan, β1,6-glucan and α1,3-glucan. Of these, β1,3-glucan is the most abundant form of glucan, making up 30-80% of total cell wall mass (Free, 2013). This form of glucan is synthesized at the plasma membrane by β1,3-glucan synthase (named Fks1 in most fungi), an integral membrane protein that synthesizes β-1,3-glucan in a vectorial manner from an intracellular pool of UDP-glucose (Douglas et al., 1994). Fks1 is activated by the GTP-bound form of Rho1, which is in turn regulated at the plasma membrane by the GDP/GTP exchange factor Rom2 (Qadota et al., 1996; Sekiya-Kawasaki et al., 2002). Both Fks1 and Rho1 localize to areas of cell wall remodelling (Qadota et al., 1996), and Fks1 has also been observed to colocalize with actin patches in *S.cerevisiae* (Utsugi et al., 2002). Studies of β1,3-glucan synthase regulation and localization are few in filamentous fungi, in part due to the difficulty in generating a functional fluorescent fusion of this enzyme. However, a recent study in *Neurospora crassa* achieved live-cell imaging of a GFP-tagged Fks1 (Sánchez-León and Riquelme, 2015). This revealed localization to hyphal apices and the outer region of the Spitzenkörper (an intracellular complex of secretory vesicles situated at the tips of growing hyphae), and to hyphal branching sites, but surprisingly not to developing septa, suggesting that β1,3-glucan may not be a major component of the cell wall in these structures. It was also found that Fks1 was transported to the hyphal tip in macrovesicles, which are perhaps analagous to the chitosomes observed in chitin synthase fusions (discussed later). Intriguingly, the distribution of these macrovesicles at the Spitzenkörper appears to differ from that of the smaller chitosomes, suggesting possible 'functional stratification' of the Spitzenkörper (Verdín et al., 2009). As in *S.cerevisiae*, Fks1 is believed to be regulated by Rho1 in filamentous fungi (Beauvais et al., 2001). However, an additional regulator has also been identified in *N.crassa*, known as GS-1 (Glucan synthase-1). Fluorescently-tagged GS-1 localizes to the Spitzenkörper in a very similar manner to Fks1, although co-localization has not yet been attempted (Verdín et al., 2009). Deletion of GS-1 severely impacts β1,3-glucan synthesis, but its precise role is unknown (Enderlin and Selitrennikoff, 1994).

The synthesized β1,3-glucan is a non-crystalline polymer that adopts a helical structure thought to impart both tensile strength and elasticity to the cell wall (Krainer et al.,

1994) (Klis et al., 2002). The precise structure of β1,3-glucan in terms of branching pattern and chain length likely vary between species. In *S.cerevisiae*, β1,3-glucan chains of ∼1500 residues long are branched at 3% of the residues by the addition of β1,3-glucan chains via a 1,6 linkage (Manners et al., 1973a). In *A.fumigatus*, the overall structure is similar, except for the presence of β1,4-glucan interspersed throughout the β1,3-chains, which is synthesized by the predicted glycosyltransferase Tft1 (Fontaine et al., 2000; Samar et al., 2015). This β1,4-glucan moiety has also been observed in *N.crassa* (Maddi and Free, 2010).

Most filamentous fungi (including *M.oryzae*) have just a single β1,3-glucan synthase, the deletion of which is assumed to be lethal, although this is based on limited experimental data (Oliveira-Garcia and Deising, 2013). A notable exception is *A.fumigatus*, where a viable deletion strain of *FKS1* was successfully generated, which demonstrated extremely reduced growth, and lethality in combination with inhibitors of septum formation (Dichtl et al., 2015). In other fungi, lethality can be avoided by reducing expression of *FKS1* by RNAi, rather than deleting the gene (Mouyna et al., 2004). In these cases, defects are observed consistent with catastrophic loss of cell wall integrity, for example hyphal bursting and loss of conidial viability in *Fusarium solani* (Ha et al., 2006) and 'exploding' appressoria in the Maize pathogen *Colletotrichum graminicola* (Oliveira-Garcia and Deising, 2013). Given the essential role of β1,3-glucan in maintaining cellular integrity, it is likely to be a component of the cell wall during all developmental stages of the fungal life-cycle. However, during pathogenic interactions, fragments of β1,3-glucan can be recognized by the host cells. This is true both in mammals, where fragments bind to Dectin-1 (Brown and Gordon, 2001), and in plants, where linear or branched β1,3-glucan fragments are recognized by an unknown receptor (Klarzynski et al., 2000; Yamaguchi et al., 2000). In both cases, the perception of β1,3-glucan as a foreign molecule (or Pathogen Associated Molecular Pattern (PAMP)) has dire consequences for the fungus, as it results in the activation of PAMP-triggered immunity (PTI), which allows the host to destroy or attenuate the invading fungus. This presents pathogenic fungi with something of a dilemma: should they reduce the amount of β1,3-glucan in their walls in order to avoid detection but as a result compromise wall strength, or should they maintain strong walls but risk detection? It appears that fungal pathogens have evolved a number of distinct strategies

to overcome this challenge. The first involves the shielding of immunostimulatory cell wall components, a strategy common to many pathogenic fungi. This can be achieved by upregulation of another cell wall component, such as α1,3-glucan or chitosan, so that the β1,3-glucan is no longer exposed at the surface of the fungi (these are discussed in detail later). In some fungi, walls are also covered by a layer of hydrophobins, which also act as a shield to prevent immune recognition (Aimanianda et al., 2009). The second strategy, which is complementary to the first, is to reduce the β1,3-glucan content of the cell wall. This was observed in *C.graminocola*, where a dramatic reduction in *FKS1* expression during the biotrophic phase of infection occurred, whereas forced overexpression of *FKS1* at this stage resulted exposure of β1,3-glucan on biotrophic hyphae and triggering of PTI (Oliveira-Garcia and Deising, 2013). The third potential strategy is to alter the molecular composition of β1,3-glucan such that it can no longer be recognized by its receptor. Recent evidence suggests that β-glucan in the cell walls of *C.albicans* differs according cell type: in yeast cells it is in a linear form (β1,3-glucan with β1,6 branches), whereas hyphal glucan demonstrated a unique, cyclical structure. Importantly, the hyphal form of glucan was a much more potent inducer of an immune response than the yeast form (Lowman et al., 2014). However, there is no suggestion that this is a specific strategy used by this fungus in order to avoid immune detection. Rather, this provides some evidence that changing the molecular structure of β1,3-glucan, perhaps by branching or cross-linking with other components could serve to render them less detectable. Further work is required to determine whether this is the case in other species of pathogenic fungi.

The role of β1,3-glucan in the cell wall of pathogenic fungi perfectly illustrates the multifaceted nature of cell wall function in these species. As a structural component of the wall, β1,3-glucan is essential for wall integrity. On the other hand, β1,3-glucan is a PAMP and forms part of the 'molecular dialogue' between the fungal and host cells. The strategies outlined above demonstrate the ability of fungi to alter the composition of their cell walls in order to alter the outcome of this 'molecular dialogue' to their favour.

As an essential component of the fungal cell wall, β1,3-glucan represents a valuable fungicide target and one that has already been exploited. The echinocandins are a group of synthetically modified lipopeptides which target β1,3-glucan synthase (Denning, 2002). The use of these drugs in clinical settings has led to more successful treatment of certain

invasive fungal infections (Denning and Bromley, 2015), though unfortunately some fungi exhibit inherent resistance to this class of fungicide (e.g. *Cryptococcus neoformans*). Another problem is the prohibitive cost of caspofungins: treatment of an *Aspergillus* infection costs over $400 per day, per patient (Saravolatz et al., 2003), making them unsuitable for use on crops, even without taking into consideration issues of stability and of plant uptake.

Linked to β1,3-glucan is β1,6 glucan, a minor component of the cell wall which comprises only ∼10% of total cell wall glucan in *S.cerevisiae* (Manners et al., 1973b). Interestingly, β1,6-glucan is absent in other species, including *A.fumigatus* (Fontaine et al., 2000) and *N.crassa* (Maddi and Free, 2010), but has been found in the cell wall of *M.oryzae* (Samalova *et al*, unpublished results). Despite its relatively low abundance, β1,6-glucan has a crucial role in cross-linking adjacent β1,3-glucan chains, and serving as an attachment site for other cell wall components, such as chitin, GPI-anchored proteins and mannoproteins (Cabib, 2009; Kollár et al., 1997). However, neither the enzyme responsible nor the site of synthesis for this form of glucan have been identified conclusively. Nevertheless, mutational studies have identified a number of genes required for the synthesis of β1,6-glucan. For example, *KRE6* and *SKN1* encode functionally redundant, golgi-localized, glycosyl hydrolase 16 (GH16) family proteins in *S.cerevisiae*. Deletion of these genes caused a dramatic reduction in β1,6-glucan levels and reduced growth, attesting to the critical role played by this polymer. Surprisingly, *M.oryzae* does not possess homologues of either of these proteins, despite β1,6-glucan being a component of the cell wall in this fungus (Samalova *et al*, unpublished results). This suggests that either the mode of synthesis of this polymer may not be conserved in all fungi, or that these proteins only have an indirect role in its synthesis. Many other gene deletions affecting synthesis of β1,6-glucan have been identified, which encode ER, Golgi or cell surface localized proteins (reviewed in Shahinian and Bussey (2000)). These proteins are also unlikely to be directly involved in synthesis of the β1,6-glucan, but may be required for regulating secretion or for processing of proteins involved in β1,6 glucan synthesis. As with *KRE6* and *SKN1*, deletion of these genes results in a reduction, but not complete loss, of β1,6-glucan and a concomitant growth defect. Some deletion combinations are lethal, for example when *KRE9* and *KNH1* are both deleted in *S.cerevisiae* (Dijkgraaf

et al., 1996). Again, however, homologues of these proteins are not found in *M.oryzae*. The failure to identify a 'β1,6-glucan synthase' could either be due to lethality, or the presence of multiple, functionally-redundant genes. Whichever the case, the synthesis of β1,6-glucan clearly represents an unexploited fungicide target and an inviting research opportunity.

The last commonly occurring glucan moiety is α1,3-glucan, which is known to be a component of the cell wall in most fungi, although is absent in *S.cerevisiae*. Like β1,3-glucan, α1,3-glucan is synthesized at the plasma membrane by an integral membrane protein, α1,3-glucan synthase (Ags), from a cytoplasmic pool of UDP-glucose. The α1,3-glucan found in fungal cell walls usually exists as a linear polymer, with short chains of α1,4-linked glucose interspersed between the longer α1,3-glucan sections. Interestingly, no linkages to other cell wall components have yet been identified (Choma et al., 2013). This suggests that α1,3-glucan exists as an entirely separate, non-crosslinked component of the cell wall, unlike chitin and β1,3-glucan. The reasons for this 'spatial' isolation are unclear, but it could have important consequences for the physical properties of the cell wall. Ags enzymes are usually predicted to have two catalytic domains: an intracellular domain for the synthesis of α1,3 glucan, and an N-terminal extracellular domain with a possible role in catalyzing transglycosylation reactions between α-glucan chains (Free, 2013). *AGS* genes have been characterized in a number of different species of fungi, revealing that α1,3-glucan has diverse roles, depending on the species and cell-type in question. In the fission yeast *Schizosaccharomyces pombe*, α1,3-glucan comprises approximately one-third of total glucans (Bush et al., 1974). Deletion of *AGS* in this fungus revealed α1,3 glucan is essential for cellular morphogenesis and integrity; conditional mutants of *AGS1* underwent cell lysis at restrictive temperatures and failed to maintain rod-like shapes (Hochstenbach et al., 1998). In *N.crassa* α1,3-glucan is component of the cell wall in aerial hyphae and conidia, but not vegetative hyphae, suggesting that in this fungus α1,3-glucan is specific to certain developmental stages. By deletion of *AGS1*, it was shown that α1,3-glucan is required for conidial development (Fu et al., 2014). In contrast, loss of α1,3-glucan in other fungi does not result in developmental defects or loss of integrity. For example, knockdown of *AGS1* in *Histoplasma capsulatum* had no effect on growth *in vitro* (Rappleye et al., 2004). Similarly, a triple deletion of all three *AGS* genes in *A.fumigatus*

had no effect on the growth of the fungus (Henry et al., 2012). This is despite the complete loss of α1,3-glucan, which constitutes up to 40% of total cell wall polysaccharides in this species (Maubon et al., 2006). Lastly, a recent study in *M.oryzae* revealed that α1,3-glucan was a component of the cell wall in germ tubes and appressoria, but that loss of this component did not affect morphogenesis (Fujikawa et al., 2012). Therefore, α1,3-glucan is not required for cellular integrity or morphogenesis in *H.capsulatum*, *A.fumigatus* or *M.oryzae in vitro*. Intriguingly however, when the pathogenicity of the *AGS* deletion strains in these species was tested in their respective hosts it was found to be severely reduced. In all cases, the invasion of the host by a fungus lacking α1,3-glucan resulted in activation of defense responses, which were presumably sufficient to prevent successful colonisation by the pathogen (Rappleye et al., 2007; Beauvais et al., 2013; Fujikawa et al., 2012). These studies provide strong evidence that α1,3-glucan operates as a 'stealth mechanism' in these pathogens, as discussed previously; the presence of α1,3-glucan on the outer part of the cell wall prevents exposure of PAMPs in the cell wall, such as β1,3-glucan. Thus, the pathogens remain undetected and can successfully colonize the host. As an essential cell wall component for successful host infection in these fungi, the inhibition of α1,3-glucan synthases has been proposed as a valuable fungicide target. Although none have yet been developed to inhibit this enzyme, an alternative approach has been tested in rice plants (Fujikawa et al., 2012). The expression of α1,3-glucanase in rice plants provided resistance to not only *M.oryzae*, but also to *Cochliobolus miyabeanus* and *Rhizoctonia solani*, suggesting that α1,3-glucan acts as a protective layer in these distantly-related species too. Transgenic crops producing α1,3-glucanase could therefore represent a novel strategy to confer broad-spectrum fungal resistance.

Chitin synthesis

The synthesis of chitin is perhaps the most studied aspect of the fungal cell wall. Chitin, a polymer of β1,4-N-acetylglucosamine (GlcNAc) is synthesized from a cytoplasmic pool of UDP-GlcNAc, by a conserved family of enzymes known as chitin synthases (CHS). These are glycosyl transferase enzymes, with multiple transmembrane domains which localize them to the plasma membrane. Based on their amino acid sequences, the chitin synthase family can be subdivided into seven classes (I-VII), although different studies have created

conflicting classifications (Riquelme and Bartnicki-García, 2008). Domain architecture of the chitin synthases differs according to the class to which the enzyme belongs. Classes I-III have a type-1 Chitin Synthase domain (Pfam 01644) at their N-terminus, preceded by a Chitin Synthase N-terminal domain (Pfam 08407), as well as a conserved portion of the Chitin Synthase-2 domain (Pfam 03142). Classes IV-VII have the full Chitin Synthase-2 domain, which is preceded by a cytochrome b5 domain (Pfam 00173) in classes IV, V and VII. Lastly, classes V and VII also have a myosin motor domain (Pfam 00063) at their N-terminus (Riquelme and Bartnicki-García, 2008). Interestingly, the number of chitin synthase sequences present in fungal genomes is highly variable. Numbers range from just a single chitin synthase in fungi such as *S.pombe*, to over 20 in species of *Rhizopus*. Such discrepancies likely reflect the higher chitin content of certain fungal species' cell walls, as well as more complex and varied cellular morphologies.

Unlike glucans, chitin is a highly crystalline polymer, in which individual chains are assembled into microfibrils through extensive inter-chain hydrogen bonding. This can give rise to three different crystalline forms of chitin: α, β, and γ, where the individual chitin chains are assembled in a parallel, anti-parallel or parallel/anti-parallel fashion respectively (Blackwell, 1969; Minke and Blackwell, 1978; Jang et al., 2004). However, α-chitin is the form that is found in fungal cell walls (Lenardon et al., 2010). Chitin plays a critical role in maintaining the strength and rigidity of the cell wall, despite constituting only 1-2% of total cell wall mass in *S.cerevisiae* (Klis, 1994), and 10-20% in filamentous fungi (Kong et al., 2012; Muszkieta et al., 2014). In contrast to glucan synthesis, where typically a single enzyme is responsible for the synthesis of all β1,3- or α1,3-glucan in the cell wall, the synthesis of chitin is performed by several different chitin synthases which appear to have spatially and temporally-specific roles. This is perhaps best exemplified in *S.cerevisiae*, where there are three chitin synthases (Chs1-3). Chs3 is responsible for the synthesis of the majority of cell wall chitin, at the base of emerging buds and the lateral wall, whereas Chs1 and Chs2 have roles in wall repair and septum synthesis respectively (Shaw et al., 1991; Bulawa and Osmond, 1990; Cabib et al., 1989). *C.albicans* has four chitin synthases, Chs1, Chs2, Chs3 and Chs8. As in *S.cerevisiae*, these enzymes have distinct and specific roles. Chs1 synthesises the primary septum, and is unique amongst chitin synthases in being an essential gene (Munro et al., 2001). Chs3 synthesizes the

majority of cell wall chitin during yeast and hyphal growth. The roles of Chs2 and Chs8 have only recently been conclusively established; they synthesize chitin at polarized sites and septa, as well as in response to cell wall stress (Preechasuth et al., 2015). Genes encoding chitin synthases are typically more numerous in filamentous ascomycetes such as *M.oryzae*. Gene deletion of individual chitin synthases have been performed in a wide range of species, including *Botrytis cinerea* (Soulié et al., 2003, 2006), *Fusarium oxysporum* (Martín-Urdíroz et al., 2008), *Colletotrichum graminicola* (Werner et al., 2007), and *Aspergillus nidulans* (Horiuchi et al., 1999; Fujiwara et al., 2000; Takeshita et al., 2006). These studies have revealed a whole host of defects associated with the loss of individual chitin synthase genes, but a consistent trend is that those containing a myosin motor domain (classes V and VII) appeared to be the most important for normal hyphal growth and pathogenicity. However, these studies neglect a significant proportion of the chitin synthase family, since they tend to focus on those that result in a clear phenotype when deleted. Systematic deletion and analysis of the entire chitin synthase family has only been performed in a handful of species. Analysis of all 7 *CHS* deletion strains in *M.oryzae* revealed that as in *S.cerevisiae*, different Chs enzymes have developmentally specific roles, although with some apparent overlap between them (Kong et al., 2012). For example, deletion of *CHS7* results in normal vegetative growth, but loss of appressorium development on artificial surfaces, suggesting that this enzyme is specifically required for the synthesis of chitin in the appressorium. Chs1 (class III) is also required for normal appressorium development, but appears to have an important role in conidiation too, as well as in plant penetration. Chs6 (class VII) is required for normal hyphal growth and plant penetration, although *chs6* strains are also reduced in conidiation. The precise roles of other Chs (Chs3, Chs4, Chs5) were less clear however, with some only showing slightly reduced hyphal growth under certain stress conditions. This may indicate a role in cell wall repair. *CHS* deletion strains have also been characterized in other species of fungi, including *N.crassa* and *A.fumigatus* (Fajardo-Somera et al., 2015; Muszkieta et al., 2014). In *N.crassa*, which also has 7 *CHS* genes, Chs6 (class VI) was implicated in hyphal growth and ascospore formation, CHS5 (class V) in growth of aerial hyphae, conidiation and ascospore formation and CHS3 (class I) in perithecia development whereas deletion strains of *CHS7* (class VII) had defects in all of the above processes (Fajardo-

Somera et al., 2015) (note: numbering of *CHS* between fungi is not consistent i.e. Chs1 in *M.oryzae* is not equivalent to Chs1 in *N.crassa*). *A.fumigatus* has 8 *CHS* genes, which have also been studied by systematic deletion (Fajardo-Somera et al., 2015). The findings of this study were broadly similar to those conducted in *M.oryzae* and *N.crassa*, in that deletion of some chitin synthases (in this case either alone or in combination) had little effect, whereas deletion of other chitin synthases had a severe impact on fungal growth and development. For example, deletion of *CSMA*, a class V Chs, resulted in multiple defects including cell wall disorganization and reduced hyphal growth. On the other hand, triple deletion of *CHSA/C/B* had little effect. From these data, it is clear that chitin is a vital component of the cell wall at all stages of fungal development, and it is synthesized by multiple chitin synthases that have both specific and overlapping roles. However, it is also apparent from the aforementioned studies that chitin synthases from the same class do not necessarily have conserved function across different species (Fajardo-Somera et al., 2015).

There are numerous possible reasons behind the requirement for multiple chitin synthases, in contrast with the single copies of β1,3-glucan synthases found in most fungi. Certainly, multiple genes allows for different transcriptional regulation of the chitin synthases and cell-type specific expression, a concept that is supported by experimental data. These different enzymes are likely to produce unique forms of chitin, leading to deposition of chitin with different physical or chemical properties, according to cellular requirements or sub-cellular location. Evidence for this has been found in *C.albicans*. Here, two forms of chitin fibrils were detected. The majority of cell wall chitin was composed of short microcrystalline rodlets, synthesized by Chs3. However, in bud scars and septa, chitin existed in longer, intertwined fibrils which were synthesized by Chs8 (Lenardon et al., 2007). Functional interaction with other cell wall enzymes is another possibility - certain chitin synthases may either interact directly with other enzymes involved in chitin metabolism (e.g. chitinase, chitin deacetylase), or enzymes in the cell wall may only process chitin produced by a certain class of chitin synthase. These possibilities have yet to be widely explored. Lastly, different chitin synthase enzymes may direct synthesis of chitin at a particular subcellular location. The localization of chitin synthases by fluorescent tagging has provided some evidence for this, thereby complementing the gene

deletion studies and revealing further aspects of chitin synthesis and regulation.

Early work was once again performed in *S.cerevisiae*, where GFP-tagging, immunofluorescence and cell-fractionation studies of Chs3 and Chs1 revealed two distinct locations for these enzymes. As expected, Chs3 and Chs1 localized to the plasma membrane. In addition however, both proteins were also found in endocytically derived intracellular compartments that were named as chitosomes (Chuang and Schekman, 1996; Ziman et al., 1996; Zanolari et al., 2011). Further work to characterize the role of these chitosomes in chitin synthesis discovered that they represented an intracellular store of Chs3, whereby enzyme could be transported to and from the plasma membrane as required (Valdivia and Schekman, 2003). Chitin synthases have also been localized in a number of filamentous fungi. In *M.oryzae*, GFP-tagged Chs7 localized to the tips of germ tubes and to developing appressoria (Odenbach et al., 2009), whereas GFP-tagged Chs1 localized to hyphal tips and developing conidia (Kong et al., 2012). As in *S.cerevisiae*, fluorescence was observed in intracellular bodies as well as the cell periphery, although further insights into the significance of this were not pursued. More detailed work has been performed in *N.crassa*, where Chs1, Chs2, Chs4, Chs5 and Chs7 have all been successfully localized (Fajardo-Somera et al., 2015). All of these CHS were localized in growing vegetative hyphae, where fluorescence was observed at the Spitzenkörper, at forming septa and in populations of intracellular bodies which could be equivalent to the chitosomes originally identified in *S.cerevisiae*. Interestingly, only partial colocalization of Chs1-mCherry with Chs2-eGFP or Chs5-eGFP occurred at the Spitzenkörper, and Chs2 also showed a unique septal pore localization. In *Ustilago maydis*, all chitin synthases localize to hyphal septa and Chs5, Chs6, Chs7 and Mcs1 also localize to apical regions (Weber et al., 2006). Further analysis of Mcs1, a class V Chs, provided a valuable insight into the role played by myosin motor domains in chitin synthases. It was found that deletion of this domain did not alter long-distance transport of Mcs1 by microtubules, but was required for apical-localization and exocytosis of the enzyme (Treitschke et al., 2010). Taken together, these localization studies provide some support for the notion of functional specialization within the chitin synthase family. The localization of chitin synthases to intracellular 'chitosomes' also suggests an additional layer of regulation that allows the synthesis of chitin to be dynamically and spatially regulated.

The cycling of CHS between intracellular stores (chitosomes and/or Spitzenkörper) and the plasma membrane appears to be a conserved mechanism in fungi which presumably allows rapid and dynamic control of chitin synthesis according to cellular requirements (e.g. to drive growth, or in response to stress conditions). This phenomenon poses significant questions, especially regarding how transport of Chs to and from the plasma membrane occurs and how this process is regulated. As is often the case, investigations in *S.cerevisiae* have supplied some answers to these questions. Chs3 was found to be maintained in an intracellular pool by cycling between the trans-golgi network (TGN) and early endosomes (Santos and Snyder, 1997; Valdivia et al., 2002). Exit of Chs3 from the TGN/early endosomes and transport to the plasma membrane is dependant upon proteins such as the TGN-localized Chs5 and the exomer component Chs6, which may form a protein-sorting complex to guide the loading of Chs3 into secretory vesicles (Santos and Snyder, 1997; Ziman et al., 1998; Sanchatjate and Schekman, 2006). Interestingly, these proteins are not required for normal transport of Chs1, suggesting that Chs1 and Chs3 are packaged by separate mechanisms that may maintain the compositional heterogeneity of the chitosome population.

Once delivered to the plasma membrane, additional factors are required for the regulation of the activity and localization of the chitin synthases. Chs4 is a prenylated protein that interacts directly with Chs3, and also with the scaffold protein Bni4, thereby indirectly anchoring Chs3 to septins (DeMarini et al., 1997). This interaction is required for the localization of Chs3 at the bud neck, as well as for the activity of Chs3 although the mechanism behind this activation is unknown. Thus, Chs4 is known as a chitin synthase regulator, and these proteins are conserved in all species of fungi. In contrast to the wealth of knowledge acquired in *S.cerevisiae*, very little is known of factors regulating Chs trafficking and localization in filamentous fungal species, although it would appear that secretion does not occur via the traditional ER/golgi secretory pathway (Riquelme and Bartnicki-García, 2008). This therefore represents a valuable research opportunity, and one that could potentially result in the discovery of novel fungicide targets. The chitin synthases themselves are already targets for some fungicides: nikkomycins and polyoxins are nucleoside-peptide analogues of UDP-GlcNAc that act as a competitive inhibitors of fungal and insect chitin synthases (Ruiz-Herrera and San-Blas, 2003). Polyoxin D is

currently marketed by Certis USA L.L.C. as Tavano^{TM} and OSO^{TM} for use on numerous soft fruit and vegetable crops (Certis, 2015). Nikkomycin Z is not used in agricultural contexts, but has been shown to be effective in reducing infection by *Histoplasma capsulatum* and *Coccidioides immitis* in mouse models (Hector et al., 1990), and is currently undergoing clinical trials (Denning and Bromley, 2015). However, one significant drawback of these fungicides is that not all chitin synthases show equal sensitivity, for example in *S.cerevisiae* the order of sensitivity to nikkomycin Z is Chs1>Chs3>Chs2. The lack of sensitivity of Chs2 explains why growth *S.cerevisiae* is not significantly inhibited by treatment with nikkomycin Z, as it is able to compensate for Chs3 inhibition (Gaughran et al., 1994). Many other fungi (e.g. *A.fumigatus*) show similar insensitivity to chitin synthase inhibitors, presumably for the same reason, although cell permeability and intracellular stability of the fungicides must also be considered. Further investigations are therefore required, in order improve the spectrum of fungal species that can be targeted by inhibition of chitin synthesis.

Glucan and chitin remodelling

Once synthesized by their respective enzymes, chitin and glucan are not simply inert and separate components of the cell wall. Their structure and relationship with other cell wall components is altered by a variety of carbohydrate modifying enzymes in order to create a rigid and interconnected polysaccharide matrix. These include enzymes involved in glucan chain branching, glucan elongation and chitin-glucan cross-linking. The hydrolysis of glucan and chitin is discussed later, in Chapter 5.

The elongation of β1,3-glucan chains is performed by GPI-anchored β1,3-glucanosyltransferase enzymes belonging to the Glycosyl Hydrolase 72 family (GH72). These enzymes cleave a β1,3-glucan chain and transfer it to the non-reducing end of another β1,3-glucan molecule, thereby creating a new β1,3 linkage (Mouyna et al., 2000). In *S.cerevisiae*, there are 5 β1,3-glucanosyltransferase enzymes (named Gas1-5), of which Gas1 is the best characterized. Deletion strains of *GAS1* showed slightly altered cell morphology, reduced glucan content, hypersensitivity to Calcofluor White and shed glucan from their cell wall (Ram et al., 1995, 1998). However, the remaining 4 *GAS* genes have not yet been fully characterized, although *GAS2* and *GAS4* appear to function

in ascospore formation, and *GAS5* is coexpressed with *GAS1* during vegetative growth (Ragni et al., 2007a; Primig et al., 2000). It is therefore likely that redundancy exists within the *GAS* family in this species. In *Aspergillus fumigatus*, which has 7 putative β1,3-glucanosyltransferases (named Gels 1-7), the enzymatic function of GH72 proteins is conserved, and both *GEL1* and *GEL2* can complement the *S.cerevisiae gas1* strain (Mouyna et al., 2000, 2005). In contrast to *S.cerevisiae*, deletion of even a single *GEL* resulted in serious growth defects: a *gel2* strain showed reduced mycelial growth, cell wall disorganization, abnormal conidiogenesis and reduced virulence (Mouyna et al., 2005). Surprisingly, a later study demonstrated that deletion of *GEL4* was lethal, suggesting that i) redundancy may not exist between members of the GH72 family in this species and ii) that GH72 family proteins play a vital role in development in filamentous fungi (Gastebois et al., 2010a). Recent unpublished work in *M.oryzae* has shown that redundancy is an issue when studying the 5 Gels present in this species, but that a triple *GEL1/GEL3/GEL4* knockout is non-pathogenic, displays severe, osmoremedial hyphal growth defects and reduced glucan chain length (Samalova *et al*, unpublished results). These studies all suggest that glucan chain elongation is critical for the correct assembly of β1,3-glucan in the cell wall, and is therefore crucial for fungal development. However, it is unclear as to exactly why this is the case. One possibility is that shorter β1,3-glucan chains simply have lower mechanical strength, as they are able to slide past each other more easily under stress. Additionally, chain elongation also reduces the number of terminal residues to which chitin or β1,6-glucan can be attached, which is hypothesized to have profound morphogenic consequences (Cabib and Arroyo, 2013). Despite these intriguing hypotheses, questions still remain regarding the spatial and temporal factors controlling glucan elongation. For example, are glucan chains in certain cell types or subcellular locations of a different length than those in others, and if so, what are the consequences of this on the properties of the cell wall? At what stage in glucan synthesis does elongation by Gels occur - do Gels colocalize with active β1,3-glucan synthase? Clearly, the answers to some of these questions may not be attainable with current techniques, and so technological and methodological advances will likely play a role in driving novel research in this area.

β1,3-glucan, although synthesized as linear chains, does not remain so in the cell wall.

As mentioned previously, the β1,3-glucan chains are branched by the presence of β1,6-linkages. An enzyme with glucan-branching activity was first isolated from *C.albicans* and characterized *in vitro*. The enzyme (named Bgl2), displayed both hydrolytic and glucosyltransferase activities, first cleaving the reducing end of a β1,3-glucan chain, then linking the removed oligosaccharide to the β1,3-glucan chain via a β1,6-linkage (Hartland et al., 1991). Deletion of *BGL2* in this fungus resulted in reduced virulence and increased sensitivity to nikkomycin Z, suggesting an increase in chitin content (Sarthy et al., 1997). Similarly, deletion of *BGL2* in *S.cerevisiae* also resulted in an increase in cell wall chitin content, although growth and cell morphology were unaffected (Kalebina et al., 2003). Investigations of this enzyme family are extremely limited in filamentous fungi. In *A.fumigatus*, two enzymes (Bgt1 and Bgt2) with similar glucosyltransferase activity to Bgl2 were characterized biochemically and deletion strains created (Gastebois et al., 2010b). Surprisingly, no phenotype was detected in either the single or double deletion strains compared to WT, nor any change in glucan branching. This suggests that, as with many enzyme families, redundancy may be preventing the study of the true phenotype. It is also likely that compensatory mechanisms allow the cell to adjust to the loss of an enzyme, by altering the composition of the cell wall e.g. increasing chitin content, as observed in *S.cerevisiae* and *C.albicans*.

Chitin and β-glucan chains can be cross-linked by a family of GPI-anchored GH16 enzymes first characterized in *S.cerevisiae* (Rodríguez-Peña et al., 2000). These enzymes (named Crh1 and Crh2) were shown to act as transglycosylases, catalyzing the transfer of chitin chains (synthesized by CHS3) to both β1,3-glucan and β1,6-glucan (Cabib, 2009). By studying the localization of GFP-tagged Crh1 and Crh2 and the incorporation of fluorescently-labelled laminari-oligosaccharides, this activity was shown to localize to bud sites and bud scars, which is coincident with the main site of chitin synthesis by CHS3 (Cabib et al., 2008). Deletion of *CRH1* and *CRH2* resulted in the loss of glucan-linked chitin and hypersensitivity to the cell wall disruptants Calcofluor White and Congo Red, suggesting defective wall organization and integrity (Cabib, 2009; Rodríguez-Peña et al., 2000). Intriguingly, cell wall remodelling by these enzymes is hypothesized to have a critical role in influencing cellular morphogenesis in fungi. It has been proposed that linkage of chitin to glucan prevents further remodelling of the glucan, as the chitin

occupies the non-reducing ends of the β1,3-glucan that would normally be occupied by β1,6-glucan and its associated mannoproteins. As a result, growth of the cell wall is prevented at these sites, namely the bud neck in *S.cerevisiae* (Cabib and Arroyo, 2013). This model implies that cellular morphogenesis is influenced by the interrelationship between the various components of the cell wall, as well as by their initial synthesis. However, it is also important to consider the direct consequences that such cell wall remodelling may have on the physical properties of the cell wall. It was recently demonstrated in *C.albicans* that simultaneous deletion of three genes encoding GH16 enzymes (*CRH11*, *CRH12* and *UTR2*) resulted in increased wall elasticity and consequently, reduced resistance to hyperosmotic stress (Ene et al., 2015). The GH16 family of transglycosylases has yet to be systematically investigated in other species of filamentous fungi, although recent work in *M.oryzae* has characterized single and double deletion strains of the GH16 family. This revealed roles in cell wall organization and integrity during mycelial and *in planta* growth, although redundancy is likely to be a factor in this species, as there are 5 putative Crh members (Che-Omar *et al*, unpublished results). Thus, further work is required to investigate the how these enzymes might influence the physical properties of the cell wall and morphogenesis in *M.oryzae*.

Taken together, these studies support the notion that the initial synthesis of the core cell wall components is just the beginning of the complex process of cell wall biogenesis. Given the severe phenotypes observed when cell wall remodelling genes are deleted, it is clear that the modification of chitin and glucan in the wall is equally as important as the initial synthesis itself. However, the relationship between cell wall remodelling, the physical properties of the cell wall and cellular morphogenesis is complex and requires further investigation. The relationships between different types of wall remodelling enzymes also needs to be determined. It is known that, in the absence of one particular remodelling enzyme, another can be upregulated to compensate. For example, in the *gas1* mutant of *S.cerevisiae*, a number of genes involved in cell wall biogenesis and remodelling are upregulated, including *CRH1* and *BGL2* (Lagorce et al., 2003). Thus, the cross-linking or branching of glucans may demonstrate at least partial redundancy of function with glucan elongation. Understanding these relationships could be key to deciphering the roles of the different forms of cell remodelling. The key steps of elongation, branching

and cross-linking clearly represent potential targets for fungicides that at present remain unexploited. There are also likely to be many remodelling enzymes that are currently unknown, for example those involved in integrating β1,6-glucan chains or mannan into the cell wall. Some such enzymes may even be class- or genus-specific, since many species of fungi contain novel linkages that do not appear to be broadly conserved. Further investigations in this field will require considerable ingenuity and novel techniques, in order to detect the activities and phenotypes of remodelling enzymes which are not always forthcoming.

Chitin deacetylation

A unique feature of chitin (β1,4-*N*-acetylglucosamine) is that it can be deacetylated by a family of carbohydrate esterase enzymes known as chitin deacetylases (CDA) to form chitosan, a polymer of β1,4-glucosamine (Figure 1.3). There is, however, no strict definition of the degree of deacetylation that needs to be achieved in order for a polymer to be described as chitosan rather than chitin. In fact, it is likely that a complete spectrum of chitin/chitosan polymers exist in nature, potentially demonstrating anywhere between 0 and 100% deacetylation. As well as the overall degree of deacetylation, the pattern of deacetylated residues probably also varies, depending on both the enzymatic mechanism of deacetylation and the nature of the substrate (Zhao et al., 2010). For example, an exo-type CDA from *Mucor rouxii* was shown to fully deacetylate chitin oligomers in a multiple-attack mechanism (Tsigos et al., 1999) whereas a CDA from *Colletotrichum lindemuthianum* only partially deacetylates chitin oligomers (Tokuyasu et al., 1997). Although informative, these studies have a significant limitation in that enzymatic activity is tested on short oligomers of chitin which do not represent the native form of chitin found in fungal cell walls, which is most likely to be crystalline. Interestingly, all CDAs tested so far have demonstrated very low activity on crystalline chitin *in vitro*, presumably due to the inaccessibility of the substrate (Win and Stevens, 2001). This suggests that *in vivo*, either a) chitin is deacetylated soon after synthesis, prior to crystallisation b) additional proteins or enzymes may act in concert with CDAs to increase substrate accessibility, or c) some chitin synthases synthesize chitin that does not crystallize, allowing it to be deacetylated later. Of course, it is possible that all of the

above may be true to some degree, although at present there is little evidence to either support or refute any of these hypotheses.

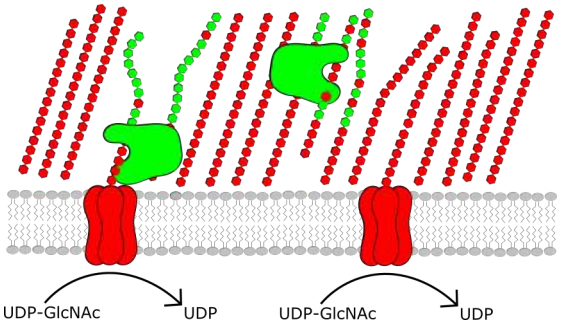

Figure 1.3: Cartoon of chitin deacetylation. Chitin deacetylases (green) remove acetyl groups from the *N*-acetylglucosamine residues of chitin (red), producing a polymer known as chitosan. CDAs may either deacetylate nascent chitin chains, prior to crystallization, or act upon crystalline microfibrillar chitin.

Chitin deacetylases are conserved in all fungi (Ruiz-Herrera and Ortiz-Castellanos, 2010), suggesting that chitosan plays a role in the cell wall of most species, at least during some part of their life-cycle. The purpose of chitin deacetylation likely relates to the relative physical and chemical properties of chitin and chitosan. Chitin, as described previously, is a rigid, crystalline polymer with low chemical reactivity. However, deacetylation creates primary amine groups. With a pKa value of 6.7, this means that some of these amine groups are protonated and charged at physiological pH. Consequently, chitosan is a polycationic, more hydrophilic and non-crystalline polysaccharide, in stark contrast to its parent polymer chitin. This could have profound consequences on the structure and properties of the fungal cell wall. On the one hand, chitosan is theoretically much more flexible than chitin. On the other, the newly exposed amine groups could be free to interact with other cell wall components in an ionic or covalent manner, potentially increasing wall rigidity. At present, there is little data to support either of these hypotheses, as the role of chitin deacetylation has only been investigated in a few species of fungi.

The role of chitin deacetylation was first described in *S.cerevisiae*. Here, there are two functionally redundant CDAs which deacetylate chitin specifically in the cell wall of ascospores (Mishra et al., 1997; Christodoulidou et al., 1996). Deletion of the two genes together resulted in complete loss of chitosan from the ascospore wall. Although formation and viability of the ascospores themselves was unaffected, spores of the double

deletion strain were shown to be more susceptible to treatment with lysing enzymes, ether and heat shock, suggesting possible disorganization and increased permeability of the ascospore wall. This was confirmed through further experimentation, which showed that the outer dityrosine layer was absent in *CDA* deletion strains, although unexpectedly total chitin content was also lower (Christodoulidou et al., 1999). It was hypothesized subsequently that the dityrosine is cross-linked to the amine groups of the chitosan, thereby creating a rigid and impermeable ascospore cell wall, although no direct evidence for this has been presented (Suda et al., 2009). In *Schizosaccharomyces pombe*, a single *CDA* was also expressed specifically during sporulation, as in *S.cerevisiae*. The deletion of *CDA1* resulted in slightly reduced sporulation (Matsuo et al., 2005). Similarly, chitosan was shown to be a component of spore wall in *Ashbya gossypii*. Surprisingly, deletion of the single *CDA* in this species resulted in a complete loss of sporulation, suggesting that chitosan is required for spore development. On the other hand, filamentous growth of the fungus was entirely unaffected (Lickfeld and Schmitz, 2012). In both *S.cerevisiae* and *S.pombe*, the defects arising from *CDA* deletion are similar, if not as severe, as deletion of a chitin synthase (encoding Chs3 in *S.cerevisiae* and Chs1 in *S.pombe*). This suggests that the CDAs specifically deacetylate the chitin make by those particular CHS, perhaps indicating a degree of collaboration between CDAs and CHS. The final species in which detailed characterization of CDAs has been performed is *C.neoformans*, where chitosan is actually 3-5 times more abundant than chitin in the cell wall of vegetatively growing cells (Banks et al., 2005). Deletion of 3 of the 4 *CDA* genes (*CDA1-3*) in this fungus is sufficient to completely abolish chitosan synthesis (Baker et al., 2007). These triple deletion strains are more susceptible to various cell wall perturbants, including Congo Red, SDS, caffeine and NaCl, are less virulent and also leak melanin from their cell walls (Baker et al., 2011). Together, these findings suggest that chitosan has an important role in cell wall integrity in this fungus. In addition, and consistent with findings in *S.cerevisiae* and *S.pombe*, deletion of one particular chitin synthase (Chs3) also results in complete loss of chitosan. This is despite the presence of 8 different chitin synthase enzymes in *C.neoformans*, some of which are expressed at the same stage of development, supporting the hypothesis of CHS-CDA collaboration (Banks et al., 2005). Further to this, it was also found that the GPI-anchor of Cda2, and therefore plasma membrane

localization, is required for chitosan synthesis by this enzyme (Gilbert et al., 2012). The GPI-anchor could conceivably serve to place Cda2 in close proximity to Chs3, so that deacetylation of nascent chitin can take place.

From the studies outlined above, it is clear that chitosan plays an important role in fungal development and cell wall integrity, although exactly how this relates to the unique properties of chitosan remains unclear. In addition, no such studies have yet been conducted in phytopathogenic fungi, and it is likely that there is an extra dimension to the role of chitosan in these species. Chitin is a well-characterized PAMP that is recognized in rice plant cells by the Pattern Recognition Receptor (PRR), CEBiP (Chitin Elicitor Binding Protein) (Shimizu et al., 2010). The release of chitin oligomers from fungal cell walls either as a result of endogenous cell wall remodelling enzymes, or due to the action of plant chitinases results in binding of these oligomers to CEBiP. This induces dimerization of CEBiP and association with CERK1 (Chitin Elicitor Receptor Kinase-1), resulting in phosphorylation and activation of CEBiP (Hayafune et al., 2014). Activation of a pattern recognition receptor such as CEBiP triggers PAMP Triggered Immunity (PTI), resulting in a range of responses including production of reactive oxygen species (ROS) and hydrolytic enzymes (glucanases and chitinases), callose deposition and accumulation of salicylic acid (Liu et al., 2013). All of the above prevent successful colonization of the plant by the invading fungus. However, the fungi themselves appear to have evolved two ways of preventing chitin from triggering PTI. The first is the secretion of chitin-binding effectors, which compete with the chitin receptors for binding of chitin oligomers. These have been shown to be necessary for the full pathogenicity of a number of fungal species, including *Cladosporium fulvum* and *M.oryzae* (de Jonge et al., 2010; Mentlak et al., 2012). The second strategy is the deacetylation of chitin to chitosan, which has two hypothesized benefits. The first is that unlike chitin, chitosan is not a PAMP and cannot cause activation of CEBiP (Hayafune et al., 2014). Although several studies have shown that chitosan can actually induce a defence response in plant cells, this is most likely a non-specific response due to the polycationic nature of chitosan which causes membrane disruption (Lin et al., 2005; Agrawal et al., 2002; Zuppini et al., 2004). In addition, the concentrations of chitosan required to induce such responses in these studies is many times higher than for chitin, bringing into question the

physiological relevance of these observations. The second benefit of chitin deacetylation is that it provides protection from plant chitinases, since chitosan is a poor substrate for these enzymes. Thus, the conversion of chitin to chitosan is hypothesized have two interlinked roles during fungal pathogenesis: i) to prevent fungal cell wall degradation by plant chitinases and ii) to avoid activation of pattern triggered immunity (i.e. to act as a 'stealth mechanism'). Although there is no functional evidence for these roles of chitosan in plant-pathogen interactions, circumstantial evidence does exist. Firstly, localization of chitosan with anti-chitosan antibodies and the chitosan-specific dye eosin Y revealed that multiple species of plant pathogen, including *Puccinia graminis* and *M.oryzae* convert exposed chitin on the surface of appressoria and invasive hyphae, to chitosan (Gueddari et al., 2002; Fujikawa et al., 2009). Secondly, transgenic rice plants expressing chitosanase demonstrated a modest increase in resistance to *M.oryzae* infection (Kouzai et al., 2012). However, chitosan is not the only cell wall component that is thought to act as a stealth mechanism. As discussed previously, α1,3-glucan has also been shown to play a similar role. Crucially, this is supported by ample experimental evidence showing that loss of α1,3-glucan alone is sufficient to prevent successful infection in a number of species, including *M.oryzae*. This raises an important question. Presumably, synthesis of chitosan was unaffected by the loss of α1,3-glucan, although this was not determined. If this is the case, it suggests that chitosan alone is insufficient to provide protection, and it is α1,3-glucan that acts as the primary defence mechanism in these fungi. Alternatively, the primary role of chitosan in pathogenic fungi may not be as a protective/stealth mechanism at all. As discussed above, chitin deacetylation could theoretically have important developmental consequences because of its unique physical and chemical attributes. Investigating chitin deacetylation in phytopathogenic fungi will allow us to resolve these questions, and to determine whether chitosan plays a developmental role, a protective role, or both. A small amount of previous work suggests that the former may be true in *M.oryzae*: deletion of a putative chitin deacetylase called Cbp1 resulted in defective appressorium formation on artificial surfaces, suggesting chitin deacetylation may be required for appressorium development (Kamakura et al., 2002). During infection of root tissues, *M.oryzae* forms a structure known as a hyphopodium, rather than an appressorium (Sesma and Osbourn, 2004). Intriguingly, deletion of Cbp1

also prevented hyphopodium and pre-invasive hypha formation on artificial surfaces (but not root surfaces), indicating that chitosan could play a role in multiple infection-related cellular differentiation events (Tucker et al., 2010). However, chitosan synthesis was not reduced in the *cbp1* mutant and neither was the chitin deacetylase activity of Cbp1 proven, so the results remain inconclusive. Nevertheless, this work provides a platform from which further work on characterizing the role of chitin deacetylation in *M.oryzae* can be undertaken. Importantly, if chitin deacetylases do prove to be critical for development or pathogenicity, they would represent a novel and valuable fungicide target.

Cell wall-associated proteins

Although the fungal cell wall is largely composed of polysaccharides, proteins also make up a significant minority by mass, estimated to be ∼10% although this varies considerably depending on growth conditions, the species in question and methodology (Nguyen et al., 1998; Bowman and Free, 2006). Cell wall proteins can be divided into 3 broad categories: Those with defined enzymatic activities (as described above, and many others besides), those with putative structural roles, and those that have roles in cell-environment interactions. Whatever their role, most proteins residing within the cell wall are *N*- and/or *O*-glycosylated, although the precise nature of the linked oligosaccharides varies between species. In *S.cerevisiae* and *C.albicans* these chains are rich in mannose residues, whereas in *N.crassa* and *A.fumigatus* they are composed of galactomannan (a mixture of both galactose and mannose residues). In either case, synthesis of these oligosaccharide moieties occurs in the secretory pathway, prior to presentation of the protein at the cell wall. In *S.cerevisiae*, a series of ER and golgi-localized mannosyltransferases catalyse the synthesis of α1,6-linked mannose chains, which are decorated with branches of α1,2-mannose and α1,3-mannose. In *N.crassa* and *Aspergillus spp.*, a similar set of mannose chains exists, except these are terminated oligosaccharides of β1,5-linked galactose residues (Bardalaye and Nordin, 1977; Nakajima et al., 1982). Many of these cell wall glycoproteins are covalently linked to cell wall β1,3-glucan by their polysaccharide side-chains (Kollár et al., 1997). In other cases, it is the GPI-anchor of a cell wall protein that is covalently linked to β1,6-glucan, a reaction which occurs via an unknown transglycosylation mechanism (Kapteyn et al., 1996; Kollár et al., 1997). These covalent

linkages provide stable and long-term attachment of proteins to the cell wall, which may particularly important for those where presentation at the cell surface is critical for their function (e.g. adhesins).

Investigations employing different extraction techniques have resulted in the identification of numerous cell wall-associated proteins which do not have identifiable enzymatic activities or protein domains (De Groot et al., 2005). These proteins could perhaps be considered as 'structural' proteins, although many are hesitant to use such a term, as these proteins may simply catalyse reactions that have yet to be characterized. One such family of putative structural proteins has been characterized in *S.cerevisiae*. The Pir (= Protein with Internal Repeats) family comprises 4 structurally related proteins, which are serine/threonine-rich, have a characteristic N-terminal repeat sequence and are thought to be highly *O*-glycosylated (Mrša and Tanner, 1999). These proteins were also found to be covalently-linked to the cell wall through a novel glutamate-glucose linkage, postulated to occur via a novel transglutaminase-type reaction (Ecker et al., 2006). *PIR* deletion strains exhibited slight growth and morphological defects and increased sensitivity to Congo Red and Calcofluor White, suggesting some role in cell wall integrity, although the precise physiological role of these proteins remains unknown (Mrša and Tanner, 1999). Numerous other proteins with putative structural roles have also been identified in *S.cerevisiae*, including Ccw12, a small mannoprotein which when deleted, also result in significant growth and cell wall defects (Ragni et al., 2007b). Many of these structural proteins identified in *S.cerevisiae* and closely related species do not have homologues in filamentous fungi, however. In fact, few cell wall proteins of this type have been characterized in filamentous species. One exception is the putative GPI-anchored protein EMP1 in *M.oryzae*, which has homologues in other species including *Fusarium oxysporum* (FEM1) (Ahn et al., 2004; Cornelissen and Haring, 2001). *EMP1* is highly expressed during appressorium development, and deletion of this gene resulted in reduced appressorium formation and pathogenicity, although the reason for this phenotype was not deduced. In *A.fumigatus*, a repeat-rich GPI-anchored cell wall protein, CspA, was identified and characterized. Deletion of CspA resulted in a disorganized and weakened cell wall, and reduced adhesion to extracellular matrix, suggesting a role in maintaining cell wall integrity (Levdansky et al., 2010). In conclusion, the role of so-called structural

proteins in the fungal cell wall remains elusive. The cross-linking of these proteins to cell wall polysaccharides may act to stabilize the glucan matrix of the wall. Alternatively, the presence of such proteins may be required for the organization of the cell wall, by directing the assembly of nascent polysaccharide chains into the correct configuration. These hypotheses are not mutually exclusive, but the study of these proteins is complicated by the fact that their deletion only results in a definable phenotype in a minority of cases, which may suggest a degree of functional redundancy between these proteins. However, it is also the likely that previous studies simply have not performed the correct experiments or applied sufficiently sensitive techniques to determine the true function of these proteins.

Proteins involved in cell-environment interactions perfectly illustrate the capacity of the cell wall to act as an interface between the fungal cell and its immediate environment. One class of protein that is well known to have roles in these interactions is the hydrophobins. Hydrophobins are a type of small, cysteine-rich amphipathic protein which self-assemble into monolayers at hydrophilic-hydrophobic interfaces. They can be divided into two classes: class I hydrophobins, which form distinctive, insoluble rodlet assemblies, and class II hydrophobins, which do not form rodlets, and have distinct hydrophobicity profiles (Sunde et al., 2008). By assembling on the surface of the cell wall, hydrophobins of both classes are able to confer hydrophobicity to the cells in question. This hydrophobicity can be crucial for numerous processes over the life-cycle of a fungus. For example, hydrophobin rodlet layers are commonly found on the surface of conidia, where they inhibit wetting and facilitate dispersal in the air (Stringer et al., 1991; Bell-Pedersen et al., 1992). Hydrophobins are also required for the formation of aerial hyphae in many species of fungi (van Wetter et al., 1996). In this case however, the hydrophobins are not attached to the wall of the fungal cell, but accumulate at the water-air interface, thereby reducing surface tension and allowing the hyphae to escape the liquid phase (Wösten et al., 1999). As well as modulating interactions with water, hydrophobins can also mediate interactions with hydrophobic surfaces. The best example of this is in *M.oryzae*, where the class I hydrophobin Mpg1 is required for hydrophobic surface sensing, as discussed previously in Section 1.1.2 (Talbot et al., 1996). In *Schizophyllum commune*, the hydrophobin Sc3 was also shown to mediate attachment of hyphae to Teflon, by accumulating between the cell

wall and the hydrophobic surface (Wösten et al., 1994). Apart from physical interactions, it is also apparent in some cases that hydrophobins are required for successful interaction between a pathogenic fungus and its host. In *A.fumigatus*, the hydrophobin RodA forms rodlet layers on the surface of conidia. Removal of this layer resulted in activation of a Dectin1-mediated host response and prevention of infection, suggesting that in this case, the hydrophobins were acting to mask immunostimulatory cell wall components, much like α1,3-glucan, as discussed previously (Aimanianda et al., 2009; de Jesus Carrion et al., 2013).

The second major class of proteins with well-characterized roles in cell-environment interactions is the adhesins. These are a class of highly-glycosylated, cell wall associated proteins which promote cellular adhesion, either to other cells, or to abiotic surfaces. Attached to the cell wall by a C-terminal GPI-anchor, the N-terminus of adhesins is able to protrude into the immediate vicinity of the fungal cell, and mediate interactions often via a sugar or amino acid binding domain (Verstrepen and Klis, 2006). These interactions serve several purposes during fungal growth. In *S.cerevisiae*, a family of the mannose-binding adhesins including Flo1 mediate cell-cell interactions, thereby causing flocculation (i.e. aggregation) of yeast cells (Kobayashi et al., 1998). Such interactions are also important for mating in this fungus, although in this case, cellular adhesion is mediated by Aga1 and Aga2, which together form **a**-agglutinin and are required to bind the protein Sag1 on the surface of cells of the opposite mating type (Lipke et al., 1989). In pathogenic fungi, adhesins are also important for interactions with host cells. In *C.albicans*, the critical first step in pathogenesis is the adhesion of the fungal cells to the host surface. This adhesion has been found to be mediated by adhesins of the Als family, which bind to a range of extracellular matrix components, including collagen, fibronectin and laminin (de Groot et al., 2013). Lastly, adhesins are also able to cause cellular adhesion to abiotic surfaces such as glass or plastic. This is of particular medical relevance, since it is a significant factor in fungal infections associated with implanted medical devices (e.g. catheters). In *C.albicans*, the cause of many such infections, surface hydrophobicity associated with upregulation of the Als family of adhesins is responsible (Beaussart et al., 2012). Little is known of the presence or function of adhesins in fungi outside of the Saccharomycotina subphylum, in contrast to the wealth of knowledge briefly

outlined above. In the insect pathogen *Metarhizium anisopliae*, the adhesins Mad1 and Mad2 were required for conidial adhesion to insect cuticle and plant surfaces respectively. Unexpectedly, deletion of *MAD1* also caused multiple morphogenic defects, which may suggest that conidial adhesion itself could be a signal for normal development (Wang and St Leger, 2007). As of yet, no adhesins have been characterized in phytopathogenic species, although it is quite possible that the spore-tip mucilage necessary for conidial adhesion in *M.oryzae* may contain adhesin-like proteins.

Wall-associated proteins clearly have diverse and crucial roles in fungal lifestyles, which in turn serves to illustrate the multifaceted role of the cell wall. These proteins can have roles in cellular integrity, morphogenesis and interactions. The composition of the cell wall is central to the correct functioning of these proteins. This is particularly apparent for the adhesins, which are covalently linked to glucan moieties via their GPI-anchor, and the association of hydrophobins with the cell wall may also be influenced by wall composition. Further work is required in order to determine the possible roles of wall-associated proteins in phytopathogenic fungi such as *M.oryzae*. Of particular interest are proteins which may occur on the surface of invasive hyphae and determine interactions with the plant cell, or those on germ tubes and conidia that interact with the plant surface.

Melanin synthesis

Melanins are a family of molecule that form a complex, darkly pigmented polymer of unknown molecular structure. In fungi, two main forms of melanin exist, classified depending on the constituent molecule: DHN-melanin is synthesized from monomers of 1,8 Dihydroxynapthalene (DHN), whereas DOPA-melanin is synthesized from 3,4-dihydroxyphenylalanine (DOPA).

DHN-melanin is a common form of melanin found in many species of fungi, including *M.oryzae*. The precursor molecule for the synthesis of DHN-melanin is either acetyl-CoA or malonyl-CoA, which are joined together by a polyketide synthase (PKS) enzyme into 1,3,6,8-tetrahydroxynapthalene (1,3,6,8-THN). This is then reduced and dehydrated in a number of steps, forming 1,8-dihydroxynapthalene (DHN), which is polymerized to form melanin. DOPA-melanin is only found in a limited number of fungi, including the

mammalian pathogen *Cryptococcus neoformans*. In this case, the precursor molecule is either L-DOPA or tyrosine, which are converted in a number of steps into dihydroxyindoles, which polymerize to form the melanin (Eisenman and Casadevall, 2012). All of the above synthesis steps occur intracellularly, although the precise location is unclear. It has been hypothesized that melanin biosynthesis and subsequent trafficking to the cell wall occurs in vesicles named melanosomes, although no conclusive evidence has yet been presented. Once deposited in the cell wall, the melanin is observed in different configurations depending on the species in question. In *C.neoformans*, which forms DOPA-melanin, discrete granules 40-130 nm in diameter are found in concentric layers in the cell wall (Eisenman et al., 2005). A recent study also revealed that this melanin was covalently linked to the polysaccharides of the cell wall (Chatterjee et al., 2015). In contrast, in the appressoria of *M.oryzae*, the melanin is observed as a discrete layer in the inner part of the cell wall (Wang et al., 2007).

Melanins have numerous roles in the life cycle of many fungi. As a structural component of the cell wall, it is important in imparting strength and rigidity. It is also highly impermeable, capable of acting as a diffusion barrier. These properties mean that melanin is a crucial component of the appressorium cell wall in *M.oryzae* (as discussed in Section 1.1.2), as well as in other species of appressorium-forming fungi (Chen et al., 2004; Gachomo et al., 2010). Melanins are also known to be virulence factors in a number of mammalian pathogens. For example in *C.neoformans* and *Penicillium marneffei*, strains unable to melanize were less virulent in mice (Salas et al., 1996; Woo et al., 2010), and in a *Cryptococcus gattii* outbreak, higher expression of genes involved in melanization was associated with greater virulence (Ngamskulrungroj et al., 2011). The likely reason for the association between melanin and virulence in these fungi is that, as an impermeable layer in the cell wall, melanin can provide protection against a broad range of chemical factors, including lytic enzymes, oxidising agents and detergents. There is also evidence that melanin can provide protection against fungicides: melanized strains of *C.neoformans* and *H.capsulatum* were less susceptible to amphotericin B and caspofungin, due to binding of the drugs to the melanin (van Duin et al., 2002). Similarly, unmelanized strains of the pathogen *Wangiella dermatitidis* were also shown to be less resistant to vorinconazole and amphotericin B (Paolo et al., 2006). Melanin also appears

to have roles beyond just being a simple physical barrier. In an intriguing study, melanin in the cell wall of the phagocytosed conidia of *Aspergillus fumigatus* was shown to be necessary to prevent apoptosis of the macrophage, suggesting that the melanin functions to manipulate host-cell signalling (Volling et al., 2011). Taken together, it is clear that melanin is a key virulence factor that can contribute to fungal survival and pathogenicity in a number of ways.

A number of fungicides already target melanin biosynthesis, including the inhibitors of DHN-melanin biosynthesis tricyclazole and carpromatid, as discussed in Section 1.1.2. However, there are no fungicides targeting DOPA-melanin biosynthesis. Although melanin is not an absolute requirement for virulence in those fungi which produce DOPA-melanin (e.g. *C.neoformans*, *H.capsulatum*), it is known to hinder treatment with fungicides, as mentioned above. Therefore, inhibition of melanin biosynthesis in these fungi could be considered as a way to improve efficacy of current anti-fungal treatments.

1.3 Summary

- *Magnaporthe oryzae* is a destructive pathogen and a model organism for the study of phytopathogenic fungi.
- The fungal cell wall has roles in maintaining cellular integrity, controlling cellular morphogenesis and influences the interactions of fungi with their environment and other organisms.
- The cell wall is a valuable target for fungicides, although exploitation of this target is hindered by a lack of understanding of the processes involved in cell wall synthesis and remodelling.
- The interactions of a pathogenic fungus with its host usually involves infection-specific changes in cell wall structure and composition in order to remain undetected or to protect itself from host defence responses.
- One such observed change is the deacetylation of chitin to form chitosan. Chitin deacetylation could both protect the cell wall from digestion by plant chitinases, and reduce the exposure of PAMPs.
- Chitosan also differs significantly in its chemical and physical properties compared with chitin, so chitin deacetylation could also be required for morphogenesis.
- *Magnaporthe oryzae* is an ideal organism in which to test the hypotheses regarding the roles of chitin deacetylation - it is genetically tractable, and a small amount of previous work suggests an intriguing role for chitin deacetylation during appressorium development.

1.4 Aims and Objectives

The overall aim of this study is to test the key hypotheses regarding chitin deacetylation in fungi, namely its putative roles as either a 'stealth mechanism' or as a critical determinant of cell wall flexibility during cellular morphogenesis. This will be achieved by:

- Characterizing the role of chitin deacetylation during appressorium development. Deletion strains for chitin deacetylases operating during this process will be created and analysed for their ability to develop appressoria.
- Characterizing the role of chitin deacetylation during vegetative growth. Deletion strains for chitin deacetylases operating during this process will be created and vegetative growth and development evaluated.

An additional aim of the study is to investigate whether the hydrolysis of chitosan is also required for cell wall remodelling during morphogenesis. This will be achieved by creating a deletion strain for the sole gene encoding a putative chitosanase in *M.oryzae*.

Chapter 2

Materials and Methods

In the following chapter, the complete Materials and Methods employed in this thesis are detailed. Unless otherwise stated, all reagents were acquired from Sigma-Aldrich (St Louis, Missouri).

2.0.1 Media and Solutions

Appendix A details the recipes of the media used for the culture of all organisms used in this thesis. Appendix B details the solutions used for protocols in this thesis.

2.0.2 Culturing *Magnaporthe oryzae*

Routine culturing of *Magnaporthe oryzae* was carried out on solid or in liquid medium, depending upon experimental requirements. In all cases, procedures involving the manipulation of fungal material were carried out in a Gelaire BSB4 Class II biological safety cabinet, in accordance with Animal and Plant Health Agency (APHA) licensing.
A table of the media used is shown in Appendix A. All strains used in this study are listed in Appendix F and in Figure 2.1.

Growth on solid media

For routine growth, 100 mm circular Petri dishes (ThermoFisher Scientific) filled with 25-30 ml complete medium (CM), were inoculated with filter papers containing dessicated conidia and mycelium of *Magnaporthe oryzae* (See 'long-term storage of *M.oryzae*'). The plates were then sealed with Micropore tape (3M) and incubated in a Panasonic MLR-350 or a Panasonic MLR-352H-PE incubator at 24°C for 10-14 days (with a light/dark cycle of 14 hr light/10 hr dark, to induce conidiation).
For evaluating growth of a deletion strain on solid media, a protocol was employed that yielded reliable and reproducible results. Circular petri dishes (100mm diameter) were filled with exactly 30 ml of medium. A 5 mm plug of mycelium from the growing edge of a 10-11 day old plate of *M.oryzae* growing on CM was inoculated onto the centre of the

Figure 2.1 *(following page)*: Table of *M.oryzae* strains used in this study. All strains, with the exception of Guy11 and Ku70 (Villalba et al., 2008), were constructed during this study. The table details the genotypes of the strains, the background strain used for their construction, and antibiotic resistance markers present. The transformant line N_o column details which of the successful transformants were used for experimentation.

Genotype	Background strain	Resistance markers	Description	Transformant line N° used
Guy11	None	None	WT strain of *Magnaporthe oryzae*	
Ku70	Guy11	Sulphonylurea	Deletion strain for *ku70*	
Δ*cda2*	Guy11	Hygromycin	Deletion strain for *MGG_09159*	8
Δ*cbp1*	Guy11	Hygromycin	Deletion strain for *MGG_12939*	11, 14
Δ*cda3*	Guy11	Hygromycin	Deletion strain for *MGG_04172*	34
Δ*cda1*	Guy11	Hygromycin	Deletion strain for *MGG_14966*	38
Δ*cda4*	Guy11	Bialaphos	Deletion strain for *MGG_08774*	3
Δ*cda5*	Guy11	Hygromycin	Deletion strain for *MGG_01868*	8b
Δ*csn*	Ku70	Bialaphos/sulphonylurea	Deletion strain for *MGG_07656 (Chitosanase)*	
Δ*csn*	Guy11	Bialaphos	Deletion strain for *MGG_07656 (Chitosanase)*	9, 46
ΔΔ*cda2/cbp1*	Δ*cda2* (line 8)	Bialaphos/Hygromycin	Double deletion strain for *MGG_09159* & *MGG_12939*	52
ΔΔ*cda2/cda3*	Δ*cda2* (line 8)	Bialaphos/Hygromycin	Double deletion strain for *MGG_09159* & *MGG_04172*	10
ΔΔ*cbp1/cda3*	Δ*cbp1* (line 11)	Bialaphos/Hygromycin	Double deletion strain for *MGG_12939* & *MGG_04172*	8, 9
ΔΔ*cda4/cda5*	Δ*cda4* (line 3)	Bialaphos/Hygromycin	Double deletion strain for *MGG_08774* & *MGG_01868*	13, 23
ΔΔΔ*cda2/cbp1/cda3*	ΔΔ*cda2/cbp1* (line 52)	Bialaphos/Hygromycin/ Sulphonylurea	Triple deletion strain for *MGG_09159* , *MGG_12939 & MGG_04172*	5, 12
ΔΔΔ*cda2/cbp1/cda4*	ΔΔ*cda2/cbp1* (line 52)	Bialaphos/Hygromycin/ Sulphonylurea	Triple deletion strain for *MGG_09159* , *MGG_12939 & MGG_08774*	30
CDA2:mCherry	Δ*cda2* (line 8)	Bialaphos/Hygromycin	Deletion strain expressing C-terminal mCherry tagged MGG_09159 (expressed by native promoter)	3, 11, 14, 16
CBP1:mCherry	Δ*cbp1* (line 11)	Bialaphos/Hygromycin	Deletion strain expressing C-terminal mCherry tagged MGG_12939 (expressed by native promoter)	21, 23, 31
CDA1:mCherry	Δ*cda1* (line 38)	Bialaphos/Hygromycin	Deletion strain expressing C-terminal mCherry tagged MGG_14966 (expressed by native promoter)	17
CDA4:mCherry	Guy11	Hygromycin	C-terminal fusion of mCherry to MGG_08774 (expressed by native promoter)	2, 8, 12
CDA4:mCherry	Δ*cda4* (line 3)	Bialaphos/Hygromycin	Deletion strain expressing C-terminal mCherry tagged MGG_08774 (expressed by native promoter)	1, 29, 22
CDA1:mCherry/ CHS1eGFP	MGG_08774: mCherry (line 2)	Bialaphos/Hygromycin	Co-expression of *MGG_08774* mCherry fusion and *MGG_01802 (chitin synthase I)* eGFP fusion	2, 18, 19, 20
MGG_06064:2xYFP	Guy11	Hygromycin	C-terminal fusion of 2 copies of YFPvenus to MGG_06064 (chitin synthase VII), expressed by native promoter	10, 18, 23
MGG_06064:2xYFP/ CDA2mCherry	MGG_06064:2xYFP (line 23)	Bialaphos/Hygromycin	Co-expression of *MGG_06064* YFP fusion and *MGG_09159* mCherry fusion	17, 21, 24
MGG_06064:2xYFP/ CBP1mCherry	MGG_06064:2xYFP (line 23)	Bialaphos/Hygromycin	Co-expression of *MGG_06064* YFP fusion and *MGG_12939* mCherry fusion	17, 18, 21
pRP27:CBP1mCherry	Guy11	Hygromycin	C-terminal fusion of mCherry to *MGG_12939* , expressed by *RP27* promoter (overexpression)	5, 6, 9, 11
pEF1:CDA1mCherry	Guy11	Hygromycin	C-terminal fusion of mCherry to *MGG_14966* , expressed by EF1 promoter (overexpression)	7, 8, 33
CSN:eGFP	Δ*csn* (lines 9 & 46)	Bialaphos/Hygromycin	C-terminal fusion of eGFP to *MGG_07656*	2
pRP27:CSN	Guy11	Bialaphos	Expression of *MGG_07656* (chitosanase) by *RP27* promoter (overexpression)	22, 27
pRP27:CSN $^{1\text{-}275}$	Guy11	Bialaphos	Expression of truncated form (residues 1-275) of *MGG_07656* (chitosanase) by *RP27* promoter (overexpression)	9, 19
pCSN 3xYFP	Guy11	Hygromycin	Expression of 3 copies of YFPvenus by the native chitosanase promoter	2, 9, 24
EV	Guy11	Bialaphos	Strain containing empty expression vector	2, 3

plate. Plates were then sealed with Micropore tape and incubated for 10 days at 24°C. In some cases (plates with CFW or CR), incubation in the dark was required, in which case the plates were wrapped in aluminium foil. Colony diameters were measured twice for each plate (at perpendicular angles). Appendix C details the treatments used in plate growth assays.

Growth in liquid media

Growth in liquid medium was necessary to provide fungal material for a number of downstream experiments (for example, transformation or cell wall analysis). First, conidia were harvested from 10-14 day old plates by pipetting of 5ml sterile MilliQ water onto the fungal colony, followed by gentle scraping of the colony with a sterile scalpel, and filtering of the resulting suspension through two layers of sterile Miracloth (Merck Millipore), to isolate the conidia. The conidia were centrifuged at 2850g in a Beckman-Coulter Allegra X-15R for 5 min, the supernatant discarded, and the conidia resuspended in 1 ml sterile dH_2O. The concentration of conidia was determined by counting on a haemocytometer, and adjusted as required. Typically, conical flasks containing 300 ml of liquid CM (or less, depending on experimental requirements) were then inoculated with the conidial suspension. Penicillin and streptomycin (50 µg/ml each, final concentration) were added to prevent bacterial growth, and the flasks sealed with a foil cap. Incubation was performed in a New Brunswick Scientific innova 4230 Refrigerated Incubator Shaker at 24°C with shaking at 150 rpm in the dark. Incubation period depended on experimental requirements.

For evaluating growth of deletion strains in liquid media, 100 ml conical flasks (VWR) containing 50 ml of medium were inoculated with precisely 5 x 10^4 conidia (from a stock suspension of 5 x 10^5 conidia/ml, harvested as above). Penicillin and streptomycin were added, and the flasks were sealed and incubated as discussed above. After the incubation period, flasks were removed and their contents filtered under vacuum through pre-weighed Whatman GF/A 47 mm glass microfibre filters. The filters containing the fungal material were then dried overnight at 80°C, and re-weighed to determine the biomass. For growth assays employing stress treatments, for example as shown in Figure 4.7, treatments were added at 48 hpi and biomass harvested at 120-144 hpi. Appendix C details the treatments

used in liquid growth assays.

Long-term storage of *M.oryzae*

In order to make a stock for long-term storage, a 100 mm petri dish containing 25-30 ml CM was first inoculated with the strain of interest. Small (approx. 5 mm x 5 mm) squares of sterile Whatman filter paper were then placed on the plate, such that the original inoculum was surrounded by ∼50 squares of paper. The plate was sealed, and incubated as discussed previously. Once sufficient growth had occurred to cover the filter papers, they were removed with sterile forceps, and placed into 50 mm petri dishes, which were then sealed with Micropore tape. These were dessicated thoroughly by placing them in an airtight container with silica gel, for 1-2 weeks. Once dry, the filter papers could either be stored in a cool, dry place (for medium-term storage) or at -20°C (for long-term storage).

2.0.3 DNA extraction

Two different DNA extraction protocols were performed, depending on the downstream applications. A more laborious method resulted in high quality gDNA, but this was impractical for processing of large numbers of samples, for example during screening of transformants. In this case, a second protocol was used that resulted in very low quality DNA that was nevertheless sufficient for subsequent diagnostic protocols.

For high-quality gDNA

For the isolation of high quality gDNA, fungal tissue (100-200 mg) was first collected by scraping of 10-14 day old *M.oryzae* colonies with a sterile scalpel. Tissue could be frozen in liquid nitrogen and stored at -80°C if required. Frozen tissue was thoroughly ground in liquid nitrogen using a pestle and mortar, and DNA was isolated using a Qiagen DNeasy Plant Mini kit, according to manufacturers instructions. Quality and quantity of the resulting DNA was analysed by gel electrophoresis and by spectrophotometry.

For screening of transformants

For the screening of large numbers of transformants, the following protocol was employed that allowed rapid isolation of low quality gDNA from large numbers of samples.
A small amount (∼100 mg wet weight) of fungal tissue was first collected by scraping of a portion of a fungal colony growing on a selection plate (as detailed in 2.0.7). In a 1.5 ml Eppendorf tube, the tissue was ground in the presence of 400 µl DNA extraction buffer, using a sterile plastic micropestle, and then left at room temperature for 30-60 min for extraction to occur. The tubes were then centrifuged in a microcentrifuge at 16,000 g for 5 min, and the supernatant (300 µl) transferred to a new tube. To the supernatant, 300 µl of isopropanol was added, mixed, and incubated at room temperature for 2 min. Samples were centrifuged again at 16,000 g for 5 min, and the resulting pellet dried at room temperate for 30-60 min. The dried pellet was then resuspended in 50 µl TE buffer (pH 7.5).

2.0.4 RNA extraction and gDNA removal

In order to isolate high-quality, undegraded RNA it is crucial to maintain an RNAse free environment in which to perform RNA extraction. In order to provide such an environment, bench areas and equipment were cleaned using RNaseZap (ThermoFisher Scientific) before use. Pipette tips and tubes used were either certified RNase free, or were treated with DEPC before use.
Fungal tissues to be used for RNA extraction were frozen in liquid nitrogen immediately after harvesting and stored at -80°C if necessary. Material was first ground thoroughly in liquid nitrogen using a pestle and mortar, then RNA extraction was performed using the Qiagen RNeasy Plant Mini Kit, according to manufacturers instructions. Before the isolated RNA could used for downstream procedures, contaminating gDNA was removed. This was achieved by using an Ambion Turbo DNA-free^{TM} Kit, according to manufacturers instructions. Quality and quantity of the isolated RNA was analyzed by gel electrophoresis and spectrophotometry. If necessary, concentration could be increased by performing RNA precipitation, as follows: To a starting volume of 200 µl of RNA, 20 µl of 3M sodium acetate (pH 5.3), 1 µl of GlycoBlue and 220 µl isopropanol were added. This mixture was kept at -20°C overnight, then centrifuged in a microcentrifuge

at 16,000 g at 4°C for 60 min. The supernatant was removed, and the pellet washed with 1 ml ice-cold 70% ethanol. Samples were spun at 16,000 g at 4°C for 20 min and the supernatant removed. The pellet was then allowed to dry at room temperate, and was resuspended in 10-20 µl of nuclease-free water.

2.0.5 cDNA synthesis

Reverse transcription of RNA into cDNA was performed by using the Maxima First Strand cDNA synthesis kit (ThermoFisher Scientific), according to manufacturers instructions. Reactions both without the reverse transcriptase (-RT control) and without template RNA (No Transcript Control (NTC)) were included, in order to control for the presence of contaminating gDNA in subsequent PCR reactions (see 2.0.6). Synthesized cDNA was aliquoted into separate tubes (to reduce freeze-thaw cycles) and stored at -80°C.

2.0.6 PCR

PCR was employed for the amplification of target DNA sequences. Three different protocols were used, depending on whether the DNA amplification was for diagnostic purposes, for the construction of cloning fragments and gene deletion cassettes or for the quantification of transcript levels.

Amplification of cloning fragments and construction of gene deletion cassettes

The amplification of DNA sequences without the introduction of errors is crucial for successful cloning and construction of gene deletion cassettes. With this in mind, a protocol was followed that employed a high-fidelity DNA polymerase (Herculase II fusion DNA polymerase (Agilent)).

For the amplification of cloning fragments, high quality genomic DNA was used as a template (detailed in 2.0.3). A 50 µl reaction comprised the following reagents, added in this order: 36 µl dH_2O, 10 µl Herculase reaction buffer, 1 µl dNTPs (25 mM each), 1 µl DNA template (typically 100-300 ng gDNA), 1.25 µl of each primer (from 10 µM stock) and 1 µl of Herculase II DNA Polymerase.

The reaction mixture was placed in a BioRad PTC-100 thermocycler, and the following

programme run:

Step 1: 95°C for 4 min

Step 2: 95°C for 20 sec

Step 3: 57-63°C for 30 sec (depending on primer annealing temperature)

Step 4: 72°C for 1-3 min (depending on target length)

Step 5: 72°C for 10 min

Steps 2-4 were repeated 34 times.

Upon completion of the programme, amplified DNA was used in downstream cloning reactions (discussed in 2.0.9), or for the creation of deletion cassettes, as discussed below. In all cases, it was necessary to perform a PCR cleanup reaction to remove unincorporated dNTPs, primers, enzyme etc. This was achieved by using a Qiagen PCR purification kit according to manufacturers instructions. In the event that a mixture of PCR products was obtained, gel extraction was used to purify the intended product. This was achieved using a Qiagen QiaQuick Gel extraction kit, according to manufacturers instructions.

For the creation of gene deletion cassettes, fusion PCR was used to create a linear DNA fragment of 4-5 kb in length, by joining together three smaller DNA fragments (an antibiotic resistance gene, and two 1-1.5 kb fragments homologous to sequences flanking the gene of interest). Three different antibiotic resistance genes were used in deletion cassettes, encoding resistance to Hygromycin B (*HPH*), Bialaphos (*BAR*) or Sulphonylurea (resistant allele of *ALS*). However, the large size of *ALS* prohibited successful fusion PCR, and so Yeast gap-repair cloning was used in this case (see section 2.0.9). The first step in fusion PCR involved amplification of the three constituent parts by high fidelity PCR, as described above, with one important difference: primers were designed such that a 20-30 bp complementary overhang existed between the DNA fragments that were to be joined together (primers used are listed in Appendix E). Two products from the first round of PCR (usually a flanking fragment and the resistance gene) were then joined in a second polymerase reaction. Finally, a third round of PCR joined the third DNA fragment to the product from the second round PCR. As obtaining a pure product in these reactions was a rare occurrence, it was often necessary to perform a gel extraction, as explained

above. Once successfully purified, the deletion cassette was used in transformation, as explained in 2.0.7.

PCR for screening of transformants

Diagnostic PCR for the screening of transformant lines usually involved several tens or even hundreds of simultaneous reactions, and so use of high fidelity PCR here would have been both unnecessary and expensive. Therefore, the high fidelity DNA polymerase was substituted for recombinant Taq Polymerase (ThermoFisher Scientific), in the following 50 µl reaction mixture: 36 µl dH_2O, 5 µl reaction buffer (as supplied), 5 µl $MgCl_2$, 0.5 µl dNTPs (10 mM each), 1 µl DNA template, 1 µl of each primer (from 10 µM stock) and 0.5 µl Taq DNA Polymerase. Typically, three different reactions were run for each transformant: One to test for the presence of the gene of interest (negative in successful deletions) and two reactions testing for integration of the resistance gene at the correct locus. Reactions were run as described in the previous subsection, and 20 µl loaded onto a 1% Agarose gel (with 0.1 µg/ml Ethidium Bromide) for visualization.

RT-PCR

Semi-quantitative RT-PCR as employed in this thesis required a cDNA template synthesized from RNA isolated from a sample of interest (e.g. germlings). RNA extraction and cDNA synthesis are outlined in 2.0.4 and 2.0.5. A 25 µl reaction comprised the following: 17.25 µl dH_2O, 2.5 µl reaction buffer (as supplied), 2.5 µl $MgCl_2$, 0.25 µl dNTPs (10 mM each), 0.5 µl of each primer (from 10 µM stock), 0.5 µl Taq DNA Polymerase (ThermoFisher Scientific) and 1 µl cDNA template. Reactions were run on a BioRad PTC-100 thermocycler essentially as described above, except that the extension time was shortened to 1 min (due to small product lengths), and the cycle number was varied between 20-35 depending on transcript abundance. In all experiments, both -RT and NTC controls were included, to control for the possibility of gDNA contamination in the cDNA (see 2.0.5). 20 µl of each reaction was loaded onto a 2-3% agarose gel (with ethidium bromide) for visualization.

2.0.7 DNA-mediated transformation of *Magnaporthe oryzae*

Transformation was used to introduce foreign DNA constructs into protoplasts of *M.oryzae*. These constructs included gene deletion cassettes (as discussed in 2.0.6), or plasmids containing fluorescent gene fusions (as described in 2.0.9). All solutions and media used in this protocol are detailed in Appendix B and Appendix A respectively.

The first step in the transformation process was growth of the background strain in liquid culture (as described in 2.0.2), to provide material for the generation of protoplasts. Usually, conidia from one 10 day old colony growing on solid CM were inoculated into 300 ml of liquid CM, and incubated as described previously (2.0.2), for 72 hr. The resulting mycelium was harvested by filtering the culture through two layers of sterile miracloth, and excess medium removed by drying on sterile paper towels. The dried mycelium was then divided into two separate 50 ml falcon tubes each containing 50 ml OM buffer, and cut into smaller fragments with a sterile scalpel. Tubes were sealed with Parafilm (Bemis), and incubated in darkness at 30°C, with shaking at 150 rpm, for 3-4 hr. Digested mycelium (containing the protoplasts) was then divided into 4 falcon tubes (25 ml in each), and gently overlayed with 25 ml cold ST buffer, such that a distinct boundary was visible between the buffer and the digested mycelium. The tubes were centrifuged at 2850g in a Beckman Coulter Allegra X-15R with a SX4750 rotor, for 15 min at 4°C. Protoplasts accumulated at the interface between the ST buffer and digestate, and were harvested with a sterile plastic pipette, and placed in a new 50 ml Falcon tube. The protoplasts were overlayed with 10 ml cold STC buffer, and centrifuged at 2000g for 10 min at 4°C. The supernatant was removed, and the protoplasts resuspended in 10 ml STC buffer. At this point, protoplasts from the separate tubes could be combined if desired. The centrifugation and resuspension steps were then repeated more three times, except that in the final step protoplasts were resuspended in 150 µl of STC buffer. The protoplast concentration was determined by counting on a haemocytometer, and adjusted to 2-5 x 10^8 protoplasts/ml.

For transformation, 140 µl of protoplasts were combined with 10 µl of DNA (containing 5-15 µg of DNA, depending on the size of the construct) in a 1.5 ml Eppendorf tube and incubated at room temperature for 20 min. To the DNA and protoplasts, 1 ml of PTC buffer was added, mixed by inverting the tube, then incubated for a further 15 min at

room temperature. Finally, the protoplast/DNA/PTC buffer mixture was pipetted into molten OCM or BDCM agar (depending on selection requirements), and mixed before being poured into Petri dishes (15-20 mls per plate). The plates were allowed to set, and were then wrapped in aluminium foil and incubated at room temperature for 16-24 hr, before being overlayed with selection media (∼35 mls per plate). The nature of the overlay depended on the antibiotic being used for selection; these are outlined in Appendix A. Hygromycin B (Merck Millipore, Cat.No. 400051) was used at a final concentration of 300 µg/ml, Bialaphos (Gold Biotechnology) was used at a final concentration of 60 µg/ml, and chlorimuron ethyl (sulphonylurea - a generous gift from the Talbot laboratory, Exeter University) at a final concentration of 100 µg/ml. Once overlayed, the plates were wrapped in aluminium foil again, and incubated at 24°C for 7-14 days.

Transformants usually appeared from 7 days onwards, and could be selected from the original transformation plates and inoculated onto 50 mm Petri dishes containing the appropriate medium for the second round of selection. Antibiotic concentration was reduced at this stage of selection: Hygromycin and Bialaphos were both used at 1/3 the original concentration, and chlorimuron ethyl at 1/5 the original concentration. Selection plates were once again incubated at 24°C, for 7-14 days, after which sufficient growth should have occurred to allow for DNA extraction from the surviving colonies (as described in 2.0.3).

2.0.8 Southern blot analysis

Southern blotting was used to confirm the number and location of inserted antibiotic resistance genes in putative gene deletion strains. High-quality gDNA (5-10 µg, isolated as described in 2.0.3), was first digested overnight (in a 50 µl reaction) by restriction enzymes (New England Biosciences). The particular enzymes used were chosen such that the resulting fragment that contained the antibiotic resistance gene in question would be 4-7 kb in length. An additional requirement was that the restriction enzymes did not cut twice within the deletion cassette used in the transformation. This ensured that both the location and number of insertions could be determined from the digest. Once digested, the DNA was mixed with loading dye loaded onto a 0.8% agarose gel (without ethidium bromide), together with DNA ladder (either GeneRuler 1 kb Plus or GeneRuler 1 kb,

mixed with ethidium bromide (ThermoFisher Scientific)). The gel was run overnight in TAE buffer at 20-30V (1.5-2 V/cm), until the DNA had run the full length of the gel, thus ensuring good band separation. The gel was then imaged on a Syngene G-box alongside a ruler, in order to make note of the physical position of the DNA ladder band sizes on the gel before blotting. To ensure efficient transfer of the DNA from the gel onto the membrane, the gel was placed in a plastic box and washed by shaking at ∼50 rpm on an orbital shaker with depurination buffer (10-20 min), denaturation buffer (30-60 min) and neutralisation buffer (30-60 min). DNA was transferred from the gel onto a positively charged nylon membrane (Hybond N+ (Amersham)) by the capillary transfer method (Sambrook and Russell, 2005). Once the DNA had been successfully transferred, it was cross-linked to the membrane by UV treatment (Stratalinker UV Crosslinker (Stratagene)). The membrane could then be used immediately, or dried and stored until ready for hybridisation.

Hybridisation of the membranes was performed as follows: Membranes were first placed in a hybridisation tube, and treated with 7 ml hybridisation buffer (Perfect Hyb-Plus Hybridisation buffer), by rotating at 65°C in a Hybaid Shake 'n' stack (ThermoFisher Scientific) for 20-60 min. Membranes were hybridised with ^{32}P labelled DNA, synthesized by the Invitrogen Random Primer labelling kit, as per manufacturers instructions: ∼25ng of template DNA was amplified in the presence of ^{32}P labelled dCTP (50 µCi). The radiolabelled DNA was purified from unincorporated nucleotides by mixing with an equal volume of Dextran Blue (50 mg/ml) and separating through an Illustra^{TM} Nick^{TM} Sephadex G-50 column (GE). The purified DNA was denatured by boiling for 10 min, then added to the membrane and left to hybridize overnight.

Following hybridisation, the radiolabelled DNA and hybridisation buffer were removed, and the membrane washed as follows: Two 30 min washes with 2x SSC/0.1% SDS solution, one 20 min wash with 1x SSC/0.1% SDS solution and two 20 min washes with 0.1x SSC/0.1% SDS. All washes were performed at 65°C in a rotating Hybaid Shake 'n' stack, with ∼50 mls washing solution. After the unhydridised DNA had been removed by washing, the membrane was sealed in a plastic pocket, placed in a lead-shielded cassette and exposed to Amersham HyperFilm MP at -80°C for 1-14 days. Finally, the film was developed with Kodak autoradiography GBX developer and Kodak autoradiography

GBX fixer. Successful transformants could be identified by the presence of a single band of the expected size (which depended on the restriction enzymes used).

2.0.9 Cloning

Two forms of cloning were used in this thesis. Restriction based cloning in *E.coli* was used for the construction of fluorescent gene fusions and overexpression constructs. Yeast gap-repair cloning was used for making gene deletion cassettes containing *ALS*, as this gene was too large for successful fusion PCR.

Restriction based cloning in *E.coli*

A map of the plasmid (pUCAP) used in this type of cloning is shown in Appendix D. The first step in cloning the DNA sequence of interest was the amplification of this sequence by high-fidelity PCR, as discussed in 2.0.6. However, the design of the primers used was slightly different, since restriction sites had to be included in the primer sequence. A list of the primers used is shown in Appendix E. Following successful DNA amplification and purification, both the plasmid and insert DNA were digested with complementary restriction enzymes (New England Biosciences) according to manufacturers instructions. In most cases, *Asc*I and/or *Sbf*I were the restriction enzymes used, since these have 8 bp restriction sites and so rarely cut in the insert DNA. The digested plasmid was then dephosphorylated with Calf-Intestinal Alkaline Phosphatase (CiP)(New England Biosciences), according to manufacturers instructions, to prevent re-circularization. This was followed by phenol-chloroform extraction (to remove the enzymes) and DNA precipitation (to concentrate the DNA), performed as follows: 200 µl DNA as mixed with 200 µl phenol-chloroform, vortexed vigorously and then centrifuged in a microcentrifuge at 16,000 g for 2 min. The top layer (∼200 µl, containing the DNA) was removed, and 6 µl of 5 M NaCl and 618 µl of ethanol were added to precipitate the DNA. After mixing, the tube was place at -20°C overnight. The following day, the tube was spun at 16,000 g at 4°C for 60 min, the pellet washed with 70% ethanol and allowed to dry. Precipitated DNA was resuspended in 10-20 µl water and could then be run on an agarose gel to check concentration and purity.

DNA ligation was performed in a 10 µl reaction as follows: 1 µl digested vector, 1-2 µl

digested insert (depending on concentration), 1 µl T4 DNA ligase buffer, 1 µl T4 DNA ligase enzyme (ThermoFisher Scientific), 5 µl H_2O. A negative control reaction was also included, which did not include the insert DNA. The reaction mixtures were placed in a 16°C water bath overnight, for ligation to occur, and then transformed into heat-shock competent *E.coli* cells (DH5α) as follows: 5 µl of ligation reaction was mixed with 50 µl of cells, and incubated on ice for 20 min. The mixture was then placed in a 42°C water bath for 2 min, followed by addition of 1 ml Xbroth medium and incubation at 37°C for 1 hr (shaking at ∼200 rpm.) The transformed cells were then centrifuged at 1100 g in a microcentrifuge for 5 min and resuspended in 200 µl of liquid LB. This cell suspension was spread onto Peri dishes containing solid LB, with Ampicillin (100 µg/ml) as a selectable marker. The plates were sealed with parafilm and incubated overnight at 37°C. After this incubation, colonies were usually visible. Success of the cloning could be judged by comparing the number of colonies from cells transformed with the control vs. experimental ligation reactions; normally very few colonies should be visible on the negative control plate. Colonies were then picked off with a sterile toothpick or pipette-tip, and placed in 5 ml LB (with 100 µg/ml Ampicillin) and incubated overnight at 37°C, shaking at 200 rpm. Finally, the cells were pelleted by centrifugation for 15 min at 4700g in a Beckman Coulter Allegra X-15R, and the plasmid DNA isolated by using a Qiagen Spin Miniprep Kit, according to manufacturers instructions. Isolated plasmids were screened for the presence of the correct insertion by either PCR or restriction digestion. Confirmed plasmids were in most cases also sent for sequencing (Source Biosciences), to confirm that no changes to the insert had occurred during PCR or cloning.

Yeast gap-repair cloning

Yeast gap-repair cloning exploits the ability of *S.cerevisiae* cells to homologously recombine linear fragments of DNA with high efficiency, to produce circular plasmids. The first step in this process was the amplification of the target DNA sequences. This was performed in a manner similar to as described previously for the creation of gene-deletion cassettes: Primers (listed in Appendix E) were designed such that the amplified DNA sequences would have a ∼30 bp overlap with the DNA fragments or plasmid that they were to recombine with. Once the insert DNA fragments had been successfully ampli-

fied, the plasmid (shown in Appendix D) was linearized by *Hind*III digestion and treated with Calf intestinal alkaline phosphatase (CiP)(New England Biosciences), to prevent re-circularization. The digested plasmid and the amplified DNA fragments were combined with *S.cerevisiae* cells (strain D599) in an Eppendorf tube as follows: 50 µl salmon sperm DNA (boiled for 5 min and cooled on ice before use), 6 µl (200 ng minimum) linearized vector, 8 µl PCR product (300-500 ng of each fragment) and 50 µl *S.cerevisiae* cells. To this mixture, 32 µl 1 M Lithium acetate and 240 µl 50% PEG4000 were added, mixed by pipetting and incubated at 30°C for 30 min. The cells were then subjected to heat shock by incubating at 45°C for 15 min, then centrifuged in a microcentrifuge at 380 g for 2 min and resuspended in 200µl H_2O. Transformed cells were spread onto Yeast Synthetic drop-out media and incubated at 30°C for ∼2 days. From the resulting transformants, 5-10 colonies were picked off, inoculated into 50 ml of liquid Yeast drop-out media and incubated at 30°C, 120 rpm overnight. Following the incubation, cells were pelleted by two centrifugaton steps. First, the 50 ml cultures were centrifuged at 500 g for 5 min in a Beckman Coulter Allegra X-15R, and the pellet resuspended in 500 µl sterile H_2O. This was then centrifuged at 16,000 g in a microcentrifuge for ∼5 secs, to obtain a pellet of yeast cells.

The plasmid DNA was isolated from the yeast cells according to the following protocol: To the pelleted cells, 250 µl of Yeast lysis buffer, 250 µl phenol:chloroform:isoamylalcohol (25:24:1) and 300 mg acid washed glass beads were added. This mixture was vortexed for 30 min, to lyse the cells, then 250µl TE buffer (pH 8) added. The tubes were centrifuged at 16,000 g for 15 min, and the aqueous phase containing the DNA transferred to a new tube. One-tenth the volume of sodium acetate (pH 5.5) and 1 ml of 96% ethanol were added, and the tubes incubated at -20°C for 30 min. Tubes were then centrifuged at 16,000 g for 30 min, and the supernatant discarded. The resulting pellet was resuspended in 400 µl TE, to which 4 µl RNase A (10 mg/ml) (ThermoFisher Scientific) was added, then incubated at 37°C for 10 min, until the pellet was dissolved. Then, 10 µl of 4 M ammonium acetate and 1 ml 96% ethanol were added, then the tubes centrifuged for 15 min at 16,000 g. The supernatant was discarded, and the pellet washed with 500 µl 70% ethanol. Finally the pellet was left to air-dry and resuspended in 50 µl dH_2O.

The isolated plasmid DNA (6-8 µl) could then be transformed into super-competent *E.coli*

cells (DH5α) by heat-shock, and screened for successful recombination as described in the previous sub-section.

2.0.10 Preparation of heat-shock competent *E.coli* cells

Heat-shock competent *E.coli* cells were used in the cloning of plasmids, as described in Section 2.0.9, and were prepared according to the following protocol. *E.coli* cells (strain DH5α) were streaked onto a Petri dish containing LB (without antibiotic), and incubated overnight at 37°C. Two of the resulting colonies were removed with a sterile toothpick and inoculated into 5 ml liquid LB (without antibiotic), and incubated overnight at 37°C, with shaking at 200 rpm. The following day, 500 µl of the cell cultures were inoculated into flasks containing 50 ml of liquid LB (without antibiotic). These flasks were incubated at 37°C with shaking at 200 rpm for 2-3 hr until OD^{595} reached 0.45-0.55. The flasks were then cooled on ice for up to 30 min, and the contents transferred into pre-cooled falcon tubes. The tubes were centrifuged at 4°C for 5 min at 2850g in a Beckman Coulter Allegra X-15R, and the supernatant discarded. The cells were gently resuspended in 25 ml 0.1M $CaCl_2$ (filter sterilized) and incubated on ice for 30 min. The cells were then centrifuged again at 4°C for 5 min at 2850g in a Beckman Coulter Allegra X-15R, and the supernatant discarded. Pelleted cells were gently resuspended in 5 ml 88 mM $CaCl_2$ with 12.5% (v/v) glycerol. The cell suspension was then aliquoted into sterile Eppendorf tubes and frozen in liquid nitrogen. Cells could be stored at -80°C until required.

2.0.11 Cell wall staining

Visualization of the fungal cell wall was achieved using a variety of fluorescently labelled probes, dyes, lectins and antibodies in conjunction with epifluorescence or confocal microscopy (detailed in 2.0.12).

Antibodies

Two different anti-chitosan antibodies were used. The first, mAbG7, was a generous gift from the laboratory of Stefan Schillberg (Schubert et al., 2010). Germlings developed on either Menzel coverslips or onion epidermis were first blocked with 2% BSA (w/v) in PBS for 1 hr at room temperature. Samples were washed 3 times with PBS/T (PBS +

0.05% Tween 20), for 5 min each on an orbital shaker (~70rpm) and then incubated with the primary antibody (mAbG7, at 10 μg/ml in PBS) for 1.5 hr at room temperature. This incubation was followed by 3 more washing steps as described above, and incubation with the secondary antibody (FITC-labelled anti-Mouse IgM, 5 μg/ml in PBS) at room temperature for a further 1.5 hr. Finally, the secondary antibody was removed by 3 more washing steps with PBS/T as described previously and viewed under an epifluorescence or confocal microscope. A negative control was included in all experiments, in which samples were only incubated with the secondary antibody.

A second anti-chitosan antibody was a generous gift from the laboratory of Holger Deising (Gueddari et al., 2002). Staining with this antibody was performed as described for mAbG7, except that the antibody was used at a dilution of 1/100 from the original antiserum, and the secondary antibody (a FITC-labelled anti-rabbit IgG) was used at 10 μg/ml (in PBS).

Staining of germlings was also attempted with the anti-pectin antibodies JIM5, JIM7 and LM19 (a generous gift from the laboratory of Ian Moore). Germlings at 16 hpi were first washed once with PBS, then incubated for 2 hr with the primary antibodies (diluted 1/20, 1/50 or 1/100 in PBS + 1% BSA) at room temperature. Primary antibodies were removed by washing 3 times for 5 min each with PBS. This was followed by incubation with the secondary antibody (TRITC-labelled anti-Rat IgG, IgA, IgM, 10 μg/ml in PBS) for 2 hr, washing 3 more times as above and viewing under the confocal microscope. A negative control with only secondary antibody was included in all experiments.

Lectins

The lectins Wheat Germ Agglutinin (WGA) and Concanavalin A (ConA) were used to stain for chitin and mannan respectively.

For staining with WGA-FITC, mycelial pellets were incubated with 2% BSA in PBS for 1 hr, before being washed 3 times with PBS/T. WGA-FITC (10 μg/ml in PBS) was added and the pellets incubated on ice for 3-4 hr. Finally, the pellets were again washed 3 times with PBS/T and viewed under the confocal microscope.

Staining of germlings with ConA-FITC was performed as follows: Germlings developed on an artificial surface were stained with ConA-FITC (20 or 40 μg/ml in PBS) for 20

min on ice, before being washed gently with H_2O twice, then viewed under the confocal microscope.

Calcofluor white, Eosin Y

The fluorescent dyes Calcofluor White (CFW) and Eosin Y were used to stain for chitin and chitosan respectively. In all experiments, unlabelled samples were included to control against autofluorescence.

For staining of germlings and mycelia with CFW, samples were incubated with 0.05% CFW (w/v) for 20 min at room temperature, washed briefly with H_2O and then viewed under epifluorescence or confocal microscopes.

Staining of conidia with eosin Y was performed essentially as described previously (Baker et al., 2007). Briefly, conidia were harvested as described in Section 2.0.2, pelleted by centrifugation at 2850g in a Beckman Coulter Allegra X-15R, then resuspended in McIlvaine buffer (pH 6). Conidial concentration was adjusted to 1 x 10^6 conidia/ml. To 500µl of conidial suspension, 10 µl eosin Y (5mg/ml) was added, and incubated on ice for 30 min. Conidia were washed by centrifugation of the labelled spore suspension at 16,000 g for 5 min, removal of the supernatant, and resuspension in 1 ml McIlvaine buffer. This was repeated 3 times, except after the last wash, conidia were resuspended in 100 µl of McIlvaine buffer. Labelled conidia could then be viewed under epifluorescence or confocal microscopes.

OGA488, COS488

The probes OGA488 and COS488 were used to stain for chitosan and polygalacturonic acid respectively, and were generous gifts from the laboratory of William Willats (Mravec et al., 2014). Staining was performed as described previously (Mravec et al., 2014): Samples (germlings or mycelia) were washed briefly with 25 mM MES (pH 5.6), then incubated with OGA488 or COS488 (diluted 1/1000 in 25 mM MES) for 15 min on ice. This was followed by 2-3 brief washes with 25 mM MES, after which samples could be mounted and viewed under the confocal microscope.

2.0.12 Microscopy

Three different microscopes were used, depending on experimental requirements.

Brightfield and epifluorescence microscopy

Brightfield microscopy was performed on an Olympus BX-50, typically for examining and recording spore germination assays. Samples were viewed under 20X/0.5 UPlanFL N or 40X/0.75 UPlanFL objective lenses. Pictures were recorded by a Q-Imaging Retiga EX-i Fast 1394 camera and Qcapture Pro software.

Epifluorescence microscopy was also performed on the Olympus BX-50, with UV illumination. The filter set used depended on the fluorophor in question: The NIBA filter was used for eosin Y or FITC, WU was used for CFW. Detector gain and exposure time were adjusted according to fluorescence levels.

Confocal microscopy

Confocal microscopy was performed on either a Zeiss LSM510 Meta or a Leica SP5. The resulting images presented in this thesis are displayed as maximum projections along the z-axis, unless otherwise stated.

For the Zeiss LSM510, samples were viewed under a Zeiss C-Apochromat water immersion 40X/1.2NA lens and collected at 8 bit data depth. Line averaging was set at either 4 or 8, scan intervals at 0.5-2 μm depending on sample thickness and pinhole diameter, which was set at ∼1 Airy unit (AU), depending on signal strength. Settings used for excitation and emission depended on the fluorophors in question. For visualization of CFW stained samples, excitation was at 405 nm from a blue diode laser, and emitted light collected at 500-530 nm. For visualization of eGFP tagged proteins or FITC labelled samples, excitation was at 488 nm from an Argon laser and emitted light collected at above 505 nm. For YFP, excitation was at 514 nm from an Argon laser, and emitted light collected between 535-590 nm. mCherry or TRITC visualization was achieved by excitation at 543 nm from a Helium-Neon laser, and emitted light collected above 585 nm.

The Leica SP5 was used for dual imaging of YFP and mCherry tagged proteins. Samples were viewed under a Leica HC PL APO CS2 63X/1.2 water immersion lens, and collected at 8 bit data depth. Line averaging was set at 8, scan speed at 400 Hz, scan

intervals at 0.5 μm and pinhole at 1 Airy Unit. Dual excitation at 514 nm and 543 nm was provided by Argon and Helium-Neon lasers respectively. Emitted light was collected at 500-564 nm and 585-660 nm.

Fluorescence stereomicroscopy

Fluorescence stereomicroscopy was used for the localization of fluorescently-tagged proteins at low magnification. It was performed on a Zeiss Axio Zoom V16 in the laboratory of Professor Kevin Foster, University of Oxford. Colonies of *M.oryzae* grown on CM, expressing mCherry or eGFP tagged proteins were observed under UV-illumination. Fluorescent heat-maps were inferred from the resulting pictures using Zeiss Zen Lite software.

2.0.13 Conidial germination assays

Conidial germination assays were performed on hydrophobic glass coverslips (Menzel-Gläser), which provided consistent and convenient conditions for appressorium formation in the absence of a plant surface. Conidia were first harvested by pipetting 5 ml of water onto a 10-12 day old colony growing on CM. This was scraped with a sterile scalpel or microscope slide to create a suspension of conidia and hyphae that was filtered through two layers of Miracloth to isolate the conidia. These were centrifuged at 2850g for 5 min in a Beckman-Coulter Allegra X-15R, and the supernatant removed. The pellet of conidia was resuspended in 1 ml of dH_2O, concentration determined by counting on a haemocytometer and adjusted to 2.5 x 10^5 conidia/ml (final concentration). Droplets of conidial suspension (50 μl) were pipetted onto the coverslips which were then placed into a 'humidity chamber' (Tupperware box containing damp tissue paper). Incubations were performed at 24°C for 1-24 hr depending on experimental requirements. For germinations on hydrophilic glass coverslips (Heathrow Scientific) the protocol was identical except that only 20 μl of conidial suspension was used. Coverslips were placed in square Petri dishes with damp filter paper and sealed with Parafilm to prevent evaporation.
Germinations were also performed in the presence of various chemical inducers or inhibitors: IBMX was used at 2.5 mM (from a 250 mM stock in DMSO), 1,16 hexadecanediol at 200 μM (from a 50 mM stock in ethanol), diacylglycerol (Enzo Life Sciences) at

58 μM (from a 7.25 mM stock in DMSO), and tricyclazole at 200 μM (from a 20 mM stock in DMSO). Chitosan and its derivatives were used at a final concentration of 0.01% or 0.001%, from a 1% stock (except for FITC-chitosan which was from a 0.08% stock). For germinations in the presence of wax (1-octacosanol), the wax was first dissolved in chloroform to a concentration of 4 mg/ml. In a laboratory fume hood, 100 μl of this stock was pipetted onto a hydrophobic glass coverslip and the chloroform allowed to evaporate, leaving a layer of wax on the coverslip. Conidia were inoculated onto this surface as described above.

Germination assays were also performed on onion epidermis or Rice leaf sheaths. For germination on onion epidermis, conidia were harvested and prepared as above. Epidermis was removed from onions (Tescos) with a scalpel and placed on a Petri dish containing 2% Agar. Epidermises were kept flat by placement of coverslips on the top and bottom edges and inoculated with 50 μl droplets of conidial suspensions. Incubation was as discussed above, usually for 24 hr. For germination on Rice, sheaths were harvested from 3-4 week old plants (cultivar CO-39) and placed in a Petri dish containing 2% agar. Conidial suspension was pipetted into the centre of the sheath and incubated as discussed above.

2.0.14 Conidial adhesion assays

Adhesion assays were performed on both hydrophobic and hydrophilic glass coverslips (detailed in 2.0.13). Conidia were harvested and diluted as described previously (2.0.13). 20 μl droplets of conidial suspension (either with or without 0.01% chitosan) of each strain were pipetted onto the coverslips, which were placed into a humidity chamber and incubated at 24°C for 2 hr to allow germination. At 2 hpi, half of the coverslips were removed and placed into a 50 mm Petri dish containing 5 ml dH_2O, and shaken on an orbital shaker at 100 rpm for 5 min. Coverslips were then removed and mounted on slides for viewing under the 10X objective lens of the Olympus BX50 microscope (detailed in 2.0.12). Conidia were counted from one field of view (for hydrophobic coverslips) or three fields of view (for hydrophilic coverslips), with a conscious effort made to locate the area of the coverslip with the highest conidial density. For each strain, the number of conidia counted on the washed coverslips was compared with those counted on the unwashed coverslips, and percentage conidial adhesion calculated as: 100 - ((conidia on unwashed

coverslip - conidia on washed coverslip) ÷ conidia on unwashed coverslip) x 100.

2.0.15 Pathogenicity assays

Pathogenicity assays were performed on both rice (*Oryza sativa*, cultivar CO-39) and barley (*Hordeum vulgare*, cultivar 'Golden Promise'). For barley, leaves were harvested from 7 day old plants grown as described in Section 2.0.17, and placed on square Petri dishes containing 2% agar. The top and bottom of the leaves were weighed down with glass microscope slides to keep them flat. Conidia were harvested as described previously (2.0.13), and diluted to a final concentration of 6.25 x 10^4 conidia/ml in 0.2% gelatine (w/v). The leaves were then sprayed from a fixed distance with 2 ml of the conidial suspension, using an airbrush (Badger). Inoculated leaves were incubated at 24°C for 5 days, after which the leaves were photographed and lesions counted. For assays on rice leaves, plants were grown as described in Section 2.0.17 for 3-4 weeks. Only the first and second youngest leaves were harvested from plants, in order to achieve greater consistency. These leaves were treated with 2% bleach (v/v) for 30 seconds, then washed 3 times with dH_2O and allowed to air dry. Dry leaves were placed on square Petri dishes containing 2% agar, and kept flat with glass microscope slides as described for barley leaves. Conidia were harvested as described previously and inoculated as described above, except that the concentration used was 2.5 x 10^5 conidia/ml. Inoculated leaves were incubated at 24°C for 4 days, then photographed. A mock inoculation was included in all experiments, in which leaves were only sprayed with 0.2% gelatine (w/v).

2.0.16 Synthesis of FITC-chitosan

FITC-labelled chitosan was synthesized as described previously (Qaqish and Amiji, 1999) - One gramme of chitosan was dissolved in 100 ml of 0.1M acetic acid. To the chitosan solution, 100 ml of methanol was slowly added with continuous stirring. A 1 mg/ml solution of FITC in methanol was then slowly added, such that the final molar ratio of FITC:glucosamine was 1:50. The reaction was allowed to proceed for 1hr in the dark, at room temperature. The resulting FITC-chitosan was precipitated by the addition of 0.1M NaOH. In order to remove unreacted FITC, the precipitate was washed by suspending it in dH_2O, followed by centrifugation and removal of the supernatant. This was repeated

until the absorbance of the supernatant at 492 nm (the absorbance maximum of FITC) was <0.01. Washed FITC-chitosan was then freeze dried and stored at -20°C until needed. For use in germination assays, the FITC-chitosan was dissolved in 1% acetic acid, and the pH adjusted to ∼6 by the addition of NaOH. This solution was then dialyzed overnight against dH_2O, to remove the sodium and acetate.

2.0.17 Growth of Rice and Barley

Rice and barley plants were grown in a Weiss-Gallenkamp Fitotron SGC-120 at 24°C, 60% relative humidity. Light was provided by 36 W fluorescent tubes, supplying a maximum light intensity of 170 μmol m^{-2} s^{-1}, with 14 hr light/10 hr dark.

Rice seeds of the cultivar CO-39, which is susceptible to *M.oryzae*, were planted in John Innes no.3 compost, and placed in the growth chamber. Plants were incubated for 3-4 weeks with regular watering. For barley, seeds of the cultivar 'Golden Promise' were planted in 50% John Innes no. 2/50% multipurpose compost, and placed in the growth chamber. Plants were incubated for 7 days with regular watering.

Chapter 3

Chitin deacetylation and appressorium development

3.1 Objectives

As discussed previously, there are two key hypotheses regarding the role of chitin deacetylation. The first concerns a putative 'stealth mechanism', whereby deacetylation of chitin prevents cell wall digestion by plant chitinases, and reduces the production of chitin PAMPs which can trigger a plant defence response. The second hypothesis is that chitin deacetylation causes a significant change in the properties of the cell wall and is therefore important for morphogenesis. Clearly, these hypotheses are not mutually exclusive, although it is possible that the protective role and the developmental role of chitosan may be spatially or temporally separated. The process of appressorium development presents an opportunity to test both of these hypotheses simultaneously. The production of the large, dome-shaped appressorium from the tip of a narrow germ tube should conceivably require a large increase in localized cell wall flexibility that may come about as a result of chitin deacetylation. In addition, successful appressorium development on a leaf surface requires protection from destructive factors; this was shown in the α1,3-glucan synthase deletion strain, where loss of α1,3-glucan resulted in the destruction of the germling even before plant penetration (Fujikawa et al., 2012). Thus, loss of chitosan during germling morphogenesis could either result in defective appressorium development, or destruction of appressoria on plant surfaces (or a combination of both). Another reason for the suitability of appressorium formation as a system in which to test hypotheses regarding chitin deacetylation is the availability of intriguing previous data. Firstly, chitosan has been found to be a component of germ tubes and appressoria in *M.oryzae* (Fujikawa et al., 2009). Secondly, deletion of a putative chitin deacetylase called Cbp1 resulted in defective appressorium formation on artificial surfaces, although no loss of chitosan was observed and appressorium formation was restored on plant surfaces and by chemical inducers (Kamakura et al., 2002; Tucker et al., 2010). This previous work provides a good basis for continued characterization of the role of chitin deacetylation during appressorium development.

The objectives of this Chapter are to:

- Confirm the presence of chitosan during appressorium development
- Identify which chitin deacetylases are expressed during appressorium development

- Perform targeted deletion of identified genes, in order to abolish chitin deacetylation during appressorium formation
- Investigate appressorium development and pathogenicity in the deletion strains

3.2 Results

Chitosan is a component of the cell wall in germ tubes and appressoria

Previous work investigating the localization of chitosan during appressorium development in *M.oryzae* employed the dye eosin Y (tetrabromofluorescein), which binds to chitosan via an electrostatic interaction (Fujikawa et al., 2009). However, attempts to localize chitosan using this dye were met with limited success here; the dye proved extremely susceptible to internalization, and often accumulated in the cytoplasm of conidia, germ tubes and appressoria in both live and fixed cells. In addition, the specificity of this interaction has not been directly proven; eosin Y could presumably interact and stain any cell wall component with a positive charge. With this in mind, alternative means of labelling chitosan were sought. Other studies of chitosan localization in fungi have used anti-chitosan antibodies which have proven specificity, and are therefore preferable to eosin Y. Two different antibodies were obtained: mAbG7, a monoclonal anti-chitosan antibody (a generous gift from the laboratory of Stefan Schillberg (Schubert et al., 2010)), and a polyclonal anti-chitosan antibody, a generous gift from the laboratory of Holger Deising (Gueddari et al., 2002). In order to allow labelling of unfixed germlings, conidia were first inoculated onto an artificial hydrophobic glass surface which effectively induces appressorium development in *M.oryzae* (Lee and Dean, 1994). The labelling of the unfixed germlings with these antibodies at 16 hpi confirmed the previous findings with eosin Y: chitosan localizes to the germ tube and appressorium, although weak labelling of the conidial wall was also observed in some cases, particularly with the polyclonal antibody (Figure 3.1). In addition to confirming these previous results however, it was also of interest to determine the precise time points at which chitin deacetylation occurs; if chitin deacetylation was found to occur after appressorium development, this would suggest that it is not required for this process. Although this could have been determined using the antibodies, there are two drawbacks of using antibodies for this experiment: Firstly,

staining germlings with antibodies takes in excess of 4 hours to complete, by which time appressorium formation would have occurred in live cells (although admittedly, fixing the samples would have circumvented this problem). Secondly, the anti-chitosan antibodies do not demonstrate absolute specificity for chitosan. Rather, binding affinity increases in proportion to the degree of chitin deacetylation. As a result, a small amount of binding to chitin is observed *in vitro* for these antibodies, which may explain the staining of the conidial wall observed (Schubert et al., 2010; Gueddari et al., 2002). Fortunately, a recently developed probe for chitosan addresses both of these issues (Mravec et al., 2014). OGA488 is an Alexa-fluor 488 labelled oligomer of galacturonic acid. As a negatively charged molecule, OGA488 interacts electrostatically with the polycationic chitosan. However, charge is not the only factor determining the specificity of this interaction: a molecular modelling approach demonstrated that the amine and carboxy groups of chitosan and OGA488 respectively are arranged in a unique stereochemical manner which results in highly specific binding (Mravec et al., 2014). This means that OGA488 does not bind at all to chitin, binds weakly to partially deacetylated chitin, and strongly to fully deacetylated chitin (Mravec et al., 2014). The second major advantage of OGA488 over the antibodies is that labelling can be completed in just 15 min. This allowed observation of chitin deacetylation at early stages of germling morphogenesis, in live cells. When germlings developing on an artificial hydrophobic surface were labelled with OGA488 at 1-2 hpi, weak labelling of the germ tube was observed. This labelling either covered the entire length of the germ tube, or was initially localized to a small 'patch'. OGA488 labelling appeared to intensify upon onset of germ tube hooking (2-3 hpi), and further still during appressorium development (4 hpi), covering the entirety of the germ tube and appressorium, much like the labelling observed with the anti-chitosan antibodies (Figure 3.1).

M.oryzae has 10 putative chitin deacetylases

Having established that chitin is deacetylated both prior to and during appressorium development, the next objective was to determine which CDAs were responsible. In order to do this, first all of the *CDA* genes present in the genome of *M.oryzae* needed to be identified. Using the protein sequence of Cbp1, a BLAST search was performed on

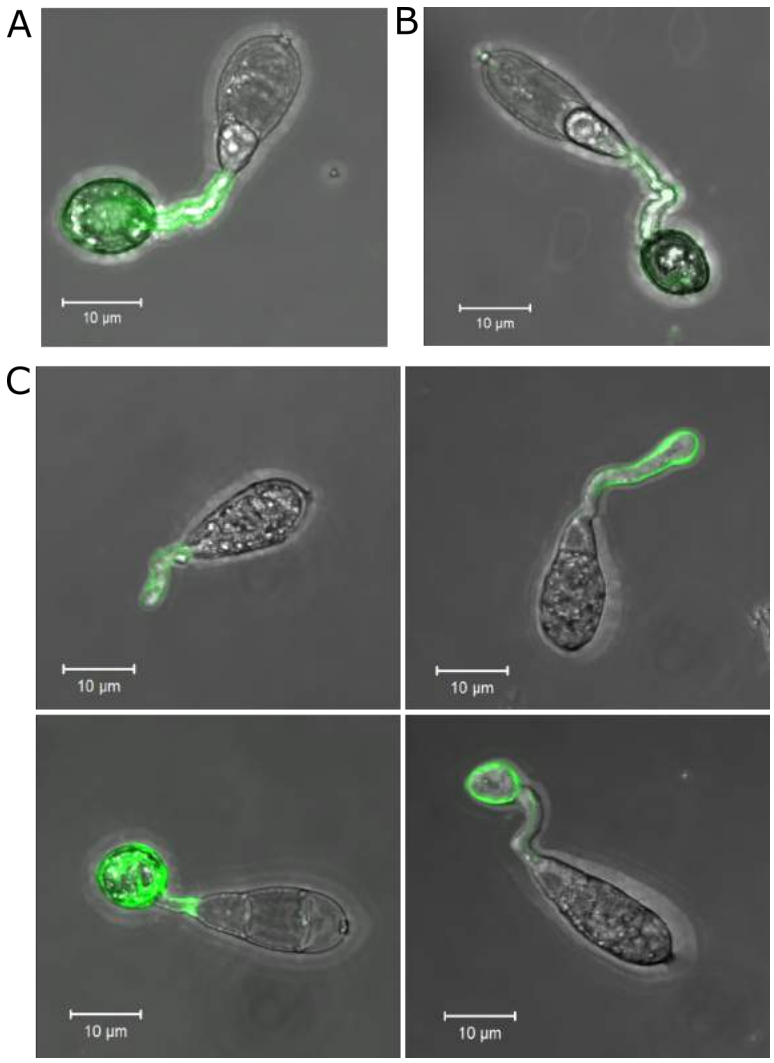

Figure 3.1: Chitosan is a component of the cell wall in germ tubes and appressoria. Germlings labelled with **A**) monoclonal anti-chitosan antibody mAbG7, **B**) polyclonal antichitosan antibody and **C**) the anti-chitosan probe OGA488. Staining of germ tubes and appressoria was observed in all cases. The rapid staining with OGA488 allowed localization of chitosan in live cells at different stages of appressorium development (2-16 hpi, clockwise from left to right). Staining with antibodies was performed at 16 hpi. Germlings were developed on a hydrophobic glass surface. Scale bars: 10 µm.

the *M.oryzae* protein database (BLOSUM62, gapped alignment, E-value cut-off of $1e^{-3}$). A Pfam domain search was performed on the resulting hits, and any sequences which did not include a Polysaccharide Deacetylase-1 domain (Pfam 01522) were discarded. Generally, these were proteins that included chitin-binding domains (Pfam 00187), but no catalytic domains. This resulted in the identification of 10 putative chitin deacetylases, shown in Figure 3.2. Subsequent BLAST searches with these newly-identified proteins did not discover any further putative chitin deacetylase sequences. All the CDAs have a polysaccharide/chitin deacetylase domain (CDA; Pfam 01522), and all CDAs except Cda9 have an N-terminal signal peptide, suggesting extracellular localization. Chitin binding domains (CBD; Pfam 00187) are also present in some CDAs, including Cbp1, which also has a serine/threonine-rich repeat region at its C-terminus, as remarked upon previously (Kamakura et al., 2002). Interestingly, Cda4, Cda5 and Cda8 have putative single transmembrane domains, suggesting membrane localization for these proteins.

The catalytic mechanism of a chitin deacetylase from the plant pathogen *Colletotrichum lindemuthianum* has been elucidated using structural and biochemical data (Hekmat et al., 2003; Blair et al., 2006). This chitin deacetylase was found to be a zinc-dependant metalloenzyme, where the zinc ion is bound by a Asp-His-His triad (Figure 3.2). Four key active-site residues were also defined: The catalytic base residue (aspartate) and catalytic acid residue (histamine), which interact with arginine and aspartate residues respectively. In order to determine whether these residues were conserved in the *M.oryzae* CDAs, the sequences were aligned using Clustal Omega (Sievers et al., 2011) (Figure 3.2). This revealed that the zinc-binding triad and active-site residues are indeed conserved in all of the sequences analyzed, with the exception of the non-catalytic aspartate in Cbp1.

A phylogenetic analysis of the chitin deacetylases was also attempted, in order to shed light on the distribution and evolutionary relationships of these enzymes amongst different species of fungi. Unfortunately, this family proved to be exceptionally difficult to resolve, primarily due to the short length of the conserved CDA domain, and the low degree of sequence conservation within it. It was therefore not possible to reliably infer a phylogeny. A previous study did investigate the evolutionary relationships of the chitin deacetylases (Ruiz-Herrera and Ortiz-Castellanos, 2010), but this only included three species of ascomycete and suffered from poor boostrap-support.

A

Gene number	Gene name	Domain architecture
MGG_12939	*CBP1*	CBD, CDA, CBD, S/T rich region
MGG_14966	*CDA1*	CDA, CBD
MGG_09159	*CDA2*	CDA, CBD, CBD
MGG_04172	*CDA3*	CDA
MGG_08774	*CDA4*	CDA
MGG_01868	*CDA5*	CDA
MGG_08356	*CDA6*	CDA
MGG_05023	*CDA7*	CDA, CBD
MGG_04704	*CDA8*	CDA
MGG_03461	*CDA9*	CDA

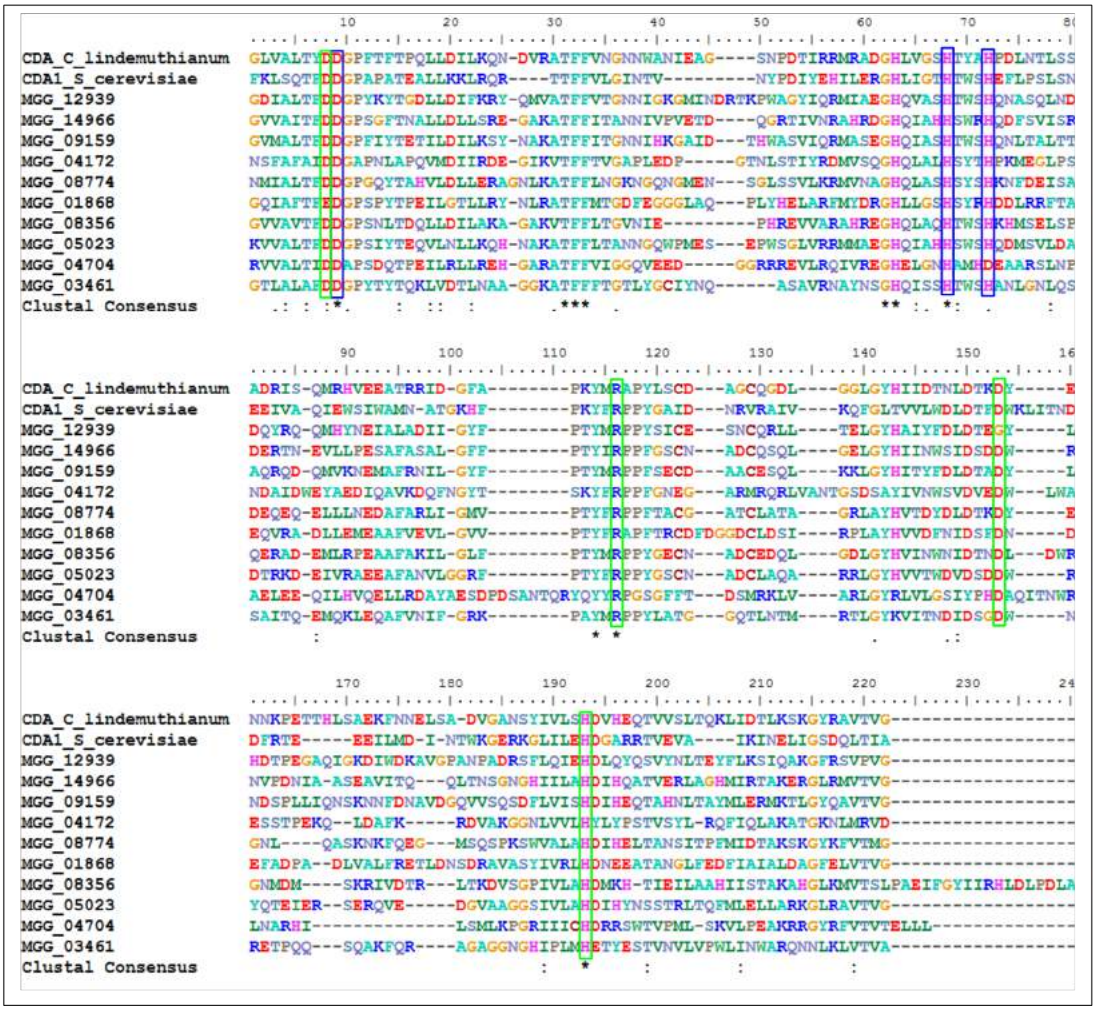

B

Figure 3.2: ***M.oryzae*** **has 10 putative chitin deacetylases.** **A**) Table of the 10 chitin deacetylase genes in *Magnaporthe oryzae*, showing gene numbers, given gene names and protein domain architectures (as defined by Pfam). **B**) Alignment of *M.oryzae* CDAs with those from *C.lindemuthianum* and *S.cerevisiae*. Conserved active site residues are marked in green boxes, and the zinc binding triad in blue boxes.

Chitin deacetylases are highly expressed during appressorium development

In order to determine which of the 10 CDAs were expressed during appressorium development, two transcriptional profiling methods were used. The first simply involved exploiting an existing transcriptomics dataset. Soanes *et al* (2012) performed genome-wide transcriptional analysis of *M.oryzae* during several stages of appressorium development on an artificial inductive surface (Soanes et al., 2012). By searching this dataset for all 10 *CDAs*, the transcript abundances for these genes at 4 hpi during appressorium development could be determined (Figure 3.3). This revealed that *CDA3* was by far the most highly expressed *CDA*, followed by *CBP1* and *CDA2*. Low or non-existent expression was found for the remaining genes. To independently verify this data, a second method was employed. Semi-quantitative RT-PCR was performed on RNA isolated from germlings developing either on rice leaves (harvested at 4 hpi) or teflon (harvested at 5 hpi). Teflon is a hydrophobic surface which can artificially induce appressorium formation in *M.oryzae*, although development of appressoria was observed to occur more slowly on this surface (not shown), hence the harvesting of germlings at 5 hpi instead of 4 hpi. Results of the RT-PCR experiments were broadly in line with those from the transcriptomics dataset; *CDA3*, *CBP1* and *CDA2* had the greatest transcript abundance, although transcript levels for *CDA4* also appeared to be comparable to *CDA2* in this analysis (Figure 3.3). Results from RT-PCR analysis of germlings harvested from teflon were slightly different from those on rice leaves, in that expression was detected for a number of *CDA* genes that were not detected on rice leaves. However, this is likely due to the much higher proportion of fungal RNA present in germling samples from Teflon compared with those from rice leaves (which is mainly plant RNA). Reducing the number of amplification cycles would have been beneficial in this case. In all cases, parallel experiments were performed in which the RNA had not been reverse transcribed (-RT control). No amplification was observed in these experiments, proving that any observed amplification was due to cDNA and not gDNA contamination. Semi-quantitative RT-PCR experiments were repeated a total of two times with independently prepared RNA samples; identical results were obtained in each case.

Gene name	Expression at 4hpi (FPKM)	RT-PCR (Leaves)	RT-PCR (Teflon)
CBP1	1232	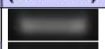	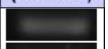
CDA1	71		
CDA2	275		
CDA3	26564		
CDA4	125		
CDA5	5		
CDA6	0		
CDA7	5		
CDA8	3		
CDA9	46		
β-tubulin	2063		

Figure 3.3: Chitin deacetylases are highly expressed during appressorium development. Expression of *CDA* genes during appressorium formation, comparing data from transcriptomics (Soanes et al., 2012), expressed in Fragments per Kilobase per Million (FPKM), and semi-quantitative RT-PCR of RNA isolated from germlings developing on rice leaves or teflon (an artificial inductive surface). β-tubulin is included as the reference gene. Primers used are listed in Appendix E (primers 84-107).

Deletion of chitin deacetylases

The data outlined above suggests that there are at least three *CDA* genes correlated with chitin deacetylation during appressorium development: *CBP1*, *CDA2*, and *CDA3*. Although *CBP1* has previously been deleted and characterized, as discussed previously (see section 3.1), it was considered that redundancy may exist between these identified genes. With this in mind, single, double and triple deletion strains were generated by the targeted gene replacement approach, whereby the genes of interest were replaced by an antibiotic resistance gene (Figure 3.4A). Homologous recombination between the gene replacement cassette and the flanking regions of the gene of interest results in gene replacement (Figure 3.4A). In most cases, the entire coding region of the gene was replaced. However, in the case of *CBP1*, due to apparent misannotation of this gene, only the first ~2 kb of the ~2.6 kb coding sequence was replaced. Since this included the signal peptide and catalytic domain, it can still be considered a functional knockout strain. Primers used for the creation of deletion cassettes are listed in Appendix E (Primers 1-26).

Putative deletion strains were first screened by PCR, to confirm the loss of the target gene and the integration of the resistance gene at the correct locus (not shown). Confirmed strains were then subjected to Southern blot analysis, to confirm the presence of a single insertion of the deletion cassette at the desired locus. In all single gene deletion

strains, genes were replaced with *HPH*, conferring resistance to hygromycin. Restriction-digested genomic DNA of these putative deletion strains was therefore hybridised with α-^{32}P-labelled DNA encoding *HPH*. Hybridisation with *Xho*I digested gDNA of 7 putative *CBP1* deletion strains, resulted in the expected 5 kb band in all lines, with no ectopic insertions. *Bgl*I digest of gDNA from putative *CDA2* deletion strains resulted in an expected band at 3.7 kb, although with an additional insertion in one of the lines. For putative *CDA3* deletion strains, *Eco*RI digest resulted in the expected 4.7 kb band, although with additional insertions in two of the lines (Figure 3.4B).

Once the single deletion strains had been successfully generated, they were used as the background strains for the creation of double deletion strains. Because *CDA2* was the most challenging gene to delete, the *cda2* mutant was used as a background strain for two of the deletions (*cda2/cbp1* and *cda2/cda3*). *CDA3* proved to be the easiest gene to delete, and so the *cbp1* mutant was used as the background strain for *cbp1/cda3*. In these strains, the target sequence was replaced by *BAR*, conferring resistance to bialaphos. Southern blot analysis therefore involved hybridisation of α-^{32}P-labelled DNA encoding *BAR* to restriction digested gDNA of the putative deletion strains. However, since both *HPH* and *BAR* have similar promoter sequences, some cross-hybridisation was apparent; faint bands resulted from the *BAR* probe hybridising to *HPH* from the first deletion. In fact, this could be considered beneficial, since it allowed both gene deletions to be confirmed in the same analysis. For *cda2/cbp1*, *Xho*I digestion gave the expected 4.5 kb band, but also a faint 5.3 kb band resulting from hybridisation of *BAR* to *HPH* at the *CDA2* locus (the *cda2* strain was included as a control). An ectopic insertion was apparent in one of the *cda2/cbp1* lines (band at 10 kb). For *cda2/cda3*, *Eco*RI digestion resulted in the expected 4.2 kb band, as well as the expected 8.6 kb band for hybridisation to *HPH* at the *CDA2* locus. Lastly, for *cbp1/cda3*, *Cla*I digestion resulted in the expected 4.7 kb band, as well as the expected ∼9 kb band for hybridisation of the *BAR* probe to *HPH* at the *CBP1* locus (Figure 3.4C).

Lastly, a triple deletion strain *cda2/cbp1/cda3* was made in the *cda2/cbp1* background strain. In this case, *CDA3* was replaced by the sulphonylurea-resistant allele of acetolactate synthase (*ALS*). Because the background strain already contains the WT allele of this gene, hybridisation of the *ALS* probe to both alleles is expected in the Southern

blot analysis. *Eco*RI digest of gDNA from two putative triple knockouts resulted in the expected 6.1 kb band for replacement of *CDA3*, and also a band at 19 kb, as expected for hybridisation to the WT *ALS* allele (Figure 3.4D). All deletion strains are listed in Appendix F.

Chitosan is required for appressorium development on artificial surfaces

CBP1 is known to be required for normal appressorium development in *M.oryzae* (Kamakura et al., 2002). To confirm these previous findings, and to investigate appressorium development in the other deletion strains, conidia of each of the strains were inoculated onto an artificial hydrophobic glass surface (Menzel coverslips). In the WT strain, over 80% of conidia developed appressoria after an 8hr incubation. However, in *cbp1*, almost no appressoria formed, and germ tubes were abnormally elongated and failed to even undergo early differentiation events (e.g. germ tube hooking), consistent with the previous report (Figure 3.5)(Kamakura et al., 2002). Conidial germination of *cbp1* at 1 hpi was not lower than WT, suggesting that the lack of appressorium development was not due to delayed or reduced germination. Extending the incubation to 16 hr did result in appressorium formation in *cbp1*, although these were frequently misshapen (Figure 3.5B). In the *cda2*, *cda3* and *cda2/cda3* strains, appressorium development and conidial germination were similar to WT. However, deletion of *CDA2* together with *CBP1* resulted in much more severe defects in appressorium development than observed in the single deletion strains. *cda2/cbp1* failed to form appressoria by 8 hpi, as in *cbp1*, but extending the incubation period to 24 hpi did not result in appressorium development, in contrast to *cbp1*. Instead, germ tubes appeared even more elongated, yet remained smooth and undifferentiated (Figure 3.5). This phenotype was also observed when conidia were germinated on other hydrophobic surfaces, including plastic and Parafilm (not shown). *CDA2* and *CBP1* therefore exhibit partial redundancy. Conversely, deletion of

Figure 3.4 *(following page)*: Targeted deletion of *CBP1*, *CDA2* and *CDA3*. **A**) Targeted gene deletion strategy, whereby the gene of interest is replaced by a gene encoding resistance to an antibiotic, due to homologous recombination between flanking sequences (green). Southern blots showing successful single **B**), double **C**) and triple **D**) knockouts of chitin deacetylases. Blots containing restriction digested gDNA of putative deletion strains were hybridised with α-^{32}P labelled DNA homologous to the hygromycin, bialaphos or sulphonylurea resistance genes respectively. The cartoon above each blot shows the expected band size based upon the position of the restriction enzyme sites at each locus. Size markers show band size in kilobases (kb).

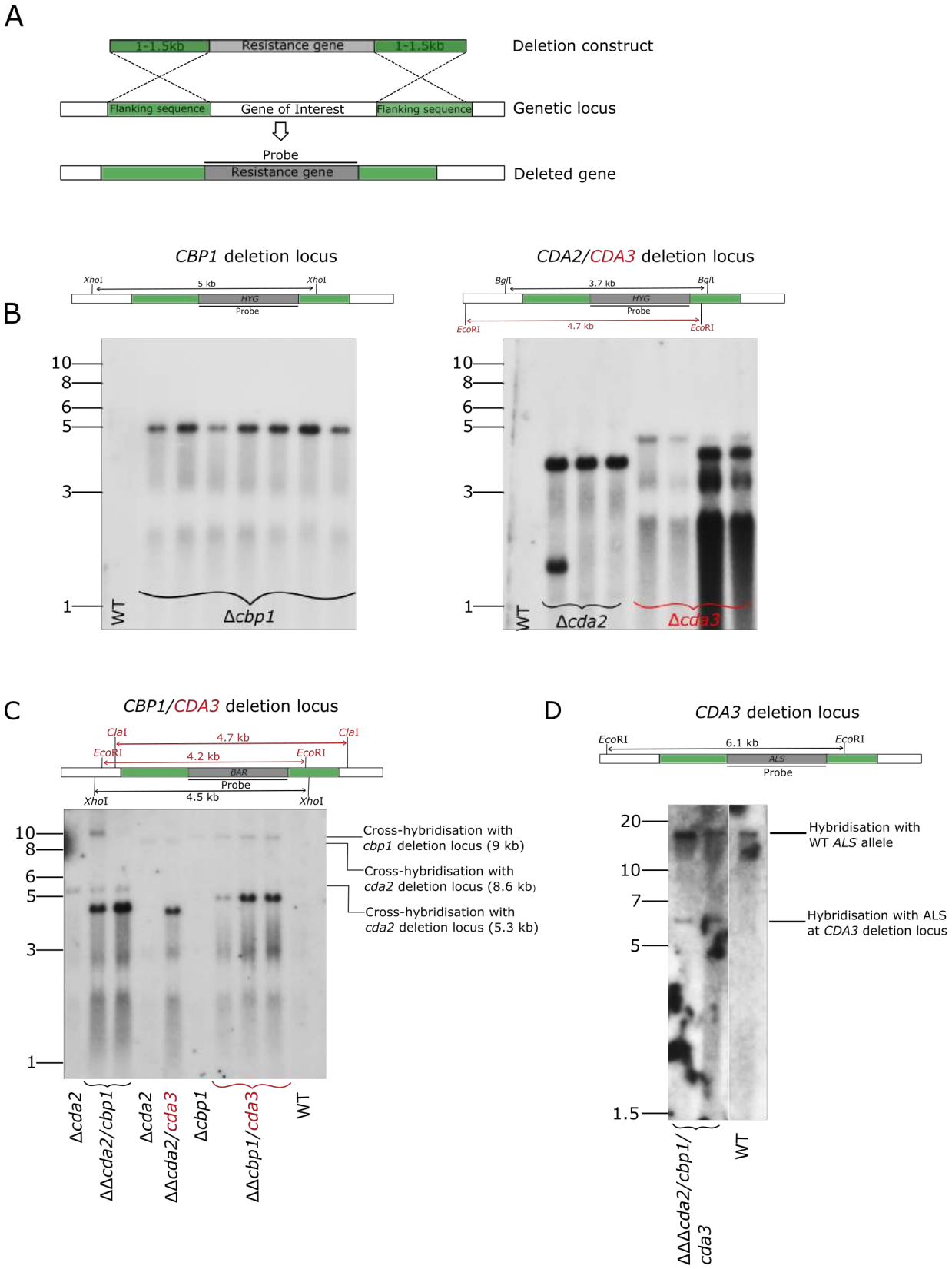
A
1-1.5kb
Resistance gene
1-1.5kb
Deletion construct
Flanking sequence
Gene of Interest
Flanking sequence
Genetic locus
Probe
Resistance gene
Deleted gene
B
CBP1 deletion locus
XhoI
5 kb
XhoI
HYG
Probe
10
8
6
5
3
1
WT
Δcbp1
CDA2/CDA3 deletion locus
BglI
3.7 kb
BglI
HYG
Probe
EcoRI
4.7 kb
EcoRI
10
8
6
5
3
1
WT
Δcda2
Δcda3
C
CBP1/CDA3 deletion locus
ClaI
4.7 kb
ClaI
EcoRI
4.2 kb
EcoRI
BAR
Probe
XhoI
4.5 kb
XhoI
10
8
6
5
3
1
Cross-hybridisation with cbp1 deletion locus (9 kb)
Cross-hybridisation with cda2 deletion locus (8.6 kb)
Cross-hybridisation with cda2 deletion locus (5.3 kb)
Δcda2
ΔΔcda2/cbp1
Δcda2
ΔΔcda2/cda3
Δcbp1
ΔΔcbp1/cda3
WT
D
CDA3 deletion locus
EcoRI
6.1 kb
EcoRI
ALS
Probe
20
10
7
5
1.5
Hybridisation with WT ALS allele
Hybridisation with ALS at CDA3 deletion locus
ΔΔΔcda2/cbp1/cda3
WT

CDA3 had no additive effects on appressorium development under the conditions tested: *cbp1/cda3* demonstrated an identical phenotype to *cbp1*, and *cda2/cbp1/cda3* an identical phenotype to *cda2/cbp1*.

Germlings of the deletion strains were then stained for chitosan, using the chitosan-specific probe OGA488. Germlings of the WT strain developed on an artificial hydrophobic surface for 16 hr demonstrated strong staining of the cell wall in germ tubes and appressoria as described previously, and similar staining was observed in *cda2/cda3* (Figure 3.5). In *cbp1* and *cbp1/cda3* appressoria continued to show labelling with OGA488, but little fluorescence was observed on the elongated germ tubes of these strains. However, in *cda2/cbp1* and *cda2/cbp1/cda3* no chitosan staining was observed at all, suggesting complete loss of chitin deacetylation in these strains, and providing further evidence of the redundancy between *cbp1* and *cda2*. Staining was also performed at 24 hpi. At this timepoint, a small proportion (10-20%) of germ tubes in *cda2/cbp1* and *cda2/cbp1/cda3* (Figure 3.5) did form appressoria. However, no chitosan was detected in these appressoria (Figure 3.14B), suggesting that it is not an absolute requirement for appressorium morphogenesis.

The highly elongated germ tubes observed in *cbp1*, *cda2/cbp1* and *cda2/cbp1/cda3* were a curious feature. In order to determine whether these germ tubes were a single cell or were in fact multiple cells, Calcofluor White staining was performed. This revealed that the germ tubes were indeed septate; septa appeared to be distributed along the germ tubes of *cbp1* and *cda2/cbp1* at regular intervals (Figure 3.5C).

Taken together, these data suggest a clear link between the loss of chitin deacetylation, and loss of appressorium development. However, the mechanism by which chitin deacetylation promotes appressorium development remains unclear.

Localization of chitin deacetylases

In an attempt to shed further light on the mechanism by which chitin deacetylation by Cbp1 and Cda2 promotes appressorium development, fluorescent protein fusions were created. *CBP1* and *CDA2* (without the stop codons) were amplified using primer pairs 47/48 and 49/50 respectively (Appendix E), then cloned into the pUCAP vector at the *Asc*I site (Appendix D). This created a C-terminal mCherry fusion to the respective proteins

A

Strain	Germination (%)	Appressoria (8hpi) (%)	Appressoria (24hpi) (%)
WT	54 ± 4	84 ± 7	96 ± 1
Δ*cbp1*	74 ± 2	3 ± 3	83 ± 4
Δ*cda2*	49 ± 7	78 ± 7	95 ± 3
Δ*cda3*	53 ± 2	77 ± 3	96 ± 2
ΔΔ*cda2/cbp1*	58 ± 18	0 ± 0	27 ± 20
ΔΔ*cda2/cda3*	66 ± 10	88 ± 1	97 ± 1
ΔΔ*cbp1/cda3*	41 ± 9	9 ± 8	78 ± 4
ΔΔΔ*cda2/cbp1/cda3*	ND	0 ± 0	7 ± 6

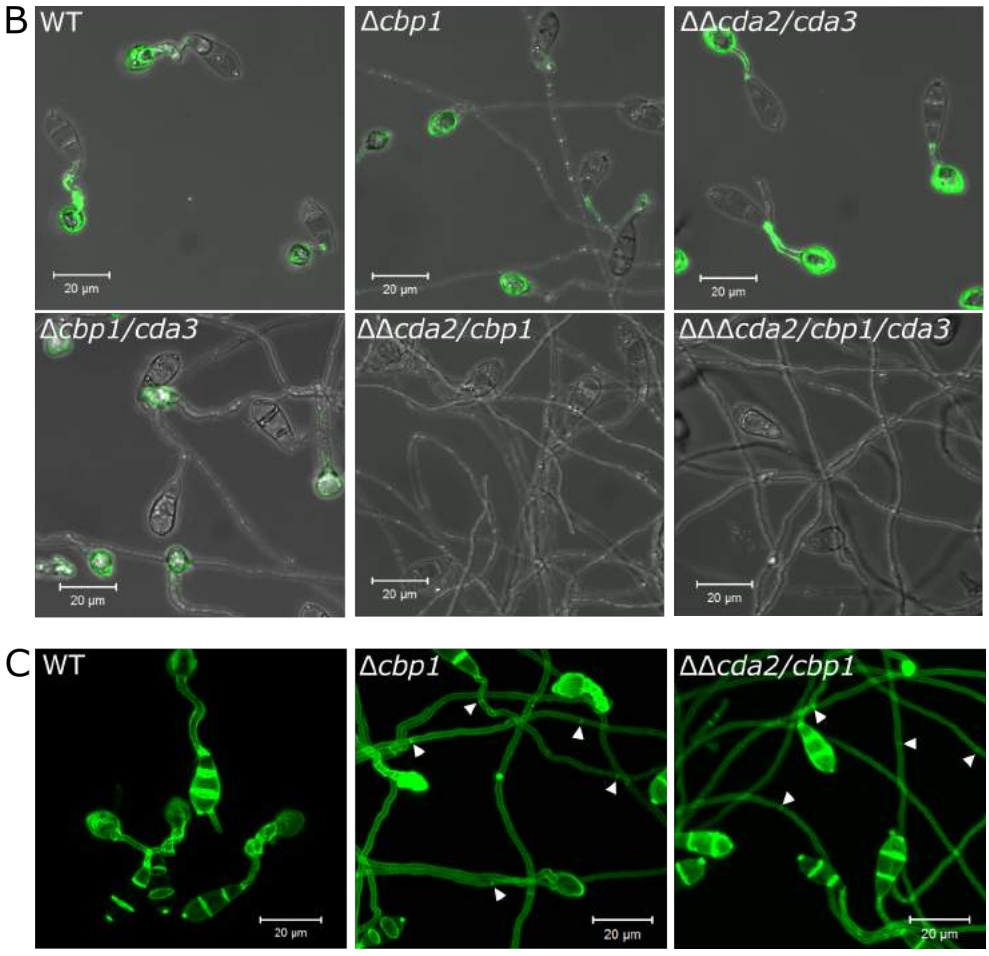

Figure 3.5: Appressorium development and chitin deacetylation are dramatically reduced in the *CDA* deletion strains. **A**) Table showing percentage conidial germination (at 1 hpi), and appressorium formation (at 8 hpi) on an artificial inductive surface (Menzel glass coverslips) (± SD, n=3), showing highly reduced appressorium formation in certain deletion strains. **B**) Fluorescent labelling of chitosan on the germlings of *CDA* deletion strains at 16 hpi, showing lack of staining in the *cda2/cbp1* and *cda2/cbp1/cda3* strains. **C**) Calcofluor White staining of germlings at 16 hpi, showing abnormally elongated, septate germ tubes (white arrow heads). Scale bars: 20 µm.

when expressed. In both cases, expression of the fusion constructs was driven by native promoters: ∼2 kb of upstream sequence was included for *CBP1mCherry*, and ∼1.3 kb for *CDA2mCherry* (due to proximity of a neighbouring gene). The fusion constructs were transformed into the deletion background strains, and the resulting antibiotic-resistant transformants screened for fluorescence. For each construct, several transformant lines were identified exhibiting identical patterns of fluorescence (listed in Appendix F), which were examined during appressorium development on a hydrophobic glass surface.

Strains expressing Cbp1:mCherry exhibited fluorescence at all stages of appressorium development (Figure 3.6). Unexpectedly, fluorescence was observed at conidial apices (Figure 3.6A), even in conidia which had not yet been harvested from the mycelium. Substantial intracellular fluorescence was also observed at this stage, most likely localized to vacuoles. During stages of germ tube growth (1-2 hpi), weak fluorescence was observed at the lateral walls of the germ tube, but not the tip (Figure 3.6B). In addition, small punctae of intracellular fluorescence were sometimes observed along the length of the germ tube which could either be vacuoles or other intracellular compartments of unknown identity. At later stages of appressorium development (3-5 hpi), wall-localized fluorescence became stronger and localized to the entire germ tube and appressorium, although intracellular fluorescence was still apparent in some appressoria (Figure 3.6C). The appressorial wall remained fluorescent even at later stages (8-16 hpi), although intensity decreased noticeably. In order to determine whether the Cbp1:mCherry fusion protein was functional, appressorium development was tested in the complemented strains. Conidia of the complemented strains germinated on an artificial hydrophobic surface for 8 hr demonstrated identical appressorium development to the WT strain (Figure 3.6D), confirming the functionality of Cbp1:mCherry. This was found for all three lines of the complemented strain, but only quantified for one.

Similar to Cbp1:mCherry, strains expressing Cda2:mCherry also exhibited fluorescence during appressorium development, although it was notably absent at the very earliest stages of conidial germination i.e. in conidia or in germ tubes. The earliest point at which Cda2mCherry fluorescence was observed was typically after hooking of the germ tube (Figure 3.6E). Strong fluorescence was also observed during subsequent appressorium formation (Figure 3.6F), and remained present at later stages (8-16 hpi), as

observed with Cbp1:mCherry. Unlike Cbp1:mCherry however, fluorescence was only very rarely observed intracellularly. Since the *cda2* strain was apparently identical to the WT strain, functionality of the fusion protein could not be determined in the complemented strain.

An attempt was also made to create a Cda3:eGFP fusion protein. Unfortunately, no fluorescent transformants were obtained for this construct, suggesting instability of the fusion protein.

Cbp1:mCherry and Cda2:mCherry colocalize with Chs7:2xYFP

Chitin synthase 7 (Chs7) has previously been found to be required for appressorium development in *M.oryzae* (Odenbach et al., 2009; Kong et al., 2012). In fact, deletion of *CHS7* resulted in a phenotype that is identical to that observed in *cda2/cbp1* and *cda2/cbp1/cda3*. Furthermore, Chs7:eGFP localized to germ tubes and developing appressoria, in a similar fashion to Cbp1:mCherry and Cda2:mCherry. It was hypothesized that these proteins may colocalize, perhaps indicating a degree of coordination between chitin synthesis and deacetylation. To test this hypothesis, first a Chs7:eGFP fusion was created, in precisely the same way as reported previously (Kong et al., 2012): *CHS7* was amplified using primers 58 and 59 (Appendix E), and cloned into the AscI site of the pUCAP plasmid (Appendix D). This created a C-terminal eGFP fusion in the resulting protein, which was expressed by the native promoter (∼1 kb of upstream sequence). This construct was previously shown to be able to complement the defects in the *chs7* mutant, suggesting full functionality of the protein (Kong et al., 2012). However, when transformed into the WT background strain, only weak fluorescence was observed, which made imaging challenging. To overcome this problem, a new construct was created, in which two copies of YFPvenus replaced the single eGFP. Transformants expressing this construct displayed stronger fluorescence, but with apparently identical localization to the eGFP construct. The *CBP1:mCherry* and *CDA2:mCherry* constructs were transformed into the *CHS7:2xYFP* background strain, and resulting antibiotic-resistant transformants screened for fluorescence. As before, several independent lines for each construct were visualized, exhibiting identical patterns of fluorescence (listed in Appendix F).

In strains co-expressing Chs7:2xYFP and Cbp1:mCherry, partial colocalization were

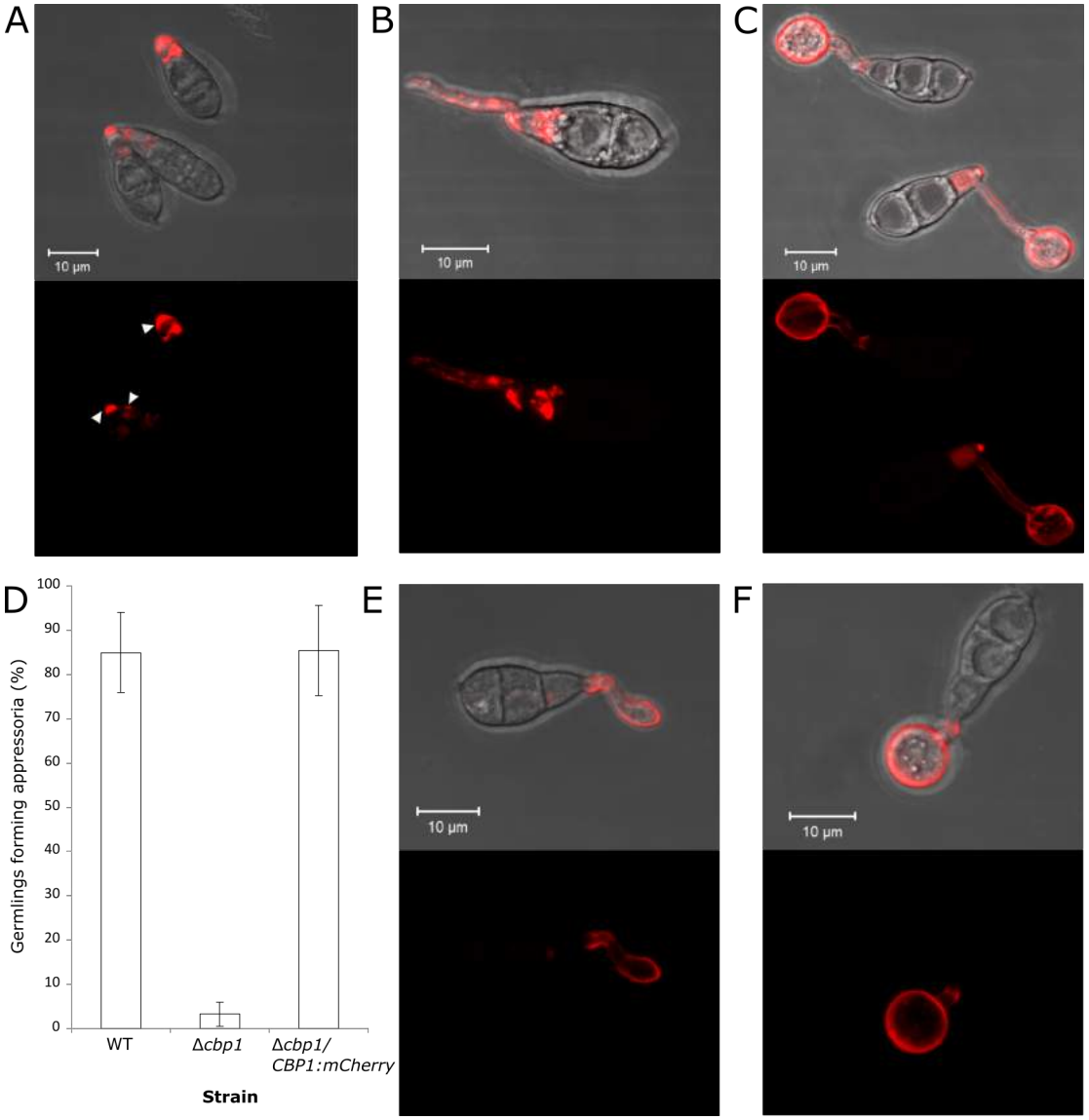

Figure 3.6: Localization of mCherry tagged Cbp1 and Cda2. A-C) Confocal fluorescence microscopy images of germlings expressing Cbp1:mCherry, showing fluorescence in conidial apices (white arrow heads), germ tubes and appressoria at 0-4 hpi on hydrophobic glass. **D**) Successful complementation of *CBP1* deletion strain by expression of the *CBP1:mCherry* fusion construct. Appressorium development was fully restored in the complemented strain at 8 hpi. Error bars show SD, n=3. **E** & **F**) Confocal fluorescence microscopy images of germlings expressing Cda2:mCherry at 2-4 hpi. Scale bars: 10 µm.

observed, depending on the developmental stage in question (Figure 3.7). During germ tube growth, Cbp1:mCherry localized to lateral walls of the germ tube, and intracellularly as described previously. Chs7:2xYFP also localized intracellularly, and partially colocalizaed with Cbp1:mCherry in the germ tube, and particularly in the apical cell of conidia (Figure 3.7A). However, unlike Cbp1:mCherry, Chs7:2xYFP was observed at plasma membrane of the germ tube tip, as reported previously (Odenbach et al., 2009), but not at the lateral walls. Thus, colocalization of these proteins at the cell periphery was not observed during germ tube growth. During appressorium development, colocalization was observed; Chs7:2xYFP localized to the cell periphery of the appressorium, as did Cbp1:mCherry (Figure 3.7B). Importantly however, the distribution of fluorescence was not identical for both fusion proteins. Chs7:2xYFP appeared to be restricted to the bottom 1-2 μm of the appressorium, forming a band of fluorescence at the base of the appressorium. In contrast, Cbp1:mCherry localized to the entire appressorium. Intracellular fluorescence was also observed during appressorium formation for Chs7:2xYFP, which also colocalized with Cbp1:mCherry.

In strains co-expressing Chs7:2xYFP and Cda2:mCherry, partial colocalization at the cell periphery was observed at the germ tube hooking stage (3.7C). In developed appressoria, Chs7:2xYFP localized to the cell periphery at the base of the appressorium, and Cda2:mCherry localized to the entire cell wall of the appressorium (3.7D).

Exogenous chitosan can rescue *CDA* deletion strains

The highly elongated germ tubes observed upon deletion of *CDA* genes were similar to that resulting from deletion of the hydrophobin gene *MPG1* (Talbot et al., 1993). Interestingly, it was reported that appressorium development could be rescued in the *mpg1* mutant by co-inoculation with WT conidia, suggesting that Mpg1 could act in trans (Beckerman and Ebbole, 1996). To test whether chitosan could also act in a similar manner, exogenous chitosan was added to conidia of the *cda* mutants during germination on an artificial hydrophobic surface. Surprisingly, the addition of 0.01% (w/v) or 0.001% (w/v) chitosan could restore appressorium development in all of the *cda* deletion strains (Figure 3.8). In the *cbp1*, *cda2/cbp1* and *cbp1/cda3* strains, 70-85% of conidia formed appressoria after an 8 hr incubation in the presence of 0.01% or 0.001% chitosan,

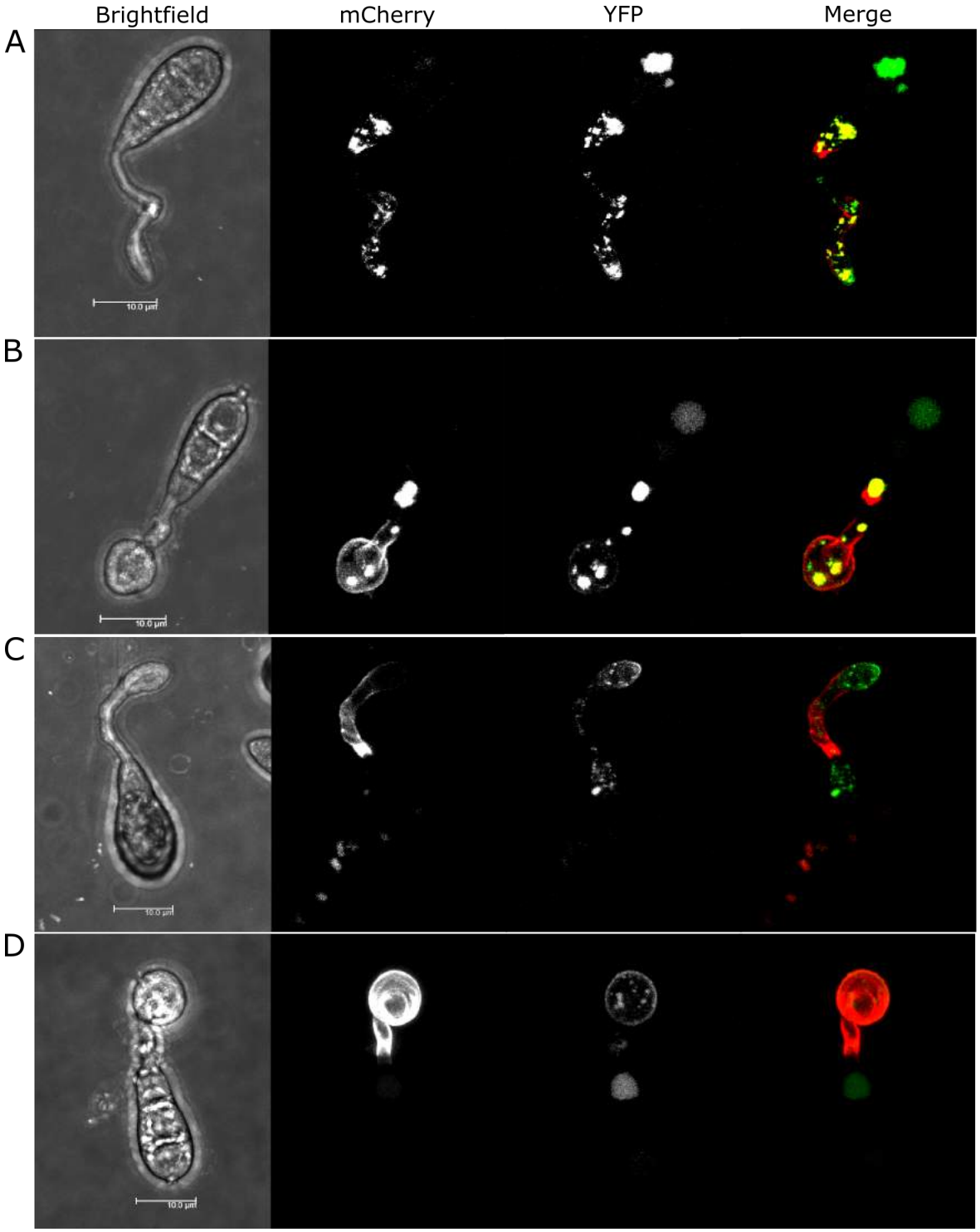

Figure 3.7: Cbp1:mCherry and Cda2:mCherry colocalize with YFP-tagged Chitin Synthase VII. Confocal fluorescence microscopy images, showing colocalization of **A** & **B**) Cbp1:mCherry and **C** & **D**) Cda2:mCherry with YFP tagged chitin synthase VII, during appressorium development. Colocalization at the cell periphery was particularly evident during germ tube hooking and early stages of appressorium differentiation. In addition, colocalization of intracellular punctae in strains co-expressing *CBP1:mCherry* and *CHS7:2xYFP* also occurred. Fluorescence has been pseudocoloured white in the mCherry and YFP panels, for clarity. Scale bars: 10 μm. Note: Picture brightness and contrast have been increased to improve clarity upon printing.

compared with 0-10% in the control treatment (water). In the triple deletion strain *cda2/cbp1/cda3* rescue was slightly lower (55% ±17 and 70% ±16 appressoria at 8 hpi for 0.01% and 0.001% chitosan respectively), although extending in incubation time was observed to increase rescue (not shown). In the WT strain, 70-85% of conidia formed appressoria in all treatments. To further investigate the relationship between chitosan and appressorium development, different derivatives and formulations of chitosan were tested for their ability to restore appressorium development in the deletion strains (structures are shown in Figure 3.8C). Glycol chitosan, a soluble derivative of chitosan could restore appressorium development in *cda2/cbp1/cda3* at a concentration of 0.01% but not 0.001%. Carboxymethylchitosan, in which an anionic carboxymethyl group has been introduced, could not restore appressorium formation at either concentration. Lastly, the addition of chitosan in oligomeric form (oligochitosan) could partially restore appressorium formation at 8 hpi (with more complete rescue observed after a 16hr incubation (not shown)), whereas glucosamine showed no restorative effects at all. Taken together, these data suggest that the cationic nature of exogenous chitosan is the most important factor determining rescue, with steric factors also having some influence. Polymer length appears to be of little importance, given the broad ranges capable of restoring appressorium development.

To investigate how exogenous chitosan was able to restore appressorium development in the *cda* mutants, fluorescently labelled chitosan was used. FITC-chitosan was synthesized according to Qaqish *et al* (Qaqish and Amiji, 1999), and added to conidia of the WT and *cda2/cbp1/cda3* strains germinating on an artificial hydrophobic surface. After a 16hr incubation, the FITC-chitosan was removed by washing, and the germlings imaged on a confocal microscope. The FITC-chitosan was able to restore appressorium formation in *cda2/cbp1/cda3*, and showed clear localization to the cell wall of germ tubes and appressoria (Figure 3.9). In the WT strain, weak fluorescence was occasionally observed

Figure 3.8 *(following page)*: Exogenous chitosan can restore appressorium development in the *CDA* deletion strains. **A**) Rescue of appressorium formation in the *cda2/cbp1/cda3* deletion strain with exogenously supplied chitosan (0.01%). Pictures were taken at 8 hpi, scale bars: 20 μm. **B**) Comparison of appressorium formation in WT (white bars) and *cda2/cbp1/cda3* deletion strain (grey bars) in the presence of different derivatives and formulations of chitosan (shown in **C**). Conidia were germinated on an artificial inductive surface for 8 hr in the presence of different types of chitosan at a final concentration of 0.01% or 0.001%, after which appressorium formation was scored. Error bars show SD, n=3. DDA: degree of deacetylation.

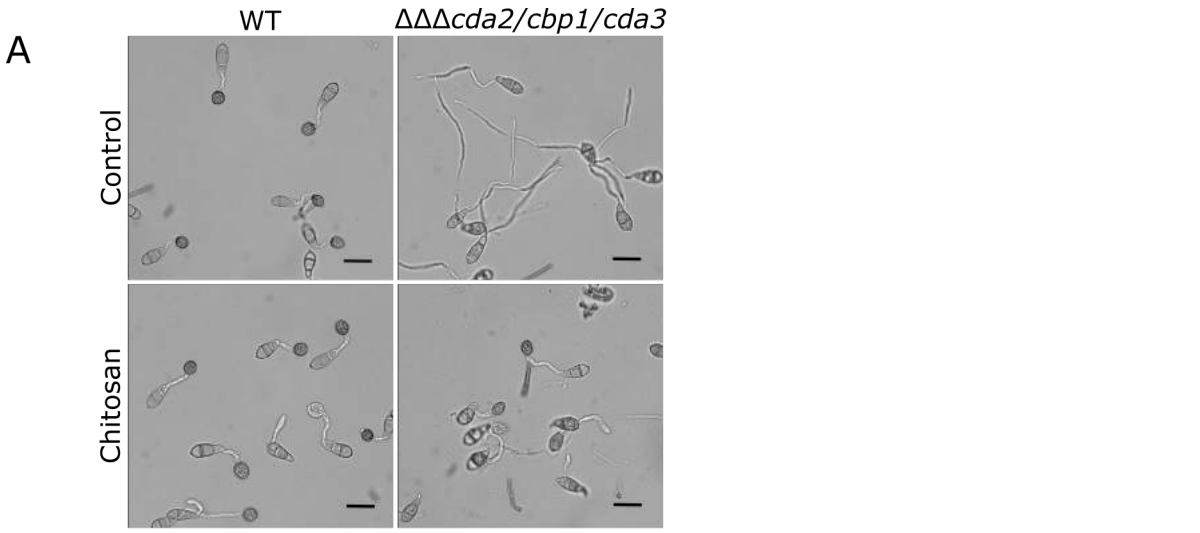
A
WT
ΔΔΔcda2/cbp1/cda3
Control
Chitosan

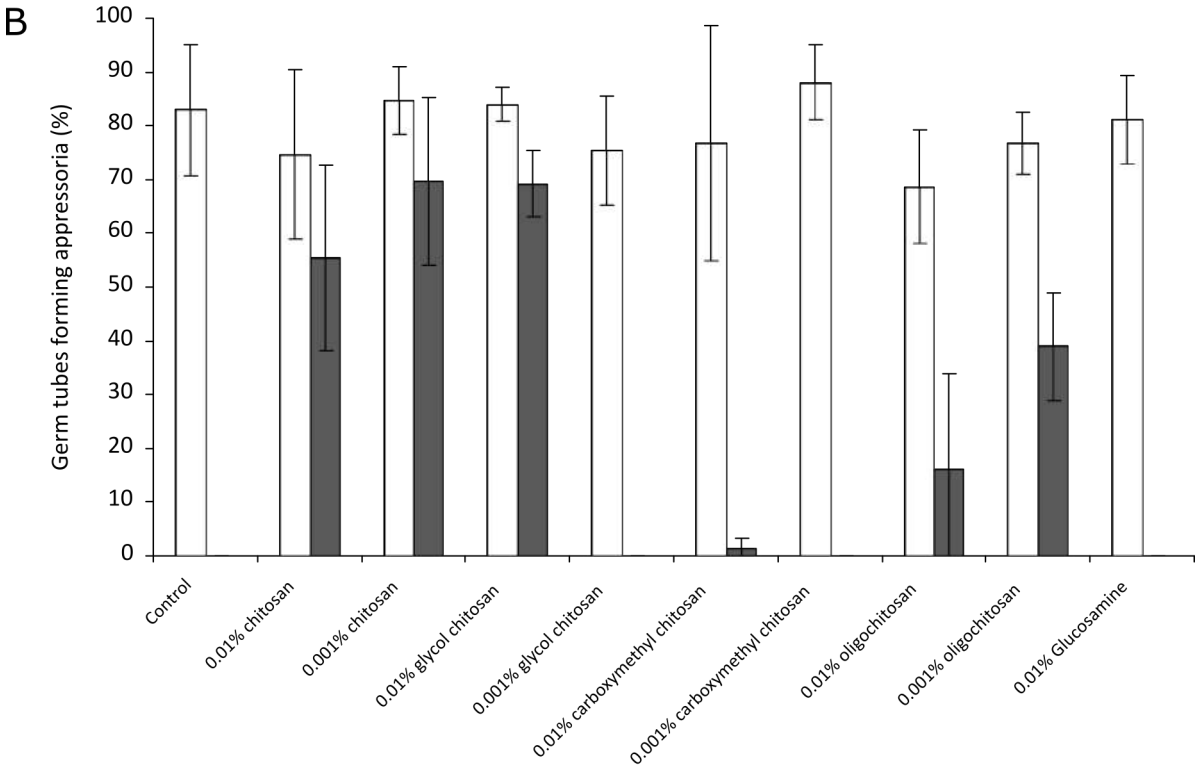
B
Germ tubes forming appressoria (%)
100
90
80
70
60
50
40
30
20
10
0
Control
0.01% chitosan
0.001% chitosan
0.01% glycol chitosan
0.001% glycol chitosan
0.01% carboxymethyl chitosan
0.001% carboxymethyl chitosan
0.01% oligochitosan
0.001% oligochitosan
0.01% Glucosamine

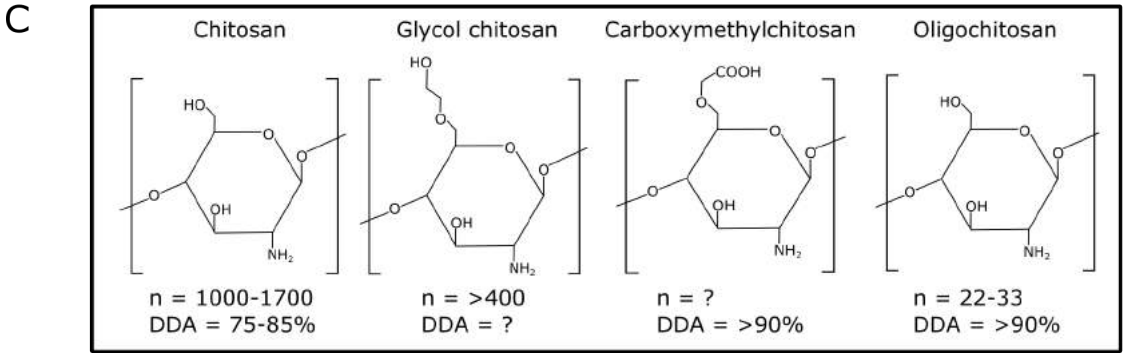
C
Chitosan
Glycol chitosan
Carboxymethylchitosan
Oligochitosan
n = 1000-1700
DDA = 75-85%
n = >400
DDA = ?
n = ?
DDA = >90%
n = 22-33
DDA = >90%

in the germ tubes. Exogenous chitosan is therefore incorporated into the cell wall of the deletion strains.

In a previous experiment, chitosan was observed to localize to the germ tube prior to appressorium development (Figure 3.1). To determine whether germ tube-localized chitosan was sufficient to induce appressorium development, FITC-chitosan was added to germinating conidia of the WT or *cda2/cbp1/cda3* strains for just 2 hr, before being washed off, and the germlings incubated for a further 16 hr. In this way, chitosan was only present during the initial germ tube stage of germling morphogenesis, and was removed before appressorium development occurred. Surprisingly, appressorium development was restored in the deletion strain by this short incubation with FITC-chitosan. In this case, fluorescence was only observed in the germ tube, and not the appressoria of *cda2/cbp1/cda3* germlings, with similar localization in the WT (Figure 3.9B).

Lastly, to investigate whether chitosan could restore appressorium development at later stages of germling morphogenesis, conidia were incubated for 16hr on an artificial surface, then FITC-chitosan added, and the conidia incubated for a further 8hr. Again, appressorium development was restored in the *cda2/cbp1/cda3* strain, although of course the germ tubes were highly-elongated in this case (Figure 3.9C). Fluorescence was observed along the entire length of these elongated germ tubes, although appeared to be more intense at regions proximal to the point of emergence from the conidium. In this case, WT germlings also exhibited fluorescence in both germ tubes and appressoria, contrary to previous observations from the first experiment.

The incorporation of chitosan into the cell walls of *cda* mutants was a curious phenomenon. As described previously, carboxymethylchitosan, in which an anionic carboxy group is introduced onto the normally cationic chitosan, was unable to restore appressorium development. Thus, charge appears to be a critical factor in the rescue of appressorium development by exogenous chitosan. This led to the hypothesis that an electrostatic interaction between the polycationic chitosan, and an anionic component of the cell wall may be responsible for chitosan incorporation. However, little is known of anionic cell wall components, although a number of previous studies have detected uronic acids as a component of the fungal cell wall, in *Botrytis cinerea* (Cantu et al., 2009), *Rhizopus oryzae* (Mélida et al., 2015) and a number of *Fusarium* species (Schoffelmeer et al., 1999).

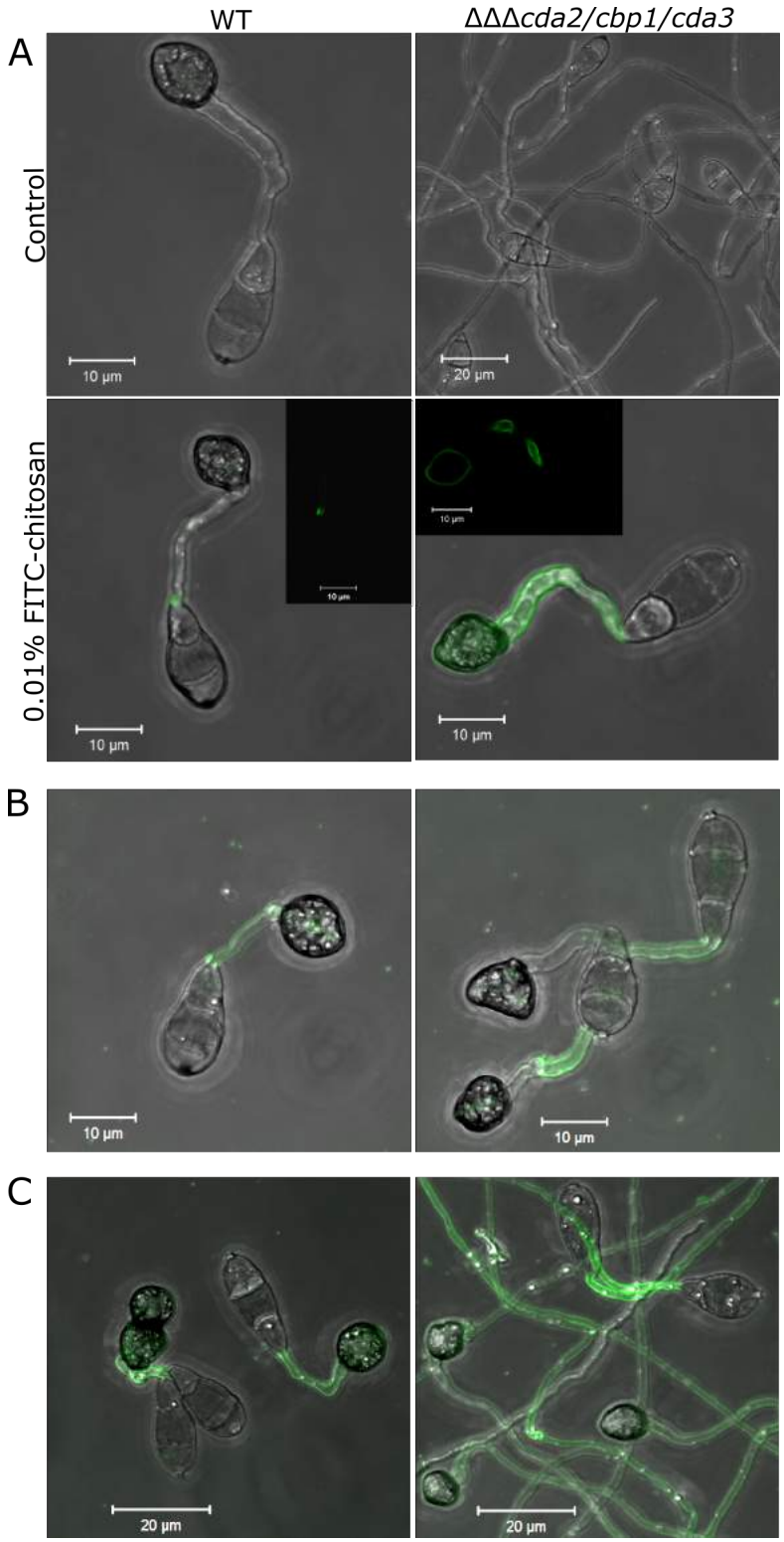

Figure 3.9: Exogenous chitosan is incorporated into the cell wall of *CDA* deletion strains. **A**) Rescue of appressorium development in the *cda2/cbp1/cda3* deletion strain using exogenous, fluorescently labelled chitosan following a 16hr incubation, showing clear localization to the cell wall of the germ tube and appressorium (single z-section inset). **B**) Rescue of appressorium development after a 2hr incubation with FITC-chitosan, followed by washing and a further 16hr incubation, showing germtube-localized FITC-chitosan. **C**) Rescue of appressorium development after addition of FITC-chitosan at 16 hpi, and incubation for a further 8 hr. Note: Picture brightness and contrast have been increased in B and C to improve clarity upon printing.

As discussed previously, OGA488, a fluorescently labelled oligomer of galacturonic acid is able to act as a highly-specific probe for chitosan, due to a specific electrostatic interaction. However, the inverse of this is also true: fluorescently labelled oligomers of chitosan (named COS488) can act as a highly specific probe for poly-β1,4-galacturonic acid (PGA) (Mravec et al., 2014). To test whether PGA is a component of the *M.oryzae* cell wall, vegetative hyphae and germlings were labelled with COS488. Only weak fluorescence was observed in hyphae stained with COS488, with some internalization of the probe evident (Figure 3.10B). Stronger fluorescence was observed in the cell walls of appressoria and germ tubes in the WT germlings, and on the elongated germ tubes of the triple deletion strain (Figure 3.10). Staining of the *cda2/cbp1/cda3* germlings was similar to that observed with the incorporation of FITC-chitosan at 16 hpi (Figure 3.9C), in that fluorescence was stronger at parts of the germ tube proximal to the point of emergence from the conidium. In order to independently verify this data, attempts were made to stain germlings with the anti-pectin antibodies JIM5, JIM7 and LM19 (a generous gift from Ian Moore, University of Oxford). These antibodies all recognize epitopes containing polygalacturonic acid, although with some dependancy upon degrees and patterns of methyl-esterification (Mravec et al., 2014). However, no staining of WT germlings was observed with any of these antibodies (not shown). In a separate experiment, germlings were treated with a pectinase enzyme cocktail, which included polygalacturonase. WT and *cda2/cbp1/cda3* germlings at 16 hpi were treated with 12.5 units of the enzyme cocktail for 5 hr, then washed and stained with COS488. However, no consistent reduction in labelling was observed in the WT germlings (not shown). Intriguingly however, treatment of *cda2/cbp1/cda3* germlings with the pectinase cocktail led to complete failure of the germlings to adhere to the hydrophobic glass surface, which prevented successful staining.

Pathogenicity is unaffected in the *CDA* deletion strains

Appressorium development is highly defective on artificial surfaces in *cda* mutants. It was therefore expected that pathogenicity would be reduced in these strains. To determine whether this was the case, equal concentrations of conidia of the deletion strains were inoculated onto rice leaves. As reported previously for *cbp1* (Kamakura et al., 2002) and

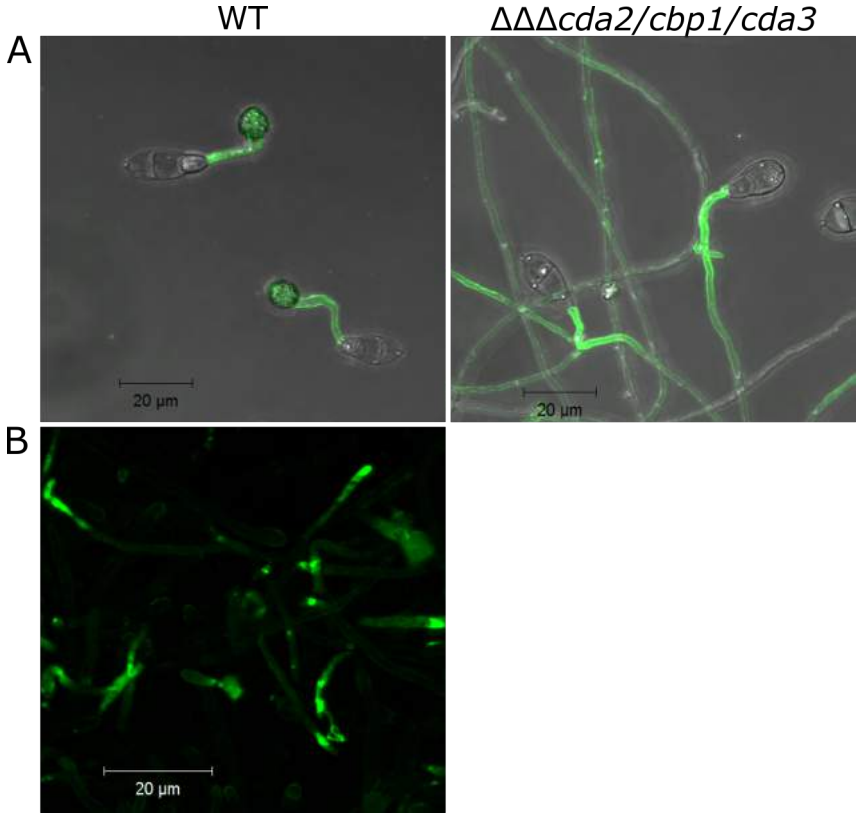

Figure 3.10: Polygalacturonic acid may be a component of the cell wall in *M.oryzae*. **A**) Labelling of WT and *cda2/cbp1/cda3* germlings at 16 hpi with the COS488 probe, which has been used to localize polygalacturonic acid (Mravec et al., 2014). **B**) Staining of WT mycelium with COS488, showing weak labelling of hyphae, and internalization of probe. Scale bars: 20 µm.

cda3 (Saitoh et al., 2012), and as expected for *cda2*, pathogenicity was unaffected (not shown). Surprisingly however, the double and triple deletion strains were also able to successfully infect rice leaves, causing similar lesion numbers to the WT strain (Figure 3.11). Previously, appressorium development was found to be restored in the *cbp1* strain on rice leaves (Kamakura et al., 2002). To see if this was also the case in the other deletion strains, rice leaf sheaths were inoculated with conidia of the *cda2/cbp1/cda3* strain, and incubated for 24 hr. This revealed that appressorium development was indeed restored upon germination on a leaf surface. Not only this, but the appressoria of *cda2/cbp1/cda3* were able to penetrate rice cells with similar efficiency to the WT: 67% (±7 (SD), n=3) of WT appressoria had invasive hyphae at 24 hpi, compared with 47% (±10 (SD), n=3) of *cda2/cbp1/cda3*. To see if this effect was specific to the rice leaf surface, the experiment was repeated on onion epidermis. Again, appressorium development was restored in the *cda2/cbp1/cda3* strain; conidia produced short germ tubes, and functional appressoria (as evidenced by visible invasive hyphae at 24 hpi) (Figure 3.11).

One factor that is present on leaves, but not artificial hydrophobic surfaces are the cuticular waxes. To test whether wax was sufficient to restore appressorium development in the *cda2/cbp1/cda3* strain, hydrophobic glass coverslips were coated with the wax molecule 1-octacosanol, which has previously been used to induce appressorium development in *M.oryzae* (Liu et al., 2011). Conidia of *cda2/cbp1* (not shown) and *cda2/cbp1/cda3* germinated on this surface for 24 hr did form appressoria, but germ tubes remained extremely elongated, unlike on onion epidermis or rice leaves (Figure 3.11). Unfortunately, accurate quantification of appressorium development on this surface was challenging using brightfield microscopy, as the opacity of the wax crystals prevented clear visualization of germlings.

Figure 3.11 *(following page)*: Pathogenic development in the *CDA* deletion strains is normal on plant surfaces. A) Pathogenicity of the *cda2/cbp1/cda3* deletion strain on rice leaves, showing comparable lesion density to the WT strain (two independent triple deletion lines are shown). A mock inoculation of 0.2% gelatine was included as a negative control. Scale bars: 1 cm. **B**) Quantification of lesion numbers on rice leaves inoculated with different *cda* deletion strains, normalized to the Guy11 WT strain (±SD, n=3). **C**) Pathogenic development of the WT and *cda2/cbp1/cda3* strains on rice leaves, onion epidermis, and glass slides coated with the wax molecule 1-octacosanol. Pathogenic development was fully restored in the *CDA* deletion strains on plant surfaces and partially restored by the presence of wax molecules (white arrow heads show appressoria). Scale bars: 20 μm.

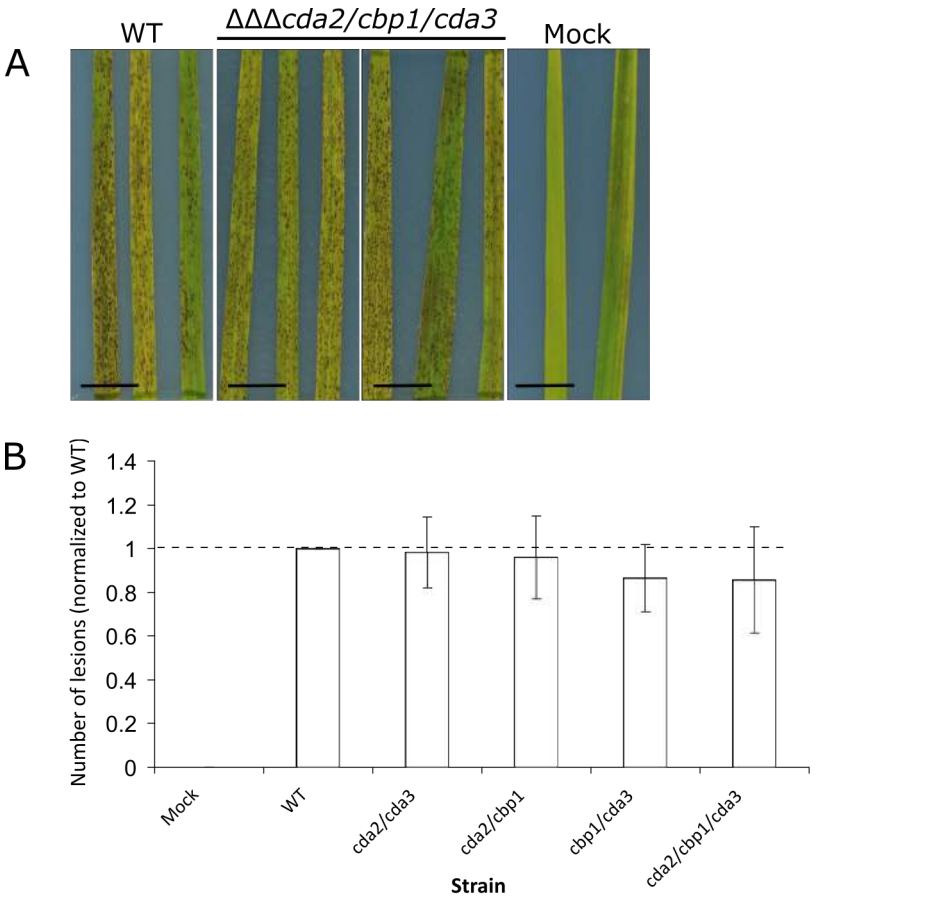
A
WT
ΔΔΔcda2/cbp1/cda3
Mock
B
Number of lesions (normalized to WT)
1.4
1.2
1
0.8
0.6
0.4
0.2
0
Mock
WT
cda2/cda3
cda2/cbp1
cbp1/cda3
cda2/cbp1/cda3
Strain
C
Rice leaf sheath
Onion epidermis
Wax (1-octacosanol)
WT
ΔΔΔcda2/cbp1/cda3

Chitosan is not required for appressorium development on plant surfaces

The rescue of appressorium development on plant surfaces was a perplexing result. It was hypothesized that chemical factors present on the leaf surface (e.g. wax, cutin) could cause upregulation of additional chitin deacetylases, which are functionally redundant and can therefore restore chitin deacetylation. To test this, conidia of the *cda2/cbp1/cda3* and WT strains were germinated on rice leaf sheaths or onion epidermis, then stained with the chitosan-specific probe OGA488. This revealed that chitosan remained completely absent in the triple deletion strain, whilst strong labelling of germ tubes and appressoria was observed in the WT (Figure 3.12). This again suggests that chitosan is not an absolute requirement for appressorium development; instead, this requirement appears to be surface dependant.

The appressoria of *M.oryzae* contain an impermeable melanin layer in their cell wall. To test whether the melanin was preventing detection of chitosan in the appressoria of *cda2/cbp1/cda3*, two approaches were taken. The first involved staining germlings for chitosan at 4 hpi, prior to melanization of the appressoria. However, staining with OGA488 remained completely absent in unmelanized *cda2/cbp1/cda3* germlings, suggesting the melanin was not preventing the detection of chitosan (Figure 3.12B). The second approach was to germinate conidia in the presence of tricyclazole, an inhibitor of melanin biosynthesis, prior to staining for chitosan with OGA488. Unexpectedly, a dramatic reduction in OGA488 labelling was observed in tricyclazole treated germlings of the WT strain. This was true of germlings developed on both onion epidermis (not shown) and on an artificial hydrophobic surface (Figure 3.12C).

Chemical inducers can restore appressorium development in *CDA* deletion strains

Appressorium development in *M.oryzae* is controlled by a number of regulatory pathways, which respond to the physical and chemical cues present on the leaf surface. Previously, it was shown that appressorium development in *cbp1* could be restored by the addition of chemical activators of these pathways, such as cAMP, 1,16 hexadecanediol (cutin monomer) or diacylglycerol (Kamakura et al., 2002). To investigate whether this is also the case in the other deletion strains, conidia were germinated on a hydrophobic glass

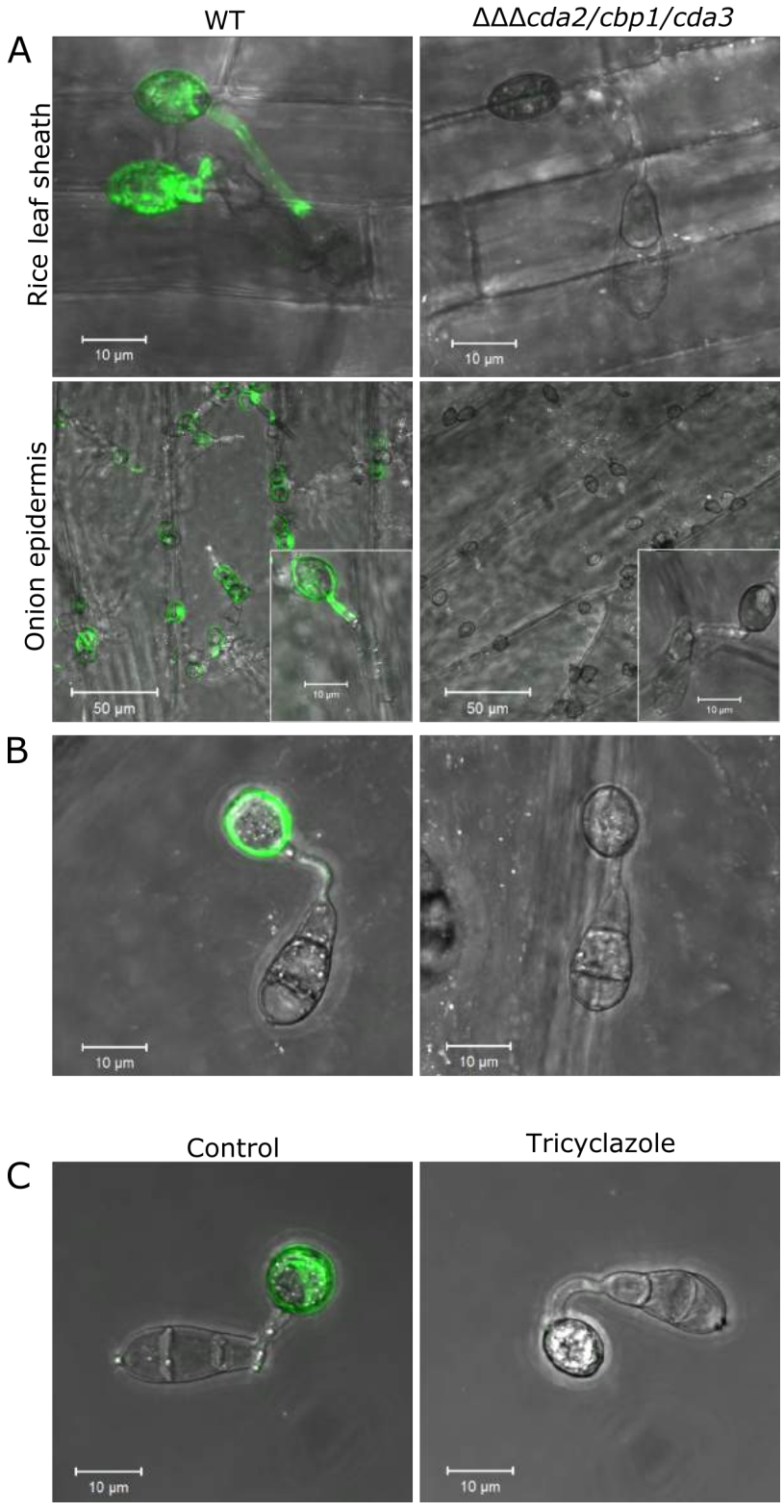

Figure 3.12: Restored pathogenic development on plant surfaces is not accompanied by restored chitin deacetylation. Fluorescent labelling of chitosan with OGA488 in WT and *cda2/cbp1/cda3* germlings germinated on **A**) rice leaf sheaths or onion epidermis for 24 hr, showing complete absence of chitosan in the *cda2/cbp1/cda3* strain. **B**) Fluorescent labelling of chitosan in WT and *cda2/cbp1/cda3* germlings germinated on onion epidermis for 4 hr, showing absence of chitosan in unmelanized appressoria of the deletion strain. **C**) Dramatic reduction of chitosan labelling following germination of WT conidia on an artificial hydrophobic surface in the presence of the melanin biosynthesis inhibitor tricyclazole for 16 hr. Scale bars: as stated in pictures

surface in the presence of 2.5 mM IBMX (a phosphodiesterase inhibitor that increases intracellular levels of cAMP), 200 μM 1,16 hexadecanediol (HDD, a cutin monomer) or 58 μM diacylglycerol (DAG, an activator of protein kinase C). Consistent with the previous report, all of the treatments could restore appressorium development in *cbp1* (Figure 3.13). Although the proportion of germ tubes forming appressoria was unchanged in this case (since observations were made at 16 hpi), germling morphology of *cbp1* was now similar to WT, as evidenced by a reduction in germ tube lengths (Figure 3.13). *cbp1/cda3* showed similar sensitivity to the chemical inducers as *cbp1*, although the proportion of germ tubes forming appressoria in the control treatment was slightly lower. Intriguingly however, *cda2/cbp1* was far less susceptible to all of the chemical inducers: neither HDD or DAG could restore appressorium development in this strain, and IBMX could only cause a partial rescue. The same was true in *cda2/cbp1/cda3*, except that IBMX was even less effective in this strain, with only a small proportion of germ tubes forming aberrant appressoria by 16 hpi. Rescue of *cbp1* by HDD and DAG is therefore dependant upon *CDA2*, and rescue by IBMX is dependant upon both *CDA2* and *CDA3*.

In order to further characterize the response of the *cda2/cbp1/cda3* mutant to chemical inducers, the above experiment was repeated, except observations were made at 24 hpi, and germinations were performed on both hydrophobic and hydrophilic glass surfaces. At 24 hpi on the hydrophobic surface, the response of *cda2/cbp1/cda3* germlings to the inducers was much the same as at 16 hpi, although the proportion of appressoria formed with IBMX was higher (Figure 3.14A). As with the appressoria formed on a plant surface, it was important to determine whether this rescue could be explained by restored chitin deacetylation. IBMX-treated germlings of the WT and *cda2/cbp1/cda3* strains were stained with OGA488 at 24 hpi. This revealed that chitosan was indeed present on the germ tubes and appressoria of the triple deletion strain, albeit to a much lesser extent than the WT germlings (Figure 3.14B). This suggests that rescue by IBMX is simply due to upregulation of redundant chitin deacetylases, as observed in *cbp1*, rather than the activation of an otherwise inactive signalling pathway.

Hydrophobicity is one of the key physical cues inducing appressorium development, and is perceived in a cAMP-dependant manner (Lee and Dean, 1993). In order to further examine the relationship between hydrophobic surface sensing, chitosan and the chemical

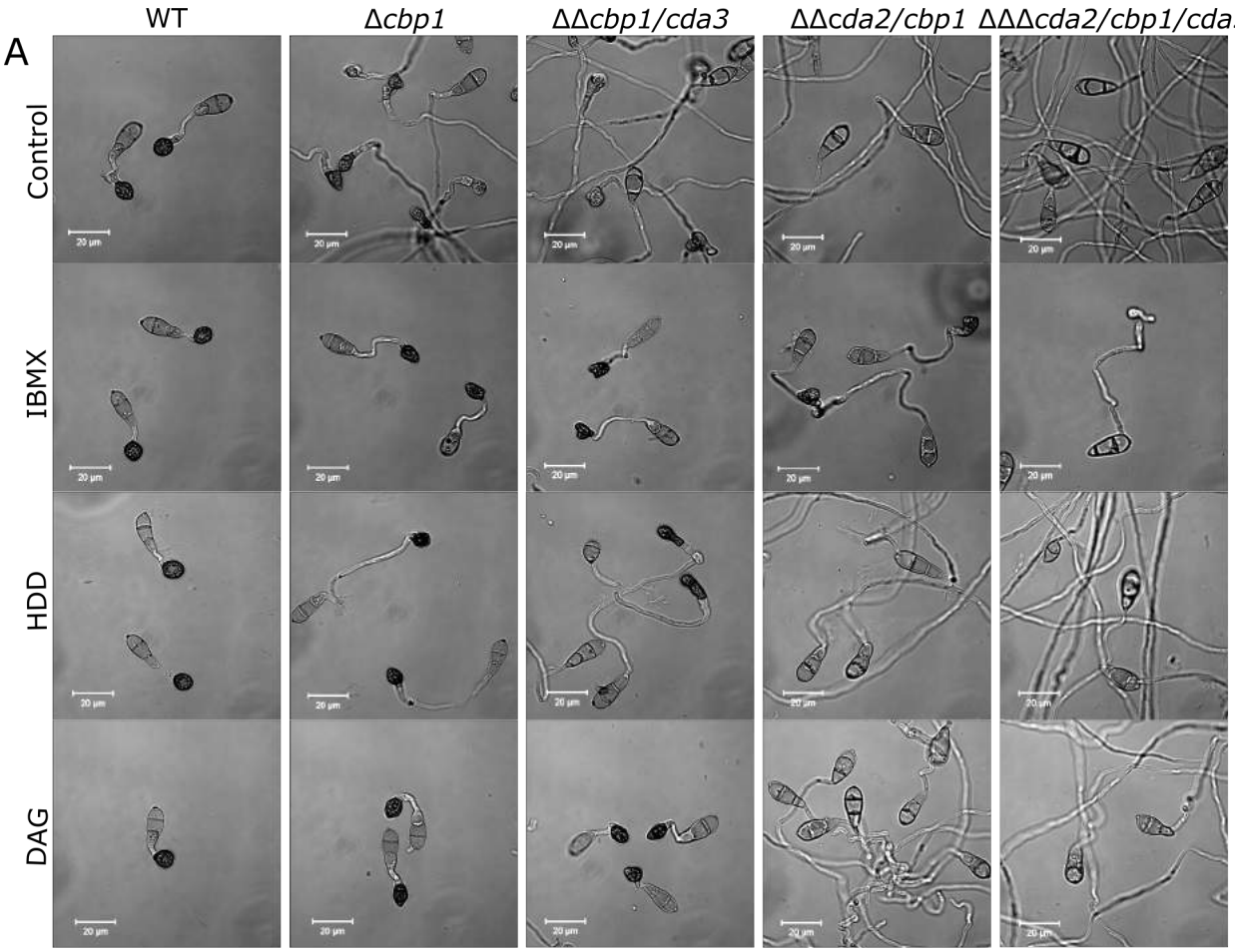

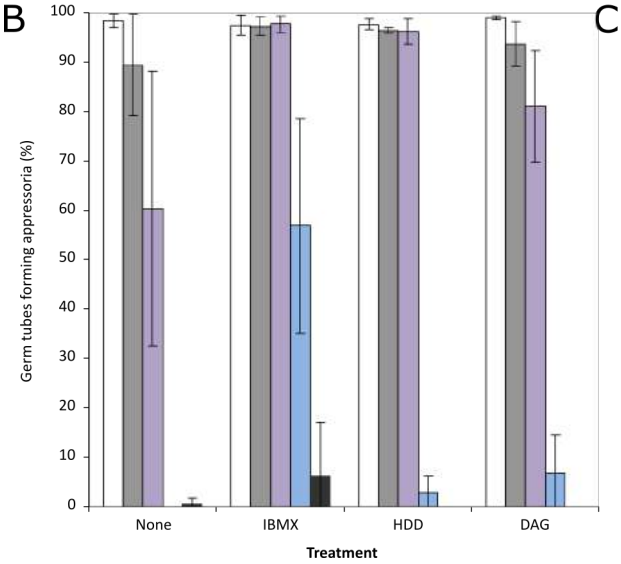

C

	Control	IBMX	HDD	DAG
WT	31 ± 6	18 ± 4	35 ± 2	16 ± 3
Δcbp1	264 ± 37	26 ± 6	115 ± 14	37 ± 11
ΔΔcbp1/cda3	322 ± 56	37 ± 9	122 ± 8	59 ± 17
ΔΔcda2/cbp1	487 ± 42	93 ± 16	ND	ND
ΔΔΔcda2/cbp1/cda3	ND	ND	ND	ND

Figure 3.13: The *CDA* deletion strains show distinct sensitivity to chemical inducers of appressorium development. **A**) Pictures of germlings at 16 hpi in presence or absence of IBMX, 1,16 hexadecanediol (HDD) or diacylglycerol (DAG), showing drastically reduced inductive effects in *cda2/cbp1* and *cda2/cbp1/cda3* strains. Scale bars: 20 μm. **B**) Quantification of appressorium development as visualized in **A**, WT: white bars, *cbp1*: grey bars, *cbp1/cda3*: purple bars, *cda2/cbp1*: blue bars and *cda2/cbp1/cda3*: dark grey bars. Error bars show SD, n=3. **C**) Table showing mean germ tube lengths of germlings as quantified in **B**, lengths in µm ± SD, n=3. ND = Not Determined.

inducers, germinations were repeated on a hydrophilic glass surface. As expected, no appressorium development was observed in the WT strain after a 24hr incubation, but could be restored by the addition of IBMX or HDD. However, these inducers remained ineffective on *cda2/cbp1/cda3* (Figure 3.14C). As discussed previously, exogenous chitosan can fully restore appressorium development in the *CDA* deletion strains on a hydrophobic surface. To see if this was also true on a hydrophilic surface, conidia were germinated in the presence of 0.01% (w/v) chitosan for 24 hr. However, no appressoria were formed in the WT or *cda2/cbp1/cda3* strains. Next, combined treatments of chitosan and IBMX or HDD were applied. Interestingly, these combined treatments were able to induce appressorium development in the *cda2/cbp1/cda3* mutant. This experiment revealed two important facts: i) chitosan acts independently of surface hydrophobicity, and ii) chitosan acts through a separate pathway to IBMX or HDD. An additional experiment was also performed, in which IBMX and HDD were added in combination. However, this did not induce appressorium development in the triple deletion strain (not shown). In a recent study, rapamycin was found to induce of appressorium development in a Pmk1 dependant manner (Marroquin-Guzman and Wilson, 2015). To test whether rapamycin could induce appressorium development in the *cda2/cbp1/cda3* strain, 55nM rapamycin was added either alone, or in combination with chitosan, IBMX or HDD, to conidia germinating on hydrophilic glass. Unfortunately, the findings of this study could not be reproduced; rapamycin did not induce appressorium development in either the WT or triple deletion strain (not shown).

Chitosan is required for germling adhesion

During the course of this study, it was observed that the germlings of *CDA* deletion strains were more easily washed off artificial surfaces. To investigate this further, adhesion of WT and *cda2/cbp1/cda3* germlings was quantified on both hydrophilic and hydrophobic glass surfaces at 2 hpi. As expected, germlings of the triple deletion strain demonstrated much lower adhesion than the WT, on both surfaces (Figure 3.15). This loss of adhesion could not be explained by lower conidial germination in the *cda2/cbp1/cda3* strain; 95% ($\pm$ 2, (SD) n=3) of WT conidia had germinated by 2 hpi, compared with 98% ($\pm$ 1, (SD) n=3) in *cda2/cbp1/cda3*. Remarkably, adhesion could be fully restored by germinating

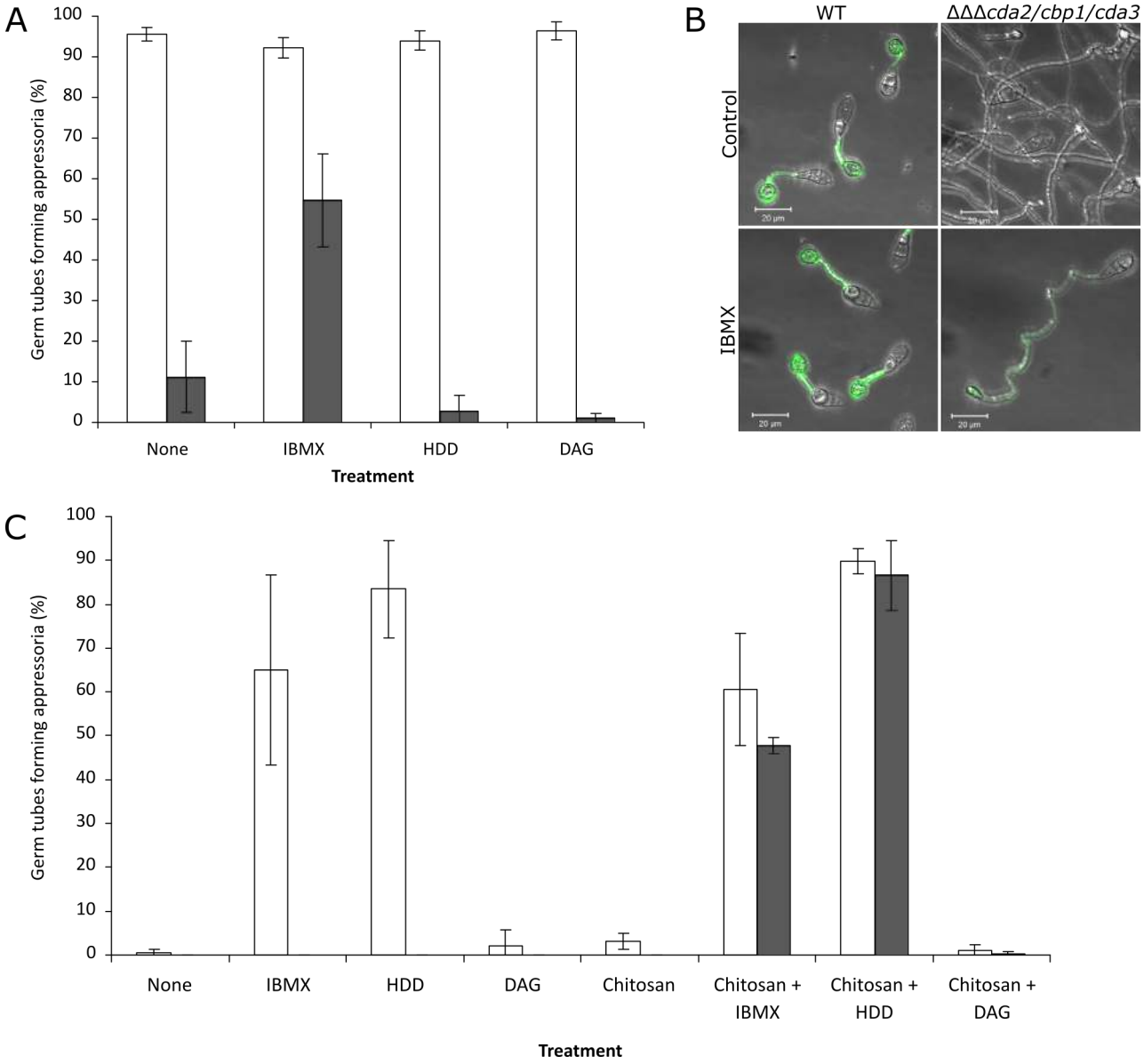

Figure 3.14: Combinations of chemical inducers are required to restore appressorium development in *cda2/cbp1/cda3*. Induction of appressorium development in the *cda2/cbp1/cda3* strain by chemical inducers, on **A**) hydrophobic and **C**) hydrophilic surfaces. Appressorium formation could be partially restored in the triple deletion strain (grey bars) after a 24hr incubation with IBMX, although chitosan staining of these germlings (**B**) showed that the appressorium formation was associated with an increase in chitosan in the germlings of the *cda2/cbp1/cda3* mutant, suggesting upregulation of functionally redundant chitin deacetylases. **C**) Appressorium development on hydrophilic surfaces could be restored to levels similar to the WT strain by combinations of 0.01% (w/v) chitosan and 2.5 mM IBMX or 200 µM 1,16 hexadecanediol (HDD). White bars: WT, grey bars: *cda2/cbp1/cda3*. Error bars: SD, n=3. Two independent *cda2/cbp1/cda3* lines were used which gave identical results, although only one of these is shown.

the conidia in the presence of 0.01% chitosan.

The adhesion of fungal cells to surfaces such as glass or plastic is often mediated by cell wall glycoproteins. A commonly used method for the detection of such glycoproteins is staining with the fluorescently-labelled mannose-binding lectin Concanavalin A (FITC-ConA). Staining of WT or *cda2/cbp1/cda3* germlings at 2 hpi with FITC-ConA revealed strong fluorescence of the germ tube in WT germlings, but only weak fluorescence in the deletion strain (Figure 3.15).

Ectopic expression of *CBP1:mCherry*

One of the original hypotheses regarding the role of chitin deacetylation was in reducing cell wall rigidity. In an attempt to investigate this hypothesis, *CBP1:mCherry* was ectopically expressed by the ribosomal protein promoter *RP27*, in the WT background strain. The *RP27* promoter has previously been used in *M.oryzae* to give strong, constitutive expression of genes (Samalova et al., 2014). *pRP27* and *CBP1* were amplified with primer pairs 70/75 and 76/48 respectively, then joined by fusion PCR (Primers 70 and 48). The *pRP27:CBP1* fusion was cloned into the pUCAP plasmid at the *Asc*I site (Appendix D), creating a C-terminal mCherry fusion. Following transformation, several independent lines ectopically expressing *CBP1:mCherry* (Appendix F) were characterized during vegetative growth and pathogenic development.

During mycelial growth, fluorescence was absent in growing hyphae at the colony margins, but in mature hyphae strong fluorescence localized to the hyphal septa, with weaker fluorescence at the lateral walls (Figure 3.16). In germlings, fluorescence was primarily observed in walls of germ tubes and appressoria, but occasionally also to conidia, typically the apical compartment. Additionally, intracellular (most likely vacuolar) fluorescence was also observed in the appressoria. During *in planta* growth, the cell walls of invasive hyphae also showed strong fluorescence. In all cases however, growth and cellular morphology appeared to be unaffected by ectopic expression of Cbp1:mCherry. Colonies ectopically expressing Cbp1:mCherry looked identical to the WT, and hyphae showed no signs of cell bursting or bulging. Similarly, conidia formed appressoria with similar morphology to WT, and were able to penetrate rice cells and form invasive hyphae (Figure 3.16).

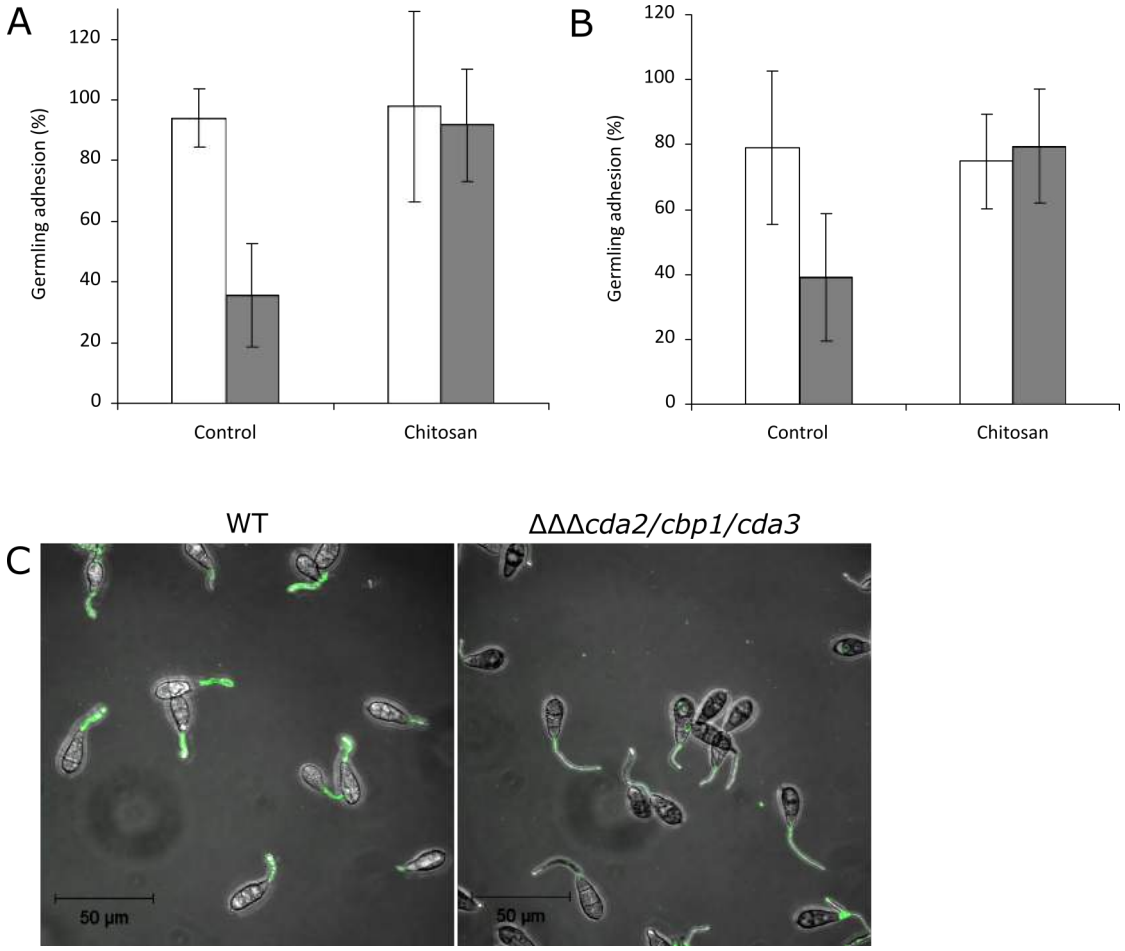

Figure 3.15: Germling adhesion is reduced in the *cda2/cbp1/cda3* strain. Adhesion of WT (white bars) and *cda2/cbp1/cda3* germlings (grey bars) on **A**) hydrophobic and **B**) hydrophilic glass surfaces, with or without 0.01% chitosan. Conidial suspensions of equal concentration were inoculated onto each surface and incubated for 2 hr, followed by 5 min washing with dH_2O on an orbital shaker. Germling adhesion was dramatically reduced in the triple deletion strain, but restored by the addition of exogenous chitosan. Two independent *cda2/cbp1/cda3* lines were tested, which gave identical results, although only one of these is shown. Error bars: SD, n=4. **C**) Labelling of germlings with FITC-Concanavalin A, showing reduced fluorescence in the *cda2/cbp1/cda3* strain. Scale bars: 50 µm.

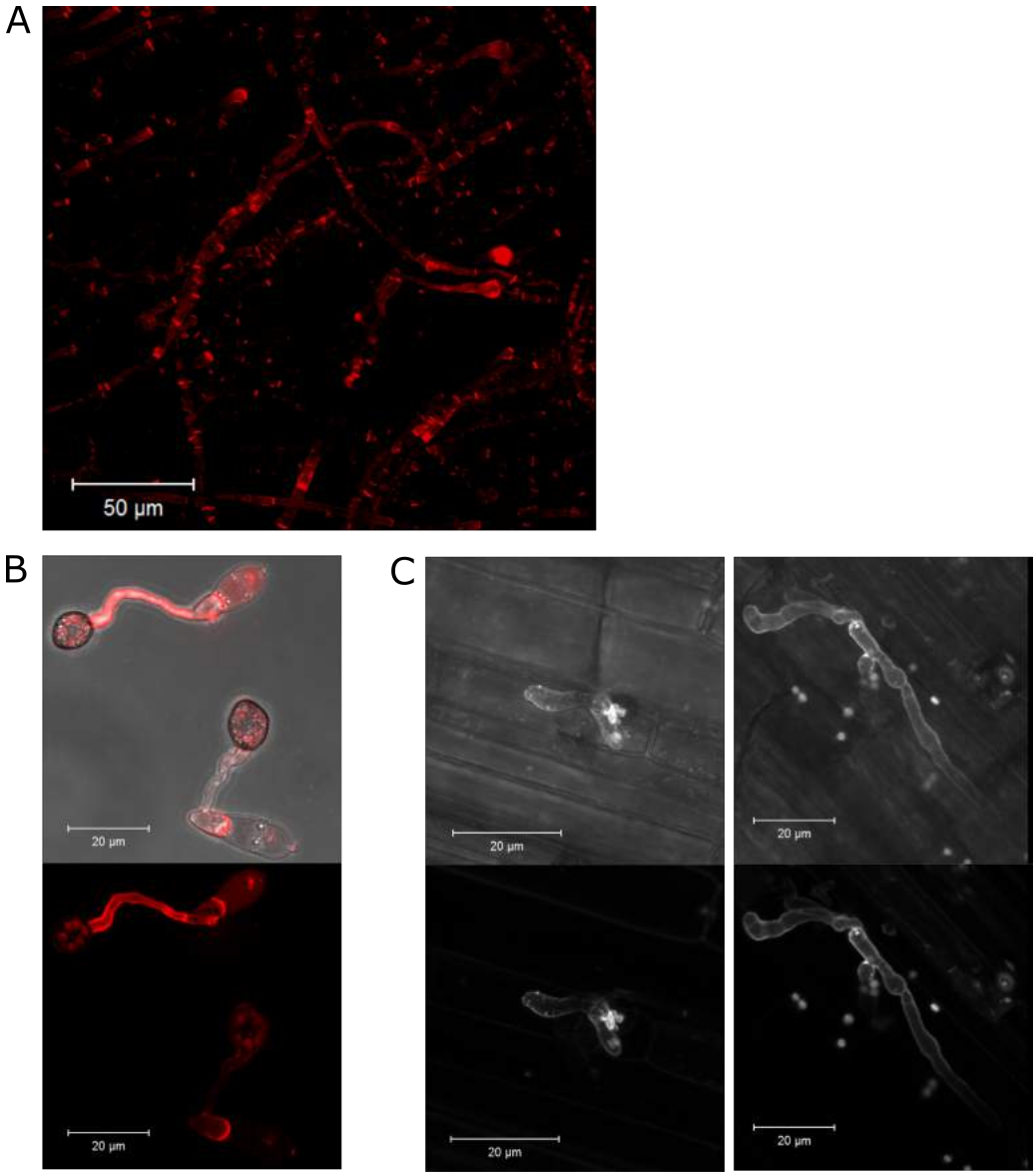

Figure 3.16: Ectopic expression of *CBP1:mCherry*. mCherry tagged Cbp1 was expressed by the constitutive *RP27* promoter. Strong, cell wall localized fluorescence was observed in **A**) Vegetative hyphae growing on complete medium, **B**) Germlings on a hydrophobic surface (at 24 hpi) and **C**) Invasive hyphae in rice (at 48 hpi). Fluorescence is pseudocoloured white in **C** for clarity. Cellular morphology appeared to be unaffected in all cases. Scale bars: 50 µm in **A**, 20 µm in **B** and **C**.

Susceptibility of *CDA* deletion strains to chitinase

Reduced susceptibility to chitinase was the second key hypothesis regarding the role of chitin deacetylation. Since chitosan was shown to be absent in the germ tubes and appressoria of *cda2/cbp1/cda3* germlings developed on plant surfaces, this provided a perfect opportunity to test this hypothesis. Conidia of both the WT and *cda2/cbp1/cda3* strain were inoculated onto onion epidermis and incubated for 16hr, after which 0.4 mg/ml chitinase or 0.4 mg/ml BSA (as a negative control) were added, and samples were incubated for a further 8 hr. Microscopic observation revealed that the chitinase treatment had little effect on either strain; conidia, germ tubes and appressoria appeared to be intact despite the treatment. However, further experimentation is required to confirm these findings, in particular the staining of chitin after chitinase treatment.

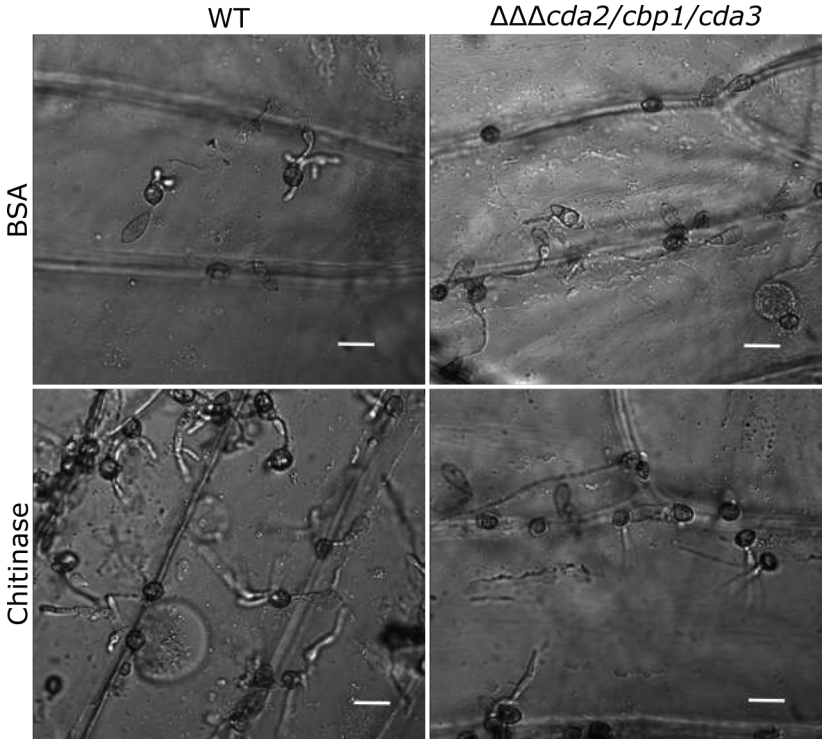

Figure 3.17: Treatment of WT and *cda2/cbp1/cda3* germlings with chitinase or BSA (control), showing lack of effect of the chitinase treatment. Spores were inoculated onto onion epidermis and incubated for 16 hr, after which 0.4 mg/ml chitinase or 0.4 mg/ml BSA were added, and the samples were incubated for a further 8 hr, before microscopic observation at 24 hpi. Scale bars: 20 μm.

3.3 Discussion

Appressorium development is regulated by two key pathways in *M.oryzae*. The Pmk1 pathway appears to operate at the earliest stage of appressorium development, and is required for sensing of wax, and possibly of surface attachment. The second, the cAMP pathway, is hypothesized to operate at the commitment phase of appressorial development, and is required for sensing of hydrophobicity and cutin monomers (Li et al., 2012). Considerable cross-talk exists between these two pathways, but activation of both is required for appressorium development. Many previous studies have been devoted to characterizing the proteins operating in these pathways. Significantly, deletion of the genes encoding these proteins results in phenotypes that are similar to those reported for the *CDA* deletion strains. Considering the data from this study in the context of previous data on signal perception in *M.oryzae* allows the role played by chitosan to be elucidated.

When germinated on an artificial hydrophobic surface, conidia of the *CDA* deletion strains *cbp1*, *cda2/cbp1* and *cda2/cbp1/cda3* failed to undergo early differentiation events, and appressorium development was either severely delayed (in *cbp1*) or rarely occurred at all (in *cda2/cbp1* and *cda2/cbp1/cda3*). Failure to differentiate appressoria on artificial surfaces is a phenotype shared by a number of other deletion strains with putative roles in surface sensing. For example, deletion strains of the signaling mucin Msb2 produce a phenotype with a striking resemblance to that reported in the present study: conidia of the *msb2* mutant germinated on an artificial hydrophobic surface produce highly elongated, undifferentiated germ tubes (Liu et al., 2011). However, when inoculated onto a plant surface appressorium development was fully restored, just as in the *cda* strains. In addition, cutin monomers were also unable to rescue *msb2*, although the effect of cAMP was not determined. These similarities may suggest a functional link between Msb2 and chitosan. Msb2 has a single transmembrane domain which anchors the protein to the plasma membrane, whilst the extracellular portion of the protein resides within the cell wall. It was recently shown that this extracellular portion alone could partially suppress the defects associated with *MSB2* deletion (Wang et al., 2015). It could therefore be the case that chitosan is required for cell wall-localization of Msb2; the absence of chitosan may result in loss of Msb2 from the cell wall, resulting in the observed phenotype. Unfortunately, the precise mechanism by which Msb2 mediates surface sensing is

unknown, which limits speculation on the putative functional link between this protein and chitosan. However, in a recent study, combined deletion of *CBP1* and *MSB2* had additive effects; virulence and Pmk1 phosphorylation (in vegetative hyphae) were shown to be more reduced in *msb2/cbp1* strains than in *msb2* strains (Wang et al., 2015). Loss of chitosan may therefore affect multiple surface-sensing related processes at the earliest stage of germling morphogenesis, which converge on the Pmk1 pathway. In support of this hypothesis, *cbp1* germlings have also been shown to be unable to form hyphopodia on artificial hydrophilic surfaces, a phenotype shared by the *pmk1* mutant, but not the *cpka* mutant (Tucker et al., 2010). In an attempt to demonstrate a link between chitosan and Pmk1 activation, a dominant active allele of the Pmk1 activating MEK kinase Mst7 was transformed into the *cda2/cbp1* strain. However, the resulting transformants failed to demonstrate restored appressorium development, although further investigations were not performed to determine whether or not this was due to a faulty construct.

Other proteins with putative roles in surface sensing are the hydrophobin Mpg1 (Talbot et al., 1993, 1996), and the putative G-protein coupled receptor Pth11 (DeZwaan et al., 1999). The *mpg1* and *pth11* mutants demonstrate very similar defects in appressorium development: Conidia produce elongated germ tubes on hydrophobic surfaces, and fail to develop appressoria as in the *cda* mutants. There are, however, several important differences in the phenotypes: Firstly, appressorium development is also defective on plant surfaces in *mpg1* and *pth11*. Secondly, germ tubes of *mpg1* and *pth11* do undergo early differentiation events (germ tube hooking). Thirdly, cAMP can restore appressorium development in both *mpg1* and *pth11* (Talbot et al., 1996), but not in the *cda* mutants, although this is complicated by the presence of redundant *CDA*s that are upregulated by cAMP (see 'regulation of chitin deacetylases'). This suggests that Mpg1 and Pth11 act upstream of the cAMP pathway, whereas chitosan does not. This hypothesis is supported by the fact that chitosan and IBMX/cutin had synergistic effects on appressorium development on a hydrophilic surface.

Yet, it is also possible that both the Pmk1 and cAMP pathways rely on the presence of chitosan, in which case the activation of just one of these by chemical or genetic means would be insufficient to restore appressorium development. The fact that germination in the presence of 1-octacosanol, which acts upstream of the Pmk1 pathway (Liu et al., 2011),

could only partially restore appressorium development in the *cda2/cbp1/cda3* strain, supports this scenario. Assuming that activation of both the Pmk1 and cAMP pathways is indeed defective, how might chitosan be required for the activation of the cAMP pathway? One mechanism could relate to the interaction between Mpg1 and the cell wall. Hydrophobins form amphipathic monolayers at the interface between hydrophobic-hydrophilic surfaces. Since leaf surfaces are highly hydrophobic, this presumably results in the assembly of an Mpg1 layer between the leaf surface and the cell wall of the germ tube. Loss of chitosan from the cell wall could alter the interaction between the germ tube cell wall and Mpg1, preventing hydrophobic surface sensing. Intriguingly, cell wall components such as β1,3-glucan have previously been found to promote rodlet formation of the class I hydrophobin Sc3 from *Schizophyllum commune* at hydrophobic interfaces (Scholtmeijer et al., 2009). In addition, the structure of hydrophobins such as EAS from *N.crassa* also provides some support for a putative interaction between Mpg1 and chitosan. EAS has both a hydrophobic area which presumably interacts with hydrophobic surfaces, and a negatively charged area on the opposite side of the protein, which may interact with the cell wall in a charge-dependant manner (Kwan et al., 2006). Although the structure of Mpg1 has not been solved, the fact that expression of EAS in the *mpg1* mutant can restore the WT phenotype (Kershaw et al., 1998) suggests the conservation of structure and function of these proteins. Unfortunately, our current lack of understanding of exactly how Mpg1 promotes appressorium development in response to hydrophobic surfaces prevents further speculation on this matter. A second mechanism by which chitosan may be required for activation of the cAMP pathway could be via its effects on the physical properties of the cell wall. In the bacterium *Staphylococcus aureus*, adhesion-force sensing was found to be dependant upon peptidoglycan cross-linking, which governs the deformability of the cell wall in response to mechanical stimuli (Harapanahalli et al., 2015). The deacetylation of chitin could have an analogous role in the germlings of *M.oryzae*: Chitosan may alter the properties of the cell wall in order to render it capable of transmitting the force of the surface adhesion to sensor proteins. The G-protein coupled receptor Pth11 could be such a sensor protein. Localized to the plasma membrane, mechanical stimulation resulting from cell adhesion to a hard surface may result in membrane perturbations, leading to conformational changes in the protein and activation

(Kumamoto, 2008). Mechanical stress has previously been shown to induce conformational changes in GPCRs such as the Angiotensin II type-1 receptor and B2-Bradykinin receptor (Yasuda et al., 2008; Chachisvilis et al., 2006), although no such investigations have yet been made in Pth11. Mechanosensitive (MS) ion channels are another possible group of sensor proteins which may mediate surface sensing in response to cell wall and membrane deformation in germlings. Such channels open in response to physical stimuli that affect the plasma membrane. As such, they have been found to be responsible for the sensing of physical stimuli in the bean rust fungus *Uromyces appendiculatus* (Zhou et al., 1991) and in *C.albicans* (Brand et al., 2007). However, the roles of these channels have not yet been characterized in *M.oryzae*, and it is unclear how the activation of these would influence the pathways regulating appressorium development.

An alternative explanation, although one that is not mutually exclusive with those proposed above, is that the phenotypes observed in the *cda* deletion strains arise from a lack of germling adhesion. Germlings of *cda2/cbp1/cda3* were much more easily detached than those of the WT, even under the relatively gentle washing conditions employed in the experiment. This suggests that the adhesive properties of the germ tube are defective in the absence of chitosan. In this scenario, germ-tube localized chitosan is not required for transmitting the force of the adhesion (as described above), but is required for the adhesion of the germ tube to the surface itself, and is therefore required for surface sensing. Thus, chitosan may act directly as a polysaccharide 'glue', or is required for the attachment of various adhesin-like proteins to the cell wall (or a combination of both). Lack of chitosan in *cda2/cbp1/cda3* did result in a reduction of Concanavalin A staining, suggesting a reduction of mannan in the cell wall, but there are several possible explanations for this: i) chitosan is required for attachment of mannoproteins to the cell wall, ii) overall cell wall structure is altered by the loss of chitosan, including a reduction in non-protein associated mannan, iii) mannoproteins are produced, but secretion to the outer wall is affected by loss of chitosan or, iv) lack of surface sensing and activation of Pmk1 and/or cAMP pathways means that production of the mannoproteins does not occur in the first place, i.e. reduced germling adhesion is a consequence, and not the cause of defective surface sensing. Further investigations are required to distinguish between these possibilities.

Germling attachment and surface sensing are critical stages of pathogenic development in a number of fungi, including *Ustilago maydis* (Mendoza-Mendoza et al., 2009), *Botrytis cinerea* (Doehlemann et al., 2006) and *Colletotrichum graminicola* (Chaky et al., 2001). It would therefore be of interest to determine whether chitosan is also required for surface sensing in these species. Whilst the characterization of chitin deacetylases has not yet been performed in plant pathogenic species other than *M.oryzae*, transcriptomics data does suggest the involvement of these enzymes in pathogenic development. In *B.cinerea* for example, the chitin deacetylases *CDA1* and *CDA3* demonstrated upregulation in the early stages of spore germination (Leroch et al., 2013). Similarly, several chitin deacetylases in *U.maydis* are induced during germination on a hydrophobic surface (Lanver et al., 2014).

Model for the role of chitosan in appressorium development

The role of chitosan in appressorium development is an intriguing one, and there remain many unanswered questions, as discussed above. Despite this, the following model (Figure 3.18) is consistent with all of the data presented in this study, and with data from previous studies characterizing surface sensing proteins in *M.oryzae*. In this model, germ-tube localized chitosan is required for the activation of the Pmk1 MAP kinase pathway in response to a surface, but independently of surface hydrophobicity. Activation of the cAMP pathway may also require chitosan, but it is not possible to conclusively determine whether just one or both of the signalling pathways are defective in *cda* mutants from the current data. Chitosan-mediated activation of these pathways may be due to:

- A direct interaction between the chitosan and cell wall-associated proteins involved in surface sensing e.g. Msb2 or Mpg1, where chitosan is required for the correct localization or conformation of the protein.
- Chitosan imparting particular physical properties (e.g flexibility) to the cell wall, which is required for transmitting the force of surface adhesion to membrane-localized sensors.
- Germ tube adhesion, which is either directly mediated by chitosan, or due to glycoproteins which are dependant upon chitosan for wall localization.

Clearly, none of the above hypotheses are mutually exclusive, and it is possible that chitosan is required for a number of processes relating to surface sensing.

Various chemical inducers are able to by-pass the requirement for certain stimuli. cAMP and cutin monomers (e.g. 1,16 hexadecanediol) both activate the cAMP pathway, and can induce appressorium development in WT germlings in the absence of hydrophobicity. However, neither can compensate for the absence of chitosan in *cda* mutants. This is either because the cAMP pathway operates normally in *cda* mutants, or because both the Pmk1 and cAMP pathways are defective, and activation of both is required for appressorium development. Chemical stimuli present on leaf surfaces are able to activate both pathways simultaneously, leading to normal appressorium development in the absence of chitosan: Wax is perceived by Sho1 and Msb2, which activate Pmk1 (Liu et al., 2011), and cutin activates the cAMP pathway through Pth11 (DeZwaan et al., 1999). There are also likely to be additional factors which have yet to be discovered.

Evidence for additional roles of chitosan

The deacetylation of chitin was hypothesized to cause profound changes to the chemical and physical properties of the cell wall, which could be crucial for cellular morphogenesis. However, no evidence for this has been found in the present study. Germlings of the *cda2/cbp1/cda3* strain developed appressoria that were morphologically indistinguishable from the WT strain on plant surfaces despite the absence of detectable chitosan. Additionally, appressorium development in *cda2/cbp1/cda3* was restored by a short incubation with FITC-chitosan that was only incorporated into the germ tube, although admittedly, subsequent chitosan staining of germlings was not performed in this experiment. Not only was chitosan not required for morphogenesis of appressoria, but appressorium function also seemed to be unaffected by the absence of chitosan, since plant penetration continued to be achieved successfully. Chitosan is therefore unlikely to be a key structural component of the cell wall, in contrast to *Cryptococcus neoformans* where loss of chitosan impaired cellular integrity (Baker et al., 2007). On the other hand, it is also possible that compensatory changes in cell wall composition occurred in the absence of chitosan, which were not investigated. The upregulation of other cell wall components may be sufficient to maintain cell wall integrity in the *cda* mutants. In a similar vein, it is

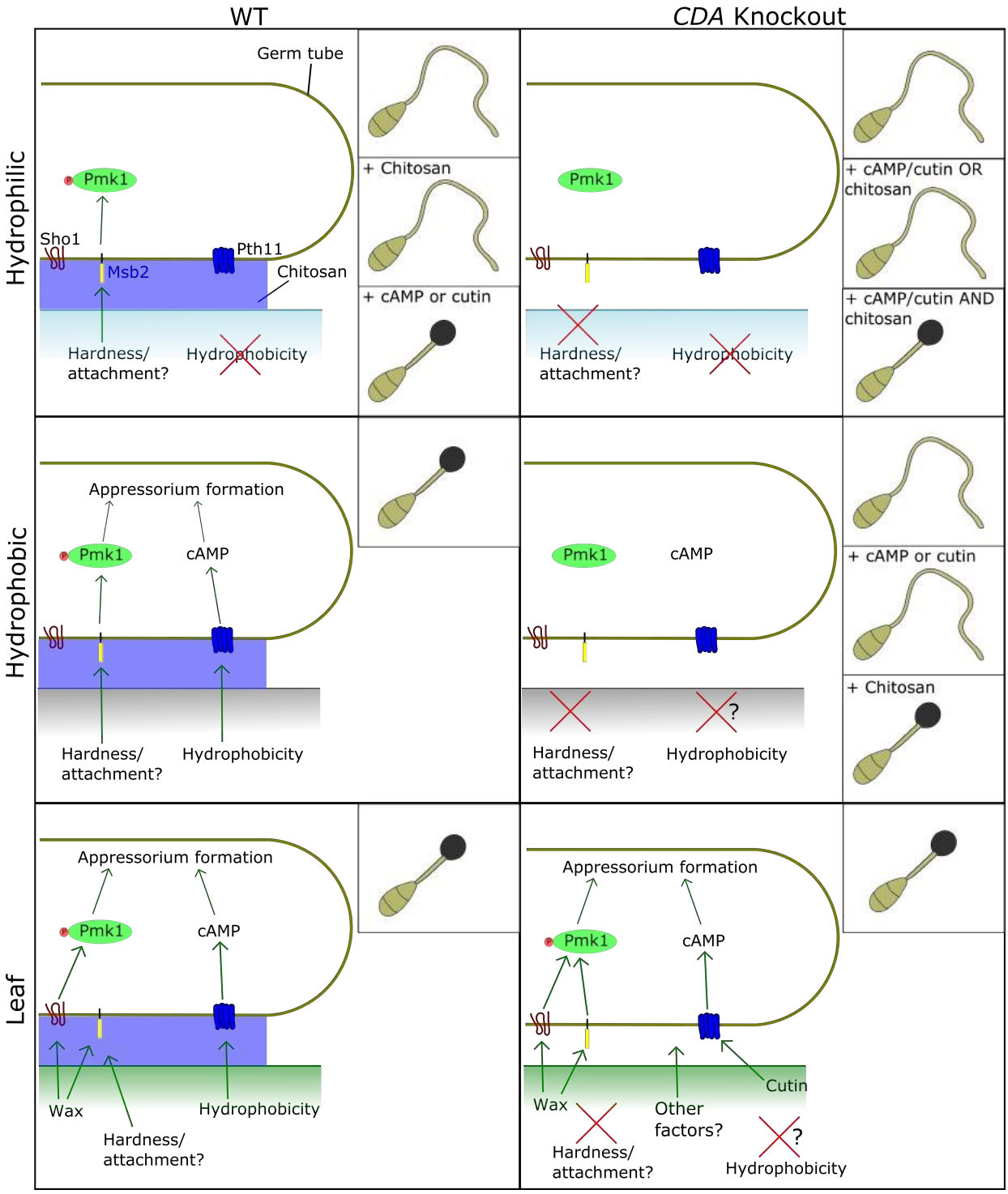

Figure 3.18: Model describing the role of chitosan in appressorium development. Germling development on three different surfaces is shown (hydrophilic, hydrophobic and leaf), with observed phenotypes shown inset. Successful appressorium development is dependant upon activation of both the Pmk1 and cAMP pathways. The absence of chitosan prevents complete activation of the Pmk1 pathway and possibly the cAMP pathway. The addition of exogenous chitosan and/or chemical inducers of these pathways can fully restore appressorium development in the *CDA* deletion strains. Thus, germ tube localized chitosan likely acts upstream of both the Pmk1 and cAMP pathways to induce appressorium development.

not inconceivable that compensatory changes were also responsible for allowing appressorium morphogenesis to occur in the absence of chitosan. This is perhaps less likely since cellular morphogenesis requires a very specific and highly regulated interplay between synthesis of cell wall components and cellular growth. In a separate attempt to discover the consequences of chitin deacetylation on the properties of the cell wall, Cbp1:mCherry was ectopically expressed. Unfortunately, this failed to reveal any morphological consequences of deregulated chitin deacetylation. It should be noted that chitosan staining was not performed in the *pRP27:CBP1mCherry* strains, although Cbp1:mCherry is known to be functional as it successfully complemented the deletion strain.

A second hypothesized role of chitosan is in the protection from plant chitinases. Since this did not transpire to be the primary focus of this study, there is currently insufficient evidence to conclusively confirm or refute this hypothesis. Nevertheless, the preliminary findings presented here, together with evidence from previous studies do not fully support this role for chitosan. Germlings of *cda2/cbp1/cda3* in which chitosan was absent remained intact on leaf surfaces, in contrast to those of the *ags* mutant which lack α1,3-glucan and were destroyed, presumably by degradative enzymes on the leaf surface (Fujikawa et al., 2012). Even the addition of exogenous chitinase was apparently insufficient to cause noticeable loss of cellular integrity, although further experimentation is required to fully characterize the effect of chitinase treatment on the *cda* mutants. Taken together, these data suggest that α1,3-glucan may be the cell wall component with the protective role in *M.oryzae* germlings. Upon reflection, it would perhaps have been more valuable to investigate the hypothesized protective effects of chitin deacetylation during *in planta* growth. Chitosan staining was not performed on invasive hyphae in the *cda* mutants, although the lack of any *in planta* fluorescence in the mCherry tagged *CDA* strains suggests that the chitin deacetylases operating during appressorium development may not also expressed during invasive growth.

Regulation of chitin deacetylases

The three *CDA* genes characterized in this study have redundant roles in chitin deacetylation during appressorium development. Yet it is also clear that their regulation differs considerably, such that the redundancy is only apparent under certain conditions. The

rescue of appressorium development in *cbp1* had been previously demonstrated by the addition of chemical inducers such as IBMX, 1,16 hexadecanediol or diacylglycerol (Kamakura et al., 2002). However, in this study it was shown that this rescue is dependant upon the other two *CDA* genes, *CDA2* and *CDA3*. Restored appressorium development in *cbp1* is therefore likely due to the upregulation or activation of *CDA2* and *CDA3* due to activation of the cAMP, Pmk1 or cell wall integrity pathways by the chemical inducers. The regulation of these genes by the aforementioned pathways has been noted in previous studies: *CDA2* and *CDA3* were found to be upregulated by cAMP treatment (Franck et al., 2013; Irie et al., 2003) and *CDA2* was significantly downregulated in the *pmk1* strain (Soanes et al., 2012). Appressorium development could also be restored in the *cda2/cbp1/cda3* strain by the addition of IBMX or by germination on plant surfaces. In the case of IBMX-treated germlings, restored chitosan staining was observed (Figure 3.14), suggesting the upregulation of yet another CDA. However, no staining was observed in germlings on plant surfaces, suggesting that in this case, rescue was not due to upregulation of redundant CDAs.

In the absence of artificial pathway activation, the temporal regulation of *CBP1* and *CDA2* appeared to be different; Cbp1:mCherry fluorescence was observed at much earlier stages of germling morphogenesis than Cda2:mCherry. Most intriguingly, Cbp1:mCherry localized to the apical conidial cell wall even prior to harvesting of conidia (Figure 3.6). It could be speculated that the chitosan synthesized by Cbp1 at the earliest stage of conidial germination is required for activation of the Pmk1 and cAMP pathways, which in turn leads to upregulation of *CDA2* and *CDA3*. *CDA2* and *CDA3* may therefore be part of a positive feedback loop, leading to stable cellular differentiation in response to surface signals.

A final aspect of the regulation of chitin deacetylation was discovered from the inhibition of melanization. Germination of conidia in the presence of tricyclazole led to a dramatic decrease in detectable chitosan on both germ tubes and appressoria. This could indicate that melanization is a key step in cell wall biosynthesis; lack of melanization may prevent down-stream activation of other cell wall enzymes either at a transcriptional or post-translational level.

Possible coordination between chitin synthesis and deacetylation

In *Cryptococcus neoformans*, all chitin that is later deacetylated into chitosan is synthesized by a single chitin synthase, which suggested possible coordination between these enzymes (Banks et al., 2005). Evidence from this study also supports this hypothesis. Deletion of *CHS7* results in an almost identical phenotype to multiple *CDA* deletion (Odenbach et al., 2009), suggesting that Cbp1, Cda2 and Cda3 may deacetylate the chitin synthesized by Chs7. The colocalization of Cbp1:mCherry and Cda2:mCherry with Chs7:2xYFP provides some evidence for possible coordination, but also raises further questions. For example, colocalization was not observed to occur at the cell periphery in germ tubes: Chs7 localized to the tip, whereas Cbp1 localized to the lateral walls. Only during germ tube hooking and appressorium development was colocalization observed. This could be significant, because it may indicate that the timing of chitin deacetylation differs according to developmental requirements. Chitin synthesized at the germ tube tip may have crystallized once it is part of the lateral walls, leading to a lower degree of deacetylation by Cbp1. Conversely, in developing appressoria the colocalization of chitin synthases and chitin deacetylases may mean that chitin is deacetylated as soon as it is synthesized, and so is deacetylated to a greater extent. The timing of chitin deacetylation could therefore influence the properties of chitosan, and possibly the cell wall as a whole.

The specificity of the putative coordination between Chs7 and the chitin deacetylases cannot be determined from the current data. However, the fact that *chs7* germlings can form appressoria on plant surfaces or in response to cAMP and 1,16 hexadecanediol treatment does offer some clues. Rescue of appressorium development in response to these treatments could be a result of upregulation of a partially redundant chitin synthases such as Chs1, which is also required for normal appressorium development (Kong et al., 2012). If this is indeed the case, it would be of interest to determine whether chitosan is also present, as it would suggest that the chitin deacetylases can deacetylate chitin from multiple chitin synthases.

Chitin synthases are known to be cycled between the plasma membrane and intracellular bodies in *S.cerevisiae* (Ziman et al., 1996). Whether this is also the case in *M.oryzae* is currently unknown, but the intracellular localization of Chs7:2xYFP suggests that this may be the case. Whilst some of the larger compartments observed were

almost undoubtedly vacuoles, the smaller fluorescent punctae may represent endosomal or Golgi compartments acting as intracellular stores of Chs7. Intriguingly, colocalization with Cbp1:mCherry was observed in these intracellular compartments, which could suggest that these proteins are co-transported to and from the plasma membrane. If co-transportation does occur, then this, in turn, may suggest that a physical association exists between the chitin synthases and chitin deacetylases. Clearly, these questions require a great deal of further investigation.

Polygalacturonic acid: a novel cell wall component in *M.oryzae*?

By using the probe COS488, which was originally developed for localizing homogalacturonan in plant tissue samples (Mravec et al., 2014), polygalacturonic acid (PGA) was tentatively identified as a novel component of the cell wall in the germlings of *M.oryzae*. The specificity of COS488 for PGA has been well-characterized: COS488 requires a degree of polymerization of at least 5 in the target PGA molecule in order to binding to occur, although binding increases with target length. No binding was found to oligomers of chitin or β1,3-glucose (Mravec et al., 2014). This suggests COS488 is highly-specific for PGA. However, binding specificity was not evaluated on targets such as polyglucuronic acid, which are more similar in structure to PGA. Given that the target of COS488 in the cell walls of *M.oryzae* appeared not to be sensitive to polygalacturonase treatment, this could indicate that PGA is not the target. On the other hand, it may simply mean that the PGA was not accessible to the enzyme treatment, either due to its position in the cell wall, or its relationship with other cell wall components.

The data showing rescue of appressorium development with exogenous chitosan (Figure 3.8) and its incorporation into the cell wall (Figure 3.9) suggest an electrostatic interaction between chitosan and PGA. Chitosan and PGA may therefore form what is known as a polyelectrolyte complex (PEC) in the cell wall (Dakhara et al., 2010). The formation of such a PEC would explain the relative efficacy of different types of chitosan in restoring appressorium development (Figure 3.8). The energetic favourability of the hypothesized interaction of chitosan with PGA obviously depends on the charge of the interacting molecules; carboxymethylchitosan was unable to rescue appressorium development, presumably because it has anionic groups, which inhibit its association with PGA.

Similarly, the glycol moiety in glycol chitosan may have prevented stereochemical fitting of the chitosan and PGA, reducing the stability of the complex. The role of molecular weight in this interaction is less intuitive, but the energetic favourability of an interaction between two polyelectrolytes increases with the length of the molecule (Dakhara et al., 2010). Therefore, short oligomers of chitosan would not form as stable complexes with the PGA as longer polymers, explaining the reduced efficacy of oligochitosan.

The presence of PGA in the cell wall begs the question of how it is synthesized. Intriguingly, and unlike most fungi, *M.oryzae* lacks a putative UDP-glucose-6-dehydrogenase, the enzyme required for the synthesis of UDP-glucuronic acid. UDP-glucuronic acid-4-epimerase, which catalyses the production of UDP-galacturonic acid is also absent in fungi. Therefore, any uronic acids in the cell wall of *M.oryzae* are likely to be synthesized by a non-conventional pathway, perhaps by *in situ* oxidation of galactose residues by secreted galactose oxidases.

3.4 Conclusions

The investigation of chitin deacetylation during appressorium development has yielded unexpected and intriguing results. It appears that chitosan is required for surface sensing in germlings, although the mechanism behind this is unclear. The cell wall therefore plays a crucial role in the perception of physical stimuli in the germlings of *M.oryzae*, demonstrating a novel way in which the cell wall is crucial in acting as an interface between fungal cells and their environment. Evidence for additional roles of chitosan are incomplete; further investigations are required to determine whether chitin deacetylation also plays a role as a 'stealth' mechanism in *M.oryzae*. In addition, no evidence was found for the hypothesized role of chitin deacetylation in cellular morphogenesis. In the following chapter, this hypothesis is further pursued by characterizing the role of chitin deacetylation during vegetative growth and development.

Chapter 4

Chitin deacetylation and vegetative growth

4.1 Objectives

In the previous chapter, the role of chitin deacetylation during appressorium development was investigated. This revealed an unexpected role in surface sensing, but failed to confirm a role for chitosan in morphogenesis. In order to further investigate how chitin deacetylation may influence cellular morphogenesis, this chapter describes the characterization of CDAs and their role during vegetative growth.

During vegetative growth, a number of changes in cell shape occur, for example during hyphal extension, hyphal branching or conidiation. Such changes may require localized increases in cell wall flexibility brought about, at least in part, by chitin deacetylation. Currently, little is known regarding the role of chitosan during vegetative growth in filamentous fungi. In *Ashbya gossypii*, chitosan is a component of the spore cell wall, and deletion of the sole *CDA* present in the genome (*CDA1*) resulted in almost complete loss of sporulation (Lickfeld and Schmitz, 2012). However, filamentous growth was unaffected by *CDA1* deletion, although the presence of chitosan as a hyphal wall component was not determined. In *Neurospora crassa*, chitosan was localized to hyphal septa, using the chitosan-specific probe OGA488 (Mravec et al., 2014), but chitin deacetylases have not yet been characterized in this fungus. Investigating the role of chitin deacetylation during vegetative growth in *M.oryzae* could therefore result in novel and valuable data.
The objectives of this chapter are to:

- Determine whether chitosan is a component of the cell wall in vegetative hyphae and conidia
- Identify which chitin deacetylases (if any) are expressed during vegetative growth
- Perform targeted deletion of identified genes, in order to abolish chitin deacetylation
- Characterize vegetative growth in the deletion strains

4.2 Results

Chitosan is a component of the cell wall in vegetative hyphae

In germlings, chitosan could be readily localized with either anti-chitosan antibodies or the chitosan-specific probe OGA488. However, staining of hyphae proved to be more challenging. Firstly, the penetrability of the anti-chitosan antibody mAbG7 appeared to be too low for effective labelling of hyphae grown in liquid medium, although weak labelling was observed (Figure 4.1A). Secondly, in order to label hyphae grown on solid medium, hyphae were grown over a glass coverslip, which had previously been overlayed with complete medium. During extensive washing and labelling steps, the agar and hyphae were prone to dislodge from the coverslip, making staining with the antibody impossible. However, OGA488 is well-suited to staining these tissues; its small molecular size means it has far superior penetrability compared with the antibody, and the rapid labelling means that samples remain intact during the protocol.

Unfixed hyphae, grown on both solid medium and in liquid medium, stained with OGA488 suggesting that chitosan is a component of the cell wall during vegetative growth. For hyphae grown on solid complete medium, fluorescence was not observed in hyphae growing at the outermost edge of the colony, but was first observed 1.5-2 mm from this point, and increased in intensity with increasing distance from the colony edge. Here, strong labelling of septa was observed, as well as weaker labelling of lateral walls and occasionally of hyphal tips (Figure 4.1C). Unfortunately, the extreme hydrophobicity of hyphae grown on solid medium prevented labelling of all but the outer $\sim$5 mm of the colony, as washing buffer and OGA488 failed to penetrate beyond the surface hyphae. In an attempt to circumvent this problem, conidia were inoculated into liquid CM, incubated for 72 hr and the resulting mycelial pellets labelled with OGA488. Again, strong fluorescence was associated with the septa, with weaker fluorescence of the lateral walls (Figure 4.1B). Strikingly, only the outer edges of septa were labelled, resulting in a 'ring' of fluorescence at each septum, although this may simply be a result of incomplete penetration of OGA488 into the inner regions of the septa. Unfortunately, the organization of hyphae was unclear upon microscopic observation of mycelial pellets; it was difficult to know whether the hyphae being observed were from the growing edge of the pellet or

the older hyphae from the middle. As such, the spatial distribution of hyphae stained with OGA488 could not be directly compared between the two protocols.

Chitosan is known to be a component of the cell wall in the spores of *A.gossypii* and *S.cerevisiae*. To determine whether this was also the case in the conidia of *M.oryzae*, staining was performed with both eosin Y and OGA488. Whilst no staining was observed with OGA488, consistent with the labelling of germlings in the previous chapter, weak fluorescence was observed in the cell wall of conidia labelled with eosin Y (Figure 4.1D). Given the superior specificity of OGA488, these data suggest that chitosan is most-likely not a component of the conidial cell wall.

Chitin deacetylases are highly expressed during mycelial growth

Having established that chitin is deacetylated during hyphal growth, the next objective was to determine which chitin deacetylases were responsible. As determined in the previous chapter, there are 10 putative chitin deacetylases present in the genome of *M.oryzae* (Figure 3.2). In order to find which of these genes were expressed during vegetative growth, two transcriptional profiling methods were used, as described in the previous chapter. Firstly, an existing transcriptomics dataset was exploited. As part of a study into transcriptional profiling of appressorium development, Soanes et al. (2012) also performed a transcriptomic analysis of genes expressed in mycelium following growth of *M.oryzae* in liquid CM for 36 hr. By searching this dataset for all 10 *CDA* genes, the transcript abundance for these genes could be determined (Figure 4.2). This revealed that a single *CDA* (*CDA1*) demonstrates extremely high transcript abundance under these growth conditions, whereas the transcript abundances of all other *CDA* genes appeared to be extremely low. To complement this data, semi-quantitative RT-PCR was performed on RNA extracted from mycelium grown in complete medium for 72 hr. In this case *CDA4* appeared to have the highest transcript abundance, with lower expression detected for *CDA1*, *CDA3* and *CDA8*. No amplification was observed in experiments in which the RNA had not been reverse transcribed (-RT control), proving that any observed amplification was from cDNA, and not due to gDNA contamination.

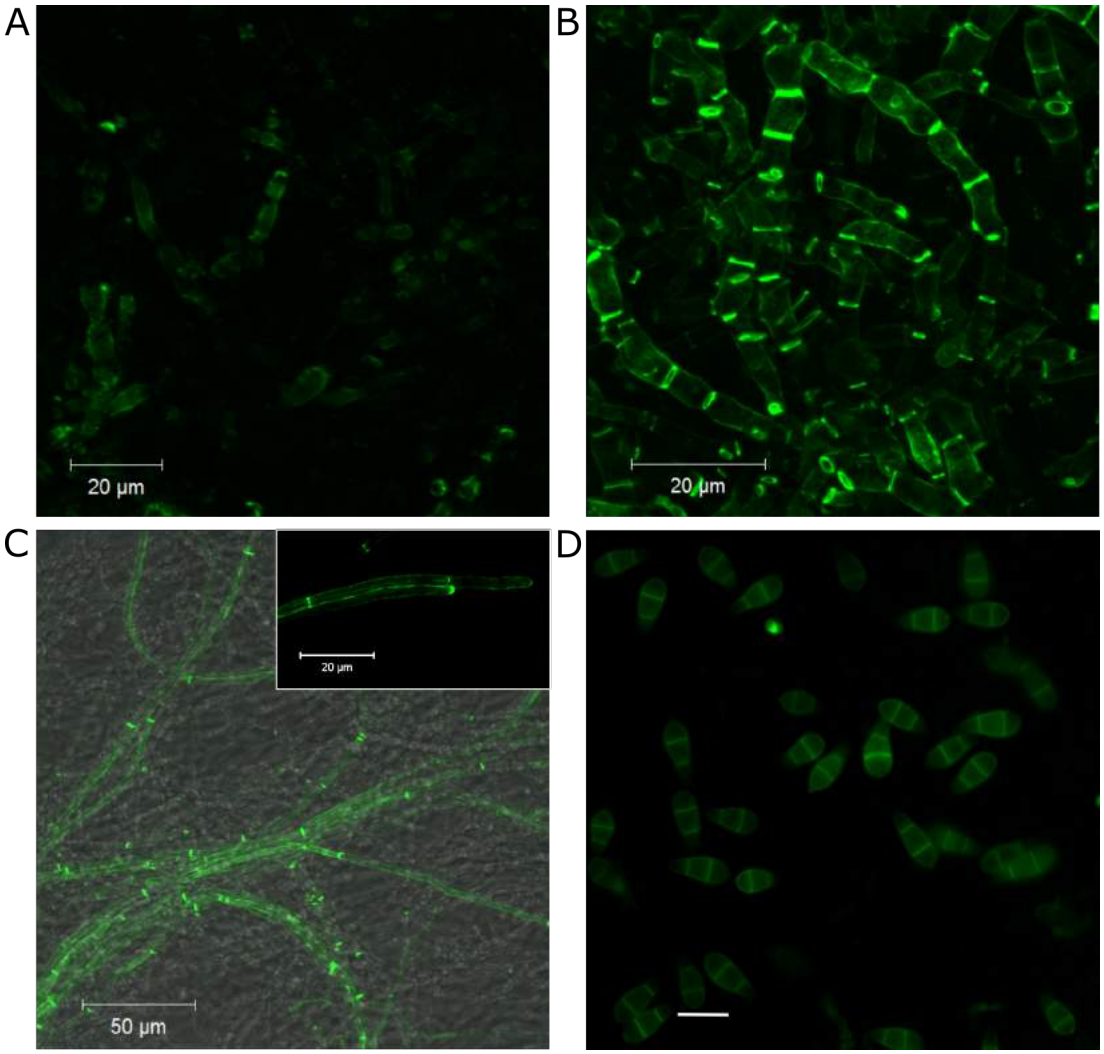

Figure 4.1: Chitosan is a component of the cell wall in the vegetative hyphae of *Magnaporthe oryzae*. The monoclonal anti-chitosan antibody mAbG7 (**A**) and chitosan-specific probe OGA488 (**B**) were used to test for the presence of chitosan in hyphae grown in liquid CM. Although staining was observed in both cases, OGA488 was both easier to use, and demonstrated stronger labelling of septa and lateral walls. **C**) OGA488 labelling of hyphae grown on solid CM, again showing labelling of septa and lateral walls, but also of hyphal tips (inset). **D**) Conidia could be labelled with the fluorescent dye eosin Y, but not OGA488 (not shown), Scale bar: 20 µm.

Gene name	Expression in mycelium (FPKM)	RT-PCR
CBP1	6	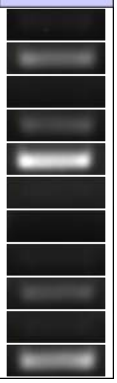
CDA1	58917	
CDA2	0	
CDA3	11	
CDA4	43	
CDA5	0	
CDA6	0	
CDA7	0	
CDA8	2	
CDA9	31	
β-tubulin	1382	

Figure 4.2: *CDA1* and *CDA4* are highly expressed during mycelial growth. Expression of *CDA* genes during vegetative growth, comparing data from transcriptomics (Soanes et al., 2012) after 36 hr growth in liquid CM (expressed in Fragments per Kilobase per Million (FPKM)), and semi-quantitative RT-PCR (30 amplification cycles) of RNA isolated from mycelium grown in liquid CM for 72 hr. *CDA1* and *CDA4* are the most highly expressed genes. β-tubulin is included as the reference gene.

Deletion of chitin deacetylases

From the data outlined above, it appears that two chitin deacetylases are responsible for chitin deacetylation during vegetative growth: *CDA1* and *CDA4*. In order to characterize the role of this chitin deacetylation, targeted deletion of these genes was performed. In addition, *CDA5* was also deleted, both alone and in combination with *CDA4*. Like Cda4, Cda5 also has a putative single transmembrane domain at its C-terminus (Figure 3.2), and so it was considered likely that it may demonstrate redundancy with Cda4. Targeted gene deletion was performed as described in Chapter 3, whereby the genes of interest were replaced by a gene encoding an antibiotic resistance gene. The entire coding regions of *CDA1* and *CDA5* were replaced with *HPH*, imparting resistance to hygromycin, *CDA4* was replaced by *BAR*, imparting resistance to bialaphos. Primers used for the construction of deletion cassettes are listed in Appendix E (Primers 1-4, 27-34 and 29-42).

Putative deletion strains were first screened by PCR, to confirm the loss of the target gene and the integration of the resistance gene at the correct locus (not shown). Confirmed strains were then subjected to Southern blot analysis, to confirm the presence of a single insertion of the deletion cassette at the desired locus (Figure 4.3). Genomic DNA of 5 putative *cda1* lines was digested with *Bam*HI, and hybridised with α-^{32}P labelled

DNA encoding *HPH*. This resulted in the expected 6.5 kb band in 4 of the 5 lines, although only two of these were free from ectopic insertions. *Eco*RI digestion of gDNA from putative *cda4* lines was hybridised with α-^{32}P labelled DNA encoding *BAR*, resulting in a visible band at 3.8 kb for three of the lines. For *cda5* and *cda4/cda5* strains, gDNA was digested with *Bgl*II and hybridised with α-^{32}P labelled DNA encoding *HPH*. As discussed previously (Chapter 3), cross-hybridisation occurs between *BAR* and *HPH*, due to a similar promoter sequence. This resulted in a 20 kb band occurring in the *cda4* background strain, and all *cda4/cda5* lines, due to hybridisation of *HPH* to *BAR* at the *CDA4* locus. In addition, the expected 6.5 kb band was also observed in putative *cda5* and *cda4/cda5* lines, indicating successful deletion of *CDA5*. In all cases, bands were absent in the WT control strain, confirming the specificity of hybridisation. All successfully generated deletion strains are listed in Appendix F.

Cell wall composition of *cda1*

Cda1 is a predicted secreted protein with a polysaccharide deacetylase domain (Pfam 01522) and a C-terminal chitin binding domain (Pfam 00187) (Figure 3.2). In order to determine whether chitin deacetylation was reduced in the *cda1* mutant, mycelial pellets resulting from 72 hr growth in liquid CM were stained with OGA488. Whilst hyphae of the WT strain demonstrated strong labelling of septa and lateral walls as discussed previously (Figure 4.1), labelling was almost absent in the hyphae of *cda1* (Figure 4.4). To test whether this decrease in chitin deacetylation was accompanied by an increase in cell wall chitin content, mycelial pellets were stained with either WGA-FITC or Calcofluor White. No clear changes in labelling were observed between hyphae of the WT and *cda1* strains, suggesting that reduced chitin deacetylation may not have resulted in a concomitant increase in chitin content. Staining with Calcofluor White also allowed hyphal and septum morphology to be observed, but these appeared to be unaffected in *cda1*. Hyphae growing on solid medium were also stained with OGA488. However, staining of the hyphae at 1.5-2 mm from the colony edge appeared to be similar in both the WT and *cda1* strains, suggesting that Cda1 may only deacetylate chitin in mature hyphae at the colony interior during growth on solid medium. Lastly, conidia were stained with the chitosan-binding dye eosin Y, but labelling was identical in both strains.

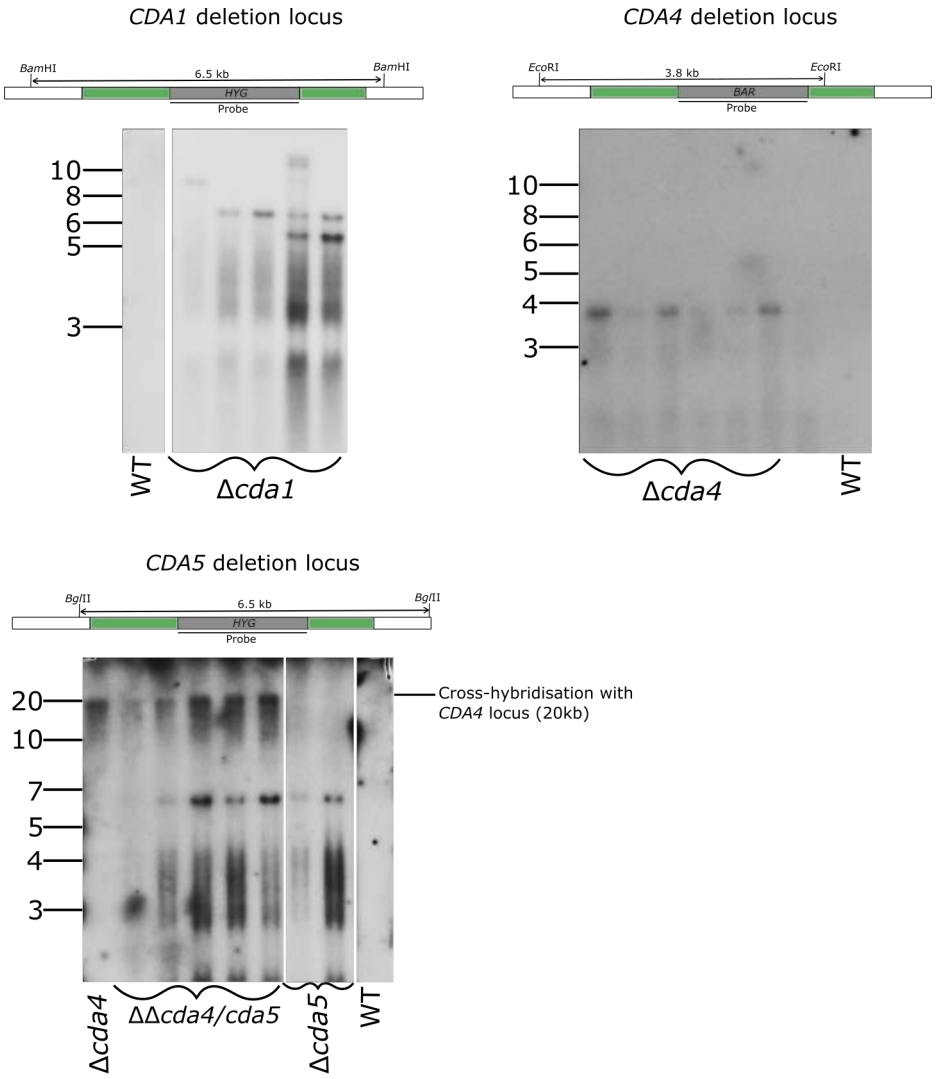

Figure 4.3: Targeted deletion of *CDA1*, *CDA4* and *CDA5*. The deletion strategy used was identical to that shown in 3.4, whereby the gene of interest is replaced by an antibiotic resistance gene. Blots containing restriction digested gDNA of putative deletion strains were hybridised with α-^{32}P labelled DNA homologous to the hygromycin (*CDA1* and *CDA5*) or bialaphos (*CDA4*) resistance genes. The cartoon above each blot shows the expected band size based upon the positions of the restriction enzymes sites at each locus. Size markers show band size in kilobases (kb).

Localization of Cda1

Having established that Cda1 may be required for chitin deacetylation in mature hyphae during vegetative growth, the *cda1* mutant was complemented by expressing an mCherry fusion of Cda1. Primers 51 and 52 (Appendix E) were used to amplify the open reading frame of *CDA1* (without the stop codon), together with 1.8 kb of 5' promoter sequence (for native expression of the construct). This was cloned into the *Asc*I site of the pU-CAP vector (Appendix D), thereby fusing mCherry to the C-terminus of Cda1. After transformation into the *cda1* background strain, antibiotic-resistant transformants were screened for fluorescence during vegetative growth. Although fluorescence was observed in a number of lines, it only appeared to be stable in one of these (Appendix F).

In strains expressing Cda1:mCherry, weak fluorescence was observed in the lateral walls of hyphae, with much stronger fluorescence associated with septa. Here, fluorescence localized both as a ring to the outer edge of the septum, or to the entire septum (Figure 4.5A). Expression of Cda1:mCherry was restricted to mature hyphae; on solid medium fluorescence was not observed in hyphae growing at the colony edge. No differences in fluorescence localization were observed between hyphae grown in liquid or on solid medium. In order to gain an insight into Cda1:mCherry expression at the colony level, colonies expressing Cda1:mCherry were observed under a fluorescence stereoscope. Fluorescence was not detected from the outer ∼5 mm of colonies, but was extremely strong in the entire colony interior (Figure 4.5B). These findings are consistent with those showing that Cda1 is not required for chitin deacetylation in hyphae at the colony margins, only in mature hyphae in the colony interior. Cda1:mCherry fluorescence was not observed at any other stages in the life-cycle, including during appressorium development, conidiation or *in planta* growth, suggesting that it is specific to the vegetative growth phase.

Figure 4.4 *(following page)*: Chitosan content is dramatically reduced in the *CDA1* deletion strain. **A**) Mycelial growth after a 72 hr incubation in liquid CM, stained with OGA488, WGA-FITC or calcofluor white to test for presence and localization of chitosan and chitin respectively. Staining with OGA488 was dramatically reduced in the *cda1* mutant, suggesting a reduction in chitosan, whereas chitin content appeared to be unaffected. **B**) Staining of hyphae grown on solid medium (approximately 1.5-2 mm from the colony edge) with OGA488, showing similar labelling in the WT and *cda1* strains. **C**) Staining of conidia with eosin Y. Scale bars: 20 μm for A and C, 50 μm for B.

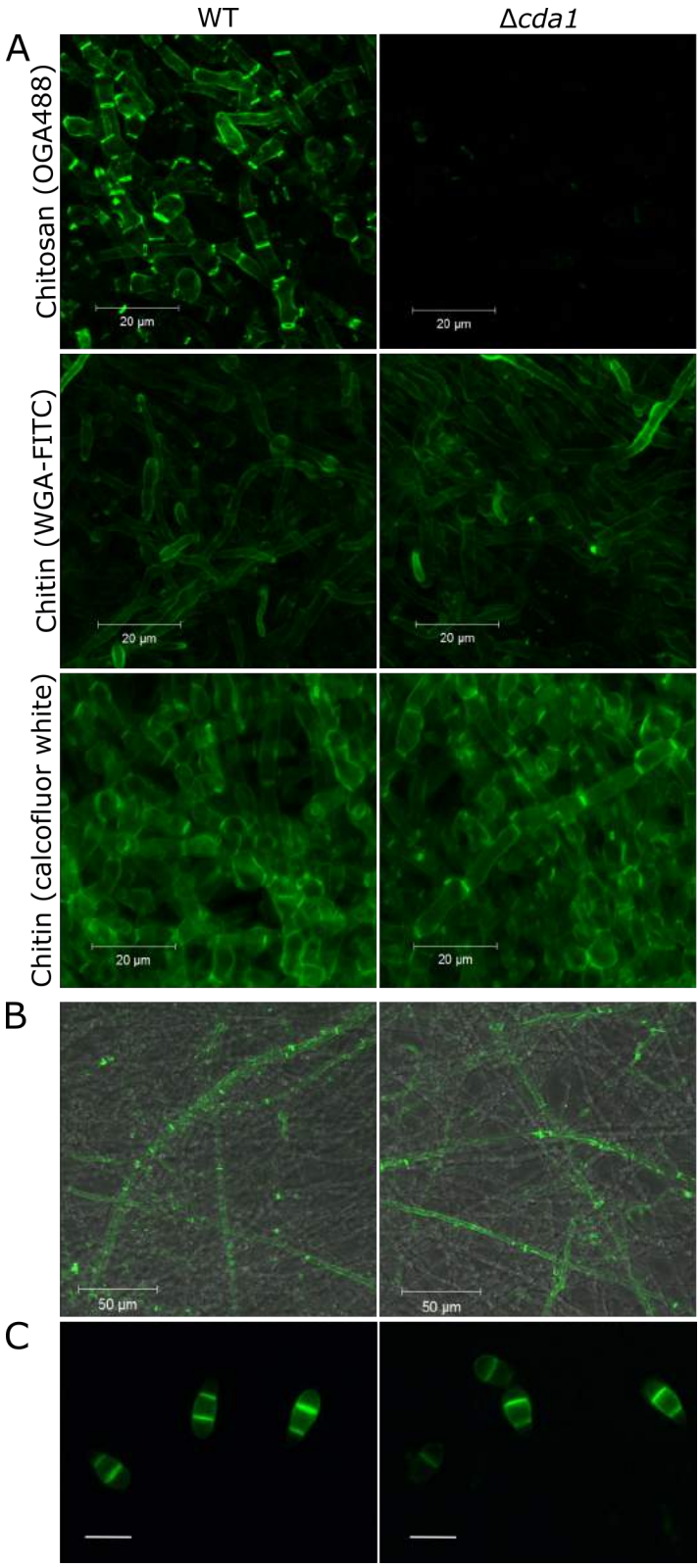
WT
Δcda1
A
Chitosan (OGA488)
Chitin (WGA-FITC)
Chitin (calcofluor white)
20 µm
B
50 µm
C

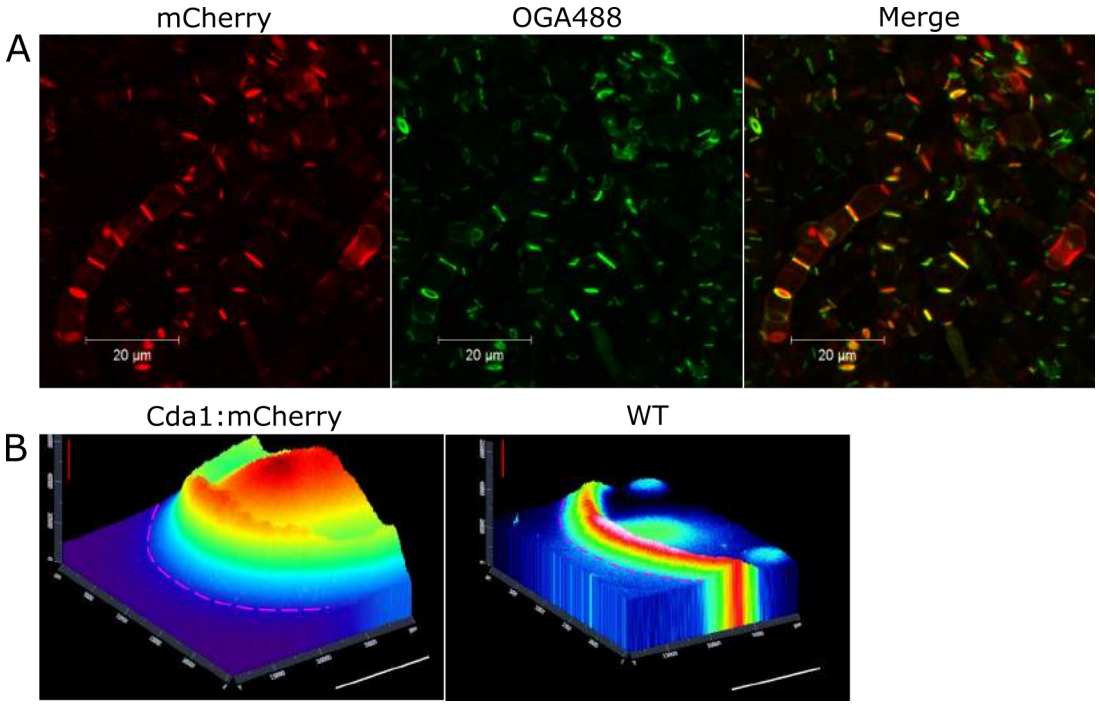

Figure 4.5: mCherry tagged Cda1 complements the deletion strain and colocalizes with chitosan. **A**) mCherry was tagged to the C-terminus of Cda1, and expressed in *cda1*. Restored staining with OGA488 was observed (middle panel), which colocalized with the mCherry fluorescence. mCherry fluorescence was most intense at the septa of vegetative hyphae (in both liquid and solid media), but was also evident in the lateral walls. Scale bars: 20 µm. **B**) Fluorescence heat map of a colony expressing Cda1:mCherry. Fluorescence was not detected at the colony margin (marked by the pink dashed line), but increased strongly towards the colony centre. A small amount of autofluorescence was observed in WT colonies. White scale bars: 10 mm, red scale bars: 20,000 fluorescence units.

To see if expression of Cda1:mCherry was able to complement *cda1*, OGA488 staining was performed on mycelial pellets grown in liquid CM. Not only was staining fully restored in the complemented strain, proving the functionality of the fusion protein, but it partially colocalized with the mCherry fluorescence of Cda1:mCherry (Figure 4.5A).

Phenotypic characterization of *cda1*

Cda1 is necessary for chitin deacetylation in the septa and lateral walls of mature vegetative hyphae. To determine the role of chitin deacetylation in these locations, growth of the *cda1* mutant was evaluated under a range of different stress conditions on solid and in liquid media. For growth on solid medium, the *cda1* mutant was subjected to chitin-binding cell wall perturbants (Calcofluor White and Congo Red) (Herth, 1980), oxidants (hydrogen peroxide), heavy metal (copper), osmotic stress (sorbitol), membrane perturbant (SDS), caffeine (an activator of the cell wall integrity pathway (Kuranda

A

	CM	MM	CFW	CR	H_2O_2	Sorbitol	Caffeine	SDS	Copper	MM-N	MM-C
WT	65.5 ± 3.7	53.4 ± 2.8	48.8 ± 1.1	49.0 ± 3.0	55.7 ± 2.1	41.8 ± 2.7	47.1 ± 1.3	49.0 ± 1.8	40.8 ± 4.3	59.2 ± 4.9	46.5 ± 3.2
Δ*cda1*	65.1 ± 3.4	51.6 ± 4.1	46.9 ± 2.6	47.6 ± 2.8	57.2 ± 2.6	40.6 ± 0.4	44.6 ± 7.4	47.7 ± 0.9	39.7 ± 2.3	56.7 ± 3.3	45.7 ± 4.6

B

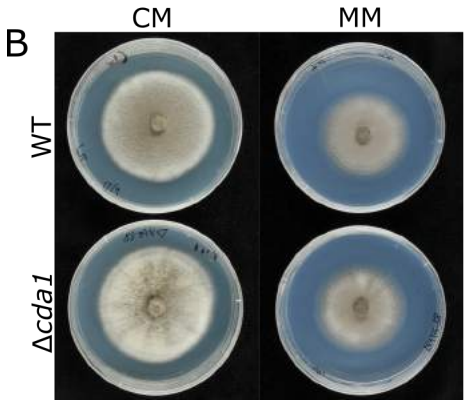

Figure 4.6: Radial growth on solid media is unaffected in *cda1*. **A**) Table showing mean colony diameters (mm, ±SD, n=3) in the WT and *cda1* strains, across a range of stress conditions. **B**) Colonies of WT and *cda1* strains growing on CM or MM. Details of treatments are shown in Appendix C. MM-C = Minimal Media without carbon, MM-N = Minimal Media without nitrogen.

et al., 2006)), and nutritional stress (MM without nitrogen or without carbon). Radial growth was measured at 10 days post-inoculation, but no significant differences were found between the WT strain and the *cda1* mutant (Student's T-test, $p<0.05$) (Figure 4.6). In addition, no consistent differences in colony appearance between the WT and *cda1* strains were observed under any conditions (Figure 4.6B). In liquid medium, growth was evaluated in the presence of lysing enzymes (a mixture of chitinases, glucanases and proteases), SDS, or hydrogen peroxide. Unexpectedly, the *cda1* mutant appeared to be more resistant to lysing enzymes and SDS, with greater biomass measured in flasks of *cda1* compared with the WT or complemented strain (Figure 4.7). However, further work is required to determine if these differences are statistically significant.

Lastly, pathogenic development was evaluated in the *cda1* mutant. Conidia of *cda1* germinated on a hydrophobic glass surface developed appressoria with identical morphology to WT. Unsurprisingly, pathogenicity was also unaffected in *cda1*; rice leaves inoculated with *cda1* conidia demonstrated similar lesion density to the WT strain (Figure 4.8). *CDA1* is therefore not required for pathogenic development in *M.oryzae*.

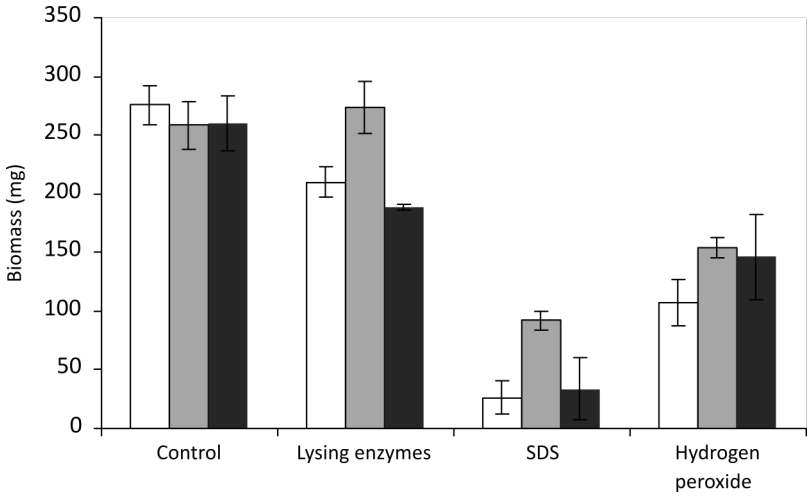

Figure 4.7: The *cda1* strain shows increased resistance to cell wall stress in liquid culture. Graph showing growth of WT (white bars), *cda1* (light grey bars) and *cda1:CDA1mCherry* (dark grey bars) in liquid complete medium, with or without various treatments. Lysing enzymes from *Trichoderma harzianum* were used at a final concentration of 4 mg/ml, SDS at 0.005% (w/v) and hydrogen peroxide at 2.5 mM. Treatments were added at 48 hpi, and biomass harvested at 120 hpi, except for flasks with hydrogen peroxide, which were harvested at 144 hpi. Error bars show SE, n=3-5.

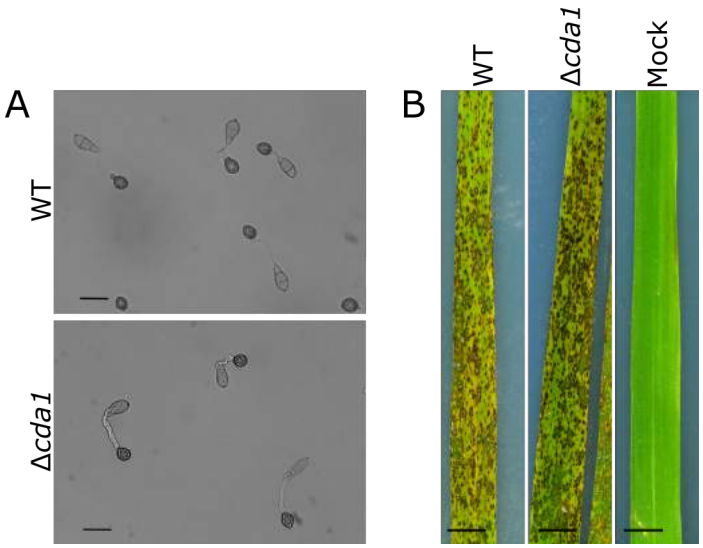

Figure 4.8: Pathogenicity is unaffected in the *cda1* strain. **A**) Appressoria of WT and *cda1* at 24 hpi on an artificial inductive surface. The deletion strain shows normal appressorium development. Scale bars: 20 μm. **B**) Pathogenicity of *cda1* on rice leaves. Leaves inoculated with conidia of *cda1* showed similar lesion density to the WT strain. A mock inoculation of 0.2% gelatine (w/v) was included as a negative control. Scale bars: 0.5 cm.

Ectopic expression of Cda1:mCherry

In the previous chapter, *CBP1:mCherry* was ectopically expressed in order to investigate how chitin deacetylation influences cell wall integrity and cellular morphology. However, these strains appeared to be identical to the WT and thus failed to answer these questions. In a further attempt, *CDA1:mCherry* was ectopically expressed in the WT background strain. In this case, expression was driven by the constitutive *EF1* promoter. Firstly, *pEF1* and the *CDA1* ORF were amplified individually using primer pairs 77/78 and 79/52 respectively (Appendix E), then joined by fusion PCR (primers 77 and 52). The *pEF1:CDA1* fusion was cloned into the *Asc*I site of pUCAP (Appendix D) to create the mCherry fusion. Following successful transformation, several independent lines ectopically expressing Cda1:mCherry were identified (Listed in Appendix F), and characterized during vegetative growth and pathogenic development.

During vegetative growth, strong fluorescence localized to the hyphal septa, with weaker fluorescence at the lateral walls, just as observed previously with the natively expressed Cda1:mCherry, and ectopically expressed Cbp1:mCherry. Such fluorescence also appeared to be restricted to the mature hyphae, and was not observed in those growing at colony margins (Figure 4.9). Both hyphal morphology and overall colony appearance were unaffected by ectopic expression of Cda1:mCherry. In conidia germinated on a hydrophobic glass surface, fluorescence was observed in the cell walls of the conidia, germ tubes and appressoria, although intracellular localization (most likely vacuolar) was also apparent. Intriguingly, a ring of fluorescence was occasionally observed at the centre of conidial septa, possibly demarcating the septal pores (not shown). Although germling morphology was identical to the WT in *pEF1:CDA1:mCherry* strains, staining with OGA488 demonstrated that ectopic chitin deacetylation had occurred in the conidial wall (Figure 4.9C). When inoculated onto onion epidermis, *pEF1:CDA1:mCherry* strains were able to penetrate the plant cells and form invasive hyphae, just as in the WT strain, with fluorescence localizing to the walls of invasive hyphae (Figure 4.9B).

Cell wall composition in *cda4*, *cda5* and *cda4/cda5*

Unlike Cda1, Cda4 and Cda5 each have a single putative transmembrane-domain at their C-terminus, suggesting that these chitin deacetylases may be membrane-localized, with

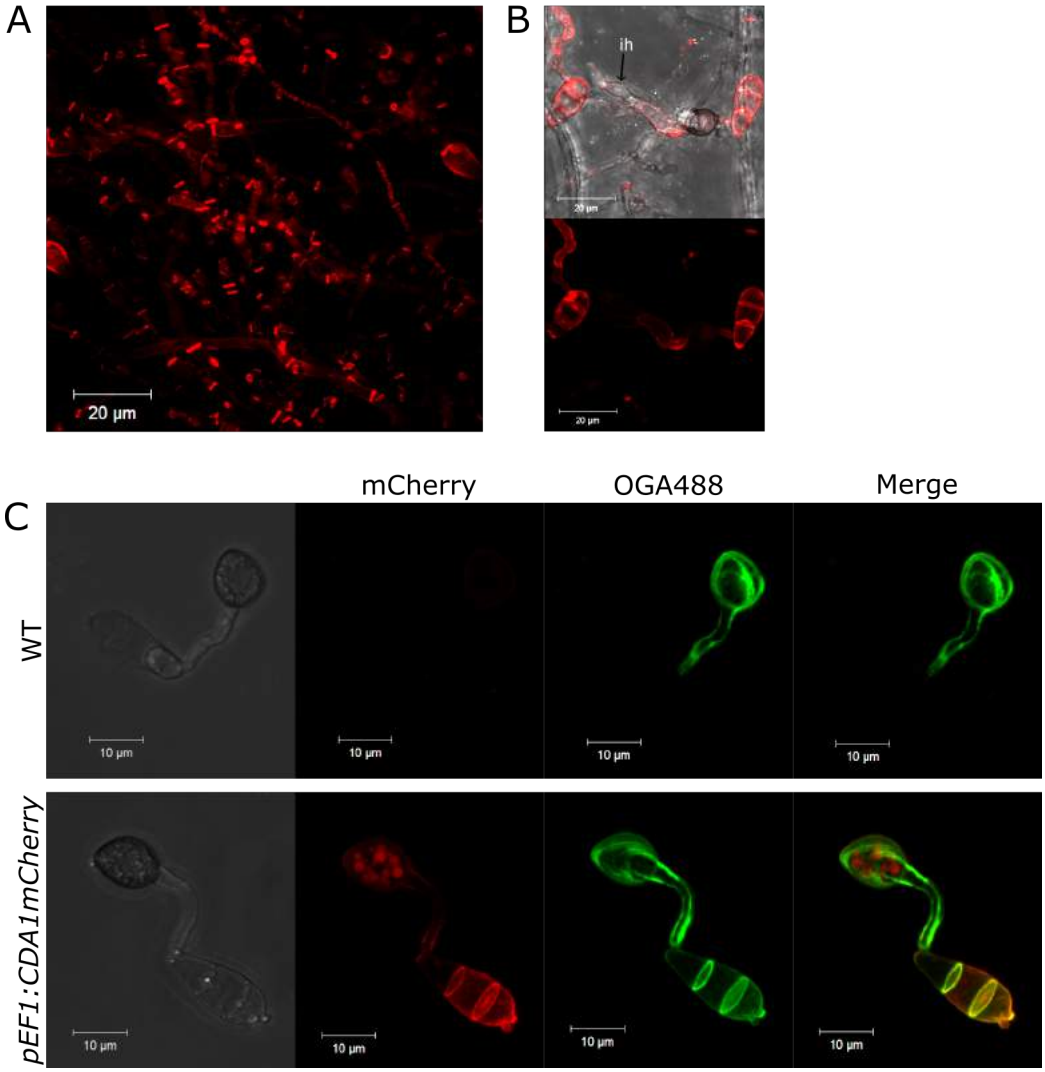

Figure 4.9: Ectopic expression of *CDA1:mCherry* by the constitutive *EF1* promoter. **A**) Localization of Cda1:mCherry in vegetative hyphae when expressed by the *EF1* promoter, showing similar localization to natively expressed Cda1:mCherry. **B**) Localization of Cda1:mCherry during invasive growth on onion epidermis at 24 hpi, showing fluorescence of invasive hyphae (ih). **C**) Localization of Cda1:mCherry at 24 hpi in germlings, and colocalization with the anti-chitosan probe OGA488. Appressorium development was unaffected in *pEF1:CDA1mCherry* strains, but ectopic chitin deacetylation was observed in the conidial cell wall. Scale bars: 20 µm in **A** and **B**, 10 µm in C. Note: Picture brightness and contrast have been increased to improve clarity upon printing.

the chitin deacetylase domain in contact with the cell wall. To determine whether Cda4 and Cda5 have roles in chitin deacetylation during vegetative growth, OGA488 staining was performed in the *cda4* and *cda4/cda5* mutants. When mycelial pellets resulting from 72 hr growth in liquid CM were stained with OGA488, no reduction in staining was observed in the deletion strains, in contrast to previous findings with the *cda1* mutant. However, when hyphae grown on solid CM were stained, reduced labelling was observed in hyphae close to the colony edge in both *cda4* and *cda4/cda5* (Figure 4.10). Staining was not completely abolished; septa in particular continued to show some fluorescence, possibly due to the action of Cda1. It was also unclear from this experiment whether staining was more reduced in *cda4/cda5*, compared with in *cda4*. Conidia of the deletion strains were stained with eosin Y, but no reduction in labelling was observed. These data suggest that Cda4 and Cda5 are required for chitin deacetylation in hyphae at the colony margins, but not those in the colony interior, in contrast to Cda1.

Localization of Cda4:mCherry

In order to gain further insight into chitin deacetylation by Cda4, an mCherry fusion was created. Primers 53 and 54 (Appendix E) were used to amplify the entire open reading frame of Cda4 (without the stop codon), including 2 kb of 5' promoter sequence (for native expression of the construct). This was cloned into the *Asc*I site of the pUCAP vector (Appendix D), thereby fusing mCherry to the C-terminus of Cda4. After transformation into both the WT and *cda4* background strains, a number of antibiotic-resistant transformants were screened for fluorescence during vegetative growth. Six independent lines (3 in each background strain, listed in Appendix F) demonstrating fluorescence in vegetative hyphae were selected for characterization. As expected, the strongest fluorescence was observed in hyphae at the colony edges. Surprisingly however, this fluorescence was entirely intracellular, as evidenced by the lack of colocalization with OGA488 (Figure 4.11A and E). In regions of the hyphae more distal to the tip, fluorescence was present in large intracellular bodies characteristic of vacuoles. At hyphal tips, Cda4:mCherry was not observed in the Spitzenkörper, but localized to tubular structures, small punctae, or in a more diffuse pattern, possibly indicating either cytoplasmic localization, or localization to very small compartments below the resolution limit of the microscope. Fluorescence was

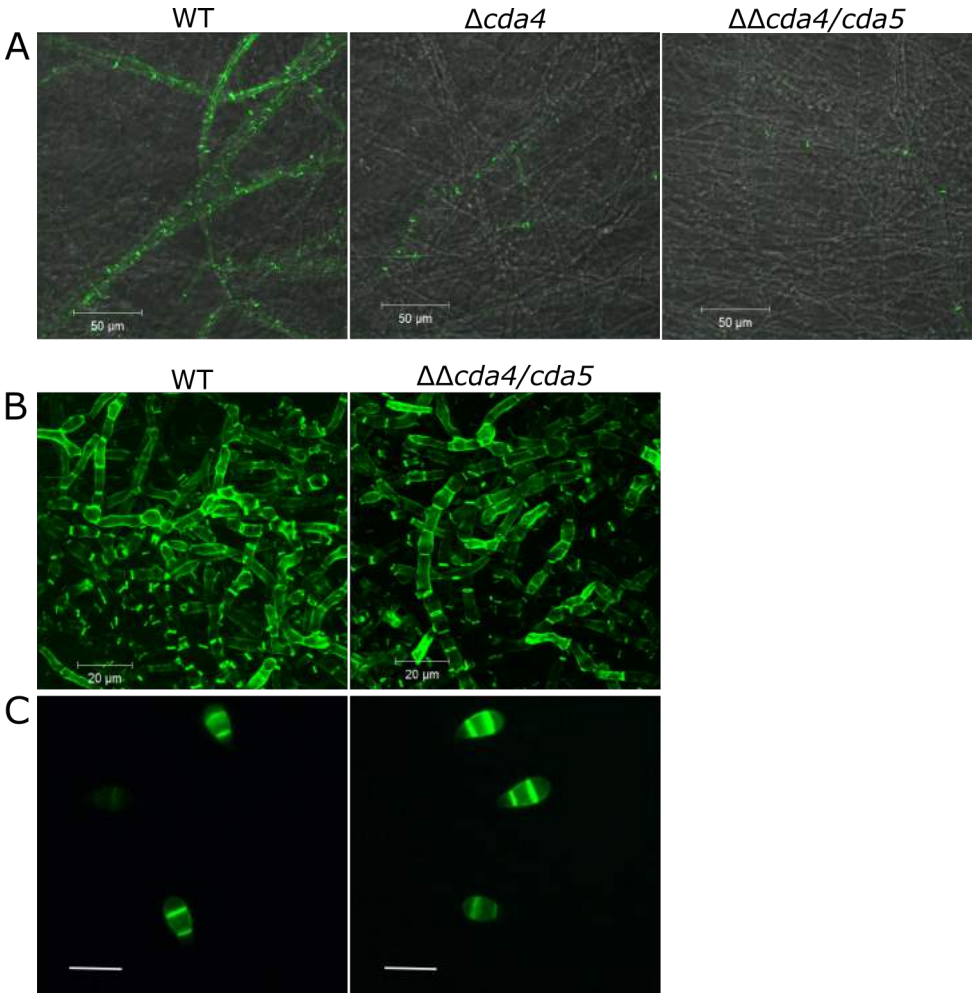

Figure 4.10: *CDA4* and *CDA5* are required for chitin deacetylation in vegetative hyphae. **A**) Staining of chitosan in vegetative hyphae grown on solid media in the WT, *cda4* and *cda4/cda5* strains, showing reduced chitosan staining in the deletion strains. Pictures were taken approximately 1.5-2 mm from the colony edge. **B**) Staining of chitosan in vegetative hyphae grown in liquid media, showing similar staining in the WT and *cda4/cda5* strains. **C**) Eosin Y staining of conidia. Staining was again unaffected in the double deletion strain. Scale bars: 50 µm in **A** and 20 µm in **B** and **C**.

also observed in developing conidia, again in intracellular bodies. Lastly, whilst no fluorescence was observed during appressorium development or in invasive hyphae, possible vacuolar fluorescence was observed in appressoria post-penetration (Figure 4.11C).

Due to the presence of a transmembrane domain at the C-terminus of Cda4, it was considered that the fusion of mCherry immediately adjacent to this (albeit with a 10aa linker sequence) may have disrupted localization of the protein. In order to independently verify the localization of Cda4 observed with the C-terminal fusion, an additional mCherry fusion was constructed. In this case, the mCherry was cloned into *CDA4* after the putative signal peptide, such that the mCherry would be at the N-terminus of the mature protein. However, strains transformed with this construct only exhibited weak fluorescence in comparison to the C-terminal fusion described above, although the localization appeared to be similar.

As with previously discussed fusion proteins, it was important to determine whether the C-terminal Cda4:mCherry fusion was functional. To do this, hyphae of the complemented strains were grown on solid CM and stained with OGA488. This revealed that chitin deacetylation was fully restored in *cda4* strains expressing *CDA4:mCherry*. In fact, staining appeared stronger than in the WT strain, suggesting over-complementation. This proves the functionality of the Cda4:mCherry fusion protein, although its level of expression may be higher than that of the native protein, possibly due to the copy number of the transformed construct, or regulatory elements which were not included in the construct.

In some cases, the absence of a fusion protein from the plasma membrane is simply due to rapid endocytic recycling of the protein, which means that it does not accumulate to detectable quantities at the cell periphery. To see if this was the case with Cda4:mCherry, hyphae were treated with latrunculin A (LatA), which prevents polymerization of actin and has previously been used to help localization of proteins to the cell membrane (Lanver et al., 2010). However, after a 30 min incubation with 1 μg/ml LatA, no fluorescence at the cell periphery was observed, and distribution of internal fluorescence also appeared to be unaffected (not shown).

The localization of Cda4:mCherry to small punctae near the hyphal tip was intriguing, and reminiscent of the localization of fluorescently-tagged chitin synthases observed in numerous previous studies (Fajardo-Somera et al., 2015; Treitschke et al., 2010). It was

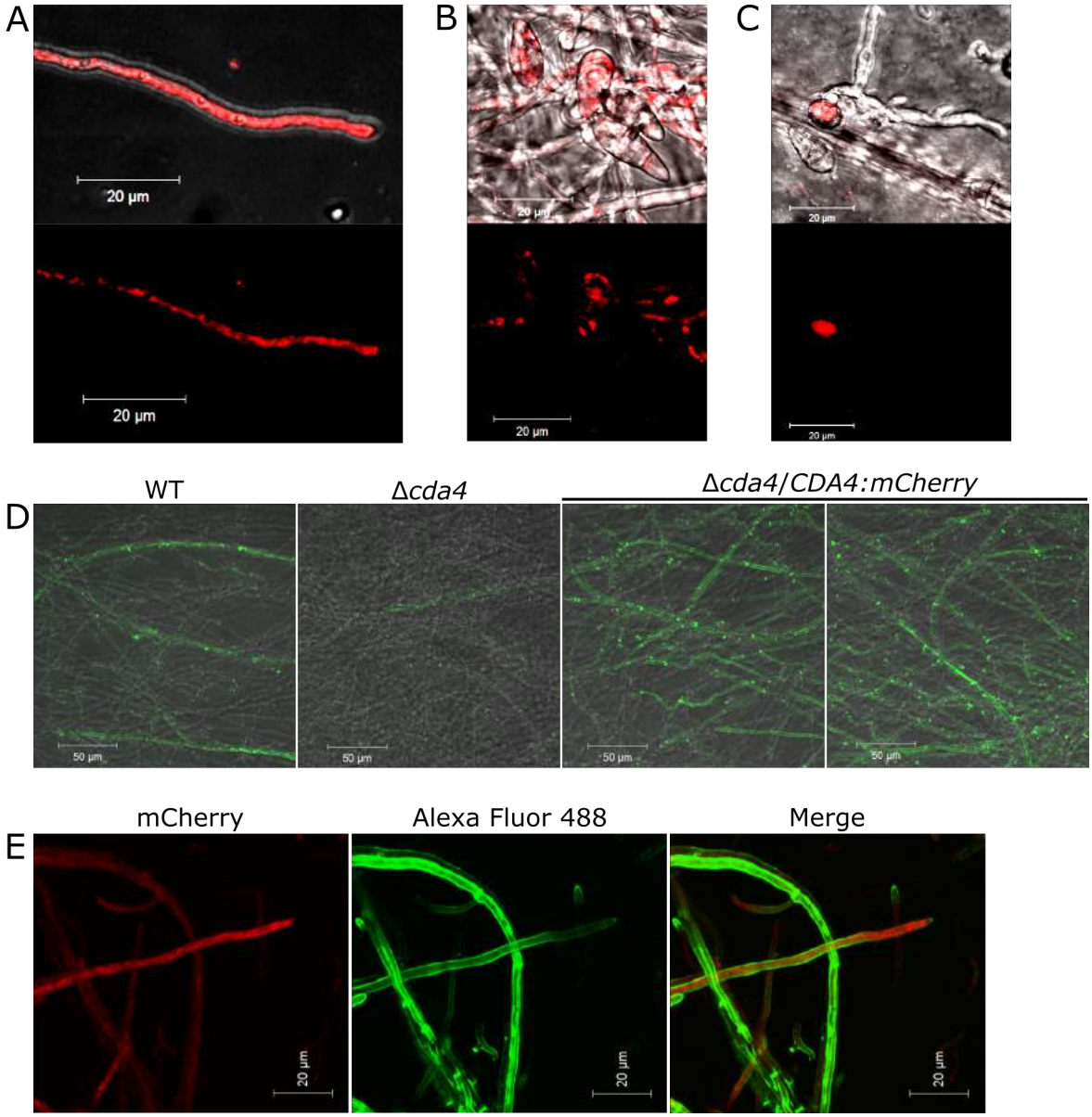

Figure 4.11: mCherry tagged Cda4 complements the deletion strain and localizes intracellularly. A) and **B**) Intracellular localization of Cda4:mCherry in vegetative hyphae and conidia respectively. During plant cell infection, fluorescence was observed in appressoria, but not in invasive hyphae (**C**). **D**) Staining of chitosan in vegetative hyphae grown on solid media, showing restored chitosan synthesis in *cda4/CDA4:mCherry* strains (two independent lines are shown). Pictures were taken 1.5-2 mm from the colony edge. **E**) Cda4:mCherry does not colocalize with OGA488 labelled chitosan. Scale bars: 20 µm in **A**, **B**, **C** and **E**, and 50 µm in **D**. Note: Picture brightness and contrast have been increased in A-C to improve clarity upon printing.

hypothesized that Cda4:mCherry may therefore colocalize with a chitin synthase, which would provide a valuable insight into possible coordinated transport of these proteins and the mechanism of chitin deacetylation. There are 7 chitin synthases in *M.oryzae*, which could possibly colocalize with Cda4:mCherry (Kong et al., 2012). However, taking into consideration previous work, three of the chitin synthases could be discounted: Chs7 is specific to appressorium development, and no fluorescence was observed in vegetative hyphae in strains expressing the Chs7:2xYFP construct used in Chapter 3. Chs5 and Chs6 both have myosin motor domains, and this class of Chs usually localizes to the Spitzenkörper and plasma membrane, which was not observed with Cda4:mCherry. This leaves Chs1, Chs2, Chs3 and Chs4 as potential colocalization partners. Previous work localizing Chs1 suggested that this was a likely candidate; Chs1:eGFP localized to hyphal tips and to developing conidia, although unfortunately only low magnification epifluorescence pictures were available for reference (Kong et al., 2012). To see if Chs1:eGFP colocalizes with Chs4:mCherry, first the Chs1:eGFP construct was cloned in precisely the same way as described previously (Kong et al., 2012): the open reading frame of Chs1, together with 1.4 kb of native promoter sequence was amplified with primers 61 and 62 (Appendix E). This was cloned into the *Asc*I-*Sbf*I sites of the pUCAP vector (Appendix D), producing a C-terminal fusion of eGFP to Chs1. This construct was previously used to complement the *chs1* mutant, suggesting full functionality of the fusion protein. The plasmid was transformed into the *CDA4:mCherry* background strain, and antibiotic resistant transformants screened for fluorescence. Several independent fluorescent lines were selected for characterization (Appendix F). Unfortunately, although Chs1:eGFP and Cda4:mCherry were often expressed in the same hyphae, colocalization of the fusion proteins was not observed. Chs1:eGFP fluorescence localized to the cell periphery and Spitzenkörper at hyphal tips, in contrast to Cda4:mCherry. In addition, although Chs1:eGFP also demonstrated intracellular localization, this only colocalized with Cda4:mCherry in the larger intracellular bodies, most likely vacuoles (Figure 4.12).

Phenotypic characterization of the *cda4*, *cda5* and *cda4/cda5* mutants

Cda4 appears to be necessary for chitin deacetylation in hyphae at colony margins. In order to determine the impact of *CDA4* and *CDA5* deletion upon cell wall integrity and

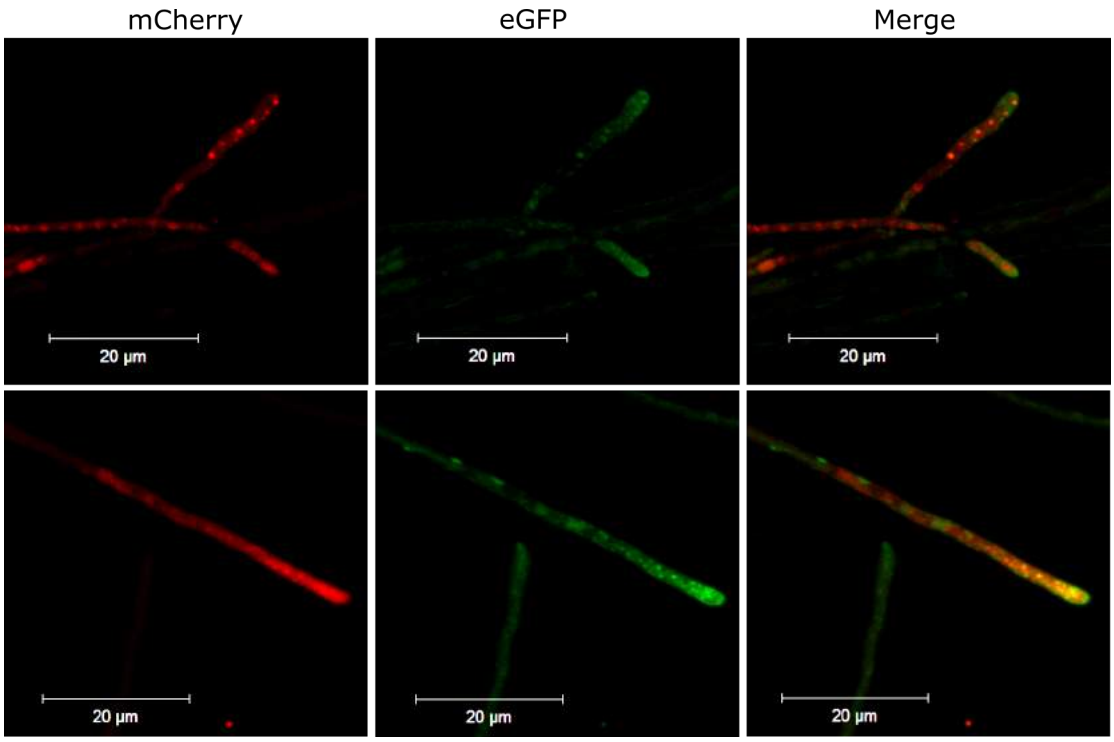

Figure 4.12: mCherry tagged Cda4 does not colocalize with eGFP tagged chitin synthase I. Chs1:eGFP localized to the cell periphery at hyphal tips, and also to intracellular punctae (possible 'chitosomes'). Some colocalization with Cda4:mCherry was observed in larger intracellular bodies, but not at the cell periphery. Scale bars: 20 µm. Note: Picture brightness and contrast have been increased to improve clarity upon printing.

hyphal morphogenesis, radial growth of the deletion strains was assessed on solid media under a range of stress conditions (as described previously for the *cda1* mutant). This revealed that small, but statistically significant (Students T-test, $p < 0.01$) reductions in growth occurred in the deletion strains compared with the WT (Figure 4.13A). However, although these growth reductions were statistically significant, in reality they generally represent less than a 10% reduction in growth, and, as such, their biological significance is questionable. For example, two independent *cda4/cda5* lines (13 and 23) were characterized in these growth experiments, but they did not demonstrate equivalent growth reductions under identical conditions. This suggests that the observed changes may not be related to the deletion of the genes themselves, but perhaps to 'cryptic' changes occurring during the transformation process. The largest reductions in growth were observed on media containing 2.5mM caffeine, where colony diameters were consistently ∼15% smaller in the deletion strains relative to the WT. Caffeine is known to activate the cell wall integrity pathway in a Tor1-dependant manner in *S.cerevisiae*. In addition, inhibition of Tor1 by the antibiotic rapamycin produced a transcriptional response that was very similar to cells treated with caffeine (Kuranda et al., 2006). However, growth of the deletion strains on media containing rapamycin was only marginally reduced, although this reduction is statistically significant.

Pathogenic development was also evaluated in the deletion strains. Unsurprisingly, given the apparent specificity of these genes to vegetative hyphae, appressorium development on hydrophobic glass and pathogenicity on rice leaves was unaffected in the deletion strains (Figure 4.14). Appressorium development from the tips of vegetative hyphae was also evaluated, but also appeared to be unaffected in the deletion strains (not shown).

A

	CM	MM	CFW	CR	H_2O_2	Sorbitol	Caffeine	SDS	MM-N	MM-C	Rapamycin
WT	65.6 ± 1.4	51.8 ± 1.1	53.0 ± 3.4	44.0 ± 0.7	49.7 ± 5.8	43.3 ± 2.7	54.1 ± 1.1	52.1 ± 1.2	55.1 ± 1.3	44.1 ± 2.2	52.1 ± 2.0
Δ*cda4*	63.2 ± 0.6	50.9 ± 1.1	51.8 ± 2.5	41.7 ± 0.9*	49.9 ± 4.0	42.0 ± 1.6	47.4 ± 1.3*	50.8 ± 1.3	54.0 ± 1.2	42.9 ± 1.6	50.7 ± 2.9
Δ*cda5*	61.3 ± 1.7*	50.9 ± 3.1	50.3 ± 2.7	41.1 ± 0.9*	50.0 ± 3.5	41.0 ± 1.9*	48.8 ± 5.5*	49.7 ± 0.7*	53.9 ± 2.3	45.5 ± 0.9	49.6 ± 1.3*
ΔΔ*cda4/cda5*_ 13	62.3 ± 1.5	50.6 ± 1.7	51.4 ± 2.9	44.4 ± 2.8	52.2 ± 5.5	41.7 ± 1.9	46.4 ± 1.7*	50.9 ± 2.1	55.2 ± 0.4	44.6 ± 1.4	49.3 ± 1.1*
ΔΔ*cda4/cda5* _23	59.9 ± 0.9*	48.8 ± 1.2	48.4 ± 2.6*	41.6 ± 0.8*	49.9 ± 5.1	40.3 ± 1.7*	46.1 ± 3.1*	47.8 ± 1.3*	54.6 ± 2.1	42.1 ± 1.1	47.0 ± 1.1*

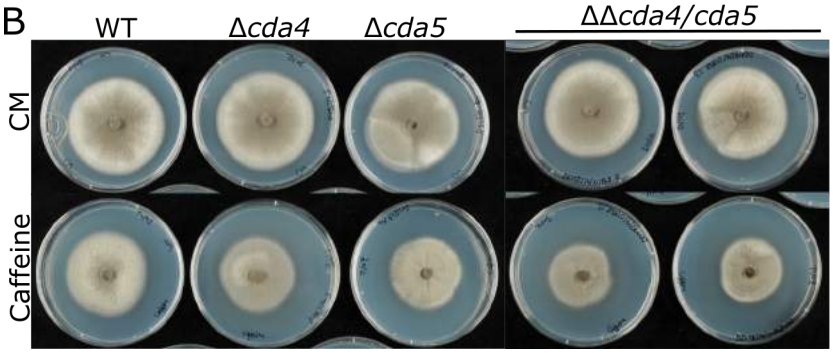

Figure 4.13: Radial growth of the *cda4* and *cda4/cda5* strains is largely unaffected on solid media. **A**) Table showing mean colony diameters (mm, ±SD, n=3) in the WT and deletion strains, across a range of stress conditions. Two independent lines (13 and 23) are shown for *cda4/cda5*. There was a statistically significant reduction in growth in a number of treatments (*), p<0.01, students T-test, n=3. Growth on caffeine was particularly reduced in the *cda4/cda5* strain (pictured in **B**). Details of treatments are shown in Appendix C.

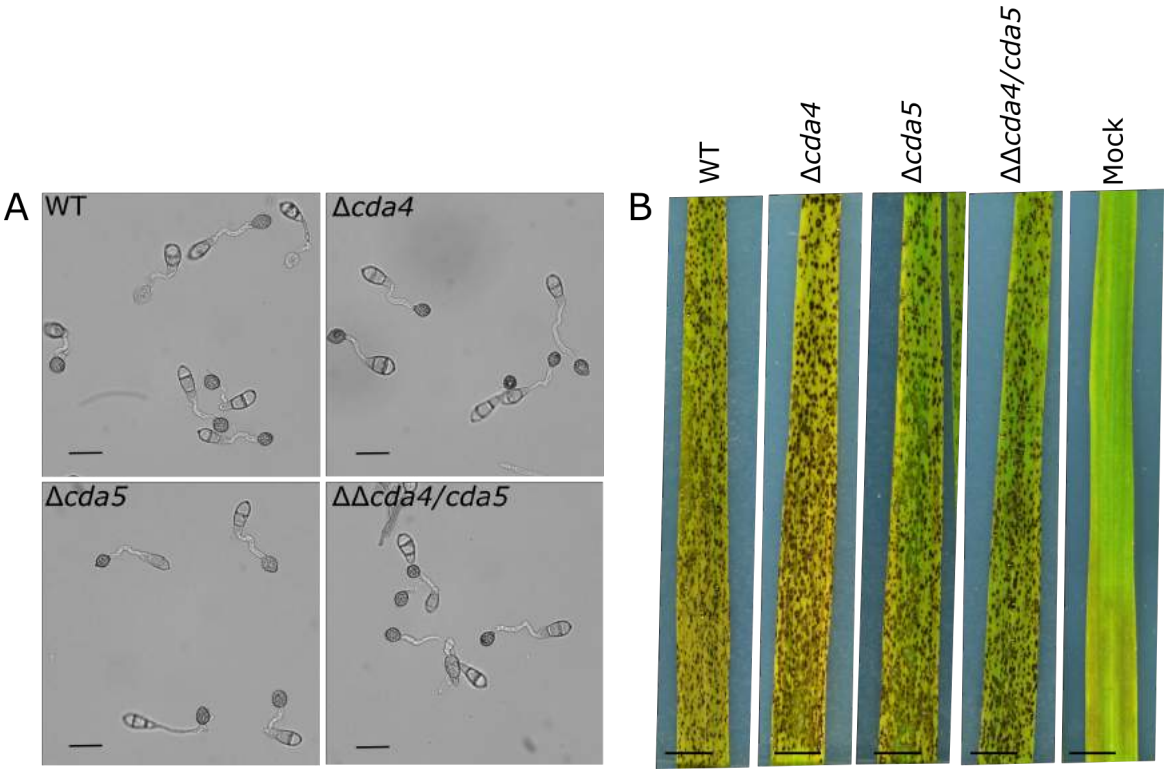

Figure 4.14: Pathogenic development is unaffected in the *cda4*, *cda5* and *cda4/cda5* strains. **A**) Appressoria of the WT and deletion strains at 24 hpi on a hydrophobic glass surface, showing normal development in all strains. Scale bars: 20 μm. **B**) Pathogenicity of the deletion strains on rice leaves. Leaves inoculated with conidia of either the WT or deletion strains showed similar lesion densities. A mock inoculation of 0.2% gelatine (w/v) was included as a negative control. Scale bars: 0.5 cm.

4.3 Discussion

Previous studies of chitin deacetylation in phytopathogenic fungi demonstrated that chitosan is a component of the cell wall during plant infection (Gueddari et al., 2002; Fujikawa et al., 2009). However, it was not known whether chitosan is also present in the cell wall at other stages of the life-cycle in these fungi. In this chapter, chitosan has been shown to be a component of the cell wall in the vegetative hyphae of *M.oryzae*, suggesting that chitin deacetylation has roles beyond those already described for appressorium development. Two chitin deacetylases (Cda1 and Cda4) were found to be necessary for chitin deacetylation in vegetative hyphae. Interestingly, they appear to be involved in two distinct modes of chitin deacetylation, in discrete zones of colonies.

Cda1, a predicted secreted protein with a chitin deacetylase domain and a single C-terminal chitin-binding domain, is required for *in situ* chitin deacetylation in the cell walls of mature hyphae located in the colony interior. The role of chitin deacetylation in these hyphae is currently unclear. Considering that expression of Cda1 is restricted to mature hyphae, it is unlikely that it plays a direct role in growth or hyphal morphogenesis. Indeed, radial growth of the *cda1* mutant on solid media was identical to the WT strain under a range of stress conditions, including cell wall perturbants (Congo Red and Calcofluor white), detergents (SDS) and hyperosmotic stress. However, in liquid media *cda1* appeared to demonstrate increased resistance to cell wall lysing enzymes and SDS. Since the susceptibility of strains to these treatments is likely to correlate with the permeability of the cell wall (De Nobel and Barnett, 1991), this could indicate that cell wall permeability is reduced in the *cda1* mutant. Chitin is known to be a highly crystalline polysaccharide, and therefore has low permeability. It is hypothesized that the deacetylation of chitin by Cda1 would cause loss of crystallinity, and therefore increased permeability. Thus, the biological role of chitin deacetylation by Cda1 could be to increase cell wall permeability in the septa and lateral walls of mature hyphae. Septa have been shown to be sites of protein secretion in hyphae (Hayakawa et al., 2011), and so efficient secretion from septa may be dependant upon high cell wall permeability. Further work is required to characterize wall permeability and to determine whether septal protein secretion is defective in *cda1*. In addition to cell wall permeability, it is also important to consider the effects that chitin deacetylation may have on cell wall charge. As discussed

previously, chitosan is a polycationic polysaccharide, whereas chitin is uncharged. The deacetylation of chitin is therefore likely to increase the positive charge of the cell wall, which would increase its interaction with a negatively charged molecule, such as SDS. In the case of the *cda1* mutant, the absence of chitosan would result in reduced interaction of SDS with the cell wall, perhaps explaining the increased resistance. Whether or not the change in cell wall charge caused by chitin deacetylation has any biological significance is another matter, and requires further investigation. Lastly, an additional role for chitin deacetylation by Cda1 in mature hyphae could be as part of a carbon-recycling mechanism. The cell wall is a major carbon source, and so its deconstruction could serve to redistribute this carbon from the aged parts of the fungal colony to the growing edge. Chitin deacetylation could either serve as a direct source of carbon in the form of acetate (released by the deacetylation reaction), or be the first step to making the cell wall of old hyphae more susceptible to degradation by chitinases and glucanases. However, no evidence for a role in carbon-recycling was found in the present study. Firstly, *CDA1* appears to be highly expressed even after a relatively short incubation in nutrient-rich complete medium, at which point carbon-recycling from the cell wall would probably not be necessary. Secondly, under conditions of carbon or nitrogen starvation on solid medium, no reduction in radial growth was observed. Yet, further investigation is required before this hypothesis can be dismissed; more sensitive methods may be required to study the efficiency of carbon recycling from the cell wall in the *cda1* mutant.

The *in situ* deacetylation of chitin by Cda1 suggests that the chitin is deacetylated post-synthesis in mature hyphae. Previously, it had been suggested that crystalline chitin in the cell wall was not susceptible to deacetylation, due to inaccessibility of the substrate (Davis and Bartnicki-Garcia, 1984b). However, data from this study suggests that this may not necessarily be the case. The chitin in the septa and lateral walls of hyphae is presumably crystalline (although there is no way to determine this), and yet it is able to be deacetylated by Cda1. In addition, ectopic expression of Cda1:mCherry resulted in ectopic chitin deacetylation in the conidial cell wall. It is therefore likely that crystalline chitin can be deacetylated *in vivo*, although the extent of deacetylation cannot be determined from the current data. Certain properties of Cda1 render it more active against crystalline chitin than previously characterized chitin deacetylases. In particular,

the presence of the chitin-binding domain may increase deacetylase activity on crystalline chitin, by increasing substrate binding of the enzyme, and/or by disrupting chitin structure and increasing accessibility (Guillén et al., 2010).

Chitosan was also found in the cell walls of vegetative hyphae located in the subperipheral zone of colonies, although Cda1 was not required for its synthesis here. Chitin deacetylation in these cells required Cda4, and perhaps to a lesser extent Cda5, two predicted secreted proteins with putative single transmembrane domains. The role of chitin deacetylation in these cells also remains unclear, but it may be associated with hyphal maturation. During this process, chitosan could serve to cross-link components of the wall, either ionically or covalently, thereby increasing the strength and rigidity of the cell wall. Another cell wall process which is associated with hyphal maturation is melanization. Cells at the growing edge of colonies are unmelanized, but become melanized with increased distance from the colony margin. As of yet, there is no evidence for a direct link between chitosan and melanin in the cell wall, and melanization proceeded normally in all the *cda* mutants (including those involved in appressorium development). A 'leaky melanin' phenotype was observed in *C.neoformans* strains lacking chitosan (Baker et al., 2007), but this is more likely to be a general symptom of reduced cell wall integrity, rather than evidence of a direct link between chitosan and melanin.

The staining of chitosan in these hyphae was reduced in the *cda4* and *cda4/cda5* strains, but the loss of chitosan had little impact on radial growth. This suggests that chitin deacetylation is not required for cell wall integrity or morphogenesis in these hyphae, although this may be due to compensatory changes in cell wall composition, which were not investigated. The deletion strains did appear to be more sensitive to caffeine, but even then the reduction in growth was less than 15% compared with the WT. Additionally, since caffeine has pleiotropic effects on cells (Kuranda et al., 2006), the increased sensitivity of the deletion strains to this chemical does not necessarily provide any particular insight into the role played by Cda4 and Cda5. However, numerous studies have found that mutations in components of the cell wall integrity signalling pathway or in genes with roles in cell wall biogenesis are also more sensitive to caffeine (Levin, 2011). The change in cell wall composition caused by deletion of *CDA4* and *CDA5* most likely causes the increased caffeine sensitivity, but the mechanism behind this is unknown.

Unlike Cda1:mCherry, the Cda4:mCherry fusion localized intracellularly, suggesting that Cda4 does not deacetylate chitin *in situ* in the cell wall. Instead, Cda4 may deacetylate nascent chitin chains in collaboration with a particular chitin synthase. Although Cda4:mCherry did not colocalize with Chs1:eGFP, it is hypothesized that Cda4 may colocalize with another chitin synthase (perhaps Chs2, Chs3 or Chs4) in intracellular vesicles (chitosomes). There are two possible models for chitin deacetylation involving Cda4. In the first, the synthesis of chitin and its subsequent deacetylation by Cda4 occurs intracellularly. The vesicles, loaded with chitin and chitosan, could then deliver their cargo to the cell wall. In support of this model, the synthesis of chitin by chitin synthases isolated from chitosomes has been demonstrated previously in *Mucor rouxii* (Davis and Bartnicki-Garcia, 1984a). This suggests that chitin synthases residing in the chitosomes are active, at least *in vitro*. However, no chitin deacetylase activity was found associated with chitosomes in this fungus (Davis and Bartnicki-Garcia, 1984a), and *in vivo* chitin synthesis in chitosomes has never been demonstrated. In the second model, the chitin synthase and Cda4 remain inactive until delivered to the plasma membrane, where deacetylation of nascent chitin chains occurs. The absence of detectable Cda4:mCherry at the cell periphery may simply be a result of very low levels of the enzyme. This would be consistent with nascent chitin chains being highly susceptible to deacetylation, and therefore only small amounts of enzyme would be required for complete deacetylation (Davis and Bartnicki-Garcia, 1984b). In both models, the transmembrane domain of Cda4 could serve to allow close association between the chitin synthase and Cda4. This may be required for sorting and loading of the enzymes into the same vesicles, as well as positioning Cda4 close to the nascent chitin chains.

It was originally hypothesized that chitin deacetylation would be required for cellular morphogenesis during vegetative growth, just as it was hypothesized to be important for appressorium morphogenesis in the previous chapter. Again, however, no evidence for this was found. Firstly, the localization of chitosan observed with OGA488 did not support a role in morphogenesis; fluorescence was only occasionally observed at hyphal tips (and even then not exclusively so), was not detected in conidia and did not specifically localize to hyphal branching sites. Secondly, deletion strains in which chitin deacetylation in the vegetative hyphae was severely reduced displayed no defects in cell shape or growth.

Lastly, the ectopic expression of Cda1:mCherry, which caused ectopic chitin deacetylation, also failed to demonstrate morphogenic defects. Taken together, it can be concluded that chitin deacetylation has no role in cellular morphogenesis during vegetative growth in *M.oryzae*.

4.4 Conclusions

The investigation of chitin deacetylation in vegetative hyphae has led to novel insights into the roles and mechanisms of chitin deacetylation in *M.oryzae*. The presence of chitosan in vegetative hyphae suggests that chitin deacetylation has roles beyond those already hypothesized during pathogenic development in phytopathogenic fungi. However, from the localization of chitosan, deletion and localization of chitin deacetylases, and ectopic expression of chitin deacetylase, it is clear that chitin deacetylation is neither required for, nor involved in, the process of cellular morphogenesis in vegetative hyphae. The actual purpose of chitin deacetylation in vegetative hyphae was not able to be determined conclusively, although it appears that this may differ according to the phase of growth. Cda1 deacetylates chitin in mature hyphae at the colony interior, which may be required for efficient protein secretion or carbon recycling from the cell wall. In contrast, Cda4 is required for chitin deacetylation in the sub-peripheral region of the colony, although there may be some overlap between Cda1 and Cda4. As well as being spatially separated, deacetylation by these CDAs also appears to occur by distinct mechanisms. Cda1 deacetylates chitin *in situ*, whereas Cda4 may collaborate with a chitin synthase to deacetylate nascent chitin chains. This gives a further insight into the possible coordination between these enzymes, as previously discussed in Chapter 3.

Chapter 5

Hydrolysis of chitosan

5.1 Introduction

In the previous chapters (Chapters 3 and 4), chitin deacetylation was revealed to play roles in appressorium development and vegetative growth. In this Chapter, the role of chitosan hydrolysis is investigated.

Roles of cell wall hydrolases in fungi

For each major polysaccharide component present in the cell wall, there is an enzyme responsible for its hydrolysis. These cell wall hydrolases include enzymes with chitinase, β1,3-glucanase, α1,3-glucanase, mannanase and chitosanase activities. The enzymatic hydrolysis of the cell wall has been shown to have numerous roles in fungi. However, there remain many aspects of this process that are poorly understood, particularly in filamentous fungi.

In fungal species with a unicellular growth phase, cell wall hydrolases have an important role in cell-separation. In *S.cerevisiae*, enzymatic degradation of the septum during cell-separation is performed by both a chitinase (Cts1) and an endo-β1,3-glucanase (Eng1) (Kuranda and Robbins, 1991; Baladrón et al., 2002). Strains in which these genes have been deleted produce clumps or chains of cells, due to failed septum degradation. Similar results have been obtained in *C.albicans*, for the chitinase Cht3 and endo-β1,3-glucanase Eng1, which are functional homologues of Cts1 and Eng1 in *S.cerevisiae* respectively (Dünkler et al., 2005; Esteban et al., 2005). In *S.pombe*, the septum is composed of both β1,3-glucan and α1,3-glucan, and cell separation requires the endo-α1,3-glucanase Agn1 and the endo-β1,3-glucanase Eng1 (Dekker et al., 2004). Another pair of glucanases, the endo-α1,3-glucanase Agn2 and the endo-β1,3-glucanase Eng2 are required for degradation of the ascus wall, and release of ascospores in *S.pombe* (Dekker et al., 2004; del Dedo et al., 2009). Recently, a pair of chitinases were also found to be required for cell-separation during the yeast-growth phase of *U.maydis* (Langner et al., 2015).

As well as being involved in cell separation, there is also evidence for a role of cell wall hydrolases in cell fusion, which requires localized degradation of the cell wall between two cells. In *S.pombe*, a number of glucanases including Agn2, Eng2 and Exg3 localize to the fusion focus and are required for efficient cell fusion (Dudin et al., 2015).

In numerous species of filamentous fungi, cell wall hydrolases have been shown to be

important for autolysis, a natural process occurring in ageing fungal cultures and those growing under nutrient-limiting conditions (White et al., 2002). During autolysis, cells are degraded in order to provide nutrients for continued growth. As a carbohydrate-rich structure, the cell wall represents a valuable source of nutrients. In *Aspergillus nidulans* the chitinase ChiB and endo-β1,3-glucanase EngA are both required for optimal autolysis during carbon starvation (Shin et al., 2009; Szilágyi et al., 2010). Similar findings were obtained in *Aspergillus niger*, where the chitinase CfcA and α1,3-glucanase AgnB were required for starvation-induced autolysis (van Munster et al., 2014). In other fungi, functional data demonstrating the involvement of hydrolytic enzymes in autolysis has not been found, although increased glucanase or chitinase activity is observed in aged cultures of *Botrytis cinerea* (Stahmann et al., 1992), *Penicillium oxilacum* (Copa-Patiño et al., 1989) and *Coprinellus congregatus* (Lim and Choi, 2009).

Apart from degrading their own cell walls, many hydrolytic enzymes have also been found to have antagonistic roles in fungi. In *A.nidulans* the C-II subgroup of chitinases are induced during interactions with *B.cinerea* and *R.solani*, and *A.nidulans* deletion strains show increased growth in mixed cultures with *B.cinerea* (Tzelepis et al., 2014). *Trichoderma* species also produce a range of chitinase, glucanases and proteases with potential roles in antagonistic interactions (Viterbo et al., 2002). In particular, a 42 kDa chitinase (Cht42) has been shown to be a key enzyme involved in mycoparasitic interactions; this enzyme is upregulated during confrontation between *T.atroviride* (Kullnig et al., 2000), and deletion of *CHT42* in *T.virens* demonstrated reduced biocontrol activities against *R.solani* (Baek et al., 1999).

Cell wall hydrolases clearly have a number of roles in large-scale degradation of the cell wall. However, it has been hypothesized that cell wall hydrolysis may also play a role in cell wall remodelling. At hyphal tips, a balance of synthase and hydrolase activities may maintain the cell wall in a pliable state, whilst at branching sites, highly regulated and restricted hydrolysis of the wall may result in enhanced localized flexibility, necessary to allow cell expansion (Bartnicki-Garcia, 1973). Currently, there is limited evidence to support these hypotheses. For example, in *C.albicans* chitinase activity was unaltered by the deletion of chitin synthases, and *vice versa*, suggesting that these enzymes are functionally independent (Selvaggini et al., 2004). Moreover, in the majority of cases

deletion of chitinases or glucanases does not result in a measurable change in growth or morphogenesis. Even a quintuple knockout of class III chitinase genes in *A.fumigatus* did not result in any growth or germination defects (Alcazar-Fuoli et al., 2011), neither did a double knockout of the chitinases CtcB and CfcI in *A.niger* (van Munster et al., 2013). Single chitinase deletions have also been performed in a number of species, including *N.crassa* (Tzelepis et al., 2012), *A.fumigatus* (Jaques et al., 2003) and *Y.lipolytica* (Park et al., 2014), which also largely failed to demonstrate morphogenic defects. Yet, there are some exceptions: Deletion of the GPI-anchored chitinase Chit-1 in *N.crassa* resulted in a reduced growth rate, supporting a possible role in wall remodelling during hyphal growth (Tzelepis et al., 2012); in *Penicillium chrysogenum* deletion of ChiB1 affected cell wall integrity (Kamerewerd et al., 2011). In *C.neoformans*, deletion of all four endochitinases did not affect vegetative growth or morphology, but prevented mating (Baker et al., 2009). Glucanases have been the subject of fewer studies than chitinases, but deletion of these too has often failed to provide evidence for morphogenic roles: Deletion strains of the endo-β1,3-glucanases Eng2 and EglC in *A.fumigatus* and *A.nidulans* respectively were identical to the WT strain (Choi et al., 2005; Hartl et al., 2011). However, a recently characterized family of glucan-modifying enzymes do appear to have intriguing roles in morphogenesis. The SUN proteins enzymes have exoβ1,3-glucanase activity and belong to a newly classified GH132 family. Deletion of *SUN1* in *A.fumigatus* resulted in a number of morphogenic defects, including intrahyphal hyphae and leaky hyphal tips, which were attributed to a possible role in cell wall biogenesis and septation (Gastebois et al., 2013). Exactly how the biochemical activity of the SUN proteins relates to their biological function remains unknown.

One significant obstacle preventing the detailed analysis of cell wall hydrolysing enzymes is their frequent functional redundancy. In most fungi, chitinases and glucanases exist in large multigene families, which are likely able to compensate for the loss of a single gene. Genetic disruption of entire gene families will therefore be required if the function of cell wall hydrolases is to be determined. Only certain species of fungi have small enough gene families for this to be possible using current gene-deletion techniques. A notable example is *Ashbya gossypii*, which has just a single chitinase gene. Interestingly, filamentous growth is unaffected by the deletion of this gene and only a mild defect

in sporulation was observed (Dünkler et al., 2008), suggesting that chitin hydrolysis is not required for hyphal morphogenesis in this fungus. A recent study in *U.maydis* also casts doubt over the involvement of chitin hydrolysis in morphogenesis. Deletion of all four chitinase genes, which led to complete loss of chitinase activity, did not impair filamentous growth or pathogenicity of the fungus (Langner et al., 2015).

The localization of cell wall hydrolysing enzymes could also offer some insight into their roles, although this has only been performed in a few cases. In *A.nidulans* an eGFP fusion of the chitinase ChiA localized to hyphal branching sites, and to conidial germination sites, thus supporting its role in morphogenesis (Yamazaki et al., 2008). However, the functionality of this fusion protein was not proven, and deletion of *ChiA* did not result in any growth defects (Yamazaki et al., 2007). Conversely, a dsRed fusion of ChiB1 in *Penicillium chrysogenum* showed no such specific localization, fluorescence was observed at the entire cell surface (Kamerewerd et al., 2011).

In summary, whilst cell wall hydrolases clearly have a multitude of roles in fungi, only some of these are supported by conclusive evidence. There is ample evidence to support a role for chitinases and glucanases in cell-separation, cell fusion, autolysis and in antagonistic interactions. However, roles in cell wall remodelling have been much more difficult to demonstrate, and our understanding of the link between cell wall hydrolysis and morphogenesis is far from complete. This is partly due to functional redundancy within the large chitinase and glucanase gene families found in most fungi. Yet, even in strains which do demonstrate morphogenic defects upon gene deletion (e.g. SUN proteins), the relationship between hydrolysis and morphogenesis is poorly understood. Further investigations are therefore required to determine the relationship between polysaccharide hydrolysis and cellular morphogenesis.

Fungal chitosanases

Chitosanases (EC 3.2.1.132) have been discovered and characterized in a broad range of organisms, including bacteria, plants and fungi (Thadathil and Velappan, 2014). They can be classified, according to sequence similarity, into five glycosyl hydrolase (GH) families: GH5, GH8, GH46, GH75 and GH80 (Hoell et al., 2010). However, all fungal chitosanases (CSN) characterized so far belong to the GH75 family, and are endo-type

chitosanases. Chitosanases can be further classified according to their substrate specificity: Class II enzymes are only able to hydrolyze a bond between two β1,4-linked glucosamine residues (GlcN-GlcN), whereas Class I and III enzymes are also able to hydrolyze β1,4-linkages between GlcNAc and GlcN residues (Fukamizo et al., 1994). Exo-β-D-glucosaminidases (EC 3.2.1.165) are also able to hydrolyze chitosan, although in this case individual glucosamine residues are cleaved from the non-reducing end of chitosan chains.

Although the structures and catalytic mechanisms have been determined for a number of bacterial chitosanases (reviewed in Hoell et al. (2010)), similar studies of fungal chitosanase are extremely limited. In *A.fumigatus*, a chitosanase was characterized as a class I CSN, and a pair of key catalytic residues (D160 and E169) identified (Cheng et al., 2006). Chitosanases from *Penicillium spp.* (Rodríguez-Martín et al., 2010; Zhu et al., 2012) and *A.oryzae* (Sugita et al., 2012) have also been cloned and characterized. Data regarding the biological roles of fungal chitosanases is also scarce, especially in comparison with those characterizing the roles of chitinases and glucanases, as discussed previously. Deletion of the chitosanase CsnB in *A.fumigatus* had no effect on vegetative growth or sporulation, although was required for growth on media containing chitosan as a carbon source (Beck et al., 2014). Similarly, silencing of *CSN1* in *Fusarium solani* also had no effect on mycelial growth or sporulation, although reduced chitosanase activity was recorded. However, overexpression of *CSN1* did result in reduced mycelial growth and virulence, although the reason for this effect was not investigated (Liu et al., 2010).

Chitin deacetylation has not been investigated in any of the organisms in which chitosanases have been characterized, and *vice versa*. Therefore, these aforementioned studies lack any frame of reference. Indeed, it is difficult to determine the role of a chitosanase without first having prior knowledge of when and where chitosan is synthesized during the life-cycle of the fungus. In this thesis, chitosan has already been shown to play a critical role in appressorium development (Chapter 3), and to be a component of the cell wall during hyphal growth (Chapter 4). In light of these data, and given the general paucity of data regarding the biological roles of fungal chitosanases, it would seem opportune to use *M.oryzae* as an organism to elucidate the role of chitosanases. In doing so, this could result in a further insight into the role of cell wall hydrolases in general. The added ben-

efit of characterizing chitosanases is that fungi contain far fewer genes encoding putative chitosanases than they do chitinases or glucanases. Redundancy is therefore much less likely to complicate the characterization of this enzyme.

5.2 Results

A single chitosanase is present in *M.oryzae*

In order to determine the number of putative chitosanase genes in the *M.oryzae*, the *A.fumigatus* Csn protein sequence (Genbank AAO41660.1) (Cheng et al., 2006) was used as a BLAST query against the *M.oryzae* protein database (Broad Institute). This identified just a single putative chitosanase: MGG07656. Further BLAST searches of the protein database using MGG07656 as a query and Pfam domain searches to find additional proteins with a GH75 domain (Pfam 07335) failed to identify further chitosanase sequences. Therefore, *M.oryzae* has just a single putative chitosanase (Csn) in its genome.

The MGG07656 *CSN* gene is 2579 nt in length, with two introns, and encodes a protein of 797 aa. This is significantly longer than all other chitosanase sequences, which are typically 250-350 aa in length. Closer inspection of the predicted protein sequence reveals that in addition to an N-terminal signal peptide (SignalP 4.0) and a chitosanase domain (Pfam 07335), the C-terminal ∼450 aa are almost entirely composed of short repeats rich in proline (P), aspartate (D) and lysine (K) residues (Figure 5.1). These are interspersed with short repeated linker sequences: Two copies of DSLKMETSGGTKDNGDMGE, and three copies of KPKLSPQGFEIIDPMAKDYNLWDKGLEGDGK (Figure 5.1). In order to confirm whether this sequence was correct, and not due to a misannotation, the gDNA was sequenced. The sequence obtained was identical to that in the genome database. Next, the cDNA was amplified, and sequenced. Again, this confirmed the presence of the repeats, and the absence of introns confirmed the sequence was from cDNA, and not gDNA (not shown). Comparison of the *M.oryzae* Csn protein sequence with the those of all other Csn in other fungi (Figure 5.2) suggests that the *M.oryzae* chitosanase is unique with regard to these repeat sequences. However, a BLAST search using these repeat sequences as a query revealed a number of bacterial cell wall proteins with similar repeat sequences, including BibA from *Streptococcus agalactiae* (Santi et al.,

2007), where the repeats are required for cell wall localization (Janulczyk et al., 2010). Repeat sequences enriched in proline, aspartate and lysine residues are often intrinsically disordered (Romero et al., 2001). To determine whether the C-terminal region of Csn is disordered, the sequence was analyzed by the PONDR (Predictor of Natural Disordered Regions) VL-XT and VLS2 algorithms (www.pondr.com). VLS2 gives accurate whole-protein prediction of disorder (Peng et al., 2006), and revealed that the entire C-terminal ∼500 aa of Csn is indeed likely to be disordered. VL-XT can be used to find localized ordered regions within disordered proteins, with possible roles in protein-protein interactions (Romero et al., 2001; Cortese et al., 2008). This algorithm revealed that there are several short ordered regions within the general disorder of the C-terminal region. These regions correspond to the three repeats of KPKLSPQGFEIIDPMAKDYNLWDKGLEGDGK as described above (Figure 5.1).

Alignment of chitosanase sequences from a number of fungi (Figure 5.1) shows that the key catalytic residues (aspartate and glutamate), as identified by Cheng et al. (2006) are conserved, suggesting that the *M.oryzae* Csn is a functional endo-chitosanase.

Chitosanases are restricted to the Pezizomycotina

Chitin deacetylases are present in all fungi, as discussed previously. To determine whether this is also true of chitosanases, a reciprocal best-hits BLAST search was performed on the protein databases of all sequenced fungal genomes, using the *M.oryzae* Csn as a query sequence. This revealed that chitosanases are restricted to the Pezizomycotina subphylum (Figure 5.2); no putative chitosanases were identified in any other subphylum of the Ascomycota, nor any phylum outside of the Ascomycota. Even within the Pezizomycotina, multiple, independent gene losses have apparently occurred; no chitosanase was identified in *Magnaporthe poae*, nor in the Ajellomycetaceae or Helotiales, to name but a few. In most of those species with putative chitosanases, just a single sequence was present. *Aspergillus sp.* were an exception, with four, as discovered previously (Cheng et al., 2006). Thus, the distribution and number of chitosanases does not mirror that of the chitin deacetylases. This suggests that the hydrolysis of chitosan may not be necessary in all fungi.

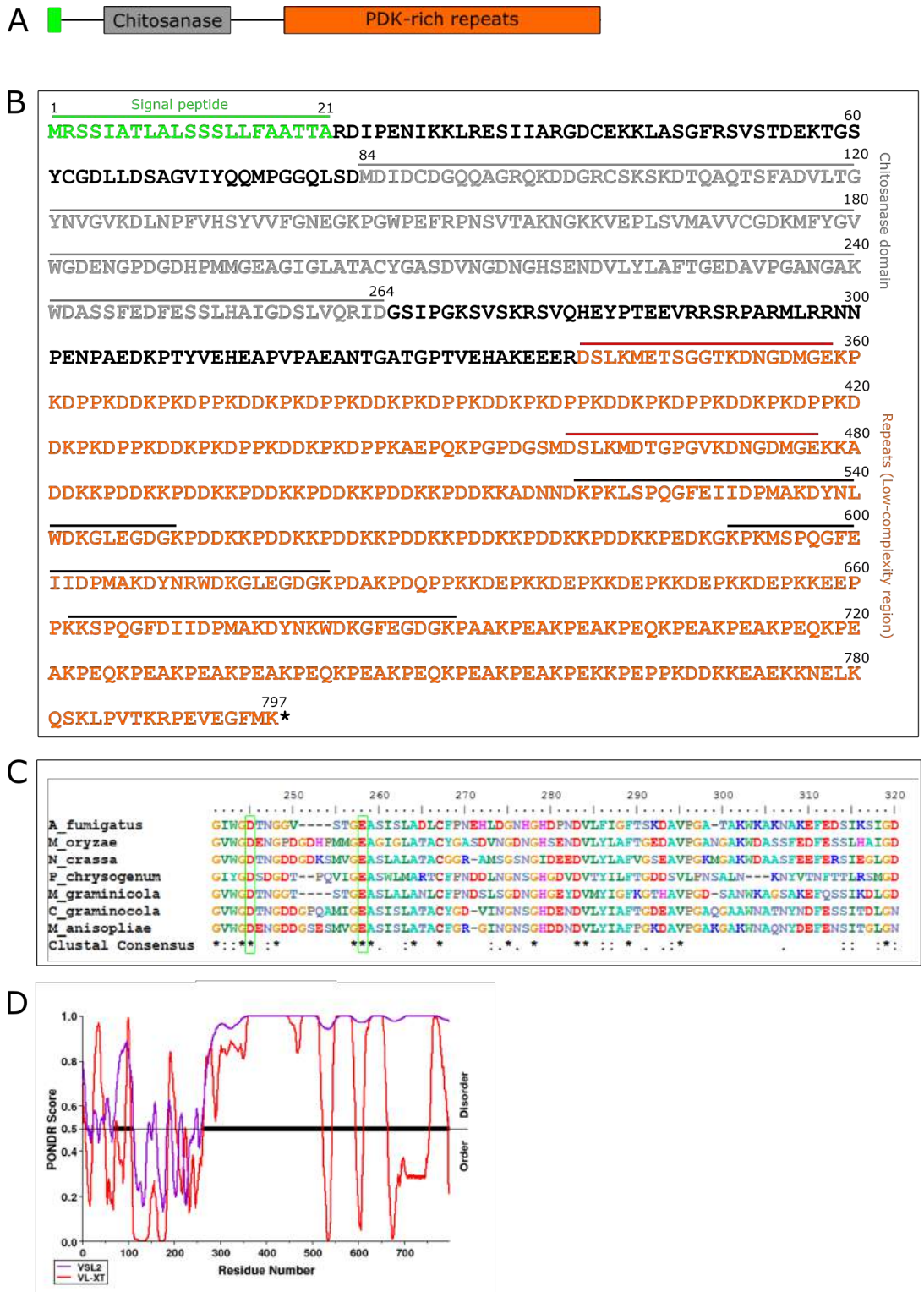

Figure 5.1: ***Magnaporthe oryzae*** **has a single gene encoding chitosanase (*CSN*).** **A**) Protein domain architecture of CSN, comprising a signal peptide, Glycosyl Hydrolase 75 domain (chitosanase) and a long section of proline, aspartate and lysine (PDK) rich repeats at the C-terminus (shown in **B**). The amino acid sequence is colour-coded to correspond to domain colours in **A**. Repeated linker sequences are marked with red or black lines above the sequence. **C**) Alignment of fungal chitosanases, showing conservation of key catalytic aspartate and glutamate residues (green boxes). **D**) Prediction of protein disorder using PONDR VSL2 (purple line) and VL-XT (red line).

Species	N° Chitosanase	Phylum	Subphylum	Class	Order	Family
Coccidioides immitis	1	Ascomycota	Pezizomycotina	Eurotiomycetes	Onygenales	Onygenaceae
Coccidioides posadasii	1	Ascomycota	Pezizomycotina	Eurotiomycetes	Onygenales	Onygenaceae
Uncinocarpus reesei	1	Ascomycota	Pezizomycotina	Eurotiomycetes	Onygenales	Onygenaceae
Histoplasma capsulatum	0	Ascomycota	Pezizomycotina	Eurotiomycetes	Onygenales	Ajellomycetaceae
Blastomyces dermatitidis	0	Ascomycota	Pezizomycotina	Eurotiomycetes	Onygenales	Ajellomycetaceae
Paracoccidioides brasiliensis	0	Ascomycota	Pezizomycotina	Eurotiomycetes	Onygenales	Ajellomycetaceae
Arthroderma benhamiae	1	Ascomycota	Pezizomycotina	Eurotiomycetes	Onygenales	Arthrodermataceae
Arthroderma otae	1	Ascomycota	Pezizomycotina	Eurotiomycetes	Onygenales	Arthrodermataceae
Arthroderma gypseum	1	Ascomycota	Pezizomycotina	Eurotiomycetes	Onygenales	Arthrodermataceae
Trichophyton rubrum	2	Ascomycota	Pezizomycotina	Eurotiomycetes	Onygenales	Arthrodermataceae
Trichophyton equinum	2	Ascomycota	Pezizomycotina	Eurotiomycetes	Onygenales	Arthrodermataceae
Trichophyton tonsurans	2	Ascomycota	Pezizomycotina	Eurotiomycetes	Onygenales	Arthrodermataceae
Trichophyton verrocosum	1	Ascomycota	Pezizomycotina	Eurotiomycetes	Onygenales	Arthrodermataceae
Aspergillus clavatus	4	Ascomycota	Pezizomycotina	Eurotiomycetes	Eurotiales	Trichocomaceae
Aspergillus fumigatus	4	Ascomycota	Pezizomycotina	Eurotiomycetes	Eurotiales	Trichocomaceae
Aspergillus flavus	4	Ascomycota	Pezizomycotina	Eurotiomycetes	Eurotiales	Trichocomaceae
Aspergillus nidulans	2	Ascomycota	Pezizomycotina	Eurotiomycetes	Eurotiales	Trichocomaceae
Aspergillus niger	2	Ascomycota	Pezizomycotina	Eurotiomycetes	Eurotiales	Trichocomaceae
Aspergillus terreus	2	Ascomycota	Pezizomycotina	Eurotiomycetes	Eurotiales	Trichocomaceae
Aspergillus oryzae	4	Ascomycota	Pezizomycotina	Eurotiomycetes	Eurotiales	Trichocomaceae
Neosartorya fischeri	4	Ascomycota	Pezizomycotina	Eurotiomycetes	Eurotiales	Trichocomaceae
Penicillium marneffei	1	Ascomycota	Pezizomycotina	Eurotiomycetes	Eurotiales	Trichocomaceae
Penicillium chrysogenum	1	Ascomycota	Pezizomycotina	Eurotiomycetes	Eurotiales	Trichocomaceae
Talaromyces stipitatus	1	Ascomycota	Pezizomycotina	Eurotiomycetes	Eurotiales	Trichocomaceae
Mycosphaerella graminicola	1	Ascomycota	Pezizomycotina	Dothideomycetes	Capnodiales	Mycosphaerellaceae
Phaeosphaeria nodorum	1	Ascomycota	Pezizomycotina	Dothideomycetes	Pleosporales	Phaeosphaeriaceae
Pyrenophora tritici-repentis	0	Ascomycota	Pezizomycotina	Dothideomycetes	Pleosporales	Pleosporaceae
Pyrenophora teres	0	Ascomycota	Pezizomycotina	Dothideomycetes	Pleosporales	Pleosporaceae
Botrytis cinerea	0	Ascomycota	Pezizomycotina	Leotiomycetes	Helotiales	Sclerotiniaceae
Sclerotinia sclerotiorum	0	Ascomycota	Pezizomycotina	Leotiomycetes	Helotiales	Sclerotiniaceae
Blumeria graminis	0	Ascomycota	Pezizomycotina	Leotiomycetes	Erysiphales	Erisiphaceae
Chaetomium globosum	2	Ascomycota	Pezizomycotina	Sordariomycetes	Sordariales	Chaetomiaceae
Chaetomium thermophilum	1	Ascomycota	Pezizomycotina	Sordariomycetes	Sordariales	Chaetomiaceae
Neurospora crassa	1	Ascomycota	Pezizomycotina	Sordariomycetes	Sordariales	Sordariaceae
Gaeumannomyces graminis	1	Ascomycota	Pezizomycotina	Sordariomycetes	Incertae sedis	Magnaporthaceae
Magnaporthe poae	0	Ascomycota	Pezizomycotina	Sordariomycetes	Magnaporthale	Magnaporthaceae
Magnaporthe oryzae	1	Ascomycota	Pezizomycotina	Sordariomycetes	Magnaporthale	Magnaporthaceae
Cordyceps militaris	2	Ascomycota	Pezizomycotina	Sordariomycetes	Hypocreales	Cordicipitaceae
Fusarium graminearum	1	Ascomycota	Pezizomycotina	Sordariomycetes	Hypocreales	Nectriaceae
Fusarium oxysporum	2	Ascomycota	Pezizomycotina	Sordariomycetes	Hypocreales	Nectriaceae
Fusarium verticillioides	2	Ascomycota	Pezizomycotina	Sordariomycetes	Hypocreales	Nectriaceae
Claviceps fusiformis	1	Ascomycota	Pezizomycotina	Sordariomycetes	Hypocreales	Clavicipitaceae
Claviceps paspali	1	Ascomycota	Pezizomycotina	Sordariomycetes	Hypocreales	Clavicipitaceae
Epichloe festucae	0	Ascomycota	Pezizomycotina	Sordariomycetes	Hypocreales	Clavicipitaceae
Metarhizium acridum	2	Ascomycota	Pezizomycotina	Sordariomycetes	Hypocreales	Clavicipitaceae
Metarhizium anisopliae	3	Ascomycota	Pezizomycotina	Sordariomycetes	Hypocreales	Clavicipitaceae
Trichoderma reesei	3	Ascomycota	Pezizomycotina	Sordariomycetes	Hypocreales	Hypocreaceae
Verticillium albo-atrum	1	Ascomycota	Pezizomycotina	Sordariomycetes	Hypocreales	Incertae sedis
Verticillium dahliae	1	Ascomycota	Pezizomycotina	Sordariomycetes	Hypocreales	Incertae sedis
Ashbya gossypii	0	Ascomycota	Saccharomycotina			
Candida albicans	0	Ascomycota	Saccharomycotina			
Clavispora lusitanae	0	Ascomycota	Saccharomycotina			
Debaromyces hansenii	0	Ascomycota	Saccharomycotina			
Kluyveromyces lactis	0	Ascomycota	Saccharomycotina			
Komagataella pastoris	0	Ascomycota	Saccharomycotina			
Lachancea thermotolerans	0	Ascomycota	Saccharomycotina			
Lodderomyces elongisporus	0	Ascomycota	Saccharomycotina			
Meyerozyma guilliermondii	0	Ascomycota	Saccharomycotina			
Ogataea parapolymorpha	0	Ascomycota	Saccharomycotina			
Saccharomyces cerevisiae	0	Ascomycota	Saccharomycotina			
Scheffersomyces stipitis	0	Ascomycota	Saccharomycotina			
Spathaspora passalidarum	0	Ascomycota	Saccharomycotina			
Yarrowia lipolytica	0	Ascomycota	Saccharomycotina			
Zygosaccharomyces rouxii	0	Ascomycota	Saccharomycotina			
Schizosaccharomyces pombe	0	Ascomycota	Schizosaccharomycetes			
Coprinopsis cinerea	0	Basidiomycota				
Cryptococcus neoformans	0	Basidiomycota				
Puccinia graminis	0	Basidiomycota				
Melampsora larici-populina	0	Basidiomycota				
Ustilago maydis	0	Basidiomycota				
Laccaria bicolor	0	Basidiomycota				
Malassezia globosa	0	Basidiomycota				
Schizophyllum commune	0	Basidiomycota				
Phanerochaete chrysosporum	0	Basidiomycota				
Encephalitozoon cuniculi	0	Microsporidia				

Figure 5.2: Chitosanases are restricted to the Pezizomycotina. Most species in the Pezizomycotina have 1-4 genes encoding putative chitosanases, although apparent gene losses have occurred in some lineages (highlighted in red). Chitosanases are absent in all other phyla, including the basidiomycota, chytridiomycota (not shown) and zygomycota (not shown).

Deletion of *CSN*

To determine the role of *CSN* in *M.oryzae*, the gene was deleted by targeted gene replacement, as described in previous Chapters. In this case, the entire deletion cassette could not be synthesized with the requisite purity. Instead, it was synthesized in two halves, each with the antibiotic resistance gene (*BAR*), and a sequence homologous to that flanking *CSN* (Figure 5.3A). This was transformed into both the Guy11 and *ku70* background strains. *ku70* is the deletion strain of *KU70*, encoding a protein involved in the non-homologous end-joining (NHEJ) pathway, and demonstrates vastly improved gene targeting efficiency (Villalba et al., 2008). Following successful transformation, transformants were first screened by PCR, to identify those in which *CSN* had been successfully replaced by *BAR* (not shown). Putative deletion strains were subjected to Southern blot analysis, to confirm the presence of a single copy of the deletion cassette at the desired locus. *Pst*I digestion of gDNA from putative deletion strains was hybridised with α-^{32}P-labelled *BAR*, and resulted in the expected 3.8 kb band in all of the lines made in the *ku70* background, and four of the lines in the Guy11 background (Figure 5.3B). No hybridisation was observed in the WT (Guy11) lane, confirming the specificity of the hybridisation. Two independent deletion lines in the Guy11 background strain were chosen for characterization (named 9 and 46).

Phenotypic characterization of *csn* mutants

Chitosan was previously found to be a component of the cell wall in vegetative hyphae (Chapter 4). To determine whether the deletion of *CSN* impacted hyphal growth, the *csn* mutants were subjected to radial growth assays on solid media. A range of stress conditions were applied, including nutritional stress (nitrogen or carbon starvation), cell wall perturbants (Calcofluor White, Congo Red), membrane perturbant (SDS), metal (copper) and osmotic stress (sorbitol and NaCl) (Figure 5.4). Although very small, yet statistically significant (Student's T-test $p<0.01$) differences in growth between the WT and *csn* strains were found, the biological significance of this is questionable, as they generally represent <10% change in growth. This is particularly apparent if one compares these results with those from Figure 5.9, which show similar growth differences in the empty vector strains. These small changes in growth in the *csn* strains are therefore

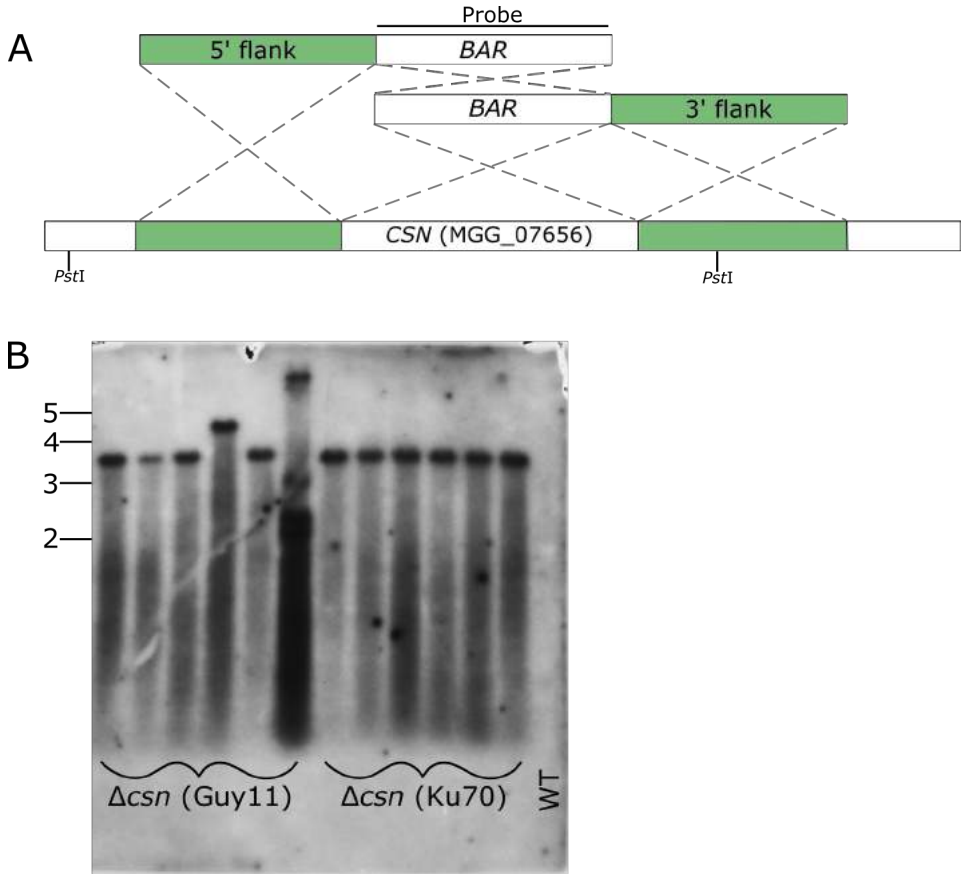

Figure 5.3: Targeted deletion of *CSN*. The gene encoding *CSN* was replaced by a gene imparting resistance to bialaphos (*BAR*). In this instance, the deletion cassette was split into two parts, each with the resistance gene, and a sequence homologous to either the 5' or 3' flanking sequence of *CSN* (**A**). **B**) Southern blot showing successful deletion of *CSN* in both the Guy11 and *Ku70* backgrounds. Restriction digested (*Pst*I) gDNA of putative deletion strains was hybridised with α-^{32}P labelled DNA homologous to *BAR*. Size markers show band size in kilobases (Kb).

likely due to 'cryptic' alterations occurring during the transformation process, and suggest that Csn is not required for growth or morphogenesis in vegetative hyphae. In future, ectopic insertion lines or complemented strains should be included in radial growth assays.

In *A.fumigatus*, deletion of *CsnB* resulted in reduced growth on media containing chitosan (Beck et al., 2014). To see if this was also true of the *csn* mutant in *M.oryzae*, growth assays with chitosan as a carbon source were performed on solid and in liquid medium (Figure 5.4). On solid medium containing 0.5% chitosan (w/v), equal growth was observed in all strains after a 14 day incubation. In some fungi, a 'halo' indicative of substrate degradation is also observed around fungal colonies grown on chitosan (Palma-Guerrero et al., 2008), but this was not observed for *M.oryzae*. In liquid medium, chitosan was clearly able to be used as a carbon source, since biomass was much higher in flasks containing 0.33% chitosan (w/v) (and 16.6 mM sodium acetate) than those containing sodium acetate alone. However, the biomass of the *csn* mutant was identical to the WT strain.

Cell wall hydrolases have previously been implicated in autolysis under starvation conditions. To determine whether Csn is required for autolysis, equal concentrations of conidia were inoculated into flasks containing minimal media, and incubated for up to 30 days, with biomass measurements taken every 4 days after an initial 5 day incubation. Biomass increased up to 17 dpi, then decreased between 21 and 30 dpi, suggesting the onset of autolysis (Figure 5.4). Similar decreases in biomass were observed in the WT and *csn* strains, suggesting that chitosanase is not required for autolysis.

It was also hypothesized that chitosanase may be required for turnover or remodelling of chitosan in the cell wall. To determine whether the amount and distribution of chitosan in the cell wall is altered in the *csn* mutant, chitosan was localized in hyphae, appressoria and conidia. In hyphae stained with OGA488 no changes in labelling intensity or localization were observed in *csn* compared with the WT (Figure 5.5). Similarly, anti-chitosan antibody labelling of germlings or eosin Y labelling of conidia also failed to show any differences between the WT and *csn* strains. It therefore appears that large-scale changes in cell wall composition have not occurred as a result of *CSN* deletion.

The cell walls of appressoria and invasive hyphae appear to have a particularly high chitosan content (Fujikawa et al., 2009). In order to determine whether Csn is required for

A

	CM	MM	CFW	CR	H_2O_2	Sorbitol	NaCl	Caffeine	SDS	Copper	MM-N	MM-C
WT	70.9 ± 1.3	54.8 ± 3.6	53.3 ± 3.0	43.2 ± 1.8	55.7 ± 3.6	44.3 ± 2.0	51.1 ± 4.5	49.4 ± 6.3	55.6 ± 1.9	39.5 ± 1.7	58.6 ± 0.5	52.7 ± 1.0
Δ*csn* _9	66.4 ± 1.4*	53.0 ± 3.4	51.0 ± 3.3	43.2 ± 0.4	60.6 ± 5.1*	42.9 ± 1.6	47.2 ± 1.8	45.0 ± 8.1	51.9 ± 0.8*	40.0 ± 2.1	58.2 ± 0.5	51.1 ± 1.8
Δ*csn* _46	68.5 ± 0.8*	54.3 ± 1.6	51.2 ± 2.8	43.4 ±0.2	60.8 ± 4.6*	42.9 ± 0.3	48.5 ± 2.7	46.2 ± 6.1	53.3 ± 1.8*	40.8 ± 2.7	58.7 ± 0.9	49.1 ± 2.5*

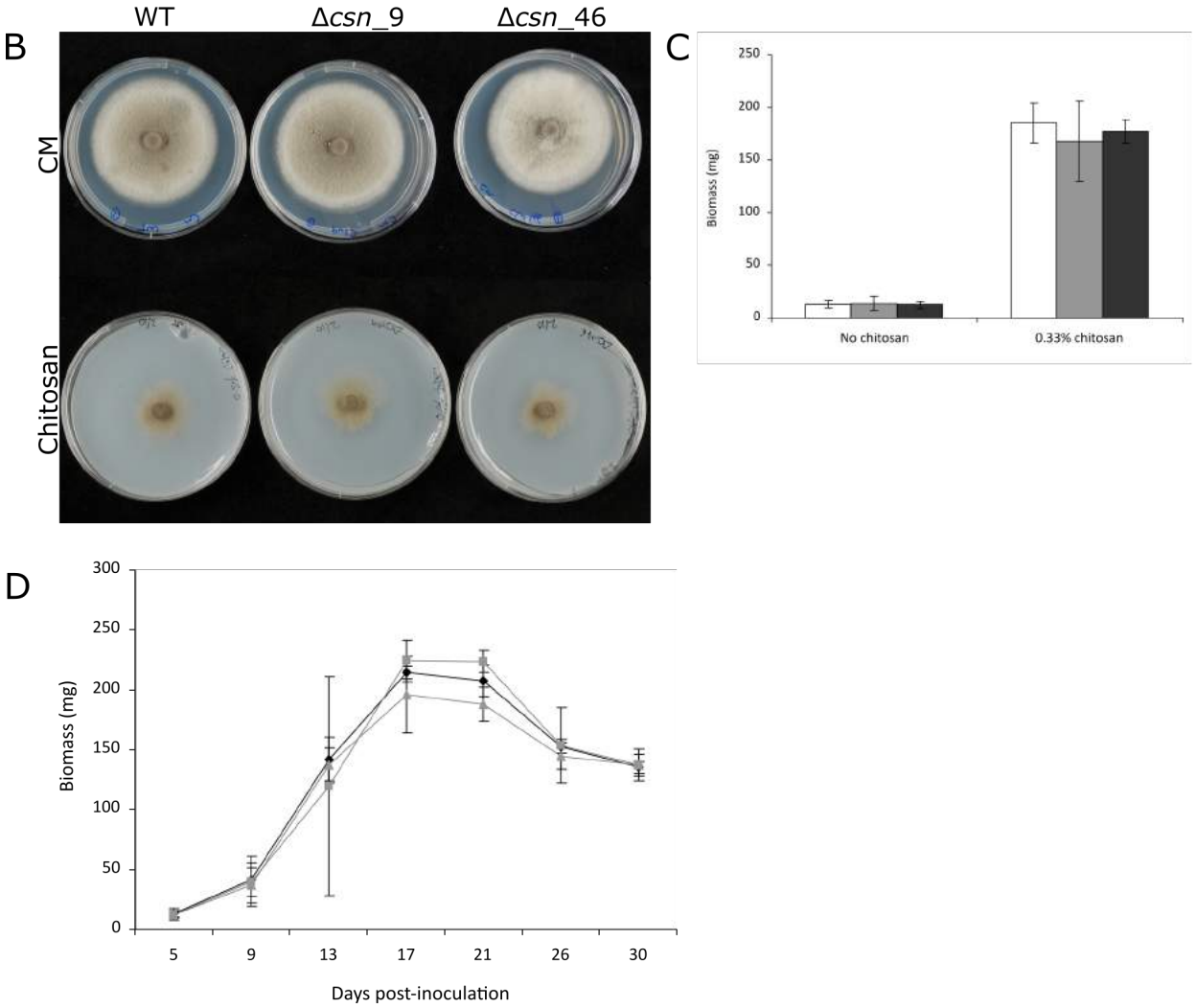

Figure 5.4: The *csn* mutant shows normal growth under a range of conditions. A) Table showing mean colony diameters (mm, ±SD, n=3) in the WT and *csn* strains, across a range of stress conditions. Two independent deletion lines were used (named 9 and 46). Small but significant differences in growth were measured under certain conditions (denoted by *, where $p<0.01$, Student's T-test). Details of treatments are shown in Appendix C. **B**) Growth of the *csn* mutant on solid medium containing 0.5% chitosan (w/v) as a sole carbon source, showing similar growth to the WT strain. **C**) Growth of the *csn* mutant (grey bars) in liquid medium with 0.33% chitosan (w/v) as a sole carbon source, showing similar accumulation of biomass to the WT strain (white bars). Error bars show SD, n=3. **D**) Long-term growth of the *csn* mutant in minimal media, showing onset of autolysis after 21 days. Autolysis proceeded similarly in the *csn* (grey lines) and WT strain (black line). Error bars show SD, n=2.

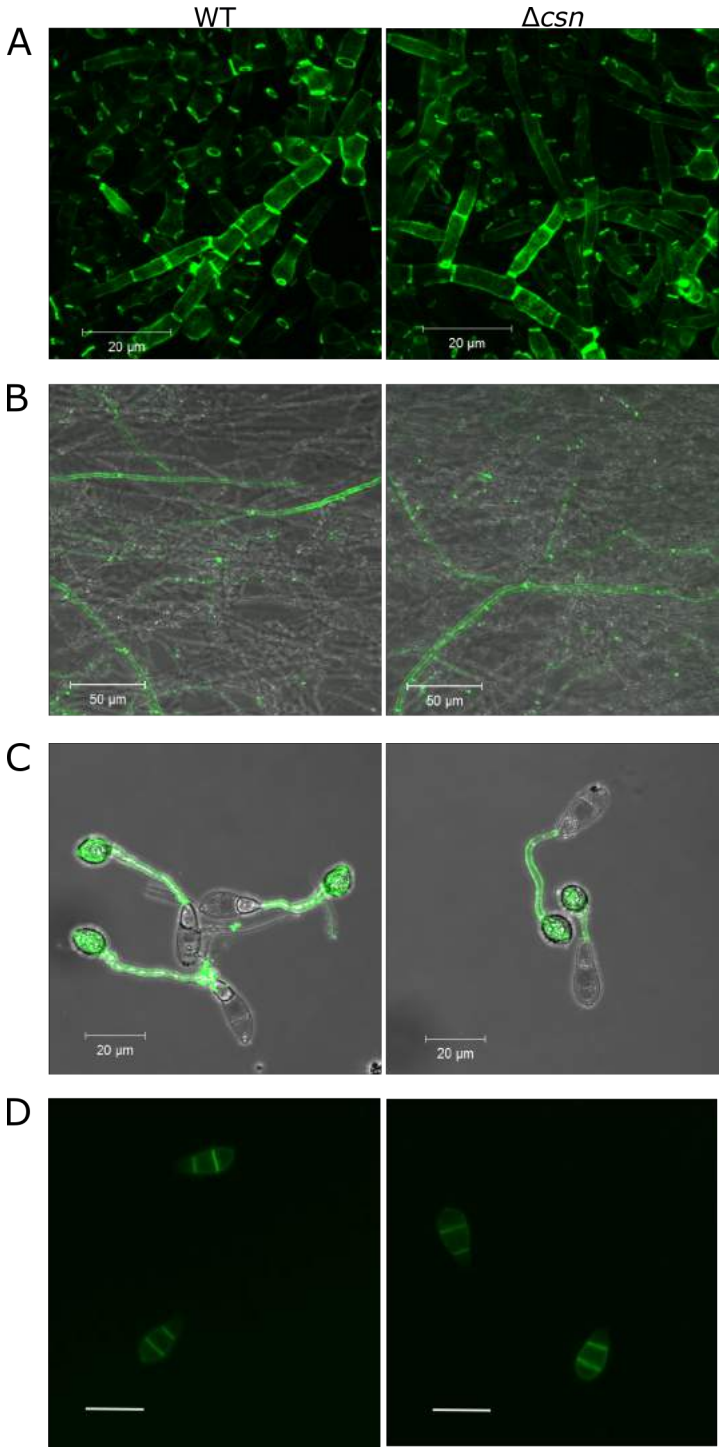

Figure 5.5: Chitosan labelling is unaffected in *csn*. **A**) and **B**) Labelling of chitosan on vegetative hyphae grown in liquid and on solid medium respectively, using the chitosan-specific probe OGA488. Similar staining was observed in both WT and *csn* strains. **C**) Staining of germlings with anti-chitosan antibody mAbG7. Germlings had been germinated on an artificial inductive surface for 16 hr prior to labelling. Both germling morphology and chitosan labelling were unaffected in the *csn* mutant. **D**) Eosin Y staining of conidia, which was unaffected in *csn*. Scale bars: 20 µm in **A**, **C** and **D**, 50 µm in **B**.

A

Strain	Germination rate (%)	Appressoria (%)
WT	50.5 ± 8.5	84.7 ± 9.8
Δ*csn_9*	46.4 ± 3.3	87.6 ± 8.3
Δ*csn_46*	41.3 ± 9.5	87.7 ± 4.7

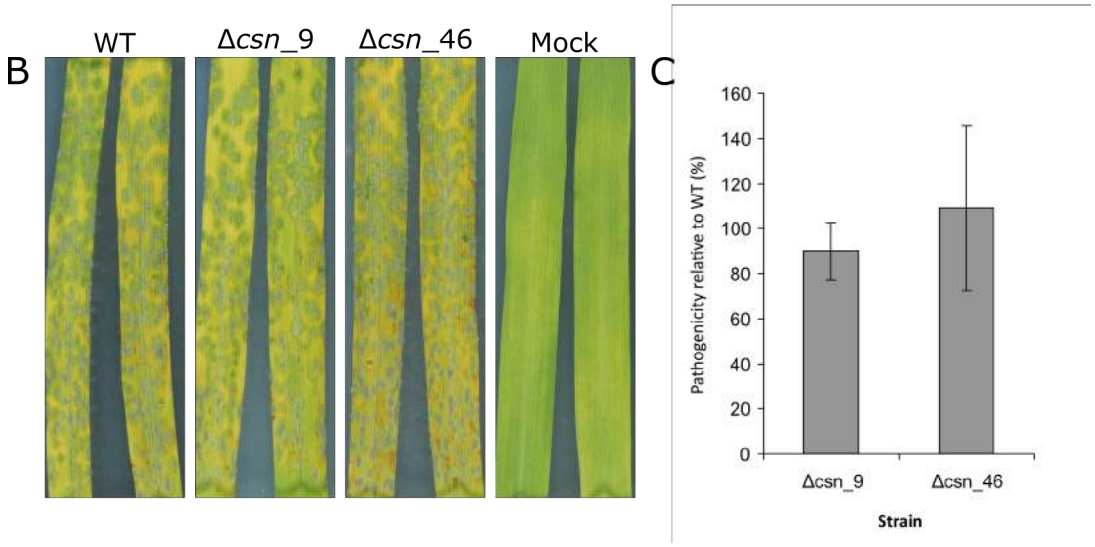

Figure 5.6: Pathogenicity is unaffected in *csn*. **A**) Table showing conidial germination (at 1 hpi) and appressorium development (at 8 hpi) on an artificial inductive surface, showing no differences between WT and *csn*. Figures are ±SD, n=3. **B**) Pathogenicity of the *csn* strain on Barley leaves, showing similar lesion numbers to the WT strain (**C**). A mock inoculation of 0.2% gelatine was included as a negative control. Error bars show SD, n=3.

morphogenesis in these structures, conidial germination, appressorium development and pathogenicity were evaluated. Germination and appressorium development on an artificial hydrophobic surface were unaffected in the *csn* mutant at all time-points (Figure 5.6). Conidia of *csn* inoculated onto barley leaves also resulted in similar lesion densities to the WT (Figure 5.6), with identical results obtained on rice leaves (not shown). Morphology of invasive hyphae in onion epidermis was also unaffected in the *csn* mutant (not shown).

Promoter analysis of *CSN*

The lack of any phenotype in the *csn* mutant was unexpected, and did not give any information regarding the role of chitosanase. To determine the localization of Csn, an eGFP fusion was created. Primers 55 and 56 (Appendix E) were used to amplify the open reading frame of *CSN* (without the stop codon), together with 1.7kb of 5' promoter sequence (for native expression of the construct). This was cloned into the *Asc*I and *Sbf*I sites of the pUCAP vector (Appendix D), thereby creating a C-terminal eGFP fusion. After transformation into the *csn* background strain, antibiotic-resistant transformants

were screened for fluorescence. A number of fluorescent lines were isolated (listed in Appendix F), and characterized.

CSN:eGFP strains demonstrated weak fluorescence in vegetative hyphae, particularly in those at the colony margins, and occasionally in conidia. However, this fluorescence appeared to be localized to the cytoplasm, rather than associated with the cell wall as expected (Figure 5.7A). No fluorescence was observed at any other stage of the life-cycle, including during appressorium development, or *in planta* growth. Western blot analysis of the Csn:eGFP fusion using an anti-eGFP antibody was unsuccessful; no specific bands were detected, so it is not known whether the fluorescence is associated with the intact fusion protein, or a degradation product. To determine whether the cytoplasmic fluorescence was due to a mislocalization of the fusion protein, additional fusion constructs were tested. Firstly, eGFP was fused to a truncated form of *CSN* (aa1-348), which lacked the C-terminal repeat region (amplified with primers 55 and 57 (Appendix E)). However, transformants carrying this construct did not demonstrate any fluorescence at all. Next, an internal eGFP fusion was attempted, of both the full length and truncated *CSN*. Here, eGFP was cloned after the Csn signal peptide, such that it would be at the N-terminus of the mature protein. Again, however, no fluorescence was detected in the resulting transformants.

Because fluorescence from the eGFP fusion construct was weak and potentially mislocalized, it could only provide limited information regarding the role of Csn. By fusing the promoter of *CSN* to three copies of YFPvenus, more sensitive information regarding spatial and temporal expression of *CSN* could be obtained. Primer pairs 62/63, 64/65 and 66/67 (Appendix E) were used to amplify three copies of *YFPvenus*, which were cloned between the *Asc*I and *Bam*HI site of the pUCAP vector (Appendix D). *pCSN* was amplified with primers 68 and 69, and cloned into the newly-created *Xho*I site 5' of the first YFPvenus, thus completing the promoter fusion. This construct was transformed into the WT background strain, and antibiotic resistant colonies were screened for fluorescence. A number of independent lines were chosen for characterization (listed in Appendix F). As with the *CSN:eGFP* strains, YFP fluorescence was observed in vegetative hyphae, and was strongest in those at the colony margins (Figure 5.7B). Additionally, fluorescence was also observed in appressoria post-penetration ($\sim$48 hpi), but not in invasive hyphae,

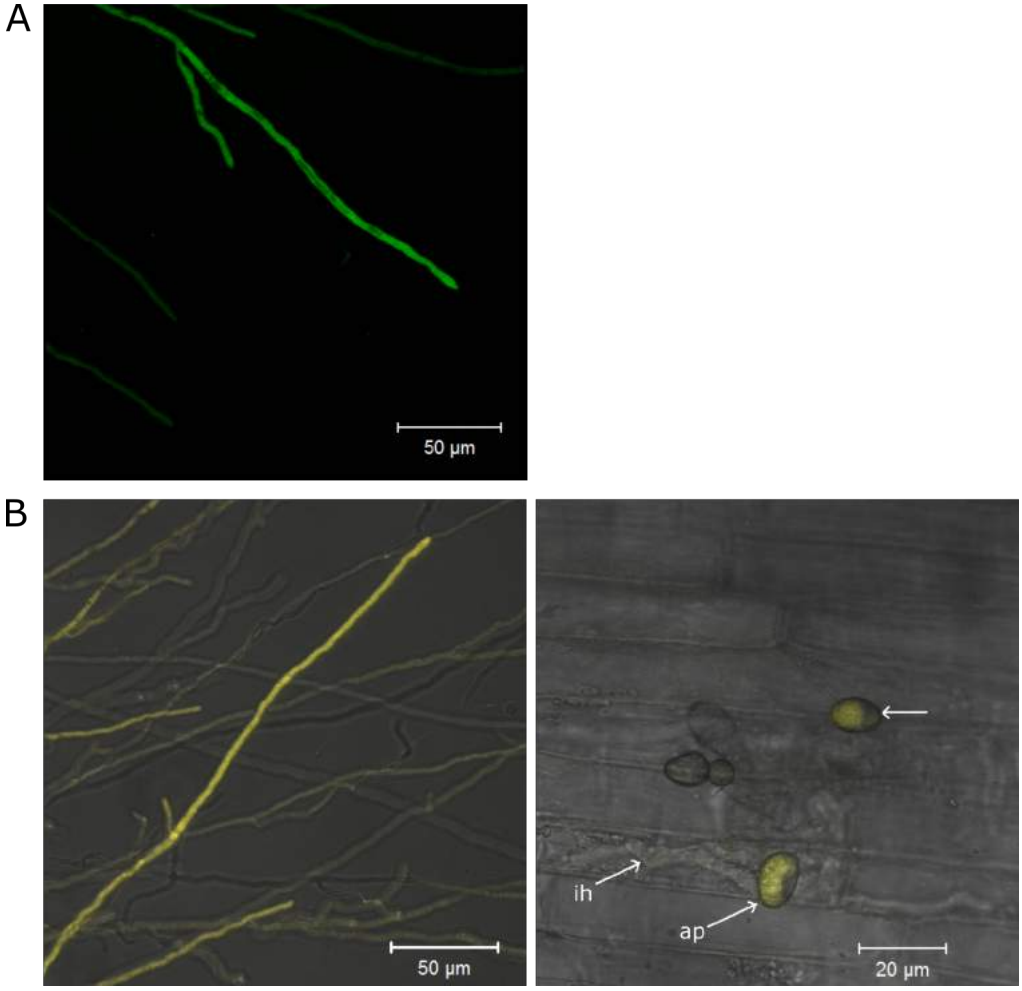

Figure 5.7: *CSN* is expressed in vegetative hyphae. A) Attempted localization of Csn by C-terminal eGFP tagging, showing cytoplasmically localized fluorescence in vegetative hyphae. **B**) Activity of the *CSN* promoter. Three copies of *YFPvenus* were placed under the control of *pCSN*. As with the eGFP fusion, fluorescence was observed in vegetative hyphae at the colony margins, but also in appressoria post-penetration. ih: invasive hyphae, ap: appressorium. Scale bars: as stated in pictures.

nor during appressorium development (Figure 5.7B). Taken together, these data suggest that Csn is involved in vegetative growth rather than pathogenic development.

Overexpression of *CSN*

The deletion of *CSN* had no discernible effect on growth or development in *M.oryzae*. In a further attempt to characterize the role of chitosan hydrolysis, *CSN* was overexpressed. The *RP27* promoter (as used for ectopic expression of *CBP1* in Chapter 3) was amplified with primers 70 and 71 (Appendix E). The full and truncated (aa1-275) forms of Csn were amplified with primer pairs 72/73 and 72/74 respectively, then fused to

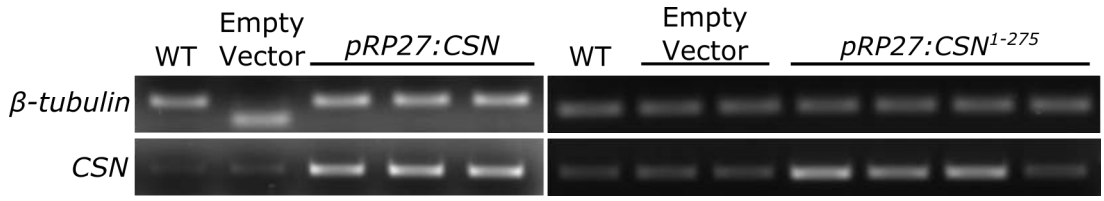

Figure 5.8: Overexpression of *CSN*. Semi-quantitative RT-PCR of *CSN* transcript, showing overexpression of both full and truncated (residues 1-275) versions of CSN.

pRP27 using primer pairs 70/73 and 70/74. Finally, the *pRP27:CSN* fusions were cloned into the pUCAP vector. The constructs were transformed into the WT background, and resulting bialaphos-resistant transformants were screened for *CSN* overexpression. Semi-quantitative RT-PCR was used to determine the transcript levels of *CSN* in mycelium after 72 hr growth in liquid CM. Primer pairs 104/105 and 106/107 were used to amplify *CSN* and *β-tubulin* transcripts respectively. In the control strains (WT and empty vector), only faint bands were detected, consistent with the low expression of *CSN* observed previously in the promoter fusion. However, several of the putative overexpressor lines demonstrated increased transcript abundance, suggesting that *CSN* was being successfully overexpressed (Figure 5.8). Amplification of non-reverse transcribed RNA (-RT control) did not result in visible bands, proving that amplification was from cDNA, and not gDNA contamination.

Two independent lines overexpressing each construct (full-length and truncated Csn) were chosen for characterization, as well an empty vector line. In an attempt to also confirm that the increased transcript resulted in increased protein levels, two antibodies raised against CsnB in *A.fumigatus* (Beck et al., 2014) were used to detect the *M.oryzae* Csn. Unfortunately, Western blot analysis using these antibodies failed to detect Csn, suggesting a lack of cross-reactivity with this protein (not shown).

Phenotypic characterization of *CSN* overexpressors

Radial growth of strains overexpressing *CSN* and $CSN^{1\text{-}275}$ was evaluated on solid media, as described previously for the *CSN* deletion strains. No differences in radial growth were found in the overexpressors compared with the empty vector strain, although in several cases the empty vector strains did themselves demonstrate significantly different growth compared with the WT, particularly on plates containing hydrogen peroxide (Figure 5.9).

Thus, small but statistically significant differences in growth characteristics can occur as a result of strains undergoing the transformation process, which must be taken into account when evaluating the growth of transformants. Growth assays were also performed on media containing chitosan as a sole carbon source. Again, however, no differences in growth were observed in the overexpressor strains, and colonies were identical in appearance (Figure 5.9). In order to more directly measure chitosanase activity, mycelial protein extracts were incubated with chitosan, and reducing ends quantified using dinitrosalicylic acid. No chitosanase activity was detected in protein extracts from the WT or overexpressing strains, although chitosanase from a commercial source (Sigma) did demonstrate activity in the same assay. This suggests that either chitosanase activity in the extracts was too low, or conditions were not correct.

To determine whether the amount or distribution of chitosan in the cell wall was altered by overexpression of Csn, germlings were labelled with the anti-chitosan antibody mAbG7. No changes in labelling were observed in the overexpressor strains; only the germ tubes and appressoria showed antibody labelling, just as in the WT and empty vector strains. Additionally, germling morphology was also unaffected.

Lastly, pathogenicity of the overexpressing strains was evaluated. Rice leaves were inoculated with equal concentrations of conidia, and lesions observed after a 4 day incubation. Leaves inoculated with conidia of the overexpressing strains demonstrated similar lesion density to the WT and empty vector strains (Figure 5.11), suggesting that overexpression of Csn had no effect on pathogenicity. Microscopic observations of onion epidermises inoculated with conidia also revealed that morphology and growth of invasive hyphae was unaffected in the overexpressor strains (not shown).

A

	CM	Caffeine	CFW	Congo Red	Sorbitol	SDS	H_2O_2	Copper
WT	65.8 ± 1.4	42.8 ± 2.7	49.1 ± 0.8	48.7 ± 1.0	40.6 ± 0.7	51.7 ± 1.2	58.1 ± 1.2	39.5 ± 1.0
Empty vector_2	67.9 ± 0.4	42.8 ± 2.7	48.2 ± 0.9	46.1 ± 0.5	41.1 ± 3.2	52.9 ± 1.8	63.4 ± 1.5	43.5 ± 0.8
pRP27:CSN _22	68.6 ± 0.1	42.7 ± 3.3	48.8 ± 0.8	45.9 ± 0.5	42.8 ± 1.8	53.1 ± 1.6	63.6 ± 0.3	43.0 ± 1.3
pRP27:CSN _27	68.8 ± 0.3	42.8 ± 2.4	48.9 ± 1.7	45.6 ± 0.1	42.0 ± 1.7	53 ± 1.3	63.5 ± 1.1	43.4 ± 1.1

B

C

	CM	Caffeine	CFW	Congo Red	Sorbitol	SDS	H_2O_2	Copper	MM	MM-N	MM-C
WT	65.7 ± 1.5	47.4 ± 1.5	48.8 ± 0.6	49.0 ± 1.8	43.2 ± 2.4	53.3 ± 1.2	58.1 ± 1.2	40.8 ± 2.5	53.4 ± 1.6	59.2 ± 2.8	47.5 ± 2.3
Empty vector_3	68.2 ± 1.4	44.8 ± 1.3	46.8 ± 2.1	49.3 ± 1.6	42.4 ± 1.9	52.3 ± 0.9	63.4 ± 1.5	41.9 ± 2.0	53.7 ± 1.8	59.3 ± 1.3	49.5 ± 2.1
pRP27:CSN $^{1\text{-}275}$ _9	66.3 ± 2.5	45.8 ± 4.5	46.8 ± 1.1	47.2 ± 2.0	42.3 ± 3.0	54.9 ± 0.7	61.4 ± 1.7	42.0 ± 3.4	54.8 ± 0.7	59.8 ± 2.6	48.5 ± 1.6
pRP27:CSN $^{1\text{-}275}$ _19	65.7 ± 2.8	41.6 ± 1.8	48.0 ± 2.0	47.3 ± 2.5	42.3 ± 2.8	51.9 ± 0.5	62.5 ± 1.2	41.1 ± 2.7	53.6 ± 1.6	59.7 ± 1.3	47.5 ± 2.4

D

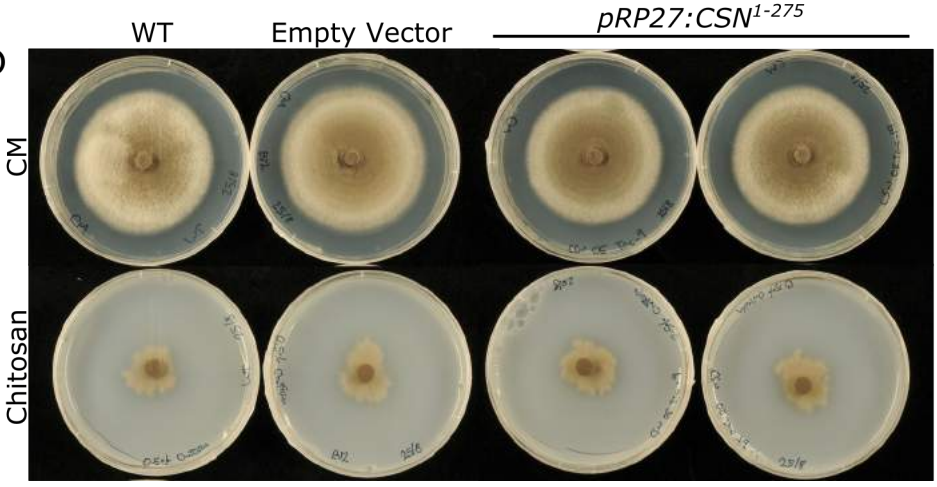

Figure 5.9: Radial growth on solid media is unaffected in *CSN* overexpressing strains. **A**) Table showing mean colony diameters (mm, ±SE, n=3-4) in the WT, empty vector and overexpressing strains, across a range of stress conditions. There were no significant differences in growth between the empty vector and *CSN* overexpressing strains. Two independent overexpressing lines were used (named 22 and 27). **B**) Growth of *CSN* overexpressing strains on media containing 0.5% chitosan (w/v) as a sole carbon source, showing no differences in growth compared with the WT or empty vector strains. **C**) Table showing mean colony diameters (mm, ±SE, n=3) in the WT, empty vector and CSN^{1-275} overexpressing strains, across a range of stress conditions. Two independent overexpressing lines were used (9 and 19). There were no significant differences in growth between the empty vector and overexpressing strains. **D**) Growth of CSN^{1-275} overexpressing strains on media containing 0.5% chitosan (w/v) as a sole carbon source, showing no differences in growth compared with the WT and empty vector. Details of growth treatments are shown in Appendix C.

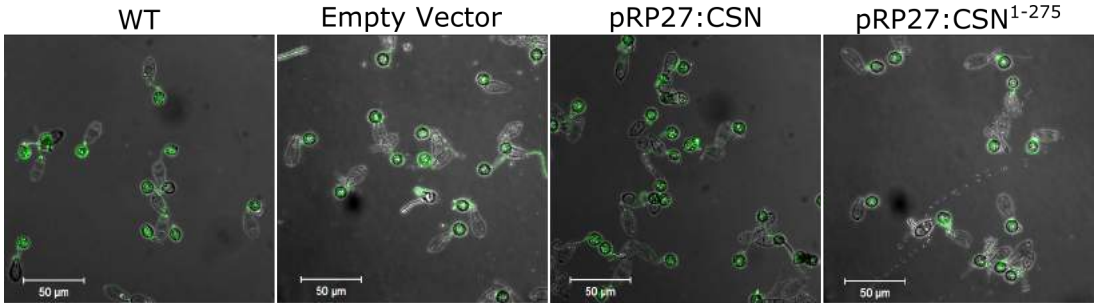

Figure 5.10: Labelling of chitosan is unaffected in *CSN* overexpressors. Labelling of germlings developed for 16 hr on an artificial inductive surface with the monoclonal anti-chitosan antibody mAbG7. Similar staining was observed in the WT, empty vector and *CSN* overexpressors. Germling morphology is also normal in the overexpressors. Scale bars: 50 µm.

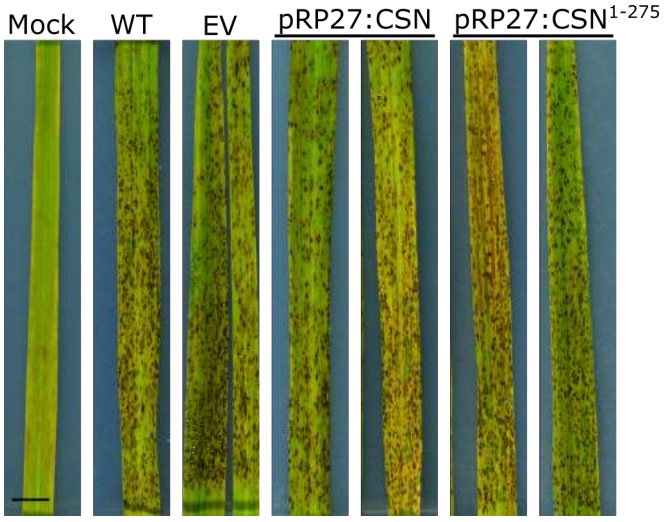

Figure 5.11: Pathogenicity is unaffected in *CSN* overexpressors. Rice leaves inoculated with equal concentrations of conidia of either the WT, empty vector or *CSN* overexpressing strains, showing similar lesion densities. A mock inoculation of 0.2% gelatine (w/v) was included as a negative control. Scale bar: 0.5 cm.

5.3 Discussion

Many aspects of cell wall hydrolysis are poorly understood. In particular, the hydrolysis of cell wall components has long been hypothesized to be required for cellular morphogenesis. However, evidence for this hypothesis is distinctly lacking and a link between cell wall hydrolysis and processes such as hyphal branching or tip-growth has yet to be demonstrated. In order to improve our understanding of cell wall hydrolysis, the role of chitosanase in *M.oryzae* was investigated.

Most cell wall hydrolysing enzymes, such as chitinases or glucanases, occur in large gene families which make characterization problematic. Functional redundancy within these families often results in compensatory responses when a gene is deleted, thereby preventing the detection of a phenotype. Fortunately, chitosanases are usually present in a single copy in the genomes of most fungi, including that of *M.oryzae*. The sole chitosanase present in *M.oryzae* appears to be unique, due to the presence of a large section of intrinsically disordered C-terminal repeats. The function of these repeats was not determined in the present study; overexpression of a truncated form of Csn did not show any phenotype, and an eGFP fusion could not be localized. In addition, given the abundance of proteins with intrinsically disordered regions (estimated at up to 50% of eukaryotic proteins (Dunker et al., 2000)), the presence of this region in Csn does not in itself give any clue as to its function. Nevertheless, the presence of similar repeats in other proteins allows speculation as to their role. A number of bacterial cell wall proteins, including BibA from *Streptococcus agalactiae* (Santi et al., 2007), have similar repeats which are required for cell wall localization (Janulczyk et al., 2010). It is therefore possible that these repeats act as a chitosan-binding or general cell wall-binding domain.

Chitosan has been demonstrated to be a cell wall component in appressoria, invasion hyphae and vegetative hyphae in *M.oryzae*, but deletion of Csn had no effects on growth or morphogenesis in any of these cell-types. In light of the expression pattern of *CSN* however, these data are perhaps not so surprising. Unexpectedly, promoter activity for *CSN* and was not detected during appressorium development or *in planta* growth, and only low expression was found in vegetative hyphae. Taken together, it appears that Csn is neither involved in, nor required for, cellular morphogenesis in cell-types with chitosan-rich cell walls. This is consistent with findings in *A.fumigatus* (Beck et al.,

2014), *F.solani* (Liu et al., 2010) and *N.crassa* (Maddi et al., 2012), where deletion or knockdown of chitosanases had no effect on vegetative growth or conidiation. There are two possible reasons why chitosanases may not be required for morphogenesis. Firstly, chitosan is hypothesized to be an inherently flexible cell wall component. As such, hydrolysis would not be necessary to render it pliable in the same way as a component such as chitin, for example. Secondly, although there is but a single chitosanase enzyme in *M.oryzae*, this does not necessarily mean that it is the only one with chitosanase activity; both chitosanases and chitinases are able to hydrolyse bonds between GlcN and GlcNAc residues (Hartl et al., 2012). Thus, chitinases are also able to hydrolyse chitosan, although this is dependant upon degree of deacetylation, since they are not able to hydrolyse bonds between two GlcN residues, unlike chitosanase. It may therefore be chitinases that are required for chitosan hydrolysis during morphogenesis.

The potential redundancy between chitosanase and chitinases may also explain a number of other observations made in this study, including the fact that many fungi, including close relatives of *M.oryzae*, lack any chitosanase sequences at all. Of course, this could also reflect differences in cell wall chitosan content or localization. Investigations of chitin deacetylation in other fungal species will be required to answer these questions. Secreted chitinases may have also been responsible for supporting growth on media containing chitosan as a sole carbon source in the *csn* mutants; the chitosan used had a degree of deacetylation of 75-85%, making it susceptible to chitinase activity. Hydrolysis of chitosan during autolysis may also be carried out by chitinases, thus explaining the lack of delay in the onset of autolysis in the *csn* mutants. However, this could also be a reflection of the relatively low chitosan content in hyphal walls; the failure to degrade this would not be expected to cause a significant delay in autolysis.

In light of these negative results, it is difficult to ascertain the role of chitosanase. The Csn:eGFP construct localized to the cytoplasm, rather than the cell wall as expected. This may not necessarily be incorrect, but without a phenotype to complement, this is impossible to determine. Certain hydrolytic enzymes involved in cell-fusion do demonstrate cytoplasmic localization: In *S.pombe*, all 7 glucanase:GFP fusions demonstrated intracellular fluorescence, despite the presence of signal peptides in some of these proteins (e.g. Agn1) (Dudin et al., 2015). These proteins were only recruited to the cell wall at

the point of fusion. It is therefore possible that Csn may be recruited to the cell wall during hyphal fusion. Unfortunately, such fusion events proved difficult to observe in *M.oryzae*, due to the extremely high density of hyphae. Cytoplasmic localization would also explain the lack of phenotype observed during overexpression of *CSN*. The accumulation of abnormal concentrations of Csn intracellularly would not cause any loss of cell wall integrity, nor any increase in growth on media containing chitosan as a sole carbon source. Further investigations are required to determine the true location and role of Csn. For example, it may be informative to determine whether Csn has a role in antagonistic interactions in *M.oryzae*, or perhaps to characterize stages of the life-cycle not examine here, such as sexual reproduction or microconidiation.

5.4 Conclusions

There remain many unanswered questions regarding the role of chitosan hydrolysis in *M.oryzae*. Firstly, it is questionable whether the hydrolysis of chitosan is even required during morphogenesis, and if it is, it appears that Csn is not involved in this process. Other enzymes, such as chitinases, may be responsible instead. Secondly, the subcellular location of Csn is unknown, and it is possible that Csn remains intracellular until recruited to the cell wall during particular processes such as hyphal fusion. Investigating chitosan hydrolysis has therefore not resulted in any further insights into the roles of cell wall hydrolysis in fungi. This serves as a reminder that the cell wall is an incredibly complex structure, and a process as apparently simple as the hydrolysis of a polysaccharide could have numerous, 'cryptic' roles in the lifecycle of a fungus.

Chapter 6

General discussion and further work

6.1 General Discussion

Chitin deacetylases (EC 3.5.1.41) are a family of carbohydrate esterase enzymes which catalyze the hydrolysis of an *N*-acetamido group in the *N*-acetylglucosamine residues of chitin, resulting in deacetylation. Chitin deacetylases are present in all fungi, although the role of these enzymes had only been characterized in four species prior to this study: *Saccharomyces cerevisiae*, *Schizosaccharomyces pombe*, *Ashbya gossypii* and *Cryptococcus neoformans*. Chitosan is a structural component of the ascospore wall in *S.cerevisiae* (Christodoulidou et al., 1996) and *S.pombe* (Matsuo et al., 2005), is required for spore development in *A.gossypii* (Lickfeld and Schmitz, 2012), and is a major component of the cell wall in the vegetative cells of *C.neoformans* (Baker et al., 2007). Clearly, chitosan has different roles in fungi depending on the cell-type or species in question. The investigation of chitin deacetylation in *M.oryzae* provided further evidence for the multifaceted nature of chitosan. At least 3 CDAs are involved in chitin deacetylation during appressorium development. Unexpectedly, chitosan was not required for morphogenesis, but was required for germling adhesion and surface sensing. In the current model, chitosan is required for activation of the Pmk1 and cAMP pathways, although the exact mechanism behind this is unknown (Figure 3.18). In vegetative hyphae, chitosan was detected in both the subperipheral zone of colonies, and the colony interior. Two CDAs were responsible for chitin deacetylation in these locations, each with apparently distinct deacetylation mechanisms and expression patterns. The role of chitin deacetylation in these cell-types was unclear, but is associated with hyphal maturation and may play a role in altering properties of the cell wall, such as permeability. The roles of the other 5 CDAs remain unknown. In a previous study, a deletion strain of MGG05023 (*CDA7*) was made, but displayed no defects in pathogenic development (Mochizuki et al., 2011). The uncharacterised CDAs are likely to operate at stages of the life-cycle which were not studied here, for example during *in planta* growth, sexual reproduction and microconidiation. Chitin deacetylation during *in planta* growth is of particular interest, as the cell walls of invasive hyphae in *M.oryzae* are known to contain chitosan (Fujikawa et al., 2009). It has been hypothesized that chitosan operates as a 'stealth mechanism' in phytopathogenic fungi. No conclusive evidence was found for this in appressoria, but this hypothesis was not tested during *in planta* development, which would perhaps have been more insightful since *in planta*

hyphae are fully exposed to the defence mechanisms of the rice plant. Recently published transcriptomic analysis of rice infected with *M.oryzae* identified three CDAs that are expressed *in planta*: MGG12939 (*CBP1*), MGG04172 (*CDA3*) and MGG08356 (*CDA6*) (Dong et al., 2015). In this study, the *cbp1/cda3* mutant was fully pathogenic, although localization of chitosan in the invasive hyphae was not performed. Deletion and mCherry fusion of MGG08356 were in fact also attempted during the course of this project. Unfortunately, no putative deletion lines were obtained, and no fluorescence was observed in the mCherry fusions. Further investigations are therefore required to determine the role of chitosan during *in planta* growth, which would perhaps require the generation of a triple *cbp1/cda3/cda6* mutant. This would also help to determine whether chitin deacetylases represent a valuable fungicide target in *M.oryzae*. Based on current evidence, the chemical inhibition of chitin deacetylation would not have any protective effect against rice blast disease.

Chitin deacetylation and chitosan hydrolysis were hypothesized to be important for increasing cell wall flexibility during cellular morphogenesis. However, the evidence presented in this thesis strongly suggests that this is not the case. Appressorium development, hyphal branching and hyphal extension all occurred normally in the absence of chitosan in the *cda* and *csn* mutants, and ectopic expression of either Cda1:mCherry or Cbp1:mCherry did not result in any morphogenic defects. In addition, localization of chitosan with OGA488 did not provide evidence for a role in morphogenesis, since labelling was not found to be specific to cell-types or subcellular locations undergoing morphogenesis. This is consistent with previous studies regarding the role of chitin deacetylation: Chitosan was not detected during vegetative growth of *S.cerevisiae* (Christodoulidou et al., 1996), and deletion of the sole chitin deacetylase in *A.gossypii* did not alter filamentous growth of the fungus (Lickfeld and Schmitz, 2012). Although it remains possible that chitin deacetylation results in a change in the physical properties of the cell wall, the relationship between cell wall dynamics and morphogenesis is much more complex than a change in a single cell wall component. Several concurrent changes in cell wall composition are most likely required during morphogenesis, including *de novo* cell wall synthesis, cell wall hydrolysis, alterations in the inter-relationships of different cell wall components, as well as re-organization of intracellular components, such as septins. As a relatively

simple example, morphogenesis at the bud neck in *S.cerevisiae* is controlled by the chitin ring (synthesized by Chs3), the linkage of this chitin to β1,3-glucan (by the transglycosylases Crh1 and Crh2), and the septin complex. Interestingly, the septin complex and chitin ring appear to have redundant functions in controlling bud neck growth (Cabib and Arroyo, 2013). Thus, one can imagine that the changes in cell-shape or morphogenesis of the various different cell-types during the life-cycle of a fungus such as *M.oryzae* requires the coordination of a large number of processes, some of which may exhibit redundancy. Future investigations in this area should therefore take a holistic view of these processes, rather than considering each in isolation.

Although not required for morphogenesis, it is clear that chitin deacetylation is associated with a remarkably diverse set of processes, including cellular development, pathogenic interactions and maintenance of cell wall integrity. For example, within *M.oryzae* chitosan was found to have different roles according to the developmental stage in question (i.e. germlings vs. vegatative hyphae). This raises the question of how a single polysaccharide can have such apparently disparate roles. The answer to this may lie in the interactions of chitosan with other cell wall components: its relationship with the rest of the cell wall may differ according to the developmental stage or cell-type in question. Unlike other cell wall polysaccharides, the primary amine groups of chitosan may allow it to form unique ionic or covalent interactions with other cell wall components. This could result in significant changes to the chemical or physical properties of the cell wall at particular subcellular locations or developmental stages. There is some evidence for this in germlings, where chitosan may form a polyelectrolyte complex with an anionic moiety, possibly polygalacturonic acid (PGA). This relationship may be critical for surface sensing in germlings, and merits further investigation. In vegetative hyphae, only extremely low levels of PGA were detected, and showed an entirely different distribution to chitosan, suggesting that the putative polyelectrolyte complex does not exist in hyphal walls. Further work is required to determine the interactions of chitosan with other cell wall components, and to establish whether this property is unique to chitosan.

The work presented in this thesis has established novel biological roles for chitosan. In addition, novel mechanistic aspects of chitin deacetylation have also been discovered. Prior to this study, the localization of chitin deacetylases had never been investigated.

However, through the use of fluorescent CDA fusions both alone and in combination with chitin synthases, a number of novel and potentially significant aspects of chitin deacetylation were revealed. Firstly, the timing of chitin deacetylation may be an important determinant of the properties of the resulting chitosan. Cbp1:mCherry and Cda2:mCherry colocalized with Chs7:2xYFP during germ tube hooking and appressorium development, and Cda4:mCherry may colocalize with a chitin synthase during hyphal growth. The proximity of the enzymes or even their physical association may result in the complete deacetylation of nascent chitin chains. Conversely, colocalization of Cbp1:mCherry and Cda2:mCherry with Chs7:2xYFP was not observed at the lateral walls of the germ tube, or at the upper, domed part of the appressorium. In addition, Cda1:mCherry was only observed in mature hyphae, where chitin synthesis may not be occurring. The action of chitin deacetylases on non-nascent chitin (which may be crystalline) may result in only partial deacetylation, due to the inaccessibility of the substrate. Therefore, the mode of chitin deacetylation could have profound effects on the properties of the resulting chitosan, and may reflect different roles of the chitosan according to cell-type or subcellular location. Data from the colocalization studies also suggests that the potential coordination between chitin synthesis and deacetylation may extend to the transport of these enzymes. In *S.cerevisiae*, Chs3 is known to cycle between the plasma membrane and intracellular trans-golgi/early endosomal compartments (Chuang and Schekman, 1996; Ziman et al., 1996). Colocalization of Cbp1:mCherry with Chs7:2xYFP was observed in intracellular bodies in germ tubes and appressoria, which may also represent an intracellular store of chitin synthase/deacetylase, from which transport of both enzymes to the plasma membrane can occur. In vegetative hyphae, the intracellular localization of Cda4:mCherry also suggested possible colocalization with a chitin synthase, although this was not confirmed. Clearly, the coordination between chitin synthesis and deacetylation is an area which merits further investigation (see 'Further work').

The investigation of chitin deacetylation and chitosan hydrolysis has also served to demonstrate the extreme complexity of the cell wall, and the limitations of our current understanding of it. In part, this lack of understanding arises from the remarkable diversity in form and function demonstrated by the fungal cell wall, both between different cell-types within a single species and between different species of fungi. A single cell

wall component, such as chitosan or α1,3-glucan, can be required for diverse processes depending on the species or developmental stage in question. Such diversity makes it difficult to predict the role of a cell wall component based on data obtained from other fungi or cell-types - the requirement for CDAs during surface sensing in the germlings of *M.oryzae* could not have been predicted based on the previous characterization of Cda1 in *A.gossypii*, for example. Similarly, the role of chitosan in the vegetative hyphae of *M.oryzae* could not have been predicted by the characterization of chitin deacetylation in germlings. This makes it impossible to create an all-encompassing model for the structure and function of the cell wall. However, it also reveals an important aspect of the cell wall, which is its functional plasticity. It appears that fungi have evolved a number of different strategies by which the cell wall can maintain cellular integrity in the face of biotic and abiotic stress, whilst also influencing cellular morphogenesis and physical or biological interactions. The deacetylation of chitin appears to be one such strategy, which has been adapted to fulfil different tasks depending on the species of fungus or developmental stage in question.

6.2 Further work

As outlined above, there are several aspects of this project which merit further investigation. These are detailed below:

Chitosan-mediated surface sensing

A key finding of this thesis was the requirement for chitosan in surface sensing during germling morphogenesis. However, the precise mechanism behind this was not elucidated. The first step in investigating this problem would be to determine the activation status of the Pmk1 and cAMP regulatory pathways in the *cda* mutants. This can be achieved relatively simply, using the Phosphoplus® p44/42 MAPK antibody (Cell Signaling Technology®) to specifically detect the phosphorylation status of Pmk1 (Zhao et al., 2005), and ELISA based protocols to quantify cAMP concentrations. This would reveal whether chitosan is required for the activation of just one, or both of these pathways. The main difficulty in these experiments would be the collection of sufficient quantities of germling tissue for the analysis.

Determining why chitosan is required for pathway activation is more challenging. As discussed previously (Chapter 3, Section 3.3), there are three main hypotheses of how chitosan may mediate surface sensing. The first hypothesis concerns the putative direct linkage between chitosan and proteins involved in surface sensing. One way to investigate this hypothesis might be to identify the proteins which are in contact with the chitosan during germling morphogenesis. Exogenous FITC-labelled chitosan was shown to be incorporated into the cell wall in germlings of *CDA* deletion strains. By instead labelling the exogenous chitosan with an amine/sulphydryl-reactive photoaffinity cross-linker, any proteins within the immediate vicinity of chitosan in the cell wall could be cross-linked, isolated, and identified by mass spectrometry. This could identify novel proteins involved in surface sensing or surface adhesion, as well as possibly confirming the putative interaction of chitosan with previously identified proteins such as the mucin Msb2. Such an approach would require rigorous preliminary testing to optimise the cross-linking protocol, which would involve testing of different cross-linking agents and experimental conditions. Any proteins identified by this method could then be tested for their involvement in surface sensing or adhesion by gene-deletion or fluorescent-labelling.

The second hypothesis concerns the possible role of chitosan in imparting the cell wall with the physical properties required to allow surface sensing through mechanical deformation. Atomic Force Microscopy (AFM) could be used to determine elasticity of the germ tube cell wall in WT and *cda* strains. However, linking this with the activation of membrane proteins would be more challenging. Chachisvilis et al. (2006) used a FRET-based approach to monitor conformational changes in a mammalian GPCR. Potentially, this could be applied to the GPCR Pth11 in *M.oryzae*, to monitor conformational changes in the WT and *cda* strains on different surfaces.

The third and final hypothesis is that chitosan directly mediates germling adhesion. In this case, investigating the structure and surface characteristics of the germ tube cell wall in WT and *cda* strains in the presence or absence of exogenous chitosan could be informative. Atomic Force Microscopy (AFM) could be used to determine the electrostatic charge and hydrophobicity of the germ tube cell wall (Butt, 1991), which may well be altered in the absence of chitosan and may influence adhesion. Surface topography of the cell wall could also be determined with AFM, as could the localization of surface-exposed mannans and chitin, using tips functionalized with ConA or WGA-lectins respectively (Alsteens et al., 2008). However, distinguishing between the direct effects of chitosan on adhesion and those occurring as a result of signalling pathway activation would be difficult. One possible way to achieve this would be by artificial pathway activation in the *cda* strain by chemical or genetic means. In this way, chitosan would remain absent, but the signalling pathways would still be activated. Germling adhesion and cell wall properties could then be examined in these strains.

The role of chitin deacetylation during *in planta* development

As described previously, investigating the role of chitin deacetylation during *in planta* development would require the creation of a *cda6* mutant strain, and possibly *cda3/cda6* and *cbp1/cda3/cda6* mutants. Once generated, the first step would be to determine that chitin deacetylation had been reduced during *in planta* growth in the deletion strains. This would be simple to achieve, by using the chitosan-specific probe OGA488. Next, the pathogenicity of the deletion strains would be evaluated, and any differences in plant defence response could be quantified by qPCR of pathogenesis-related (PR)

genes, callose staining with aniline blue and hydrogen peroxide staining with DAB (3-3'-Diaminobenzidine).

Co-ordination between chitin synthesis and deacetylation

The relationship between chitin synthesis and deacetylation is one of the key areas which merits further investigation. Due to the tractability of germling morphogenesis as an experimental system and the preliminary data already obtained, investigating the relationship between chitin synthase 7 and Cbp1 or Cda2 would likely be the most productive approach. There are a number of different experiments which would be required to investigate this area. The first thread of research would investigate the possibility of co-transportation of Chs7 and Cbp1. To do this, the identity of the intracellular bodies observed when imaging the Chs7:2xYFP and Cbp1:mCherry constructs (Figure 3.7) should be determined. This could be achieved by using fluorescently-tagged Rab5, Rab7 and carboxypeptidase Y to identify the localization of early endosomes, late endosomes and vacuoles respectively (Ramanujam et al., 2013), and to determine whether these colocalize with Chs7:2xYFP and Cbp1:mCherry. Assuming the colocalization of these proteins, live cell imaging of germlings could then be used to follow the movement of these compartments to and from the cell periphery. Endocytic recycling of Chs7 and Cbp1 could also be studied either via pharmacological inhibition (e.g. Latrunculin A treatment) or genetic disruption (e.g. *END4* deletion). The involvement of other proteins, such as the chitin synthase activators would also be of interest to pursue. The second thread of research would investigate the putative physical association between Chs7 and Cbp1 or Cda2. This could be tested in a number of ways, including co-immunoprecipitation, pull-down assay, protein cross-linking, FRET (Fluorescence Resonance Energy Transfer) or BiFC (Bimolecular Fluorescence Complementation). These analyses could well identify other proteins which are part of a proposed chitin synthase-deacetylase complex.

Cda4 was also hypothesized to colocalize with a chitin synthase in vegetative hyphae, but the enzyme in question was not identified. The localization of other chitin synthases (Chs2, 3, 4, 5 and 6) therefore needs to be tested to determine whether they colocalize with Cda4. Any putative co-transportation and protein-protein interactions can then be tested as described above.

The effect of chitin deacetylation on the chemical and physical properties of the cell wall

Chitin deacetylation is hypothesized to alter the chemical and physical properties of the cell wall. Investigating this hypothesis could be achieved by exploiting the existing deletion strains, and strains ectopically expressing chitin deacetylases. Quantifying the physical properties of the cell wall is relatively straight-forward, and could be achieved with AFM. This would determine whether reduced or ectopic chitin deacetylation results in altered cell wall elasticity. As discussed previously, AFM could also be used to produce high resolution topographical maps of the cell wall surface, quantify surface charge or hydrophobicity and to localize surface-exposed mannans and chitin.

The chemical properties of chitosan (e.g. degree of deacetylation) and its interactions with other cell wall components would be far more challenging to deduce. It would perhaps be possible to once again exploit the incorporation of exogenous chitosan into the germ tube and appressorial cell walls. Once incorporated into the cell wall, the chitosan (which could be labelled prior to incorporation) may be able to be isolated and characterized by HPLC, mass spectrometry or NMR. This could help identify any covalent linkages between chitosan and other cell wall components. Fourier-Transform Infra-Red (FT-IR) spectroscopy could also be a valuable tool to determine the chemical composition of the cell wall in *CDA* deletion strains or those ectopically expressing *CDA*s.

Polygalacturonic acid as a novel cell wall component

Polygalacturonic acid (PGA) was tentatively identified as a component of the cell wall in the germlings of *M.oryzae* (Chapter 3). In order to further investigate this, the identity of PGA would first need to be confirmed. The most effective approach would be cell wall composition analysis by GC-MS (Wang et al., 2013), although the main challenge with this method would be the collection of sufficient germling tissue for the analysis ($\sim$100mg dry weight required). Assuming that PGA is indeed a component of the cell wall, it would be of interest to investigate the role of this polysaccharide, especially given its putative relationship with chitosan. Unfortunately, in order to do this, the enzymes responsible for its synthesis need to first be identified. As discussed previously (Chapter 3), the genome of *M.oryzae* does not appear to encode the enzymes required for galacturonic

acid synthesis. This suggests a non-conventional mechanism of synthesis. It is possible that galactose oxidase enzymes are required for oxidation of galactose residues in the cell wall. The genome of *M.oryzae* encodes two predicted secreted galactose oxidase enzymes: MGG02368 and MGG10878. One of these, MGG10878, appears to be specifically expressed during appressorium development (Soanes et al., 2012). However, the oxidation of galactose by this enzyme would only produce galacto-hexodialdose, not galacturonic acid. Therefore, an additional oxidation step would be required. This may be performed by MGG05865, which is annotated as a glyoxal oxidase. MGG05865 is a predicted secreted protein, with 5 chitin binding domains, suggesting cell wall localization. It is also highly expressed during appressorium development, but not during vegetative growth (Soanes et al., 2012). Glyoxal oxidase enzymes catalyze the oxidation of aldehydes to carboxylic acids, and so this could represent the final step in the synthesis of galacturonic acid in the cell wall. Deletion of these identified genes would be necessary to test whether they are required for the synthesis of PGA. Previous studies characterizing the roles of galactose oxidase and glyoxal oxidase enzymes are few. Deletion of a membrane-bound glyoxal oxidase in *Ustilago maydis* resulted in defective cellular morphology and loss of pathogenicity (Leuthner et al., 2005), and in *Botrytis cinerea* a deletion mutant for glyoxal oxidase resulted in defects in conidial germination, hyphal growth and pathogenicity (Van Kan et al., 2004). However, it is unclear exactly why deletion of these enzymes resulted in the observed phenotype and no link to galacturonic acid was investigated.

Bibliography

Agrawal, G. K., Rakwal, R., Tamogami, S., Yonekura, M., Kubo, A., and Saji, H. (2002). Chitosan activates defense/stress responses in the leaves of *Oryza sativa* seedlings. *Plant Physiology and Biochemistry*, 40(12):1061–1069.

Ahn, N., Kim, S., Choi, W., Im, K.-H., and Lee, Y.-H. (2004). Extracellular matrix protein gene, *EMP1*, is required for appressorium formation and pathogenicity of the rice blast fungus, *Magnaporthe grisea*. *Molecules and Cells*, 17(1):166–173.

Aimanianda, V., Bayry, J., Bozza, S., Kniemeyer, O., Perruccio, K., Elluru, S. R., Clavaud, C., Paris, S., Brakhage, A. A., Kaveri, S. V., et al. (2009). Surface hydrophobin prevents immune recognition of airborne fungal spores. *Nature*, 460(7259):1117–1121.

Alcazar-Fuoli, L., Clavaud, C., Lamarre, C., Aimanianda, V., Seidl-Seiboth, V., Mellado, E., and Latgé, J.-P. (2011). Functional analysis of the fungal/plant class chitinase family in *Aspergillus fumigatus*. *Fungal Genetics and Biology*, 48(4):418–429.

Alsteens, D., Dupres, V., Mc Evoy, K., Wildling, L., Gruber, H. J., and Dufrêne, Y. F. (2008). Structure, cell wall elasticity and polysaccharide properties of living yeast cells, as probed by AFM. *Nanotechnology*, 19(38):384005.

Baek, J.-M., Howell, C. R., and Kenerley, C. M. (1999). The role of an extracellular chitinase from *Trichoderma virens* Gv29-8 in the biocontrol of *Rhizoctonia solani*. *Current Genetics*, 35(1):41–50.

Baker, L., Specht, C., Donlin, M., and Lodge, J. (2007). Chitosan, the deacetylated form of chitin, is necessary for cell wall integrity in *Cryptococcus neoformans*. *Eukaryotic Cell*, 6(5):855–867.

Baker, L. G., Specht, C. A., and Lodge, J. K. (2009). Chitinases are essential for sexual development but not vegetative growth in *Cryptococcus neoformans*. *Eukaryotic Cell*, 8(11):1692–1705.

Baker, L. G., Specht, C. A., and Lodge, J. K. (2011). Cell wall chitosan is necessary for virulence in the opportunistic pathogen *Cryptococcus neoformans*. *Eukaryotic Cell*, 10(9):1264–1268.

Baladrón, V., Ufano, S., Dueñas, E., Martín-Cuadrado, A. B., del Rey, F., and de Aldana, C. R. V. (2002). Eng1p, an endo-1, 3-β-glucanase localized at the daughter side of the septum, is involved in cell separation in *Saccharomyces cerevisiae*. *Eukaryotic Cell*, 1(5):774–786.

Banks, I. R., Specht, C. A., Donlin, M. J., Gerik, K. J., Levitz, S. M., and Lodge, J. K. (2005). A chitin synthase and its regulator protein are critical for chitosan

production and growth of the fungal pathogen *Cryptococcus neoformans*. *Eukaryotic Cell*, 4(11):1902–1912.

Bardalaye, P. C. and Nordin, J. H. (1977). Chemical structure of the galactomannan from the cell wall of *Aspergillus niger*. *Journal of Biological Chemistry*, 252(8):2584–2591.

Bartnicki-Garcia, S. (1973). Fundamental aspects of hyphal morphogenesis. *Microbial Differentiation*, 23:245–267.

Beaussart, A., Alsteens, D., El-Kirat-Chatel, S., Lipke, P. N., Kucharíková, S., Van Dijck, P., and Dufrêne, Y. F. (2012). Single-molecule imaging and functional analysis of als adhesins and mannans during *Candida albicans* morphogenesis. *ACS Nano*, 6(12):10950–10964.

Beauvais, A., Bozza, S., Kniemeyer, O., Formosa, C., Balloy, V., Henry, C., Roberson, R. W., Dague, E., Chignard, M., Brakhage, A. A., et al. (2013). Deletion of the α-(1, 3)-glucan synthase genes induces a restructuring of the conidial cell wall responsible for the avirulence of *Aspergillus fumigatus*. *Plos Pathogens*, 9(11).

Beauvais, A., Bruneau, J., Mol, P., Buitrago, M., Legrand, R., and Latge, J. (2001). Glucan synthase complex of *Aspergillus fumigatus*. *Journal of Bacteriology*, 183(7):2273–2279.

Beck, J., Broniszewska, M., Schwienbacher, M., and Ebel, F. (2014). Characterization of the *Aspergillus fumigatus* chitosanase CsnB and evaluation of its potential use in serological diagnostics. *International Journal of Medical Microbiology*, 304(5):696–702.

Becker, W., Von Jagow, G., Anke, T., and Steglich, W. (1981). Oudemansin, strobilurin A, strobilurin B and myxothiazol: new inhibitors of the bc 1 segment of the respiratory chain with an e-β-methoxyacrylate system as common structural element. *FEBS Letters*, 132(2):329–333.

Beckerman, J. L. and Ebbole, D. J. (1996). *MPG1*, a gene encoding a fungal hydrophobin of *Magnaporthe grisea*, is involved in surface recognition. *Molecular Plant-Microbe Interactions*, 9(6):450–456.

Bell-Pedersen, D., Dunlap, J. C., and Loros, J. J. (1992). The *Neurospora* circadian clock-controlled gene, *CCG-2*, is allelic to *EAS* and encodes a fungal hydrophobin required for formation of the conidial rodlet layer. *Genes & Development*, 6(12a):2382–2394.

Bernard, M. and Latgé, J.-P. (2001). *Aspergillus fumigatus* cell wall: composition and biosynthesis. *Medical Mycology*, 39(1):9–17.

Blackwell, J. (1969). Structure of β-chitin or parallel chain systems of poly-β-(1 4)-n-acetyl-d-glucosamine. *Biopolymers*, 7(3):281–298.

Blair, D. E., Hekmat, O., Schüttelkopf, A. W., Shrestha, B., Tokuyasu, K., Withers, S. G., and Van Aalten, D. M. (2006). Structure and mechanism of chitin deacetylase from the fungal pathogen *Colletotrichum lindemuthianum*. *Biochemistry*, 45(31):9416–9426.

Bowman, S. M. and Free, S. J. (2006). The structure and synthesis of the fungal cell wall. *Bioessays*, 28(8):799–808.

Brand, A., Shanks, S., Duncan, V. M., Yang, M., Mackenzie, K., and Gow, N. A. (2007). Hyphal orientation of *Candida albicans* is regulated by a calcium-dependent mechanism. *Current Biology*, 17(4):347–352.

Brown, G. D. and Gordon, S. (2001). Immune recognition: a new receptor for β-glucans. *Nature*, 413(6851):36–37.

Bulawa, C. E. and Osmond, B. C. (1990). Chitin synthase i and chitin synthase ii are not required for chitin synthesis in vivo in *Saccharomyces cerevisiae*. *Proceedings of the National Academy of Sciences*, 87(19):7424–7428.

Bush, D., Horisberger, M., Horman, I., and Wursch, P. (1974). The wall structure of *Schizosaccharomyces pombe*. *Journal of General Microbiology*, 81(1):199–206.

Butt, H.-J. (1991). Measuring electrostatic, van der waals, and hydration forces in electrolyte solutions with an atomic force microscope. *Biophysical Journal*, 60(6):1438.

Cabib, E. (2009). Two novel techniques for determination of polysaccharide cross-links show that Crh1p and Crh2p attach chitin to both β (1-6)-and β (1-3) glucan in the *Saccharomyces cerevisiae* cell wall. *Eukaryotic Cell*, 8(11):1626–1636.

Cabib, E. and Arroyo, J. (2013). How carbohydrates sculpt cells: chemical control of morphogenesis in the yeast cell wall. *Nature Reviews Microbiology*, 11(9):648–655.

Cabib, E., Farkas, V., Kosík, O., Blanco, N., Arroyo, J., and McPhie, P. (2008). Assembly of the yeast cell wall Crh1p and Crh2p act as transglycosylases in vivo and in vitro. *Journal of Biological Chemistry*, 283(44):29859–29872.

Cabib, E., Sburlati, A., Bowers, B., and Silverman, S. J. (1989). Chitin synthase 1, an auxiliary enzyme for chitin synthesis in *Saccharomyces cerevisiae*. *The Journal of Cell Biology*, 108(5):1665–1672.

Cantu, D., Greve, L. C., Labavitch, J. M., and Powell, A. L. (2009). Characterization of the cell wall of the ubiquitous plant pathogen *Botrytis cinerea*. *Mycological Research*, 113(12):1396–1403.

Cappellaro, C., Baldermann, C., Rachel, R., and Tanner, W. (1994). Mating type-specific cell-cell recognition of *Saccharomyces cerevisiae*: cell wall attachment and active sites of a-and alpha-agglutinin. *The EMBO Journal*, 13(20):4737.

Certis (2015). Tavano fungicide. [Online;accessed: 2015-03-07].

Chachisvilis, M., Zhang, Y.-L., and Frangos, J. A. (2006). G protein-coupled receptors sense fluid shear stress in endothelial cells. *Proceedings of the National Academy of Sciences*, 103(42):15463–15468.

Chaky, J., Anderson, K., Moss, M., and Vaillancourt, L. (2001). Surface hydrophobicity and surface rigidity induce spore germination in *Colletotrichum graminicola*. *Phytopathology*, 91(6):558–564.

Chatterjee, S., Prados-Rosales, R., Itin, B., Casadevall, A., and Stark, R. E. (2015). Solid-state NMR reveals the carbon-based molecular architecture of *Cryptococcus neoformans* fungal eumelanins in the cell wall. *Journal of Biological Chemistry*, 290(22):13779–13790.

Chen, Z., Nunes, M. A., Silva, M. C., and Rodrigues, C. J. (2004). Appressorium turgor pressure of *Colletotrichum kahawae* might have a role in coffee cuticle penetration. *Mycologia*, 96(6):1199–1208.

Cheng, C.-Y., Chang, C.-H., Wu, Y.-J., and Li, Y.-K. (2006). Exploration of glycosyl hydrolase family 75, a chitosanase from *Aspergillus fumigatus*. *Journal of Biological Chemistry*, 281(6):3137–3144.

Choi, C.-J., Ju, H.-J., Park, B.-H., Qin, R., Jahng, K.-Y., Han, D.-M., and Chae, K.-S. (2005). Isolation and characterization of the *Aspergillus nidulans eglC* gene encoding a putative β-1, 3-endoglucanase. *Fungal Genetics and Biology*, 42(7):590–600.

Choi, W. and Dean, R. A. (1997). The adenylate cyclase gene *MAC1* of *Magnaporthe grisea* controls appressorium formation and other aspects of growth and development. *The Plant Cell*, 9(11):1973–1983.

Choma, A., Wiater, A., Komaniecka, I., Paduch, R., Pleszczyńska, M., and Szczodrak, J. (2013). Chemical characterization of a water insoluble (1 3)-α-d-glucan from an alkaline extract of *Aspergillus wentii*. *Carbohydrate Polymers*, 91(2):603–608.

Christodoulidou, A., Bouriotis, V., and Thireos, G. (1996). Two sporulation-specific chitin deacetylase-encoding genes are required for the ascospore wall rigidity of *Saccharomyces cerevisiae*. *Journal of Biological Chemistry*, 271(49):31420–31425.

Christodoulidou, A., Briza, P., Ellinger, A., and Bouriotis, V. (1999). Yeast ascospore wall assembly requires two chitin deacetylase isozymes. *FEBS letters*, 460(2):275–279.

Chuang, J. S. and Schekman, R. W. (1996). Differential trafficking and timed localization of two chitin synthase proteins, Chs2p and Chs3p. *The Journal of Cell Biology*, 135(3):597–610.

Chumley, F. G., Valent, B., et al. (1990). Genetic analysis of melanin-deficient, nonpathogenic mutants of *Magnaporthe grisea*. *Molecular Plant-Microbe Interactions*, 3(3):135–143.

Copa-Patiño, J. L., Reyes, F., and Pérez-Leblic, M. I. (1989). Purification and properties of a 1, 3-β-glucanase from *Penicillium oxalicum* autolysates. *FEMS Microbiology Letters*, 65(3):285–291.

Cornelissen, B. and Haring, M. (2001). Fem1, a *Fusarium oxysporum* glycoprotein that is covalently linked to the cell wall matrix and is conserved in filamentous fungi. *Molecular Genetics and Genomics*, 265:143–152.

Cortese, M. S., Uversky, V. N., and Dunker, A. K. (2008). Intrinsic disorder in scaffold proteins: getting more from less. *Progress in Biophysics and Molecular Biology*, 98(1):85–106.

Dakhara, S., Anajwala, C., et al. (2010). Polyelectrolyte complex: A pharmaceutical review. *Systematic Reviews in Pharmacy*, 1(2):121.

Davis, L. and Bartnicki-Garcia, S. (1984a). The co-ordination of chitosan and chitin synthesis in *Mucor rouxii*. *Journal of General Microbiology*, 130(8):2095–2102.

Davis, L. L. and Bartnicki-Garcia, S. (1984b). Chitosan synthesis by the tandem action of chitin synthetase and chitin deacetylase from *Mucor rouxii*. *Biochemistry*, 23(6):1065–1073.

de Groot, P. W., Bader, O., de Boer, A. D., Weig, M., and Chauhan, N. (2013). Adhesins in human fungal pathogens: glue with plenty of stick. *Eukaryotic Cell*, 12(4):470–481.

De Groot, P. W., Ram, A. F., and Klis, F. M. (2005). Features and functions of covalently linked proteins in fungal cell walls. *Fungal Genetics and Biology*, 42(8):657–675.

de Jesus Carrion, S., Leal, S. M., Ghannoum, M. A., Aimanianda, V., Latgé, J.-P., and Pearlman, E. (2013). The rodA hydrophobin on *Aspergillus fumigatus* spores masks dectin-1–and dectin-2–dependent responses and enhances fungal survival in vivo. *The Journal of Immunology*, 191(5):2581–2588.

de Jong, J. C., McCormack, B. J., Smirnoff, N., and Talbot, N. J. (1997). Glycerol generates turgor in rice blast. *Nature*, 389(6648):244–244.

de Jonge, R., van Esse, H. P., Kombrink, A., Shinya, T., Desaki, Y., Bours, R., van der Krol, S., Shibuya, N., Joosten, M. H., and Thomma, B. P. (2010). Conserved fungal lysm effector Ecp6 prevents chitin-triggered immunity in plants. *Science*, 329(5994):953–955.

De Nobel, J. and Barnett, J. (1991). Passage of molecules through yeast cell walls: A brief essay-review. *Yeast*, 7(4):313–323.

Dekker, N., Speijer, D., Grün, C. H., van den Berg, M., de Haan, A., and Hochstenbach, F. (2004). Role of the α-glucanase Agn1p in fission-yeast cell separation. *Molecular Biology of the Cell*, 15(8):3903–3914.

del Dedo, J. E., Dueñas, E., Arnáiz, Y., del Rey, F., and de Aldana, C. R. V. (2009). β-glucanase Eng2 is required for ascus wall endolysis after sporulation in the fission yeast *Schizosaccharomyces pombe*. *Eukaryotic Cell*, 8(8):1278–1286.

DeMarini, D. J., Adams, A. E., Fares, H., De Virgilio, C., Valle, G., Chuang, J. S., and Pringle, J. R. (1997). A septin-based hierarchy of proteins required for localized deposition of chitin in the *Saccharomyces cerevisiae* cell wall. *The Journal of Cell Biology*, 139(1):75–93.

Denning, D. W. (2002). Echinocandins: a new class of antifungal. *Journal of Antimicrobial Chemotherapy*, 49(6):889–891.

Denning, D. W. and Bromley, M. J. (2015). How to bolster the antifungal pipeline. *Science*, 347(6229):1414–1416.

DeZwaan, T. M., Carroll, A. M., Valent, B., and Sweigard, J. A. (1999). *Magnaporthe grisea* pth11p is a novel plasma membrane protein that mediates appressorium differentiation in response to inductive substrate cues. *The Plant Cell*, 11(10):2013–2030.

Dichtl, K., Samantaray, S., Aimanianda, V., Zhu, Z., Prévost, M.-C., Latgé, J.-P., Ebel, F., and Wagener, J. (2015). *Aspergillus fumigatus* devoid of cell wall β-1, 3-glucan is viable, massively sheds galactomannan and is killed by septum formation inhibitors. *Molecular Microbiology*, 95(3):458–471.

Dijkgraaf, G. J., Brown, J. L., and Bussey, H. (1996). The *KNH1* gene of *Saccharomyces cerevisiae* is a functional homolog of *KRE9*. *Yeast*, 12(7):683–692.

Doehlemann, G., Berndt, P., and Hahn, M. (2006). Different signalling pathways involving a Gα protein, cAMP and a MAP kinase control germination of *Botrytis cinerea* conidia. *Molecular Microbiology*, 59(3):821–835.

Dong, Y., Li, Y., Zhao, M., Jing, M., Liu, X., Liu, M., Guo, X., Zhang, X., Chen, Y., Liu, Y., et al. (2015). Global genome and transcriptome analyses of *Magnaporthe oryzae* epidemic isolate 98-06 uncover novel effectors and pathogenicity-related genes, revealing gene gain and lose dynamics in genome evolution. *PLoS pathogens*, 11(4):e1004801–e1004801.

Douglas, C. M., Foor, F., Marrinan, J. A., Morin, N., Nielsen, J. B., Dahl, A. M., Mazur, P., Baginsky, W., Li, W., and El-Sherbeini, M. (1994). The *Saccharomyces cerevisiae FKS1* (etg1) gene encodes an integral membrane protein which is a subunit of 1, 3-beta-d-glucan synthase. *Proceedings of the National Academy of Sciences*, 91(26):12907–12911.

Dudin, O., Bendezú, F. O., Groux, R., Laroche, T., Seitz, A., and Martin, S. G. (2015). A formin-nucleated actin aster concentrates cell wall hydrolases for cell fusion in fission yeast. *The Journal of Cell Biology*, 208(7):897–911.

Dunker, A. K., Romero, P., Obradovic, Z., Garner, E. C., and Brown, C. J. (2000). Intrinsic protein disorder in complete genomes. *Genome Informatics*, 11:161–171.

Dünkler, A., Jorde, S., and Wendland, J. (2008). An *Ashbya gossypii cts2* mutant deficient in a sporulation-specific chitinase can be complemented by *Candida albicans* cht4. *Microbiological Research*, 163(6):701–710.

Dünkler, A., Walther, A., Specht, C. A., and Wendland, J. (2005). *Candida albicans CHT3* encodes the functional homolog of the Cts1 chitinase of *Saccharomyces cerevisiae*. *Fungal Genetics and Biology*, 42(11):935–947.

Ecker, M., Deutzmann, R., Lehle, L., Mrsa, V., and Tanner, W. (2006). Pir proteins of *Saccharomyces cerevisiae* are attached to β-1, 3-glucan by a new protein-carbohydrate linkage. *Journal of Biological Chemistry*, 281(17):11523–11529.

Eisenman, H. C. and Casadevall, A. (2012). Synthesis and assembly of fungal melanin. *Applied Microbiology and Biotechnology*, 93(3):931–940.

Eisenman, H. C., Nosanchuk, J. D., Webber, J. B. W., Emerson, R. J., Camesano, T. A., and Casadevall, A. (2005). Microstructure of cell wall-associated melanin in the human pathogenic fungus *Cryptococcus neoformans*. *Biochemistry*, 44(10):3683–3693.

Enderlin, C. S. and Selitrennikoff, C. P. (1994). Cloning and characterization of a *Neurospora crassa* gene required for (1, 3) beta-glucan synthase activity and cell wall formation. *Proceedings of the National Academy of Sciences*, 91(20):9500–9504.

Ene, I. V., Walker, L. A., Schiavone, M., Lee, K. K., Martin-Yken, H., Dague, E., Gow, N. A., Munro, C. A., and Brown, A. J. (2015). Cell wall remodeling enzymes modulate fungal cell wall elasticity and osmotic stress resistance. *mBio*, 6(4):e00986–15.

Esteban, P. F., Ríos, I., García, R., Dueñas, E., Plá, J., Sánchez, M., de Aldana, C. R. V., and del Rey, F. (2005). Characterization of the *CaENG1* gene encoding an endo-1, 3-β-glucanase involved in cell separation in *Candida albicans*. *Current Microbiology*, 51(6):385–392.

Fajardo-Somera, R. A., Jöhnk, B., Bayram, Ö., Valerius, O., Braus, G. H., and Riquelme, M. (2015). Dissecting the function of the different chitin synthases in vegetative growth and sexual development in *Neurospora crassa*. *Fungal Genetics and Biology*, 75:30–45.

Fontaine, T., Simenel, C., Dubreucq, G., Adam, O., Delepierre, M., Lemoine, J., Vorgias, C. E., Diaquin, M., and Latgé, J.-P. (2000). Molecular organization of the alkali-insoluble fraction of *Aspergillus fumigatus* cell wall. *Journal of Biological Chemistry*, 275(36):27594–27607.

Franck, W. L., Gokce, E., Oh, Y., Muddiman, D. C., and Dean, R. A. (2013). Temporal analysis of the *Magnaporthe oryzae* proteome during conidial germination and cyclic amp (camp)-mediated appressorium formation. *Molecular & Cellular Proteomics*, 12(8):2249–2265.

Free, S. J. (2013). Fungal cell wall organization and biosynthesis. *Advanced Genetics*, 81:33–82.

Froyd, J., Paget, C., Guse, L., Dreikorn, B., and Pafford, J. (1976). Tricyclazole: a new systemic fungicide for control of *Pyricularia oryzae* on rice. *Phytopathology*, 66(1):135–131.

Fu, C., Tanaka, A., and Free, S. J. (2014). *Neurospora crassa* 1, 3-α-glucan synthase, Ags-1, is required for cell wall biosynthesis during macroconidia development. *Microbiology*, 160(Pt 8):1618–1627.

Fujikawa, T., Kuga, Y., Yano, S., Yoshimi, A., Tachiki, T., Abe, K., and Nishimura, M. (2009). Dynamics of cell wall components of *Magnaporthe grisea* during infectious structure development. *Molecular Microbiology*, 73(4):553–570.

Fujikawa, T., Sakaguchi, A., Nishizawa, Y., Kouzai, Y., Minami, E., Yano, S., Koga, H., Meshi, T., and Nishimura, M. (2012). Surface α-1, 3-glucan facilitates fungal stealth infection by interfering with innate immunity in plants. *PLoS Pathogens*, 8(8):e1002882.

Fujiwara, M., Ichinomiya, M., Motoyama, T., Horiuchi, H., Ohta, A., and Takagi, M. (2000). Evidence that the *Aspergillus nidulans* class i and class ii chitin synthase genes, *chsC* and *chsA*, share critical roles in hyphal wall integrity and conidiophore development. *Journal of Biochemistry*, 127(3):359–366.

Fukamizo, T., Ohkawa, T., Ikeda, Y., and Goto, S. (1994). Specificity of chitosanase from *Bacillus pumilus*. *Biochimica et Biophysica Acta (BBA)-Protein Structure and Molecular Enzymology*, 1205(2):183–188.

Gachomo, E. W., Seufferheld, M. J., and Kotchoni, S. O. (2010). Melanization of appressoria is critical for the pathogenicity of *Diplocarpon rosae*. *Molecular Biology Reports*, 37(7):3583–3591.

Gastebois, A., Aimanianda, V., Bachellier-Bassi, S., Nesseir, A., Firon, A., Beauvais, A., Schmitt, C., England, P., Beau, R., Prévost, M.-C., et al. (2013). SUN proteins belong to a novel family of β-(1, 3)-glucan-modifying enzymes involved in fungal morphogenesis. *Journal of Biological Chemistry*, 288(19):13387–13396.

Gastebois, A., Fontaine, T., Latgé, J.-P., and Mouyna, I. (2010a). β (1-3) glucanosyltransferase Gel4p is essential for *Aspergillus fumigatus*. *Eukaryotic Cell*, 9(8):1294–1298.

Gastebois, A., Mouyna, I., Simenel, C., Clavaud, C., Coddeville, B., Delepierre, M., Latgé, J.-P., and Fontaine, T. (2010b). Characterization of a new β (1–3)-glucan branching activity of *Aspergillus fumigatus*. *Journal of Biological Chemistry*, 285(4):2386–2396.

Gaughran, J. P., Lai, M. H., Kirsch, D. R., and Silverman, S. J. (1994). Nikkomycin Z is a specific inhibitor of *Saccharomyces cerevisiae* chitin synthase isozyme Chs3 in vitro and in vivo. *Journal of Bacteriology*, 176(18):5857–5860.

Gilbert, N. M., Baker, L. G., Specht, C. A., and Lodge, J. K. (2012). A glycosylphosphatidylinositol anchor is required for membrane localization but dispensable for cell wall association of chitin deacetylase 2 in *Cryptococcus neoformans*. *mBio*, 3(1):e00007–12.

Giraldo, M. C., Dagdas, Y. F., Gupta, Y. K., Mentlak, T. A., Yi, M., Martinez-Rocha, A. L., Saitoh, H., Terauchi, R., Talbot, N. J., and Valent, B. (2013). Two distinct secretion systems facilitate tissue invasion by the rice blast fungus *Magnaporthe oryzae*. *Nature Communications*, 4.

Godwin, J., Anthony, V., Clough, J., and Godfrey, C. (1992). A. 1992. icia 5504: A novel, broad spectrum, systemic b-methoxyacrylate fungicide. In *Proceedings of the British Crop Protection Conference on Pests and Diseases*, volume 10, pages 435–442.

Gueddari, N., U., R., Moerschbacher, B., and Deising, H. (2002). Developmentally regulated conversion of surface-exposed chitin to chitosan in cell walls of plant pathogenic fungi. *New Phytologist*, 156(1):103–112.

Guillén, D., Sánchez, S., and Rodríguez-Sanoja, R. (2010). Carbohydrate-binding domains: multiplicity of biological roles. *Applied Microbiology and Biotechnology*, 85(5):1241–1249.

Ha, Y.-s., Covert, S. F., and Momany, M. (2006). Fsfks1, the 1, 3-β-glucan synthase from the caspofungin-resistant fungus *Fusarium solani*. *Eukaryotic Cell*, 5(7):1036–1042.

Hamer, J. E., Howard, R. J., Chumley, F. G., Valent, B., et al. (1988). A mechanism for surface attachment in spores of a plant pathogenic fungus. *Science*, 239(4837):288–290.

Harapanahalli, A. K., Chen, Y., Li, J., Busscher, H. J., and van der Mei, H. C. (2015). Influence of adhesion force on *icaA* and *cidA* gene expression and production of matrix components in *Staphylococcus aureus* biofilms. *Applied and Environmental Microbiology*, 81(10):3369–3378.

Hartl, L., Gastebois, A., Aimanianda, V., and Latgé, J.-P. (2011). Characterization of the GPI-anchored endo β-1, 3-glucanase eng2 of *Aspergillus fumigatus*. *Fungal Genetics and Biology*, 48(2):185–191.

Hartl, L., Zach, S., and Seidl-Seiboth, V. (2012). Fungal chitinases: diversity, mechanistic properties and biotechnological potential. *Applied Microbiology and Biotechnology*, 93(2):533–543.

Hartland, R., Emerson, G., and Sullivan, P. (1991). A secreted beta-glucan-branching enzyme from *Candida albicans*. *Proceedings of the Royal Society of London B: Biological Sciences*, 246(1316):155–160.

Hayafune, M., Berisio, R., Marchetti, R., Silipo, A., Kayama, M., Desaki, Y., Arima, S., Squeglia, F., Ruggiero, A., Tokuyasu, K., et al. (2014). Chitin-induced activation of immune signaling by the rice receptor CEBiP relies on a unique sandwich-type dimerization. *Proceedings of the National Academy of Sciences*, 111(3):E404–E413.

Hayakawa, Y., Ishikawa, E., Shoji, J.-y., Nakano, H., and Kitamoto, K. (2011). Septum-directed secretion in the filamentous fungus *Aspergillus oryzae*. *Molecular Microbiology*, 81(1):40–55.

Hector, R., Zimmer, B., and Pappagianis, D. (1990). Evaluation of nikkomycins X and Z in murine models of coccidioidomycosis, histoplasmosis, and blastomycosis. *Antimicrobial Agents and Chemotherapy*, 34(4):587–593.

Hekmat, O., Tokuyasu, K., and Withers, S. (2003). Subsite structure of the endo-type chitin deacetylase from a deuteromycete, *Colletotrichum lindemuthianum*: an investigation using steady-state kinetic analysis and ms. *Biochemical Journal*, 374:369–380.

Henry, C., Latgé, J.-P., and Beauvais, A. (2012). α1, 3 glucans are dispensable in *Aspergillus fumigatus*. *Eukaryotic Cell*, 11(1):26–29.

Herth, W. (1980). Calcofluor white and Congo red inhibit chitin microfibril assembly of *Poterioochromonas*: evidence for a gap between polymerization and microfibril formation. *The Journal of Cell Biology*, 87(2):442–450.

Hochstenbach, F., Klis, F. M., Van Den Ende, H., Van Donselaar, E., Peters, P. J., and Klausner, R. D. (1998). Identification of a putative alpha-glucan synthase essential for cell wall construction and morphogenesis in fission yeast. *Proceedings of the National Academy of Sciences*, 95(16):9161–9166.

Hoell, I. A., Vaaje-Kolstad, G., and Eijsink, V. G. (2010). Structure and function of enzymes acting on chitin and chitosan. *Biotechnology and Genetic Engineering Reviews*, 27(1):331–366.

Horiuchi, H., Fujiwara, M., Yamashita, S., Ohta, A., and Takagi, M. (1999). Proliferation of intrahyphal hyphae caused by disruption of *CSMA*, which encodes a class V chitin synthase with a myosin motor-like domain in *Aspergillus nidulans*. *Journal of Bacteriology*, 181(12):3721–3729.

Howard, R. J., Ferrari, M. A., Roach, D. H., and Money, N. P. (1991). Penetration of hard substrates by a fungus employing enormous turgor pressures. *Proceedings of the National Academy of Sciences*, 88(24):11281–11284.

Irie, T., Matsumura, H., Terauchi, R., and Saitoh, H. (2003). Serial analysis of gene expression (SAGE) of *Magnaporthe grisea*: genes involved in appressorium formation. *Molecular Genetics and Genomics*, 270(2):181–189.

Iwai, T., Seo, S., Mitsuhara, I., and Ohashi, Y. (2007). Probenazole-induced accumulation of salicylic acid confers resistance to *Magnaporthe grisea* in adult rice plants. *Plant and Cell Physiology*, 48(7):915–924.

Jang, M.-K., Kong, B.-G., Jeong, Y.-I., Lee, C. H., and Nah, J.-W. (2004). Physicochemical characterization of α-chitin, β-chitin, and γ-chitin separated from natural resources. *Journal of Polymer Science Part A: Polymer Chemistry*, 42(14):3423–3432.

Janulczyk, R., Masignani, V., Maione, D., Tettelin, H., Grandi, G., and Telford, J. L. (2010). Simple sequence repeats and genome plasticity in *Streptococcus agalactiae*. *Journal of Bacteriology*, 192(15):3990–4000.

Jaques, A. K., Fukamizo, T., Hall, D., Barton, R. C., Escott, G. M., Parkinson, T., Hitchcock, C. A., and Adams, D. J. (2003). Disruption of the gene encoding the ChiB1 chitinase of *Aspergillus fumigatus* and characterization of a recombinant gene product. *Microbiology*, 149(10):2931–2939.

Kalebina, T. S., Farkaš, V., Laurinavichiute, D. K., Gorlovoy, P. M., Fominov, G. V., Bartek, P., and Kulaev, I. S. (2003). Deletion of *BGL2* results in an increased chitin level in the cell wall of *Saccharomyces cerevisiae*. *Antonie Van Leeuwenhoek*, 84(3):179–184.

Kamakura, T., Yamaguchi, S., Saitoh, K.-i., Teraoka, T., and Yamaguchi, I. (2002). A novel gene, *CBP1*, encoding a putative extracellular chitin-binding protein, may play an important role in the hydrophobic surface sensing of *Magnaporthe grisea* during appressorium differentiation. *Molecular Plant-Microbe Interactions*, 15(5):437–444.

Kamerewerd, J., Zadra, I., Kürnsteiner, H., and Kück, U. (2011). *PcchiB1*, encoding a class V chitinase, is affected by *PcVelA* and *PcLaeA*, and is responsible for cell wall integrity in *Penicillium chrysogenum*. *Microbiology*, 157(11):3036–3048.

Kankanala, P., Czymmek, K., and Valent, B. (2007). Roles for rice membrane dynamics and plasmodesmata during biotrophic invasion by the blast fungus. *The Plant Cell*, 19(2):706–724.

Kapteyn, J. C., Montijin, R. C., Vink, E., de la Cruz, J., Llobell, A., Douwes, J. E., Shimoi, H., Lipke, P. N., and Klis, F. M. (1996). Retention of *Saccharomyces cerevisiae* cell wall proteins through a phosphodiester-linked β-1, 3-/β-l, 6-glucan heteropolymer. *Glycobiology*, 6(3):337–345.

Kershaw, M. J., Wakley, G., and Talbot, N. J. (1998). Complementation of the mpg1 mutant phenotype in *Magnaporthe grisea* reveals functional relationships between fungal hydrophobins. *The EMBO Journal*, 17(14):3838–3849.

Khang, C. H., Berruyer, R., Giraldo, M. C., Kankanala, P., Park, S.-Y., Czymmek, K., Kang, S., and Valent, B. (2010). Translocation of *Magnaporthe oryzae* effectors into rice cells and their subsequent cell-to-cell movement. *The Plant Cell*, 22(4):1388–1403.

Klarzynski, O., Plesse, B., Joubert, J.-M., Yvin, J.-C., Kopp, M., Kloareg, B., and Fritig, B. (2000). Linear β-1, 3 glucans are elicitors of defense responses in tobacco. *Plant Physiology*, 124(3):1027–1038.

Klis, F., De Groot, P., and Hellingwerf, K. (2001). Molecular organization of the cell wall of *Candida albicans*. *Medical Mycology*, 39(1):1–8.

Klis, F. M. (1994). Review: cell wall assembly in yeast. *Yeast*, 10(7):851–869.

Klis, F. M., Mol, P., Hellingwerf, K., and Brul, S. (2002). Dynamics of cell wall structure in *Saccharomyces cerevisiae*. *FEMS Microbiology Reviews*, 26(3):239–256.

Kobayashi, O., Hayashi, N., Kuroki, R., and Sone, H. (1998). Region of Flo1 proteins responsible for sugar recognition. *Journal of Bacteriology*, 180(24):6503–6510.

Kodama, O., Yamada, H., and Akatsuka, T. (1979). Kitazin p, inhibitor of phosphatidylcholine biosynthesis in *Pyricularia oryzae*. *Agricultural and Biological Chemistry*, 43(8):1719–1725.

Kollár, R., Reinhold, B. B., Petráková, E., Yeh, H. J., Ashwell, G., Drgonová, J., Kapteyn, J. C., Klis, F. M., and Cabib, E. (1997). Architecture of the yeast cell wall β (1 6)-glucan interconnects mannoprotein, β (1 3)-glucan, and chitin. *Journal of Biological Chemistry*, 272(28):17762–17775.

Kong, L.-A., Yang, J., Li, G.-T., Qi, L.-L., Zhang, Y.-J., Wang, C.-F., Zhao, W.-S., Xu, J.-R., and Peng, Y.-L. (2012). Different chitin synthase genes are required for various developmental and plant infection processes in the rice blast fungus *Magnaporthe oryzae*. *PLoS Pathogens*, 8(2):e1002526.

Kouzai, Y., Mochizuki, S., Saito, A., Ando, A., Minami, E., and Nishizawa, Y. (2012). Expression of a bacterial chitosanase in rice plants improves disease resistance to the rice blast fungus *Magnaporthe oryzae*. *Plant Cell Reports*, 31(4):629–636.

Krainer, E., Stark, R. E., Naider, F., Alagramam, K., and Becker, J. M. (1994). Direct observation of cell wall glucans in whole cells of *Saccharomyces cerevisiae* by magic-angle spinning 13c-nmr. *Biopolymers*, 34(12):1627–1635.

Kullnig, C., Mach, R. L., Lorito, M., and Kubicek, C. P. (2000). Enzyme diffusion from *Trichoderma atroviride (= T. harzianum P1)* to *Rhizoctonia solani* is a prerequisite for triggering of *Trichoderma ech42* gene expression before mycoparasitic contact. *Applied and Environmental Microbiology*, 66(5):2232–2234.

Kumamoto, C. A. (2008). Molecular mechanisms of mechanosensing and their roles in fungal contact sensing. *Nature Reviews Microbiology*, 6(9):667–673.

Kurahashi, Y., Sakawa, S., and Kinbara, T. (1997). Biological activity of carpropamid (ktu 3616). *Journal of Pesticide Science*, 22(2):108–112.

Kuranda, K., Leberre, V., Sokol, S., Palamarczyk, G., and François, J. (2006). Investigating the caffeine effects in the yeast *Saccharomyces cerevisiae* brings new insights into the connection between TOR, PKC and Ras/cAMP signalling pathways. *Molecular Microbiology*, 61(5):1147–1166.

Kuranda, M. J. and Robbins, P. W. (1991). Chitinase is required for cell separation during growth of *Saccharomyces cerevisiae*. *Journal of Biological Chemistry*, 266(29):19758–19767.

Kwan, A., Winefield, R., Sunde, M., Matthews, J., Haverkamp, R., Templeton, M., and Mackay, J. (2006). Structural basis for rodlet assembly in fungal hydrophobins. *Proceedings of the National Academy of Sciences of the United States of America*, 103(10):3621–3626.

Lagorce, A., Hauser, N. C., Labourdette, D., Rodriguez, C., Martin-Yken, H., Arroyo, J., Hoheisel, J. D., and François, J. (2003). Genome-wide analysis of the response to cell wall mutations in the yeast *Saccharomyces cerevisiae*. *Journal of Biological Chemistry*, 278(22):20345–20357.

Langner, T., Öztürk, M., Hartmann, S., Cord-Landwehr, S., Moerschbacher, B., Walton, J. D., and Göhre, V. (2015). Chitinases are essential for cell separation in *Ustilago maydis*. *Eukaryotic Cell*, pages EC–00022.

Lanver, D., Berndt, P., Tollot, M., Naik, V., Vranes, M., Warmann, T., Münch, K., Rössel, N., and Kahmann, R. (2014). Plant surface cues prime *Ustilago maydis* for biotrophic development. *Plos Pathogens*, 10(7).

Lanver, D., Mendoza-Mendoza, A., Brachmann, A., and Kahmann, R. (2010). Sho1 and Msb2-related proteins regulate appressorium development in the smut fungus *Ustilago maydis*. *The Plant Cell*, 22(6):2085–2101.

Lee, R. (2011). The outlook for population growth. *Science*, 333(6042):569–573.

Lee, Y.-H. and Dean, R. A. (1993). cAMP regulates infection structure formation in the plant pathogenic fungus *Magnaporthe grisea*. *The Plant Cell*, 5(6):693–700.

Lee, Y.-H. and Dean, R. A. (1994). Hydrophobicity of contact surface induces appressorium formation in *Magnaporthe grisea*. *FEMS Microbiology Letters*, 115(1):71–75.

Lenardon, M. D., Munro, C. A., and Gow, N. A. (2010). Chitin synthesis and fungal pathogenesis. *Current Opinion in Microbiology*, 13(4):416–423.

Lenardon, M. D., Whitton, R. K., Munro, C. A., Marshall, D., and Gow, N. A. (2007). Individual chitin synthase enzymes synthesize microfibrils of differing structure at specific locations in the *Candida albicans* cell wall. *Molecular Microbiology*, 66(5):1164–1173.

Leroch, M., Kleber, A., Silva, E., Coenen, T., Koppenhöfer, D., Shmaryahu, A., Valenzuela, P. D., and Hahn, M. (2013). Transcriptome profiling of *Botrytis cinerea* conidial germination reveals upregulation of infection-related genes during the prepenetration stage. *Eukaryotic Cell*, 12(4):614–626.

Leroch, M., Mueller, N., Hinsenkamp, I., and Hahn, M. (2015). The signalling mucin Msb2 regulates surface sensing and host penetration via BMP1 map kinase signalling in *Botrytis cinerea*. *Molecular Plant Pathology*.

Leroux, P. (2003). Mode of action of agrochemicals towards plant pathogens. *Plant Biology and Pathology*, 326(1):9–21.

Lesage, G. and Bussey, H. (2006). Cell wall assembly in *Saccharomyces cerevisiae*. *Microbiology and Molecular Biology Reviews*, 70(2):317–343.

Leuthner, B., Aichinger, C., Oehmen, E., Koopmann, E., Müller, O., Müller, P., Kahmann, R., Bölker, M., and Schreier, P. (2005). A H_2O_2-producing glyoxal oxidase is required for filamentous growth and pathogenicity in *Ustilago maydis*. *Molecular Genetics and Genomics*, 272(6):639–650.

Levdansky, E., Kashi, O., Sharon, H., Shadkchan, Y., and Osherov, N. (2010). The *Aspergillus fumigatus cspA* gene encoding a repeat-rich cell wall protein is important for normal conidial cell wall architecture and interaction with host cells. *Eukaryotic Cell*, 9(9):1403–1415.

Levin, D. E. (2011). Regulation of cell wall biogenesis in *Saccharomyces cerevisiae*: the cell wall integrity signaling pathway. *Genetics*, 189(4):1145–1175.

Li, G., Zhou, X., and Xu, J.-R. (2012). Genetic control of infection-related development in *Magnaporthe oryzae*. *Current Opinion in Microbiology*, 15(6):678–684.

Lickfeld, M. and Schmitz, H.-P. (2012). A network involving Rho-type GTPases, a paxillin and a formin homologue regulates spore length and spore wall integrity in the filamentous fungus *Ashbya gossypii*. *Molecular Microbiology*, 85(3):574–593.

Lim, H. and Choi, H. T. (2009). Enhanced expression of chitinase during the autolysis of mushroom in *Coprinellus congregatus*. *The Journal of Microbiology*, 47(2):225–228.

Lin, W., Hu, X., Zhang, W., Rogers, W. J., and Cai, W. (2005). Hydrogen peroxide mediates defence responses induced by chitosans of different molecular weights in rice. *Journal of Plant Physiology*, 162(8):937–944.

Lipke, P., Wojciechowicz, D., and Kurjan, J. (1989). Ag alpha 1 is the structural gene for the *Saccharomyces cerevisiae* alpha-agglutinin, a cell surface glycoprotein involved in cell-cell interactions during mating. *Molecular and Cellular Biology*, 9(8):3155–3165.

Liu, H., Zhang, B., Li, C., and Bao, X. (2010). Knock down of chitosanase expression in phytopathogenic fungus *Fusarium solani* and its effect on pathogenicity. *Current Genetics*, 56(3):275–281.

Liu, W., Liu, J., Ning, Y., Ding, B., Wang, X., Wang, Z., and Wang, G.-L. (2013). Recent progress in understanding PAMP-and effector-triggered immunity against the rice blast fungus *Magnaporthe oryzae*. *Molecular Plant*, 6(3):605–620.

Liu, W., Zhou, X., Li, G., Li, L., Kong, L., Wang, C., Zhang, H., and Xu, J.-R. (2011). Multiple plant surface signals are sensed by different mechanisms in the rice blast fungus for appressorium formation. *PLoS Pathogens*, 7(1):e1001261–e1001261.

Lowman, D. W., Greene, R. R., Bearden, D. W., Kruppa, M. D., Pottier, M., Monteiro, M. A., Soldatov, D. V., Ensley, H. E., Cheng, S.-C., Netea, M. G., et al. (2014). Novel structural features in *Candida albicans* hyphal glucan provide a basis for differential innate immune recognition of hyphae versus yeast. *Journal of Biological Chemistry*, 289(6):3432–3443.

Maddi, A., Dettman, A., Fu, C., Seiler, S., and Free, S. J. (2012). WSC-1 and HAM-7 are MAK-1 MAP kinase pathway sensors required for cell wall integrity and hyphal fusion in *Neurospora crassa*. *PLoS One*, 7(8):e42374.

Maddi, A. and Free, S. J. (2010). α-1, 6-mannosylation of n-linked oligosaccharide present on cell wall proteins is required for their incorporation into the cell wall in the filamentous fungus *Neurospora crassa*. *Eukaryotic Cell*, 9(11):1766–1775.

Manners, D. J., Masson, A. J., and Patterson, J. C. (1973a). The structure of a beta-(1-¿ 3)-d-glucan from yeast cell walls. *Biochemical Journal*, 135:19–30.

Manners, D. J., Masson, A. J., and Patterson, J. C. (1973b). The structure of a beta-(1-¿ 6)-d-glucan from yeast cell walls. *Biochemical Journal*, 135:31–36.

Marroquin-Guzman, M. and Wilson, R. A. (2015). GATA-dependent glutaminolysis drives appressorium formation in *Magnaporthe oryzae* by suppressing TOR inhibition of cAMP/PKA signaling. *Plos Pathogens*, 11.

Martín-Urdíroz, M., Roncero, M. I. G., González-Reyes, J. A., and Ruiz-Roldán, C. (2008). Chsvb, a class VII chitin synthase involved in septation, is critical for pathogenicity in *Fusarium oxysporum*. *Eukaryotic Cell*, 7(1):112–121.

Matsuo, Y., Tanaka, K., Matsuda, H., and Kawamukai, M. (2005). cda1+, encoding chitin deacetylase is required for proper spore formation in *Schizosaccharomyces pombe*. *FEBS Letters*, 579(12):2737–2743.

Maubon, D., Park, S., Tanguy, M., Huerre, M., Schmitt, C., Prevost, M., Perlin, D., Latge, J., and Beauvais, A. (2006). *AGS3*, an α (1–3) glucan synthase gene family member of *Aspergillus fumigatus*, modulates mycelium growth in the lung of experimentally infected mice. *Fungal Genetics and Biology*, 43(5):366–375.

Mélida, H., Sain, D., Stajich, J. E., and Bulone, V. (2015). Deciphering the uniqueness of Mucoromycotina cell walls by combining biochemical and phylogenomic approaches. *Environmental Microbiology*, 17(5):1649–1662.

Mendoza-Mendoza, A., Berndt, P., Djamei, A., Weise, C., Linne, U., Marahiel, M., Vraneš, M., Kämper, J., and Kahmann, R. (2009). Physical-chemical plant-derived signals induce differentiation in *Ustilago maydis*. *Molecular Microbiology*, 71(4):895–911.

Mentlak, T. A., Kombrink, A., Shinya, T., Ryder, L. S., Otomo, I., Saitoh, H., Terauchi, R., Nishizawa, Y., Shibuya, N., Thomma, B. P., et al. (2012). Effector-mediated suppression of chitin-triggered immunity by *Magnaporthe oryzae* is necessary for rice blast disease. *The Plant Cell*, 24(1):322–335.

Minke, R. and Blackwell, J. (1978). The structure of α-chitin. *Journal of Molecular Biology*, 120(2):167–181.

Mishra, C., Semino, C. E., McCreath, K. J., De La Vega, H., Jones, B. J., Specht, C. A., and Robbins, P. W. (1997). Cloning and expression of two chitin deacetylase genes of *Saccharomyces cerevisiae*. *Yeast*, 13(4):327–336.

Mitchell, T. K. and Dean, R. A. (1995). The camp-dependent protein kinase catalytic subunit is required for appressorium formation and pathogenesis by the rice blast pathogen *Magnaporthe grisea*. *The Plant Cell*, 7(11):1869–1878.

Mochizuki, S., Saitoh, K.-i., Minami, E., and Nishizawa, Y. (2011). Localization of probe-accessible chitin and characterization of genes encoding chitin-binding domains during rice–*Magnaporthe oryzae* interactions. *Journal of General Plant Pathology*, 77(3):163–173.

Mouyna, I., Fontaine, T., Vai, M., Monod, M., Fonzi, W. A., Diaquin, M., Popolo, L., Hartland, R. P., and Latgé, J.-P. (2000). Glycosylphosphatidylinositol-anchored glucanosyltransferases play an active role in the biosynthesis of the fungal cell wall. *Journal of Biological Chemistry*, 275(20):14882–14889.

Mouyna, I., Henry, C., Doering, T. L., and Latgé, J.-P. (2004). Gene silencing with RNA interference in the human pathogenic fungus *Aspergillus fumigatus*. *FEMS Microbiology Letters*, 237(2):317–324.

Mouyna, I., Morelle, W., Vai, M., Monod, M., Léchenne, B., Fontaine, T., Beauvais, A., Sarfati, J., Prévost, M.-C., Henry, C., et al. (2005). Deletion of *GEL2* encoding for a β (1–3) glucanosyltransferase affects morphogenesis and virulence in *Aspergillus fumigatus*. *Molecular Microbiology*, 56(6):1675–1688.

Mravec, J., Kračun, S. K., Rydahl, M. G., Westereng, B., Miart, F., Clausen, M. H., Fangel, J. U., Daugaard, M., Van Cutsem, P., Henrik, H., et al. (2014). Tracking developmentally regulated post-synthetic processing of homogalacturonan and chitin using reciprocal oligosaccharide probes. *Development*, 141(24):4841–4850.

Mrša, V. and Tanner, W. (1999). Role of naoh-extractable cell wall proteins Ccw5p, Ccw6p, Ccw7p and Ccw8p (members of the pir protein family) in stability of the *Saccharomyces cerevisiae* cell wall. *Yeast*, 15(10A):813–820.

Munro, C. A., Winter, K., Buchan, A., Henry, K., Becker, J. M., Brown, A. J., Bulawa, C. E., and Gow, N. A. (2001). Chs1 of *Candida albicans* is an essential chitin synthase required for synthesis of the septum and for cell integrity. *Molecular Microbiology*, 39(5):1414–1426.

Muszkieta, L., Aimanianda, V., Mellado, E., Gribaldo, S., Alcàzar-Fuoli, L., Szewczyk, E., Prevost, M.-C., and Latgé, J.-P. (2014). Deciphering the role of the chitin synthase families 1 and 2 in the in vivo and in vitro growth of *Aspergillus fumigatus* by multiple gene targeting deletion. *Cellular Microbiology*, 16(12):1784–1805.

Nakajima, T., Suzuki, C., and Matsuda, K. (1982). Extracellular galactomannan from *Neurospora crassa*. *Agricultural and Biological Chemistry*, 46(4):869–875.

Ngamskulrungroj, P., Price, J., Sorrell, T., Perfect, J. R., and Meyer, W. (2011). *Cryptococcus gattii* virulence composite: candidate genes revealed by microarray analysis of high and less virulent vancouver island outbreak strains. *Plos One*, 6(1).

Nguyen, T., Fleet, G., and Rogers, P. (1998). Composition of the cell walls of several yeast species. *Applied Microbiology and Biotechnology*, 50(2):206–212.

Nishimura, M., Fukada, J., Moriwaki, A., Fujikawa, T., Ohashi, M., Hibi, T., and Hayashi, N. (2009). Mstu1, an APSES transcription factor, is required for appressorium-mediated infection in *Magnaporthe grisea*. *Bioscience, Biotechnology, and Biochemistry*, 73(8):1779–1786.

Odenbach, D., Thines, E., Anke, H., and Foster, A. J. (2009). The *Magnaporthe grisea* class vii chitin synthase is required for normal appressorial development and function. *Molecular Plant Pathology*, 10(1):81–94.

Oliveira-Garcia, E. and Deising, H. B. (2013). Infection structure–specific expression of β-1, 3-glucan synthase is essential for pathogenicity of *Colletotrichum graminicola* and evasion of β-glucan–triggered immunity in maize. *The Plant Cell*, 25(6):2356–2378.

Ou, S. H. (1985). *Rice diseases*. IRRI.

Palma-Guerrero, J., Jansson, H.-B., Salinas, J., and Lopez-Llorca, L. (2008). Effect of chitosan on hyphal growth and spore germination of plant pathogenic and biocontrol fungi. *Journal of Applied Microbiology*, 104(2):541–553.

Paolo, W. F., Dadachova, E., Mandal, P., Casadevall, A., Szaniszlo, P. J., and Nosanchuk, J. D. (2006). Effects of disrupting the polyketide synthase gene *WdPKS1* in *Wangiella [Exophiala] dermatitidis* on melanin production and resistance to killing by antifungal compounds, enzymatic degradation, and extremes in temperature. *BMC Microbiology*, 6(1):55.

Park, J.-N., Han, C. P., Lee, D.-J., Cheon, S. A., and Kang, H. A. (2014). Functional characterization of extracellular chitinase encoded by the ylcts1 gene in a dimorphic yeast *Yarrowia lipolytica*. *Journal of Microbiology*, 52(4):284–291.

Peng, K., Radivojac, P., Vucetic, S., Dunker, A. K., and Obradovic, Z. (2006). Length-dependent prediction of protein intrinsic disorder. *BMC Bioinformatics*, 7(1):208.

Pérez-Nadales, E. and Di Pietro, A. (2011). The membrane mucin Msb2 regulates invasive growth and plant infection in *Fusarium oxysporum*. *The Plant Cell*, 23(3):1171–1185.

Preechasuth, K., Anderson, J. C., Peck, S. C., Brown, A. J., Gow, N. A., and Lenardon, M. D. (2015). Cell wall protection by the textitCandida albicans class I chitin synthases. *Fungal Genetics and Biology*.

Primig, M., Williams, R. M., Winzeler, E. A., Tevzadze, G. G., Conway, A. R., Hwang, S. Y., Davis, R. W., and Esposito, R. E. (2000). The core meiotic transcriptome in budding yeasts. *Nature Genetics*, 26(4):415–423.

Qadota, H., Python, C. P., Inoue, S. B., Arisawa, M., Anraku, Y., Zheng, Y., Watanabe, T., Levin, D. E., and Ohya, Y. (1996). Identification of yeast Rho1p GTPase as a regulatory subunit of 1, 3-β-glucan synthase. *Science*, 272(5259):279–281.

Qaqish, R. and Amiji, M. (1999). Synthesis of a fluorescent chitosan derivative and its application for the study of chitosan–mucin interactions. *Carbohydrate Polymers*, 38(2):99–107.

Ragni, E., Coluccio, A., Rolli, E., Rodriguez-Peña, J. M., Colasante, G., Arroyo, J., Neiman, A. M., and Popolo, L. (2007a). *GAS2* and *GAS4*, a pair of developmentally regulated genes required for spore wall assembly in *Saccharomyces cerevisiae*. *Eukaryotic Cell*, 6(2):302–316.

Ragni, E., Sipiczki, M., and Strahl, S. (2007b). Characterization of Ccw12p, a major key player in cell wall stability of *Saccharomyces cerevisiae*. *Yeast*, 24(4):309–319.

Ram, A., Brekelmans, S., Oehlen, L., and Klis, F. (1995). Identification of two cell cycle regulated genes affecting the β1, 3-glucan content of cell walls in *Saccharomyces cerevisiae*. *FEBS Letters*, 358(2):165–170.

Ram, A. F., Kapteyn, J. C., Montijn, R. C., Caro, L. H. P., Douwes, J. E., Baginsky, W., Mazur, P., van den Ende, H., and Klis, F. M. (1998). Loss of the plasma membrane-bound protein Gas1p in *Saccharomyces cerevisiae* results in the release of β1, 3-glucan into the medium and induces a compensation mechanism to ensure cell wall integrity. *Journal of Bacteriology*, 180(6):1418–1424.

Ramanujam, R., Calvert, M. E., Selvaraj, P., and Naqvi, N. I. (2013). The late endosomal HOPS complex anchors active G-protein signaling essential for pathogenesis in *Magnaporthe oryzae*. *PLoS Pathogens*, 9(8):e1003527.

Rappleye, C. A., Eissenberg, L. G., and Goldman, W. E. (2007). *Histoplasma capsulatum* α-(1, 3)-glucan blocks innate immune recognition by the β-glucan receptor. *Proceedings of the National Academy of Sciences*, 104(4):1366–1370.

Rappleye, C. A., Engle, J. T., and Goldman, W. E. (2004). RNA interference in *Histoplasma capsulatum* demonstrates a role for α-(1, 3)-glucan in virulence. *Molecular Microbiology*, 53(1):153–165.

Riquelme, M. and Bartnicki-García, S. (2008). Advances in understanding hyphal morphogenesis: ontogeny, phylogeny and cellular localization of chitin synthases. *Fungal Biology Reviews*, 22(2):56–70.

Rodríguez-Martín, A., Acosta, R., Liddell, S., Núñez, F., Benito, M. J., and Asensio, M. A. (2010). Characterization of the novel antifungal chitosanase PgChP and the encoding gene from *Penicillium chrysogenum*. *Applied Microbiology and Biotechnology*, 88(2):519–528.

Rodríguez-Peña, J. M., Cid, V. J., Arroyo, J., and Nombela, C. (2000). A novel family of cell wall-related proteins regulated differently during the yeast life cycle. *Molecular and Cellular Biology*, 20(9):3245–3255.

Romero, P., Obradovic, Z., Li, X., Garner, E. C., Brown, C. J., and Dunker, A. K. (2001). Sequence complexity of disordered protein. *Proteins: Structure, Function, and Bioinformatics*, 42(1):38–48.

Ruiz-Herrera, J. and Ortiz-Castellanos, L. (2010). Analysis of the phylogenetic relationships and evolution of the cell walls from yeasts and fungi. *FEMS Yeast Research*, 10(3):225–243.

Ruiz-Herrera, J. and San-Blas, G. (2003). Chitin synthesis as a target for antifungal drugs. *Current Drug Targets-Infectious Disorders*, 3(1):77–91.

Saitoh, H., Fujisawa, S., Mitsuoka, C., Ito, A., Hirabuchi, A., Ikeda, K., Irieda, H., Yoshino, K., Yoshida, K., Matsumura, H., et al. (2012). Large-scale gene disruption in *Magnaporthe oryzae* identifies MC69, a secreted protein required for infection by monocot and dicot fungal pathogens. *Plos Pathogens*, 8(5).

Salas, S., Bennett, J., Kwon-Chung, K., Perfect, J., and Williamson, P. (1996). Effect of the laccase gene *CNLAC1*, on virulence of *Cryptococcus neoformans*. *The Journal of Experimental Medicine*, 184(2):377–386.

Samalova, M., Meyer, A. J., Gurr, S. J., and Fricker, M. D. (2014). Robust anti-oxidant defences in the rice blast fungus *Magnaporthe oryzae* confer tolerance to the host oxidative burst. *New Phytologist*, 201(2):556–573.

Samar, D., Kieler, J. B., and Klutts, J. S. (2015). Identification and deletion of Tft1, a predicted glycosyltransferase necessary for cell wall β-1, 3; 1, 4-glucan synthesis in aspergillus fumigatus. *PloS One*, 10(2):e0117336.

Sambrook, J. and Russell, D. (2005). Southern blotting: capillary transfer of DNA to membranes. *CSH protocols*, 2006(1):40–50.

Sanchatjate, S. and Schekman, R. (2006). Chs5/6 complex: a multiprotein complex that interacts with and conveys chitin synthase iii from the trans-Golgi network to the cell surface. *Molecular Biology of the Cell*, 17(10):4157–4166.

Sánchez-León, E. and Riquelme, M. (2015). Live imaging of β-1, 3-glucan synthase Fks-1 in *Neurospora crassa* hyphae. *Fungal Genetics and Biology*.

Santi, I., Scarselli, M., Mariani, M., Pezzicoli, A., Masignani, V., Taddei, A., Grandi, G., Telford, J. L., and Soriani, M. (2007). BibA: a novel immunogenic bacterial adhesin contributing to group B *Streptococcus* survival in human blood. *Molecular Microbiology*, 63(3):754–767.

Santos, B. and Snyder, M. (1997). Targeting of chitin synthase 3 to polarized growth sites in yeast requires Chs5p and Myo2p. *The Journal of Cell Biology*, 136(1):95–110.

Saravolatz, L. D., Deresinski, S. C., and Stevens, D. A. (2003). Caspofungin. *Clinical Infectious Diseases*, 36(11):1445–1457.

Sarthy, A. V., McGonigal, T., Coen, M., Frost, D. J., Meulbroek, J. A., and Goldman, R. C. (1997). Phenotype in *Candida albicans* of a disruption of the *BGL2* gene encoding a 1, 3-β-glucosyltransferase. *Microbiology*, 143(2):367–376.

Schoffelmeer, E. A., Klis, F. M., Sietsma, J., and Cornelissen, B. J. (1999). The cell wall of *Fusarium oxysporum*. *Fungal Genetics and Biology*, 27(2):275–282.

Scholtmeijer, K., de Vocht, M. L., Rink, R., Robillard, G. T., and Wösten, H. A. (2009). Assembly of the fungal SC3 hydrophobin into functional amyloid fibrils depends on its concentration and is promoted by cell wall polysaccharides. *Journal of Biological Chemistry*, 284(39):26309–26314.

Schubert, M., Agdour, S., Fischer, R., Olbrich, Y., Schinkel, H., and Schillberg, S. (2010). A Monoclonal antibody that specifically binds chitosan *in vitro* and *in situ* on Fungal cell walls. *Journal of Microbiology and Biotechnology*, 20(8):1179–1184.

Sekiya-Kawasaki, M., Abe, M., Saka, A., Watanabe, D., Kono, K., Minemura-Asakawa, M., Ishihara, S., Watanabe, T., and Ohya, Y. (2002). Dissection of upstream regulatory components of the Rho1p effector, 1, 3-β-glucan synthase, in *Saccharomyces cerevisiae*. *Genetics*, 162(2):663–676.

Selvaggini, S., Munro, C. A., Paschoud, S., Sanglard, D., and Gow, N. A. (2004). Independent regulation of chitin synthase and chitinase activity in *Candida albicans* and *Saccharomyces cerevisiae*. *Microbiology*, 150(4):921–928.

Sesma, A. and Osbourn, A. E. (2004). The rice leaf blast pathogen undergoes developmental processes typical of root-infecting fungi. *Nature*, 431(7008):582–586.

Shahinian, S. and Bussey, H. (2000). β-1, 6-glucan synthesis in *Saccharomyces cerevisiae*. *Molecular Microbiology*, 35(3):477–489.

Shaw, J. A., Mol, P. C., Bowers, B., Silverman, S. J., Valdivieso, M. H., Durán, A., and Cabib, E. (1991). The function of chitin synthases 2 and 3 in the *Saccharomyces cerevisiae* cell cycle. *The Journal of Cell Biology*, 114(1):111–123.

Shimizu, T., Nakano, T., Takamizawa, D., Desaki, Y., Ishii-Minami, N., Nishizawa, Y., Minami, E., Okada, K., Yamane, H., Kaku, H., et al. (2010). Two lysm receptor molecules, CEBiP and OsCERK1, cooperatively regulate chitin elicitor signaling in rice. *The Plant Journal*, 64(2):204–214.

Shin, K.-S., Kwon, N.-J., Kim, Y. H., Park, H.-S., Kwon, G.-S., and Yu, J.-H. (2009). Differential roles of the ChiB chitinase in autolysis and cell death of *Aspergillus nidulans*. *Eukaryotic Cell*, 8(5):738–746.

Sievers, F., Wilm, A., Dineen, D., Gibson, T. J., Karplus, K., Li, W., Lopez, R., McWilliam, H., Remmert, M., Söding, J., et al. (2011). Fast, scalable generation of high-quality protein multiple sequence alignments using Clustal Omega. *Molecular Systems Biology*, 7(1):539.

Skamnioti, P. and Gurr, S. J. (2009). Against the grain: safeguarding rice from rice blast disease. *Trends in Biotechnology*, 27(3):141–150.

Soanes, D., Chakrabarti, A., Paszkiewicz, K., Dawe, A., and Talbot, N. (2012). Genome-wide transcriptional profiling of appressorium development by the Rice Blast fungus *Magnaporthe oryzae*. *Plos Pathogens*, 8(2).

Soulié, M.-C., Perino, C., Piffeteau, A., Choquer, M., Malfatti, P., Cimerman, A., Kunz, C., Boccara, M., and Vidal-Cros, A. (2006). *Botrytis cinerea* virulence is drastically reduced after disruption of chitin synthase class iii gene (Bc*CHS3A*). *Cellular Microbiology*, 8(8):1310–1321.

Soulié, M.-C., Piffeteau, A., Choquer, M., Boccara, M., and Vidal-Cros, A. (2003). Disruption of *Botrytis cinerea* class i chitin synthase gene Bc*CHS1* results in cell wall weakening and reduced virulence. *Fungal Genetics and Biology*, 40(1):38–46.

Stahmann, K.-P., Pielken, P., Schimz, K.-L., and Sahm, H. (1992). Degradation of extracellular β-(1, 3)(1, 6)-d-glucan by *Botrytis cinerea*. *Applied and Environmental Microbiology*, 58(10):3347–3354.

Stringer, M., Dean, R., Sewall, T., and Timberlake, W. (1991). Rodletless, a new *Aspergillus* developmental mutant induced by directed gene inactivation. *Genes & Development*, 5(7):1161–1171.

Suda, Y., Rodriguez, R. K., Coluccio, A. E., and Neiman, A. M. (2009). A screen for spore wall permeability mutants identifies a secreted protease required for proper spore wall assembly. *PLoS One*, 4(9):e7184.

Sugita, A., Sugii, A., Sato, K., Zhang, X.-Y., Dai, A.-L., Taguchi, G., and Shimosaka, M. (2012). Cloning and characterization of a gene coding for a major extracellular chitosanase from the koji mold *Aspergillus oryzae*. *Bioscience, Biotechnology, and Biochemistry*, 76(1):193–195.

Sunde, M., Kwan, A. H., Templeton, M. D., Beever, R. E., and Mackay, J. P. (2008). Structural analysis of hydrophobins. *Micron*, 39(7):773–784.

Szilágyi, M., Kwon, N.-J., Dorogi, C., Pócsi, I., Yu, J.-H., and Emri, T. (2010). The extracellular β-1, 3-endoglucanase EngA is involved in autolysis of *Aspergillus nidulans*. *Journal of Applied Microbiology*, 109(5):1498–1508.

Takeshita, N., Yamashita, S., Ohta, A., and Horiuchi, H. (2006). *Aspergillus nidulans* class V and VI chitin synthases CsmA and CsmB, each with a myosin motor-like domain, perform compensatory functions that are essential for hyphal tip growth. *Molecular Microbiology*, 59(5):1380–1394.

Talbot, N. J., Ebbole, D. J., and Hamer, J. E. (1993). Identification and characterization of *MPG1*, a gene involved in pathogenicity from the rice blast fungus *Magnaporthe grisea*. *The Plant Cell*, 5(11):1575–1590.

Talbot, N. J., Kershaw, M. J., Wakley, G. E., De Vries, O. M., Wessels, J. G., and Hamer, J. E. (1996). *MPG1* encodes a fungal hydrophobin involved in surface interactions during infection-related development of *Magnaporthe grisea*. *The Plant Cell*, 8(6):985–999.

Thadathil, N. and Velappan, S. P. (2014). Recent developments in chitosanase research and its biotechnological applications: A review. *Food Chemistry*, 150:392–399.

Thines, E., Weber, R. W., and Talbot, N. J. (2000). MAP kinase and protein kinase a–dependent mobilization of triacylglycerol and glycogen during appressorium turgor generation by *Magnaporthe grisea*. *The Plant Cell*, 12(9):1703–1718.

Thinlay, X., Finckh, M. R., Bordeos, A. C., and Zeigler, R. S. (2000). Effects and possible causes of an unprecedented rice blast epidemic on the traditional farming system of Bhutan. *Agriculture, Ecosystems & Environment*, 78(3):237–248.

Tokousbalides, M. C. and Sisler, H. (1978). Effect of tricyclazole on growth and secondary metabolism in *Pyricularia oryzae*. *Pesticide Biochemistry and Physiology*, 8(1):26–32.

Tokunaga, M., Kusamichi, M., and Koike, H. (1986). Ultrastructure of outermost layer of cell wall in *Candida albicans* observed by rapid-freezing technique. *Journal of Electron Microscopy*, 35(3):237–246.

Tokuyasu, K., Ono, H., Ohnishi-Kameyama, M., Hayashi, K., and Mori, Y. (1997). Deacetylation of chitin oligosaccharides of dp 2–4 by chitin deacetylase from *Colletotrichum lindemuthianum*. *Carbohydrate Research*, 303(3):353–358.

Treitschke, S., Doehlemann, G., Schuster, M., and Steinberg, G. (2010). The myosin motor domain of fungal chitin synthase V is dispensable for vesicle motility but required for virulence of the maize pathogen *Ustilago maydis*. *The Plant Cell*, 22(7):2476–2494.

Tsigos, I., Zydowicz, N., Martinou, A., Domard, A., and Bouriotis, V. (1999). Mode of action of chitin deacetylase from *Mucor rouxii* on n-acetylchitooligosaccharides. *European Journal of Biochemistry*, 261(3):698–705.

Tucker, S. L., Besi, M. I., Galhano, R., Franceschetti, M., Goetz, S., Lenhert, S., Osbourn, A., and Sesma, A. (2010). Common genetic pathways regulate organ-specific infection-related development in the rice blast fungus. *The Plant Cell*, 22(3):953–972.

Tzelepis, G. D., Melin, P., Jensen, D. F., Stenlid, J., and Karlsson, M. (2012). Functional analysis of glycoside hydrolase family 18 and 20 genes in *Neurospora crassa*. *Fungal Genetics and Biology*, 49(9):717–730.

Tzelepis, G. D., Melin, P., Stenlid, J., Jensen, D. F., and Karlsson, M. (2014). Functional analysis of the C-II subgroup killer toxin-like chitinases in the filamentous ascomycete *Aspergillus nidulans*. *Fungal Genetics and Biology*, 64:58–66.

Uesugi, Y. (2001). Fungal choline biosynthesis-a target for controlling rice blast. *Pesticide Outlook*, 12(1):26–27.

Utsugi, T., Minemura, M., Hirata, A., Abe, M., Watanabe, D., and Ohya, Y. (2002). Movement of yeast 1, 3-β-glucan synthase is essential for uniform cell wall synthesis. *Genes to Cells*, 7(1):1–9.

Valdivia, R. H., Baggott, D., Chuang, J. S., and Schekman, R. W. (2002). The yeast clathrin adaptor protein complex 1 is required for the efficient retention of a subset of late Golgi membrane proteins. *Developmental Cell*, 2(3):283–294.

Valdivia, R. H. and Schekman, R. (2003). The yeasts Rho1p and Pkc1p regulate the transport of chitin synthase iii (Chs3p) from internal stores to the plasma membrane. *Proceedings of the National Academy of Sciences*, 100(18):10287–10292.

van Duin, D., Casadevall, A., and Nosanchuk, J. D. (2002). Melanization of *Cryptococcus neoformans* and *Histoplasma capsulatum* reduces their susceptibilities to amphotericin b and caspofungin. *Antimicrobial Agents and Chemotherapy*, 46(11):3394–3400.

Van Kan, J., Stefanato, F., and Raats, E. (2004). A mysterious, pleiotropic growth defect caused by deletion of a glyoxal oxidase gene in *Botrytis cinerea*. In *Book of Abstracts XIII International Botrytis Symposium, Antalya, Turkey, 25-31 October 2004*, page 97.

van Munster, J. M., Dobruchowska, J. M., Veloo, R., Dijkhuizen, L., and van der Maarel, M. J. (2014). Characterization of the starvation-induced chitinase CfcA and α-1, 3-glucanase AgnB of *Aspergillus niger*. *Applied Microbiology and Biotechnology*, 99(5):2209–2223.

van Munster, J. M., Nitsche, B. M., Krijgsheld, P., van Wijk, A., Dijkhuizen, L., Wösten, H. A., Ram, A. F., and van der Maarel, M. J. (2013). Chitinases CtcB and CfcI modify the cell wall in sporulating aerial mycelium of *Aspergillus niger*. *Microbiology*, 159(9):1853–1867.

van Wetter, M.-A., Schuren, F. H., Schuurs, T. A., and Wessels, J. G. (1996). Targeted mutation of the *SC3* hydrophobin gene of *Schizophyllum commune* affects formation of aerial hyphae. *FEMS Microbiology Letters*, 140(2-3):265–269.

Verdín, J., Bartnicki-Garcia, S., and Riquelme, M. (2009). Functional stratification of the Spitzenkörper of *Neurospora crassa*. *Molecular Microbiology*, 74(5):1044–1053.

Verstrepen, K. J. and Klis, F. M. (2006). Flocculation, adhesion and biofilm formation in yeasts. *Molecular Microbiology*, 60(1):5–15.

Villalba, F., Collemare, J., Landraud, P., Lambou, K., Brozek, V., Cirer, B., Morin, D., Bruel, C., Beffa, R., and Lebrun, M.-H. (2008). Improved gene targeting in *Magnaporthe grisea* by inactivation of *MgKU80* required for non-homologous end joining. *Fungal Genetics and Biology*, 45(1):68–75.

Viterbo, A., Ramot, O., Chernin, L., and Chet, I. (2002). Significance of lytic enzymes from *Trichoderma spp.* in the biocontrol of fungal plant pathogens. *Antonie Van Leeuwenhoek*, 81(1-4):549–556.

Volling, K., Thywissen, A., Brakhage, A. A., and Saluz, H. P. (2011). Phagocytosis of melanized *Aspergillus* conidia by macrophages exerts cytoprotective effects by sustained pi3k/akt signalling. *Cellular Microbiology*, 13(8):1130–1148.

Wang, C. and St Leger, R. J. (2007). The Mad1 adhesin of *Metarhizium anisopliae* links adhesion with blastospore production and virulence to insects, and the mad2 adhesin enables attachment to plants. *Eukaryotic Cell*, 6(5):808–816.

Wang, F., Yang, H., and Wang, Y. (2013). [simultaneous determination of neutral sugars and uronic acid constituents in a novel bacterial polysaccharide using gas chromatography-mass spectrometry]. *Se pu= Chinese Journal of Chromatography/Zhongguo hua xue hui*, 31(1):53–58.

Wang, G., Li, G., Zhang, S., Jiang, C., Qin, J., and Xu, J.-R. (2015). Activation of the signalling mucin MoMsb2 and its functional relationship with Cbp1 in *Magnaporthe oryzae*. *Environmental Microbiology*.

Wang, Z., Soanes, D., Kershaw, M., and Talbot, N. (2007). Functional analysis of lipid metabolism in the rice blast fungus *Magnaporthe grisea* reveals a role for peroxisomal oxidation in appressorium-mediated plant infection. *Molecular Plant–Microbe Interactions*, 20:475–491.

Weber, I., Aßmann, D., Thines, E., and Steinberg, G. (2006). Polar localizing class V myosin chitin synthases are essential during early plant infection in the plant pathogenic fungus *Ustilago maydis*. *The Plant Cell*, 18(1):225–242.

Werner, S., Sugui, J. A., Steinberg, G., and Deising, H. B. (2007). A chitin synthase with a myosin-like motor domain is essential for hyphal growth, appressorium differentiation, and pathogenicity of the maize anthracnose fungus *Colletotrichum graminicola*. *Molecular Plant-Microbe Interactions*, 20(12):1555–1567.

Wheeler, T. and von Braun, J. (2013). Climate change impacts on global food security. *Science*, 341(6145):508–513.

White, S., McIntyre, M., Berry, D. R., and McNeil, B. (2002). The autolysis of industrial filamentous fungi. *Critical Reviews in Biotechnology*, 22(1):1–14.

Wilson, R. A. and Talbot, N. J. (2009). Under pressure: investigating the biology of plant infection by *Magnaporthe oryzae*. *Nature Reviews Microbiology*, 7(3):185–195.

Win, N. and Stevens, W. (2001). Shrimp chitin as substrate for fungal chitin deacetylase. *Applied Microbiology and Biotechnology*, 57(3):334–341.

Woo, P. C., Tam, E. W., Chong, K. T., Cai, J. J., Tung, E. T., Ngan, A. H., Lau, S. K., and Yuen, K.-Y. (2010). High diversity of polyketide synthase genes and the melanin biosynthesis gene cluster in *Penicillium marneffei*. *FEBS Journal*, 277(18):3750–3758.

Wösten, H., Schuren, F., and Wessels, J. (1994). Interfacial self-assembly of a hydrophobin into an amphipathic protein membrane mediates fungal attachment to hydrophobic surfaces. *The EMBO Journal*, 13(24):5848.

Wösten, H. A., van Wetter, M.-A., Lugones, L. G., van der Mei, H. C., Busscher, H. J., and Wessels, J. G. (1999). How a fungus escapes the water to grow into the air. *Current Biology*, 9(2):85–88.

Wu, Y., Xiao, N., Yu, L., Pan, C., Li, Y., Zhang, X., Liu, G., Dai, Z., Pan, X., and Li, A. (2015). Combination patterns of major R genes determine the level of resistance to the *M. oryzae* in rice (oryza sativa l.). *PloS One*, 10(6):e0126130.

Yamaguchi, J., Kuchiki, F., Hirayae, K., and So, K. (2002). Decreased effect of carpropamid for rice blast control in the west north area of saga prefecture in 2001. *Japanese Journal of Phytopathology*, 68:261.

Yamaguchi, T., Yamada, A., Hong, N., Ogawa, T., Ishii, T., and Shibuya, N. (2000). Differences in the recognition of glucan elicitor signals between rice and soybean: β-glucan fragments from the rice blast disease fungus *Pyricularia oryzae* that elicit phytoalexin biosynthesis in suspension-cultured rice cells. *The Plant Cell*, 12(5):817–826.

Yamazaki, H., Tanaka, A., Kaneko, J.-i., Ohta, A., and Horiuchi, H. (2008). *Aspergillus nidulans* ChiA is a glycosylphosphatidylinositol (GPI)-anchored chitinase specifically localized at polarized growth sites. *Fungal Genetics and Biology*, 45(6):963–972.

Yamazaki, H., Yamazaki, D., Takaya, N., Takagi, M., Ohta, A., and Horiuchi, H. (2007). A chitinase gene, *chiB*, involved in the autolytic process of *Aspergillus nidulans*. *Current Genetics*, 51(2):89–98.

Yasuda, N., Miura, S.-i., Akazawa, H., Tanaka, T., Qin, Y., Kiya, Y., Imaizumi, S., Fujino, M., Ito, K., Zou, Y., et al. (2008). Conformational switch of angiotensin II type 1 receptor underlying mechanical stress-induced activation. *EMBO Reports*, 9(2):179–186.

Yoshida, M., Moriya, S., and Uesugi, Y. (1984). Observation of transmethylation from methionine into choline in the intact mycelia of *Pyricularia oryzae* by 13 c nmr under the influence of fungicides. *Journal of Pesticide Science*, 9(4):703–708.

Yoshioka, K., Nakashita, H., Klessig, D. F., and Yamaguchi, I. (2001). Probenazole induces systemic acquired resistance in *Arabidopsis* with a novel type of action. *The Plant Journal*, 25(2):149–157.

Zanolari, B., Rockenbauch, U., Trautwein, M., Clay, L., Barral, Y., and Spang, A. (2011). Transport to the plasma membrane is regulated differently early and late in the cell cycle in *Saccharomyces cerevisiae*. *Journal of Cell Science*, 124(7):1055–1066.

Zhang, S. and Xu, J.-R. (2014). Effectors and effector delivery in *Magnaporthe oryzae*. *PLoS Pathogens*, 10(1):e1003826.

Zhao, X., Kim, Y., Park, G., and Xu, J.-R. (2005). A mitogen-activated protein kinase cascade regulating infection-related morphogenesis in *Magnaporthe grisea*. *The Plant Cell*, 17(4):1317–1329.

Zhao, Y., Park, R.-D., and Muzzarelli, R. A. (2010). Chitin deacetylases: properties and applications. *Marine Drugs*, 8(1):24–46.

Zhou, X.-L., Stumpf, M. A., Hoch, H. C., and Kung, C. (1991). A mechanosensitive channel in whole cells and in membrane patches of the fungus *Uromyces*. *Science*, 253(5026):1415–1417.

Zhu, X.-F., Tan, H.-Q., Zhu, C., Liao, L., Zhang, X.-Q., and Wu, M. (2012). Cloning and overexpression of a new chitosanase gene from *Penicillium sp. D-1*. *AMB Express*, 2(1):1–8.

Ziman, M., Chuang, J. S., and Schekman, R. W. (1996). Chs1p and Chs3p, two proteins involved in chitin synthesis, populate a compartment of the *Saccharomyces cerevisiae* endocytic pathway. *Molecular Biology of the Cell*, 7(12):1909–1919.

Ziman, M., Chuang, J. S., Tsung, M., Hamamoto, S., and Schekman, R. (1998). Chs6p-dependent anterograde transport of Chs3p from the chitosome to the plasma membrane in *Saccharomyces cerevisiae*. *Molecular Biology of the Cell*, 9(6):1565–1576.

Zuppini, A., Baldan, B., Millioni, R., Favaron, F., Navazio, L., and Mariani, P. (2004). Chitosan induces ca2+-mediated programmed cell death in soybean cells. *New Phytologist*, 161(2):557–568.

Appendices

Appendix A

Media

Name	Recipe	Use
Complete medium (CM)	For 1000ml: 50ml 20x nitrate salts, 1ml Trace elements, 1ml Vitamin Mix, 10g Glucose, 2g Peptone, 1g Yeast Extract ,1g Casamino acids . 15g agar for solid media. pH 6.5 (with NaOH).	Routine culturing of *M.oryzae* or as base medium for plate growth and liquid growth assays.
Minimal medium (MM)	For 1000ml: 50ml 20x nitrate salts, 1ml Trace elements, 1ml Thiamine (from 1% stock solution), 50µl Biotin (from 0.05% stock solution), 10g Glucose. 15g Agar for solid media. pH 6.5 (with NaOH).	Plate growth, liquid growth assays or overlay selection media for transformations using hygromycin.
DCM	For 1000ml: 1.7g Yeast nitrogen base without amino acids, 2g L-Asparagine, 1g Ammonium nitrate, 10g (w/v) Glucose, pH 6 (with Na_2HPO_4). 10g agar.	Overlay media for transformations selecting with bialaphos
BDCM (bottom layer)	For 1000ml: 1.7g Yeast nitrogen base without amino acids/smmonium sulphate, 1g L-Asparagine, 2g Ammonium nitrate, 10g (w/v) Glucose, 273.84g sucrose, pH 6 (with Na_2HPO_4). 15g agar.	Media for bottom layer after transformation of *M.oryzae,* when selecting with sulphonylurea.
BDCM (overlay)	For 1000ml: 1.7g Yeast nitrogen base without amino acids/smmonium sulphate, 1g L-Asparagine, 2g Ammonium nitrate, 10g (w/v) Glucose, pH 6 (with Na_2HPO_4). 15g agar.	Overlay media for transformations selecting with sulphonyurea
OCM	For 1000ml: 273.84g sucrose, 10g Glucose, 2g Peptone, 1g Yeast extract, 1g Casamino acids, 50ml 20x nitrate salts, 1ml Trace elements, 1ml Vitamin solution. pH 6.5 (with NaOH). 15g agar.	Media for bottom layer after transformation of *M.oryzae,* when selecting with hygromycin or bialaphos.
LB	For 1000ml: 10g Tryptone, 5g Yeast extract, 10g NaCl	Growth and selection of *E.coli*
Xbroth	For 1000ml: 5g Yeast extract, 20g Tryptone, 4g $MgSO_4$, 0.76g KCl, pH 7.6	Recovery of *E.coli* after heat-shock
YPD	For 1000ml: 10g Yeast extract, 20g Peptone, 20g Glucose, 20g Agar	Culturing of *S.cerevisiae*
Yeast synthetic drop-out media	For 1000ml: 1.7g Yeast nitrogen base without amino acids, 5g Ammonium sulphate, 5g Casamino acids, 20mg Adenine, 20mg Tryptophan, 20g agar.	Selection of S.cerevisiae transformants

Appendix B

Solutions

Name	Recipe	Use
20x Nitrate salts	For 1000ml: 120g $NaNO_3$, 10.4g KCl, 10.4g $MgSO_4.7H_2O$, 30.4g KH_2PO_4	As a constituent of Complete Medium and Minimal Medium.
1000x Trace elements	For 100ml: 80ml H_2O, 2.2 g $ZnSO_4.7H2O$, 1.1g H_3BO_4, 0.5g $MnCl_2.4H_2O$, 0.5g $FeSO_4.7H2O$, $CoCl_2.6H_2O$, $CuSO_4.5H_2O$, 0.15g $Na_2MoO_4.2H_2O$, 5g Na_4EDTA. Boil and cool to 60°C, pH 6.5 adjust volume to 100ml with dH_2O	As a constituent of Complete Medium and Minimal Medium.
Vitamin solution	For 100ml: 0.01g biotin, 0.01g pyridoxin, 0.01g thiamin, 0.01g riboflavin, 0.01g p-aminobenzoic acid, 0.01g nicotinic acid.	As a constituent of Complete Medium.
ST buffer	For 500ml: 54.66g Sorbitol, 50ml 1M Tris-HCl, pH 7.0	Transformation of *M.oryzae*
STC buffer	For 500ml: 109.32g Sorbitol, 5ml 1M Tris-HCl, pH 7.5, 5ml 1M $CaCl_2$	Transformation of *M.oryzae*
PTC buffer	For 100ml: 60g PEG4000, 1ml Tris-HCl, pH 7.5, 1ml 1M $CaCl_2$	Transformation of *M.oryzae* (filter sterilized before use)
OM buffer	For 100ml: 29.58g $MgSO_4.7H_2O$, 1.3g lysing enzymes from Trichoderma harzianum, 1ml 1M Na_2HPO_4. pH 5.8 with NaH_2PO_4.	Transformation of *M.oryzae* (filter sterilized before use)
1% Chitosan stock	For 100ml: 1g Chitosan, dissolved in 80ml 3% acetic acid. pH to 5-6 with solid NaOH. Dialyze against water for 24-48hrs using benzoylated dialysis tubing.	For addition to media (growth assays)
DNA extraction buffer	For 100ml: 20ml 1M Tris HCl pH 7.5, 5ml 5M NaCl, 5ml 0.5M EDTA, 5ml 10% SDS	Extraction of low quality DNA for screening of transformants.
Depurination buffer	For 1000ml: 11ml concentrated HCl, 989ml MilliQ H_2O	Southern blotting (Gel washing)
Denaturation buffer	For 1000ml: 87.88g NaCl, 20g NaOH, pH 7.5.	Southern blotting (Gel washing)
Neutralisation buffer	For 1000ml: 87.66g NaCl, 60.5g Trizmabase. pH 7-8 with concentrated HCl	Southern blotting (Gel washing)
20x SSC buffer	For 2000ml: 350.6g NaCl, 176.4g Tri-sodium citrate. pH 7	Southern blotting (Transfer)
Yeast lysis buffer	For 200ml: 4ml Triton X-100, 20ml 10% SDS, 4ml 5M NaCl, 400ul 0.5M EDTA, 2ml 1M Tris	Plasmid DNA extraction from S.cerevisiae.

Appendix C

Growth treatments

Treatment	Concentration	Base Medium	Notes
Congo Red	100µg/ml	CM + 50mM HEPES, pH 7	4mg/ml stock solution, filter sterilized and added after autoclaving of media
Calcofluor White	40µg/ml	CM + 50mM HEPES, pH 7	1mg/ml stock solution, filter sterilized and added after autoclaving of media
Hydrogen Peroxide	5mM (solid media) 2.5mM (liquid media)	CM	8.82M stock solution, filter sterilized and added after autoclaving of media
Sorbitol	1M	CM	Added prior to autoclaving
SDS	0.005%	CM	Added prior to autoclaving, from 10% stock solution.
NaCl	1M	CM	Added prior to autoclaving
Copper	2g/L	CM + 50mM HEPES, pH 7	1mg/ml stock solution of $CuSO_4.5H_2O$. Filter sterilized and added after autoclaving of media
Caffeine	2.5mM	CM	Filter sterilized and added after autoclaving of media
Rapamycin	60ng/ml	CM	5mg/ml stock solution in DMSO. Added after autoclaving of media
Chitosan	0.5% (solid media), 0.33% (liquid media)	MM (without glucose), + 25mM Na_2HPO_4, pH 5.6 (solid media) or 25mM sodium acetate, pH 5.6 (liquid media)	1% chitosan stock sterilized by microwaving, and added after autoclaving of media
Lysing enzymes (from *T. harzianum)*	4mg/ml (liquid media)	CM (liquid)	Filter sterilized and added after autoclaving of media

Appendix D

Plasmid maps

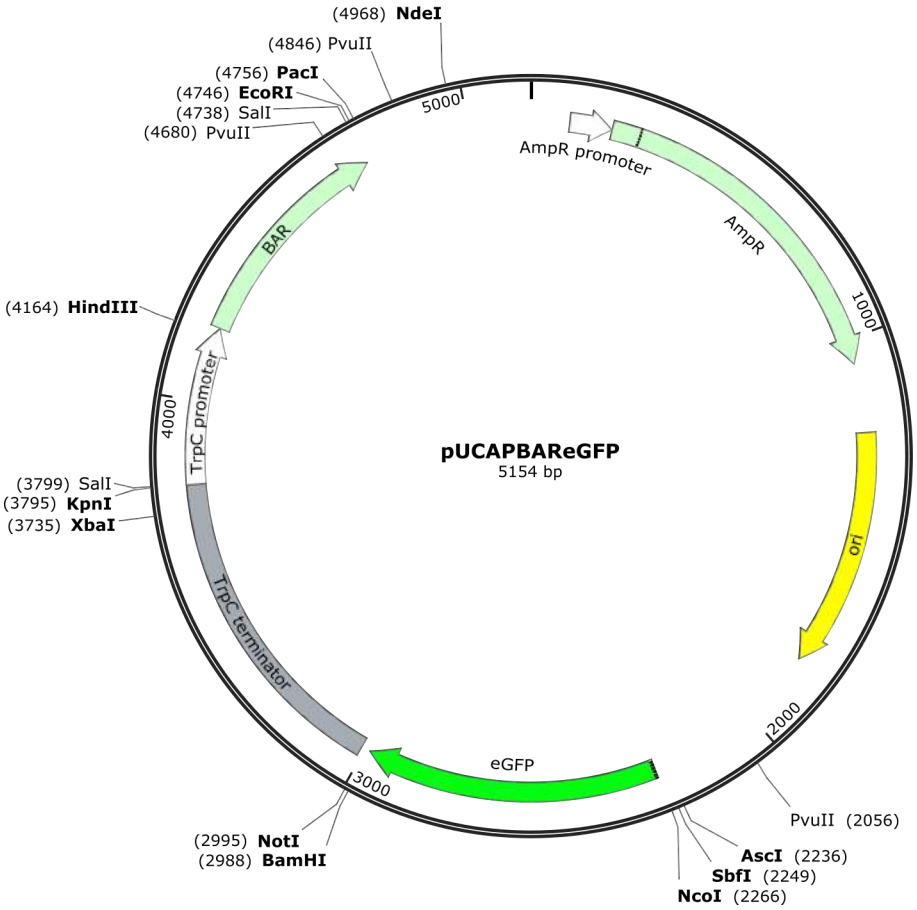

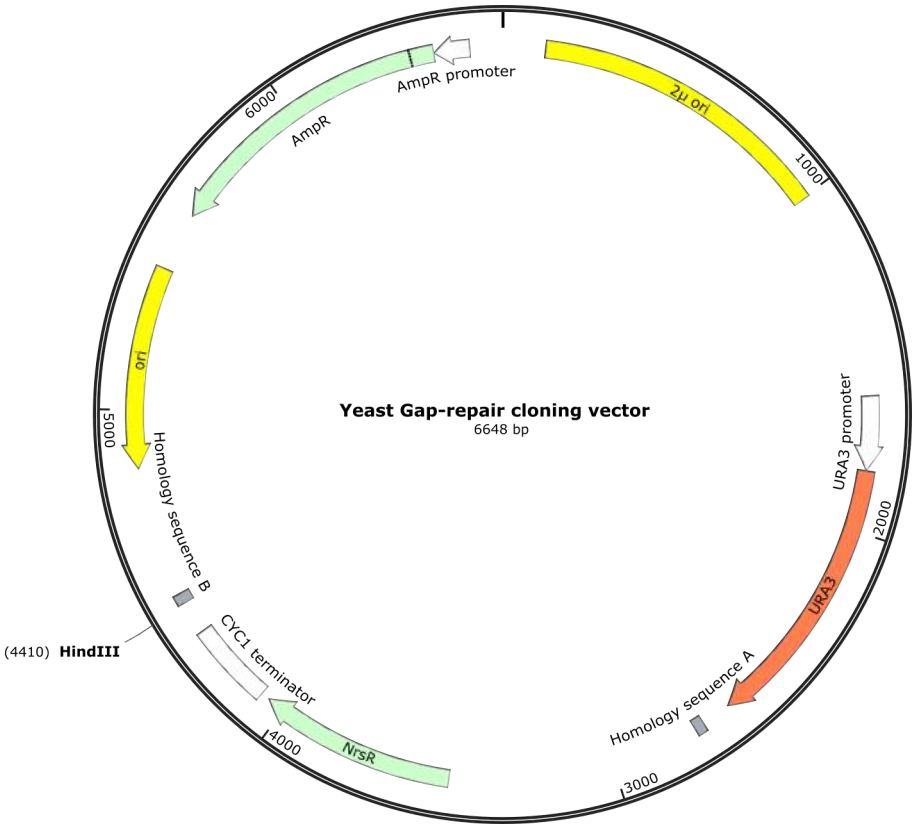
Yeast Gap-repair cloning vector
6648 bp
AmpR promoter
AmpR
2µ ori
ori
URA3 promoter
URA3
Homology sequence B
Homology sequence A
CYC1 terminator
NrsR
(4410) HindIII
1000
2000
3000
4000
5000
6000

Appendix E

Primers

No.	Primer Name	Sequence	Notes
1	BialaphosFor	GTCGACAGAAGATGATATTGAAGGAGCACTTTTTGG	Same as HygromycinFor. SalI site (underlined)
2	BialaphosRev	GTCGACCTAAATCTCGGTGACGGGCAG	SalI site (underlined)
3	HygromycinFor	GTCGACAGAAGATGATATTGAAGGAGCACTTTTTGG	Same as BialaphosFor. SalI site (underlined)
4	HygromycinRev	GTCGACGTTAACTGGTTCCCGGTC	SalI site (underlined)
5	SulR-For	GTCGACGTGCCAACGCCACAGTGCCCCACATCTCCC	SalI site (underlined)
6	SulR-Rev	GTCGACGTGAGAGCATGCAATTCCCGTGCAATAATCAATTCCC	SalI site (underlined)
7	MGG12939_KO1	ACCATGGCTACACAATTCGAGACGACG	
8	MGG12939_KO2	CTTCAATATCATCTTCTGTCGACTCGGAATTAAGGTATCTGGATAGATAAAGG	Overlaps with Hygromycin resistance gene (underlined)
9	MGG12939_KO5	ACCGGGAACCAGTTAACGTCGACACTAGCGCCTCAAGCAC	Overlaps with Hygromycin resistance gene (underlined)
10	MGG12939_KO6	TTGTTTAATAAGGGAGAGCAAAACAATAGCAGGAAG	
11	MGG12939_KO2BAR	CAATATCATCTTCTGTCGACTCGGAATTAAGGTATCTGGATAGATAAAGG	Overlaps with Bialaphos resistance gene (underlined)
12	MGG12939_KO5BAR	CGTCACCGAGATTTAGGTCGACACTAGCGCCTCAAGCAC	Overlaps with Bialaphos resistance gene (underlined)
13	MGG09159_KO1	TTCTCGGTTGTATTATTTTTGGTGTCTGGCTAGTATGTG	
14	MGG09159_KO2	CTTCAATATCATCTTCTGTCGACGTGGGTGATATTATATAAGAGAGTGTG	Overlaps with Hygromycin resistance gene (underlined)
15	MGG09159_KO5	ACCGGGAACCAGTTAACGTCGACCATTGAGAATAGGCTACAGCAG	Overlaps with Hygromycin resistance gene (underlined)
16	MGG09159_KO6	TCTGGGCTTTGGCAACGACCTCAGTGTG	
17	MGG04172_KO1	GATCTGCGCATCACGATACCTACTGTCC	
18	MGG04172_KO2	CTTCAATATCATCTTCTGTCGACTCACTTACCGCTGGTGTATGATCC	Overlaps with Hygromycin resistance gene (underlined)
19	MGG04172_KO5	ACCGGGAACCAGTTAACGTCGACAGACAGCAAGCCAGCTAAGGAGG	Overlaps with Hygromycin resistance gene (underlined)
20	MGG04172_KO6	ACATTCCACCGCTTCTCTTACGTCAACACC	
21	MGG04172_KO2BAR	CAATATCATCTTCTGTCGACTCACTTACCGCTGGTGTATGATCC	Overlaps with Bialaphos resistance gene (underlined)
22	MGG04172_KO5BAR	CGTCACCGAGATTTAGGTCGACAGACAGCAAGCCAGCTAAGGAGG	Overlaps with Bialaphos resistance gene (underlined)
23	04172TripleKO1	AACTGTTGGGAAGGGCGATCGGTGCGGGCCGATCTGCGCATCACGATACCTACTGTCC	Overlaps with Yeast cloning vector (underlined)
24	04172TripleKO2	GATGTGGGGCACTGTGGCGTTGGCACGTCGACTCACTTACCGCTGGTGTATGATCC	Overlaps with Sulphonyurea resistance gene (underlined)
25	04172TripleKO5	GCACGGGAATTGCATGCTCTCACGTCGACAGACAGCAAGCCAGCTAAGGAGG	Overlaps with Sulphonyurea resistance gene (underlined)
26	04172TripleKO6	TTCACACAGGAAACAGCTATGACCATGATTACATTCCACCGCTTCTCTTACGTCAACACC	Overlaps with Yeast cloning vector (underlined)
27	MGG14966_KO1	CTAATGTGATAAGGTTAAGCATCTGAGGCATTCG	
28	MGG14966_KO2	CTTCAATATCATCTTCTGTCGACAACGAATGTATAATTTAAACGAGAGTAGAGG	Overlaps with Hygromycin resistance gene (underlined)
29	MGG14966_KO5	ACCGGGAACCAGTTAACGTCGACAACTCGCGCACGAACCAGTAGC	Overlaps with Hygromycin resistance gene (underlined)
30	MGG14966_KO6	ACTCCCTTCCTACCGCTGAACGATTTTCACG	
31	MGG08774_KO1	AAGCCTCTATCCGTCCTGCTACGTAG	
32	MGG08774_KO2	CAATATCATCTTCTGTCGACTGTCTTGGTTGGCTGTGTATAC	Overlaps with Bialaphos resistance gene (underlined)
33	MGG08774_KO5	CGTCACCGAGATTTAGGTCGACTCTTATTCATCGCACCTGGTTAGC	Overlaps with Bialaphos resistance gene (underlined)
34	MGG08774_KO6	AGAGGCAGGGAAATATCGTGTTCTTCAG	
35	08774TripleKO1	AACTGTTGGGAAGGGCGATCGGTGCGGGCCAAGCCTCTATCCGTCCTGCTACGTAG	Overlaps with Yeast cloning vector (underlined)
36	08774TripleKO2	GATGTGGGGCACTGTGGCGTTGGCACGTCGACTGTCTTGGTTGGCTGTGTATAC	Overlaps with Sulphonyurea resistance gene (underlined)
37	08774TripleKO5	GCACGGGAATTGCATGCTCTCACGTCGACTCTTATTCATCGCACCTGGTTAGC	Overlaps with Sulphonyurea resistance gene (underlined)
38	08774TripleKO6	TTCACACAGGAAACAGCTATGACCATGATTAGAGGCAGGGAAATATCGTGTTCTTCAG	Overlaps with Yeast cloning vector (underlined)
39	MGG01868_KO1	TGGTGTCAATCTGAAGTATTGGCCAAGGTAGC	
40	MGG01868_KO2	CTTCAATATCAGTTAACGTCGACGGAATGGGTGTATTGACCAAG	Overlaps with Hygromycin resistance gene (underlined)
41	MGG01868_KO5	ACCGGGAACCAGTTAACGTCGACCTGTGCTGTTGTGATTGCTG	Overlaps with Hygromycin resistance gene (underlined)
42	MGG01868_KO6	GCTGGGCTACTAGGTTGCGAAGTCAGTGG	
43	MGG07656_KO1	TGCGACGGAGATGGAAGGCAGC	
44	MGG07656_KO2	CTTCAATATCATCTTCTGTCGACTCCGTCAGTAGTAAGCCCTGG	Overlaps with Bialaphos resistance gene (underlined)
45	MGG07656_KO5	CGTCACCGAGATTTAGGTCGACACTTATTCTGTTTGACTTTGG	Overlaps with Bialaphos resistance gene (underlined)
46	MGG07656_KO6	GAACTCTACCTTGGAATTTATATGGCATCAGTGTCGGAGC	
47	12939mCherryFor	AAAAGGCGCGCCAATTTAGATCACATCAGAAACTCG	AscI site (underlined)
48	12939mCherryRev	AAAAGGCGCGCCCCATAAACAGAACCCGTAGC	AscI site (underlined)
49	09159mCherryFor	AAAAGGCGCGCCATCGTTACAAAGCTCAAGGTTCATC	AscI site (underlined)
50	09159mCherryRev	AAAAGGCGCGCCGTTGCAAGTGCCAAAGC	AscI site (underlined)
51	14966mCherryFor	AAAAGGCGCGCCAGGTAATCGAACGACGTACG	AscI site (underlined)
52	14966mCherryRev	AAAAGGCGCGCCAGAGCAGGTGCCGAATGC	AscI site (underlined)
53	08774mCherryFor	AAAAGGCGCGCCACATCGTGGGTCTTTGG	AscI site (underlined)
54	08774mCherryRev	AAAAGGCGCGCCCATCAAGAGAGCAAATGCCGTAG	AscI site (underlined)

No.	Primer Name	Sequence	Notes
55	07656eGFPFor	AAAAGGCGCGCCAGTGCTGAGGCTTGTTCCTTCC	AscI site (underlined)
56	07656eGFPRev	AAAACCTGCAGGTTTCATGAACCCTTCGACTTCTGG	SbfI site (underlined)
57	07656trunceGFPRev	AAAACCTGCAGGACCGCTCGTCTCCATCTTGAG	SbfI site (underlined)
58	06064YFPFor	AAAAGGCGCGCCCCAATAACATTGTCTGTCTGC	AscI site (underlined)
59	06064YFPRev	AAAAGGCGCGCCCCGTTGCTGATGG	AscI site (underlined)
60	01802eGFPFor	AAAAGGCGCGCCATAGGATCGTCGTTCGAAGC	AscI site (underlined)
61	01802eGFPRev	AAAACCTGCAGGGCGACGGGCAATGCAGCAC	SbfI site (underlined)
62	YFPForSbfI	AAAACCTGCAGGAATGGTGAGCAAGGGCGAG	SbfI site (underlined)
63	YFPRevBamHI	AAAAGGATCCTTAAGAGGCGGCGGTCAC	BamHI site (underlined)
64	YFPForAscI	AAAAGGCGCGCCAATGGGATCCGTGAGCAAG	AscI site (underlined)
65	YFPRevSbfI	AAAACCTGCAGGGGATCCAGAGGCGGCGGTC	SbfI site (underlined)
66	YFPForAscIXhoI	AAAAGGCGCGCCATGCTCGAGGTGAGCAAGGGCGAG	AscI and XhoI sites (underlined)
67	YFPRevAscI	AAAAGGCGCGCCGGATCCAGAGGCGGCGGTC	AscI site (underlined)
68	pCSNForXhoI	AAAACTCGAGAGTGCTGAGGCTTGTTCCTTCC	XhoI site (underlined)
69	pCSNRevXhoI	AAAACTCGAGTCCCATGGCAGATGTATGTGTATAGAAATAG	XhoI site (underlined)
70	pRP27ForAscI	AAAAGGCGCGCCATAAATGTAGGTATTACCTG	AscI site (underlined)
71	pRP27RevCSN	GTTGCAATGCTTGATCGCAT TTTGAAGATTGGGTTC	Overlaps with MGG_07656 coding sequence (underlined)
72	CSNForpRP27	GAACCCAATCTTCAAAATGCGATCAAGCATTGCAAC	Overlaps with pRP27 (underlined)
73	CSNRevSbfI	AAAACCTGCAGGCCAAAGTCAAACAGAATAAGTATTTAGTC	SbfI site (underlined)
74	CSNTruncRevBamHI	AAAAGGATCCCTAACCGCTCGTCTCCATCTTGAG	BamHI site (underlined)
75	pRP27Rev12939	GACAACCACTTCATTTTGAAGATTGGGTTCCTACG	Overlaps with MGG_12939 coding sequence (underlined)
76	12939ForpRP27	TAGGAACCCAATCTTCAAA ATGAAGTGGTTGTCACTTGC	Overlaps with pRP27 (underlined)
77	pEF1ForAscI	AAAAGGCGCGCCATGATGTGAGTTCCTCCGTTC	AscI site (underlined)
78	pEF1Rev14966	GAAAGTGGTGTACTTCAT TTTGGCGGTTTGGTGCTC	Overlaps with MGG_14966 coding sequence (underlined)
79	14966ForpEF1	ACCAAACCGCCAAAATGAAGTACACCACTTTCGCTG	Overlaps with pEF1 (underlined)
80	MST7ForSbfI	AAAACCTGCAGGAGCTAGGTCTAGAAGTGGAGAGGA	SbfI site (underlined)
81	MST7For2mut	GAACTTATTAACGACATAGCCGAT GAGTTTGTCGGCACT	Introduces mutations (replaced codons underlined)
82	MST7Rev2mut	AGTGCCGACAAACTCATCGGCTAT GTCGTTAATAAGTTC	Introduces mutations (replaced codons underlined)
83	MST7RevNotI	AAAAGCGGCCGCCTAGTCCCGGATGTAAAGCCGA	NotI site (underlined)
84	14966RTPCRFor	TCGCTGCTCTTCTGGGTC	
85	14966RTPCRRev	GTCTGCTCGCTCTTCAAGGA	
86	08356RTPCRFor	GCACGACATGAAACACACAATC	
87	08356RTPCRRev	GCAGCGACGTAACCATTTTC	
88	05023RTPCRFor	TCCCTTATGGCGAGGTCATAAC	
89	05023RTPCRRev	TGCTCGGTGTAGATGCTGG	
90	04172RTPCRFor	GCTGGACATTTGACGGCTC	
91	04172RTPCRRev	GCACCGTGTTGAGCTTGG	
92	12939RTPCRFor	GGTGTACTCAGGAGCCACAATC	
93	12939RTPCRRev	TGGCTGTTTTGAGAGGTAGCTG	
94	09159RTPCRFor	CTACGACTGCGTCAACAACG	
95	09159RTPCRRev	TCCAGGATCGTCTCGGTG	
96	01868RTPCRFor	GACGACCGATGTATCCCAGAC	
97	01868RTPCRRev	GATGGTTCTTCAGATGTGGTGG	
98	03461RTPCRFor	CTCGCATACTTGAGCCACG	
99	03461RTPCRRev	TGTTGACAAACGCCTGCTC	
100	08774RTPCRFor	CTTTGCGCGACTCATTGG	
101	08774RTPCRRev	TCGTAGTCGGTGACATGGTAGG	
102	04704RTPCRFor	ACTCGATGCGCAAGCTAGTC	
103	04704RTPCRRev	CGTTCAGACGCCAGTTTGT	
104	07656RTPCRFor	GCGGCGACAAGATGTTCTAC	
105	07656RTPCRRev	GCGAGATACAGCACATCGTTC	
106	β-tubRTPCRFor	CTGCCATCTTCCGTGGAAAGG	
107	β-tubRTPCRRev	GACGAAGTACGACGAGTTCTTG	

Appendix F

Strains

Genotype	Background strain	Resistance markers	Description	Transformant line N° used
Guy11	None	None	WT strain of *Magnaporthe oryzae*	
Ku70	Guy11	Sulphonylurea	Deletion strain for *ku70*	
Δ*cda2*	Guy11	Hygromycin	Deletion strain for *MGG_09159*	8
Δ*cbp1*	Guy11	Hygromycin	Deletion strain for *MGG_12939*	11, 14
Δ*cda3*	Guy11	Hygromycin	Deletion strain for *MGG_04172*	34
Δ*cda1*	Guy11	Hygromycin	Deletion strain for *MGG_14966*	38
Δ*cda4*	Guy11	Bialaphos	Deletion strain for *MGG_08774*	3
Δ*cda5*	Guy11	Hygromycin	Deletion strain for *MGG_01868*	8b
Δ*csn*	Ku70	Bialaphos/sulphonylurea	Deletion strain for *MGG_07656 (Chitosanase)*	
Δ*csn*	Guy11	Bialaphos	Deletion strain for *MGG_07656 (Chitosanase)*	9, 46
ΔΔ*cda2/cbp1*	Δ*cda2* (line 8)	Bialaphos/Hygromycin	Double deletion strain for *MGG_09159* & *MGG_12939*	52
ΔΔ*cda2/cda3*	Δ*cda2* (line 8)	Bialaphos/Hygromycin	Double deletion strain for *MGG_09159* & *MGG_04172*	10
ΔΔ*cbp1/cda3*	Δ*cbp1* (line 11)	Bialaphos/Hygromycin	Double deletion strain for *MGG_12939* & *MGG_04172*	8, 9
ΔΔ*cda4/cda5*	Δ*cda4* (line 3)	Bialaphos/Hygromycin	Double deletion strain for *MGG_08774* & *MGG_01868*	13, 23
ΔΔΔ*cda2/cbp1/cda3*	ΔΔ*cda2/cbp1* (line 52)	Bialaphos/Hygromycin/ Sulphonylurea	Triple deletion strain for *MGG_09159* , *MGG_12939* & *MGG_04172*	5, 12
ΔΔΔ*cda2/cbp1/cda4*	ΔΔ*cda2/cbp1* (line 52)	Bialaphos/Hygromycin/ Sulphonylurea	Triple deletion strain for *MGG_09159* , *MGG_12939* & *MGG_08774*	30
CDA2:mCherry	Δ*cda2* (line 8)	Bialaphos/Hygromycin	Deletion strain expressing C-terminal mCherry tagged MGG_09159 (expressed by native promoter)	3, 11, 14, 16
CBP1:mCherry	Δ*cbp1* (line 11)	Bialaphos/Hygromycin	Deletion strain expressing C-terminal mCherry tagged MGG_12939 (expressed by native promoter)	21, 23, 31
CDA1:mCherry	Δ*cda1* (line 38)	Bialaphos/Hygromycin	Deletion strain expressing C-terminal mCherry tagged MGG_14966 (expressed by native promoter)	17
CDA4:mCherry	Guy11	Hygromycin	C-terminal fusion of mCherry to MGG_08774 (expressed by native promoter)	2, 8, 12
CDA4:mCherry	Δ*cda4* (line 3)	Bialaphos/Hygromycin	Deletion strain expressing C-terminal mCherry tagged MGG_08774 (expressed by native promoter)	1, 29, 22
CDA1:mCherry/ CHS1eGFP	MGG_08774: mCherry (line 2)	Bialaphos/Hygromycin	Co-expression of *MGG_08774* mCherry fusion and *MGG_01802 (chitin synthase I)* eGFP fusion	2, 18, 19, 20
MGG_06064:2xYFP	Guy11	Hygromycin	C-terminal fusion of 2 copies of YFPvenus to MGG_06064 (chitin synthase VII), expressed by native promoter	10, 18, 23
MGG_06064:2xYFP/ CDA2mCherry	MGG_06064:2xYFP (line 23)	Bialaphos/Hygromycin	Co-expression of *MGG_06064* YFP fusion and *MGG_09159* mCherry fusion	17, 21, 24
MGG_06064:2xYFP/ CBP1mCherry	MGG_06064:2xYFP (line 23)	Bialaphos/Hygromycin	Co-expression of *MGG_06064* YFP fusion and *MGG_12939* mCherry fusion	17, 18, 21
pRP27:CBP1mCherry	Guy11	Hygromycin	C-terminal fusion of mCherry to *MGG_12939* , expressed by *RP27* promoter (overexpression)	5, 6, 9, 11
pEF1:CDA1mCherry	Guy11	Hygromycin	C-terminal fusion of mCherry to *MGG_14966* , expressed by EF1 promoter (overexpression)	7, 8, 33
CSN:eGFP	Δ*csn* (lines 9 & 46)	Bialaphos/Hygromycin	C-terminal fusion of eGFP to *MGG_07656*	2
pRP27:CSN	Guy11	Bialaphos	Expression of *MGG_07656* (chitosanase) by *RP27* promoter (overexpression)	22, 27
pRP27:CSN $^{1\text{-}275}$	Guy11	Bialaphos	Expression of truncated form (residues 1-275) of *MGG_07656* (chitosanase) by *RP27* promoter (overexpression)	9, 19
pCSN 3xYFP	Guy11	Hygromycin	Expression of 3 copies of YFPvenus by the native chitosanase promoter	2, 9, 24
EV	Guy11	Bialaphos	Strain containing empty expression vector	2, 3